The Effect of Thermal Impact Factors on the Thermal Performance of Low-Slope Roofing Assemblies

By

Michael Zinoviev

A thesis submitted in partial fulfilment of the requirements for the degree

Of

Masters of Applied Science
In Civil Engineering

At

The University of Ottawa

“Research is to see what everybody has seen, and to think what nobody else has thought.”

- Albert Szent-Gyorgyi

Acknowledgements

I would first like to thank my supervisors: Dr. Suda Molleti and Dr. Beatriz Martin-Perez. Dr. Molleti for his patience, support, and guidance during my endeavors in a new field; Dr. Martin-Perez for her devotion and helpfulness in every aspect of her teaching. I would not have been able to reach this achievement without them.

I would like to give special thanks to Dr. Bas Baskaran for the opportunity to work at the National Research Council, for without him, I would not have had the opportunity to work on such an interesting and significant research topic.

I would like to thank my colleagues at the National Research Council for their guidance and willingness to help: Pascal Beaulieu, David Van Reenen, Helen Yew, Steven Ko, Jeffery Tomkins and Amour Duric.

I would like to express my gratitude to everyone who has supported me along this journey; my family, friends, and colleges.

This thesis is dedicated to my parents and brother; they have taught me that hard work and dedication will lead to success; the goal is not perfection but the integrity of the work.

Abstract

For decades materials of low thermal conductivity have been used to minimize heat flow through building systems. With advancements in sustainability and a demand for an increase in building envelope efficiency, there is a greater interest in the energy efficiency of insulating materials and their behavior in building assemblies. The heat flow in a low-slope roof system would be relatively simple to estimate if the insulation were continuous and the heat flow one-dimensional, but it becomes complex with the presence of gaps between insulation boards and thermal bridging. Over the past three decades there has been an increased focus on the problem of thermal drift in roofing insulation materials and thermal bridging. Thermal bridging is an inevitable mode of thermal loss in roof assemblies due to the use of mechanical fasteners to secure the roofing components. Similarly, thermal breaks due to gaps between insulation boards are anticipated due to installation and the dimensional stability of the boards. Currently, regulations and standards do not consider these thermal impact factors on the performance of roofing systems. As a result, proper analysis of these factors becomes more important as their relative influence on the thermal demand becomes more evident. The purpose of this research is to study these thermal impact factors and quantify their influence on low-slope roofing systems. The literature on this subject is in agreement that thermal losses resulting from these factors leads to drastic thermal inefficiencies; however, none of the studies provide general encompassing methods that may be applied to reach the building code design thermal values. This research considers an array of components and assemblies to provide generalized adjustment factors for the decrease in effective thermal resistance due to fasteners and gaps for the potential implementation in the energy codes.

Table of Contents

Acknowledgements iii

Abstract iv

Table of Contents v

List of Tables vii

List of Figures ix

Glossary xiii

Symbols xiii

Units xiii

Conversions xiii

Abbreviations xiv

Terminology xv

Chapter 1: Introduction 1

1.1. Background 1

1.2. Thesis Objective 2

1.3. Thesis Scope 3

1.4. Thesis Outline 5

Chapter 2: Energy Design of Roofs 6

2.1. Roofing Systems and Components 6

2.2. Thermal Fundamentals 11

2.2.1. Fundamentals of Heat Transfer 11

2.2.2. Fundamental Calculations of Heat Transfer 17

2.3. Thermal Transmittance of a Roof Assembly - Design Example 18

2.4. Thermal Impact Factors 20

2.4.1. Gaps between Insulation Boards 20

2.4.2. Mechanical Fasteners 26

2.4.3. Air Intrusion and Moisture 29

2.4.4. Thermal drift 30

2.4.5. Reporting Mean Temperatures 30

2.5. Concluding Remarks 31

Chapter 3: Literature Review 32

3.1. Standard Test Methods 33

3.2. Thermal Analysis via Numerical Modeling 39
3.3. Thermal Analysis via Experimental Testing 50
3.4. Concluding Remarks 55
Chapter 4: Experimental Methodology 56
4.1. Roofing Components 56
4.2. Heat Flow Meter (HFM) 58
4.3. Coefficient of Linear Expansion 61
4.4. Dimensional Stability 63
4.5. Guarded Hot Box Apparatus (GHB) 66
4.5.1. Construction of the Guarded Hot Box 68
4.5.2. Calibration 72
4.5.3. Temperature Offset 74
4.5.5. Specimen Installation 79
Chapter 5: Experimental Results and Analysis 84
5.1. Coefficient of Linear Expansion 84
5.2. Dimensional Stability Results 86
5.3. Heat Flow Meter Results 89
5.4. Guarded Hot Box Results 97
5.4.1. Data Analysis and Validation 97
5.4.2. Development of Adjustment Factors 104
Chapter 6: Data Validation and Codification 116
6.1. Joint Validation 116
6.2. Fastener Validation 121
6.3. Codification 123
Chapter 7: Concluding Remarks 127
7.1. Conclusions 127
7.2. Future Work 129
References 130
Appendices 132
Appendix A: Summary of Literature Results 132
Appendix B: Dimensional Stability Results 136
Appendix C: Heat Flow Meter Results 140
Appendix D: Guarded Hot Box Results 146

List of Tables

Table 2-1: Summary of all NECB Zone Thermal Requirements 16
Table 2-2: Summary of all ASHRAE Zone Thermal Requirements 17
Table 3-1: Summary of Dimensional Stability Test Requirements 38
Table 4-1: Manufacture Provided Thickness for Achieving Respective R-Value 57
Table 4-2: Individual Board Thickness 57
Table 4-3: Heat Flow Meter Test Mean Temperatures 59
Table 4-4: Dimensional Stability Limits of Different Insulation from Test Standards 65
Table 4-5: Calculated Temperature Offset 77
Table 4-6: Typical Fastener Density 80
Table 5-1: Coefficient of Linear Expansion Results 84
Table 5-2: Insulation Thicknesses Tested 86
Table 5-3: Percent Change in Mass 88
Table 5-4: Dimensional Stability Results 88
Table 5-5: Average R-Value and Standard Deviation of 3.125" EPS Insulation 92
Table 5-6: GHB Repeatability 103
Table 5-7: EPS – R26 – Fastener Results 105
Table 5-8: EPS – R31 – Fastener Results 105
Table 5-9: Polyiso – R26 – Fastener Results 106
Table 5-10: Polyiso – R31 – Fastener Results 106
Table 5-11: Stone Wool – R26 – Fastener Results 107
Table 5-12: Stone Wool – R31 – Fastener Results 107
Table 5-13: Fastener Density Adjustment Factors 109
Table 5-14: Top and Bottom Gap Results 113
Table 5-15: Staggered Gap Results 114
Table 5-16: Fastener and Gap Combined Test Results 115
Table 6-1: Length of Gaps per Chamber 119
Table 6-2: CTC Joint Test Results 120
Table 6-3: Calibrated Thermal Chamber Fastener Test Results 122
Table 6-4: Fastener Adjustment Factors 123
Table 6-5: Adjustment Factor Implementation Example 125
Table A-1: Summary of Literature (Lewis, 1979) 132
Table A-2: Summary of Literature (Burch, Shoback, and Cavanaugh, 1987) 132
Table A-3: Summary of Literature (Wiedland, 1988) 132
Table A-4: Summary of Literature (Wieland, 2006) 133
Table A-5: Summary of Literature (O'Brian, 2006) 133
Table A-6: Summary of Literature (Grin, Schumacher, and Smegal, 2014) 133
Table A-7: Summary of Literature (Hedlin, 1985) 134
Table A-8: Summary of Literature (Courville et al., 1989) 134
Table A-9: Summary of Literature (Petrie et al., 2000) 135
Table A-10: Summary of Literature (Building Science Corporation, 2005) 135

Table D-1: EPS R26 Temperature Offset Data 146
Table D-2: EPS R31 Temperature Offset Data 146
Table D-3: Stone Wool R26 Temperature Offset Data 146
Table D-4: Stone Wool R31 Temperature Offset Data 146
Table D-5: Polyiso R26 Temperature Offset Data 147
Table D-6: Polyiso R31 Temperature Offset Data 147
Table D-7: GHB – EPS R26 Results – Raw Data 148
Table D-8: GHB – EPS R31 Results – Raw Data 149
Table D-9: GHB – Stone Wool R26 – Raw Data 150
Table D-10: GHB – Stone Wool R31 – Raw Data 151
Table D-11: GHB – Polyiso R26 – Raw Data 152
Table D-12: GHB – Polyiso R31 – Raw Data 153

List of Figures

Figure 1-1: Work Plan Developed by the ERCR Consortium 3
Figure 1-2: Test Matrix Developed by the ERCR Consortium 4
Figure 2-1: Conventional Roof Assembly 7
Figure 2-2: Built-Up Roofing System 7
Figure 2-3: Mechanically-Attached Roofing System 8
Figure 2-4: Partially Adhered Roofing System 8
Figure 2-5: Adhesive Attached Roofing System 9
Figure 2-6: Ballasted Roof System 10
Figure 2-7: Protected Membrane Roof 10
Figure 2-8: Mechanisms of Heat Flow 12
Figure 2-9: Thickness Required to Reach the Equivalent Resistance 12
Figure 2-10: ASHRAE: U.S. and Canada Climate Zone Map 15
Figure 2-11: Canadian Climatic Zones 15
Figure 2-12: Building Envelope Requirements 16
Figure 2-13: Building Envelope Requirements for Zone 6 16
Figure 2-14: NECB Design Example 18
Figure 2-15: Thermal Resistance Values of Common Insulation 19
Figure 2-16: Insulation Gaps 20
Figure 2-17: Insulation Joints 21
Figure 2-18: Insulation Gap Formation 21
Figure 2-19: Cause of Gap Formation 23
Figure 2-20: Insulation Defect 23
Figure 2-21: In-situ Insulation Gaps #1 24
Figure 2-22: In-situ Insulation Gaps #2 25
Figure 2-23: Fasteners 26
Figure 2-24: PARS vs. MARS Roof Assemblies 26
Figure 2-25: Effect of Membrane on Fastener Density 27
Figure 2-26: Industry Fastener Densities 27
Figure 2-27: In-situ Fastener Thermal Impact 28
Figure 2-28: Air Intrusion Impact on Roofing Assemblies 29
Figure 2-29: Insulation Behaviour over Ranging Mean Temperature 31
Figure 3-1: Guarded-Hot-Plate Apparatus 33
Figure 3-2: Heat Flow Meter Apparatus 34
Figure 3-3: Typical Guarded Hot Box Schematic 35
Figure 3-4: Guarded Hot Box Reproducibility 36
Figure 3-5: Temperature Conditions for Aging 37
Figure 3-6: Standard Temperatures for Thermal Testing 38
Figure 3-7: Adjacent Insulation Gaps 39
Figure 3-8: Thermal Transmittance due to Gaps 40
Figure 3-9: Thermocouple Locations 40

Figure 3-10: Percent Increase in Thermal Transmittance 41
Figure 3-11: Fastener through (a) Bottom Layer of Insulation (b) Entire Insulation 42
Figure 3-12: System with Carbon Steel Screw (left) and Screw with Plastic Shank (right) 43
Figure 3-13: (a) Metal Fastener and Plate (b) Plastic Sleeve with Metal Fastener 44
Figure 3-14: Percentage Increase in Heat Loss with 4 Fasteners/m^2 45
Figure 3-15: Insulation Requirements and Associated Material Thickness 46
Figure 3-16: Temperature Dependent R-Value for R-30 Insulation 47
Figure 3-17: Modeled Winter Heat Flow 47
Figure 3-18: Re-Covering Assemblies 48
Figure 3-19: Reroofing Assemblies 49
Figure 3-20: (a) Reroofing and (b) Re-Covering Heat Flux Vectors 49
Figure 3-21: System Configuration 50
Figure 3-22: Measure Heat Flow along Insulation 51
Figure 3-23: Measure and Calculated Heat Flow 51
Figure 3-24: Schematic of Large Scale Climate Simulator 52
Figure 3-25: Conditions Imposed on Roof Assembly 52
Figure 3-26: R-Values for the Effects of Gaps and Fasteners 53
Figure 3-27: Thermal Resistance Variation for Polyiso Insulation 54
Figure 4-1: Insulation Boards 56
Figure 4-2: DensDeck Protection Board and PVC Membrane 57
Figure 4-3: Heat Flow Meter Test Setup 59
Figure 4-4: Manufacturer Provided Thickness for Achieving Design R26 60
Figure 4-5: Manufacturer Provided Thickness for Achieving Design R31 60
Figure 4-6: Linear Variable Displacement Transformers 61
Figure 4-7: Test Configuration and LVDT Location 62
Figure 4-8: Coefficient of Linear Expansion Test Apparatus 62
Figure 4-9: Dimensional Stability Measurement Tools 63
Figure 4-10: Board Dimensions Before and After Dimensional Stability Test 63
Figure 4-11: Dimensional Stability – Heating Chamber 64
Figure 4-12: Dimensional Stability – Cooling Chamber 64
Figure 4-13: Guarded Hot Box Chambers 66
Figure 4-14: Guarded Hot Box Apparatus 67
Figure 4-15: Insulating the Exterior Walls of the GHB 68
Figure 4-16: Insulating the Walls of the Guard Chamber 69
Figure 4-17: Air and Moisture Proofing the Chamber 69
Figure 4-18: Insulated Metering Chamber and Thermal Couple Installation 70
Figure 4-19: Assembled Guarded Hot Box 70
Figure 4-20: Climatic Chamber 71
Figure 4-21: Completed Guarded Hot Box Apparatus 71
Figure 4-22: Guarded Hot Box Precision Interval 73
Figure 4-23: Ideal Guarded Hot box 74
Figure 4-24: Chamber Temperature Scenarios 75

Figure 4-25: Temperature Offset Calibration 75
Figure 4-26: Thermocouple 78
Figure 4-27: Opaque Assembly Installation 79
Figure 4-28: Fastener Densities 80
Figure 4-29: Fastener Assembly Installation 81
Figure 4-30: Fastener Lengths and Specifications 81
Figure 4-31: All Possible Joint Configurations in 4 Foot Cross-Section 82
Figure 4-32: Top Joint 83
Figure 4-33: Bottom Joint 83
Figure 4-34: Staggered Joints 83
Figure 5-1: Coefficient of Linear Expansion, Heating Cycle 85
Figure 5-2: Coefficient of Linear Expansion, Cooling Cycle 85
Figure 5-3: Dimensional Stability of 3 1/8" EPS Boards 86
Figure 5-4: Dimensional Stability of 3 7/8" EPS Boards 87
Figure 5-5: Summary of Dimensional Changes of EPS Boards 87
Figure 5-6: R26 Components and Assembly 90
Figure 5-7: Heat Flow through Thin Insulation 90
Figure 5-8: Heat Flow through Thick Insulation 90
Figure 5-9: Typical Measured Data 91
Figure 5-10: Normalized Data 91
Figure 5-11: EPS - R25.21 Single Layer Repeatability 93
Figure 5-12: EPS - R25.21 Two Layer Repeatability 93
Figure 5-13: EPS - Thermal Resistivity 94
Figure 5-14: Measured vs. Calculated Thermal Resistance for EPS R25.21 94
Figure 5-15: Measured vs. Calculated Resistance for EPS R30.21 Insulation 95
Figure 5-16: Strip Applied Adhesive 96
Figure 5-17: Spread Applied Adhesive 96
Figure 5-18: Effect of Adhesive on R-Value 96
Figure 5-19: Metering Chamber Temperature 98
Figure 5-20: Guard Chamber Temperature 99
Figure 5-21: Climatic Chamber Temperature 99
Figure 5-22: Bottom Specimen Temperature 100
Figure 5-23: Top Specimen Temperature 100
Figure 5-24: Typical GHB Temperature Time History 101
Figure 5-25: Typical GHB Heat Flow Time History 101
Figure 5-26: Calibration of GHB – Data Comparison with HFM and CTC 102
Figure 5-27: GHB Repeatability Test Data of Polyiso Opaque Assembly 103
Figure 5-28: Opaque vs. Fastener Assembly – Heat Flow Time History 104
Figure 5-29: EPS – Effect of Fasteners 105
Figure 5-30: ISO – Effect of Fasteners 106
Figure 5-31: Stone Wool – Effect of Fasteners 107
Figure 5-32: Fastener Density per m^2 vs. Effective R-Value 108

Figure 5-33: Percent Decrease in Thermal Resistance due to Fasteners 109
Figure 5-34: Opaque vs. Gap Assembly – Heat Flow Time History.. 110
Figure 5-35: Through Gap Results 111
Figure 5-36: Gap Test Configurations 111
Figure 5-37: Effect of Gap Type on the Effective Thermal Resistance 112
Figure 5-38: Top and Bottom Gap Results 113
Figure 5-39: Staggered Gap Results 114
Figure 5-40: Gap Adjustment Curve.. 115
Figure 6-1: Thermal Chamber 116
Figure 6-2: Calibrated Thermal Chamber – Polyiso R31 System – No Gaps 116
Figure 6-3: Calibrated Thermal Chamber – Polyiso R31 System – ½” Gaps 117
Figure 6-4: GHB Insulation Dimensions 117
Figure 6-5: GHB vs. CTC Dimensions... 118
Figure 6-6: CTC Insulation Dimensions... 118
Figure 6-7: Cross-Joint 120
Figure 6-8: CTC Cross-Joints 121
Figure 6-9: Calibrated Thermal Chamber – Polyiso R31 System - Fasteners........................... 121
Figure 6-10: GHB Tested Fastener Densities 122
Figure 6-11: Fastener Adjustment Curve.. 123
Figure 6-12: Gap Adjustment Curve.. 124
Figure B-1: Dimensional Stability: 2.5” Stone Wool Insulation 136
Figure B-2: Dimensional Stability: 4” Stone Wool Insulation 136
Figure B-3: Dimensional Stability: Stone Wool Summary 137
Figure B-4: Dimensional Stability: 2” Polyiso Insulation 137
Figure B-5: Dimensional Stability: 2.5” Polyiso Insulation 138
Figure B-6: Dimensional Stability: 3.3” Polyiso Insulation 138
Figure B-7: Dimensional Stability: Polyiso Summary 139
Figure C-1: Stone Wool – R25.21 Single Layer Repeatability 140
Figure C-2: Stone Wool – R25.21 Two Layer Repeatability 140
Figure C-3: Stone-Wool Thermal Resistivity 141
Figure C-4: Measured vs. Calculated Thermal Resistance for Stone Wool R25.21.................. 141
Figure C-5: Stone Wool – R30.21 Two Layer Repeatability 142
Figure C-6: Measured vs. Calculated Thermal Resistance for Stone Wool R30.21.................. 142
Figure C-7: Polyiso – R25.21 Single Layer Repeatability 143
Figure C-8: Polyiso – R25.21 Two Layer Repeatability 143
Figure C-9: Polyiso Thermal Resistivity 144
Figure C-10: Measured vs. Calculated Thermal Resistance for Polyiso R25.21....................... 144
Figure C-11: Measured vs. Calculated Thermal Resistance for Polyiso R30.21....................... 145

Glossary

Symbols

Symbol	Description	Units	
		Metric	Imperial
A	$Area\ of\ heat\ flow\ measurement$	m^2	ft^2
C	$Thermal\ conductance$	$\frac{W}{m^2 \cdot K}$	$\frac{Btu}{ft \cdot °F \cdot hr}$
E	$Heat\ flux\ transducer\ output$	V	-
h	$Heat\ transfer\ coefficient$	$\frac{W}{m^2 \cdot K}$	$\frac{Btu}{ft^2 \cdot °F \cdot hr}$
k	$Thermal\ conductivity$	$\frac{W}{m \cdot K}$	$\frac{Btu}{ft \cdot °F \cdot hr}$
q	$Heat\ flux\ (heat\ flow\ rate, Q, through\ area\ A)$	$\frac{W}{m^2}$	$\frac{Btu}{ft^2 \cdot h}$
Q	$Heat\ flow\ rate$	W	$\frac{Btu}{h}$
R	$Thermal\ resistance\ (Imperial)$	$\frac{m^2 \cdot K}{W}$	$\frac{ft^2 \cdot °F \cdot hr}{Btu}$
ΔT	$Temperature\ difference\ across\ specimen$	℃	℉
T_c	$Temperature\ of\ cold\ plate\ surface$	℃	℉
T_h	$Temperature\ of\ hot\ plate\ surface$	℃	℉
T_m	$Mean\ temperature, \frac{T_h + T_c}{2}$	℃	℉

Units

$A - Amps$

$V - Volts$

$W - Watts$

$m - meter$

℃ $- Celsius$

℉ $- Fahrenheit$

$°K - Kelvin$

Conversions

$°K = °C + 273.15°$

$°C = \frac{5}{9} \times (°F - 32°)$

$R - value = 5.67446 \times RSI$

Abbreviations

AARS Adhesive-Applied Roof System

ANSI American National Standards Institute

ASTM American Society for Testing and Materials

ASHRAE American Society of Heating, Refrigerating, and Air Conditioning Engineering

BUR Built-Up Roof

CTC Calibrated Thermal Chamber

EPS Expanded Polystyrene Insulation

GHB Guarded Hot Box

HFM Heat Flow Meter

ISO International Organization for Standardization

MARS Mechanically Attached Roof System

PARS Partially Adhered Roof System

PMR Protected Membrane Roof

Polyiso Polyisocyanurate Insulation

VIP Vacuum Insulated Panels

XPS Extruded Polystyrene Insulation

Terminology

Air Films	Air films are layers of air on both sides of a building envelope. These air films provide a slight additional insulation resistance that should be considered when calculating the effective thermal resistance.
Apparent R-Value	Test measured thermal resistance of a material.
Blowing Agent	A blowing agent is a chemical applied to a cellular plastic at the liquid stage resulting in a chemical reaction which increases the stiffness of the material and fills the porous foam with gas. This is the method through which many types of insulations are formed.
Building Envelope	The physical barrier between the interior and exterior of the building.
Composite Assembly	An assembly made of separate parts.
Conduction	The transfer of energy through mater from particle to particle (by touch).
Convection	The transfer of thermal energy through movement.
Delta Temperature	Temperature difference across a material or assembly.
Dimensional Stability	The degree to which a material maintains its original dimensions when subjected to changes in temperature and humidity.
Effective R-Value	Test measured thermal resistance of an assembly (steel deck, insulation, cover board, membrane etc.).
Heat Flux	The rate of heat flow per unit area.
Low-Slope Roof	A roof with a height to length slope less than 1:12 (or 1 degree).

Mean Temperature	The average temperature of the top and bottom of the insulation sample.
Opaque Component	Insulation board without any gaps or fasteners.
Radiation	The transfer of energy through space like waves (solar radiation).
Rigid Cellular Plastics	Foam structures that have hardened. Most types of insulation are produced from foam, in order to turn the foam into a solid structure; a hardening phase is undergone through the use of blowing agents.
Steady-State Condition	A point of equilibrium or of unchanging condition.
Temperature Gradient	The physical quantity that describes the direction and rate of temperature change.
Thermal Bridge	A thermal bridge is a discontinuity in any thermal barrier allowing an easy path of lesser resistance through the insulation.
Thermal Conductance	The ability for a material to transfer heat through a cross-sectional area.
Thermal Conductivity	The ability of a material to transfer heat through a thickness.
Thermal Resistance	The ability of a material to resist heat flow through a cross-sectional area (the inverse of thermal conductance).
Thermal Resistivity	The ability of a material to resist heat through a thickness.
Thermal Transmittance	Also known as U-value, the rate of heat transfer through one square meter of material divided by the delta temperature across the material.

Chapter 1: Introduction

1.1. Background

The roof is a critical part of the building's envelope and the first line of protection against all hazards such as rain, wind and snow. A typical low-slope roof assembly consists of the following components: structural steel deck, insulation, cover board, membrane and fasteners. Properly designed roof systems contribute to the energy efficiency of the building - although even perfectly installed systems will experience heat loss through the assembly. The factors that affect the thermal performance of roofing assemblies are: the thermal conductivity of the insulation, thermal breaks due to fasteners and gaps, airflow and moisture migration. Heat flow through building enclosures is significantly different than heat flow through materials during testing. Building assemblies are three-dimensional and may contain conductive components such as the steel deck and metal fasteners. Airflow in the assembly will also affect the thermal performance of the enclosure by transporting a significant amount of heat and moisture. Thermal bridges are discontinuities in any thermal barrier allowing an easy path of lesser resistance through the insulation, by which, permitting more heat to bypass the thermal barrier. A thermal bridge is more prominent when the material creating the bridge is highly conductive. Similarly, a thermal break (or thermal barrier) is a material of low thermal conductivity used in an assembly to reduce the heat flow between mediums. The heat is transferred by the three mechanisms: conduction, convection, and radiation.

Improper installation of insulation boards can lead gaps between the adjacent boards, which combined with the dimensional instability of the boards due to temperature variation, can result in a compounding effect on the gap size. Other possible gaps can be caused by penetration of fasteners. It is common for damaged roofs to be reroofed or re-covered, where reroofing is the processes of replacing an existing roof cover, while re-covering is the installation of an additional roof cover over an existing one in order to repair any damaged substrate. The reroofing method of repairing a roof system leaves holes in the assembly as a result of the previously installed fasteners, while re-covering leaves existing fasteners in place while additional fasteners are installed to secure the new cover (Gulati, Suddapalli, and Srinivasan 2016). Both options leave the roofing system more susceptible to thermal losses, as both holes in the substrate and larger fastener density lead to thermal bridging and therefore greater thermal losses. A study conducted by Lewis (1979) was done with the purpose of evaluating the effects of gaps on heat loss. It was previously believed that the percent heat loss was equal to the percent gap. Therefore, a one percent gap area would lead to a one percent increase in heat loss. However, this significantly underestimates the effect of the gap area as it was found that a one percent gap will lead to a thermal transmittance of 3 to 9%, depending on the insulation dimensions. Similar studies done by Burch (1987), Wieland (1988) and Hedlin (1985) have shown the significance of thermal bridging; these studies, however, had many limitations and cannot be generalized or applied to the current energy design of roofs.

Current energy codes such as the National Energy Code for Buildings (NECB) and ASHRAE 90.1 (American Society of Heating, Refrigerating, and Air Conditioning Engineering) provide prescriptive requirements for the energy design of buildings. In the energy design of roofs, these requirements emphasis a thermal resistance of insulation and disregard the effect of thermal impact factors such as fasteners and gaps. At this time, no adequate studies exist analyzing and accounting for the thermal losses of roofing systems due to thermal impact factors. With many concerns, including the rising cost of energy and climate change, it has led to the continued increase in requirements for energy efficiency in many new and existing buildings. Building codes are improving and require higher levels of thermal control than ever before.

1.2. Thesis Objective

The purpose of this research is to quantify the magnitude of thermal breaks induced by fasteners and gaps between insulation boards in roofing assemblies through experimental testing. To account for these thermal breaks, appropriate adjustment factors will be developed. With codification as the final objective, efforts will be made to potentially implement these adjustment factors in the energy codes to update the current energy design of roofs. These factors will allow the designers to design the roofs properly and accurately, so that the actual energy performance of the roofing assembly can be established. When combined in the Canadian climatic context, this can lead to optimized roofing energy designs, realistic prediction of commercial building energy savings, and maintaining an energy efficient Canadian built environment. These adjustment factors will be universally applicable regardless of roof type, component or configuration.

1.3. Thesis Scope

This research is done in collaboration with the National Research Council of Canada as part of the Energy Resistance of Commercial Roofs (ERCR) project. The research project aims to develop scientifically supported performance data on energy resistance of roofing systems that are constructed according to field practices. The key objectives of the project are:

1. Quantification of the influencing parameters on the thermal performance of the roofing system; and,
2. Development of test methodology to evaluate roof energy resistance.

A work plan has been established by the ERCR consortium as shown in Figure 1-1. For task 1, a test matrix is established (Figure 1-2) for testing 36 different roof systems designed according to NECB and ASHRAE climatic zones 2-7. These roof systems are categorized as: category 1 (zone 2-3): R26; category 2 (zone 4, 5, and 6): R31; and category 3 (zone 7 and 8): R36. The scope of this thesis is focused on quantifying the magnitude of thermal impact factors by conducting experimental testing on R26 and R31 designed roof assemblies. Each category has three types of insulations, three fastener densities and six gap configurations. A total of 84 tests are conducted to quantify the thermal impact factors and develop associated adjustment factors.

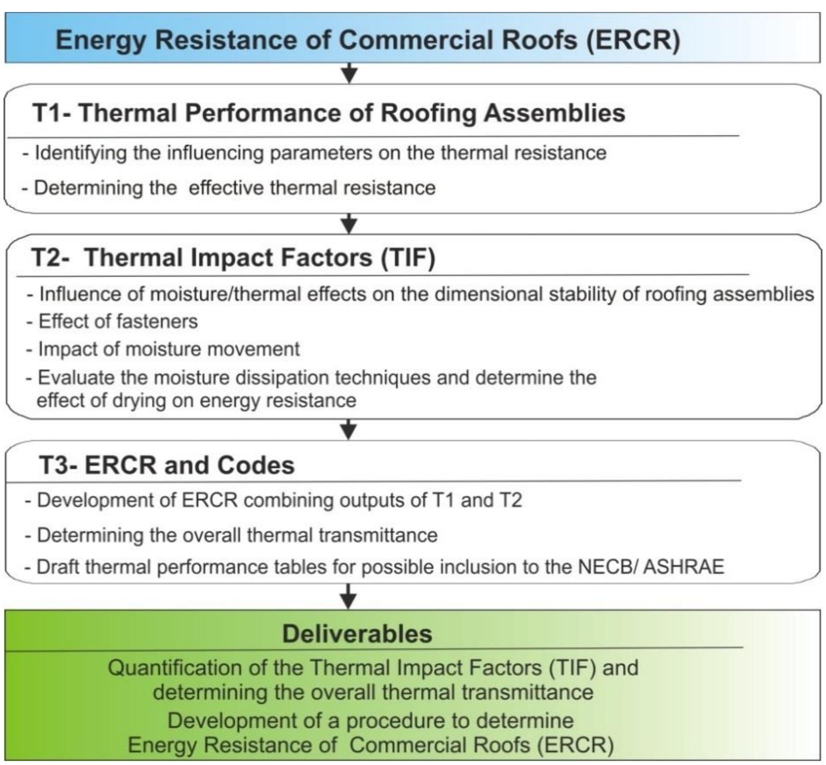

Figure 1-1: Work Plan Developed by the ERCR Consortium

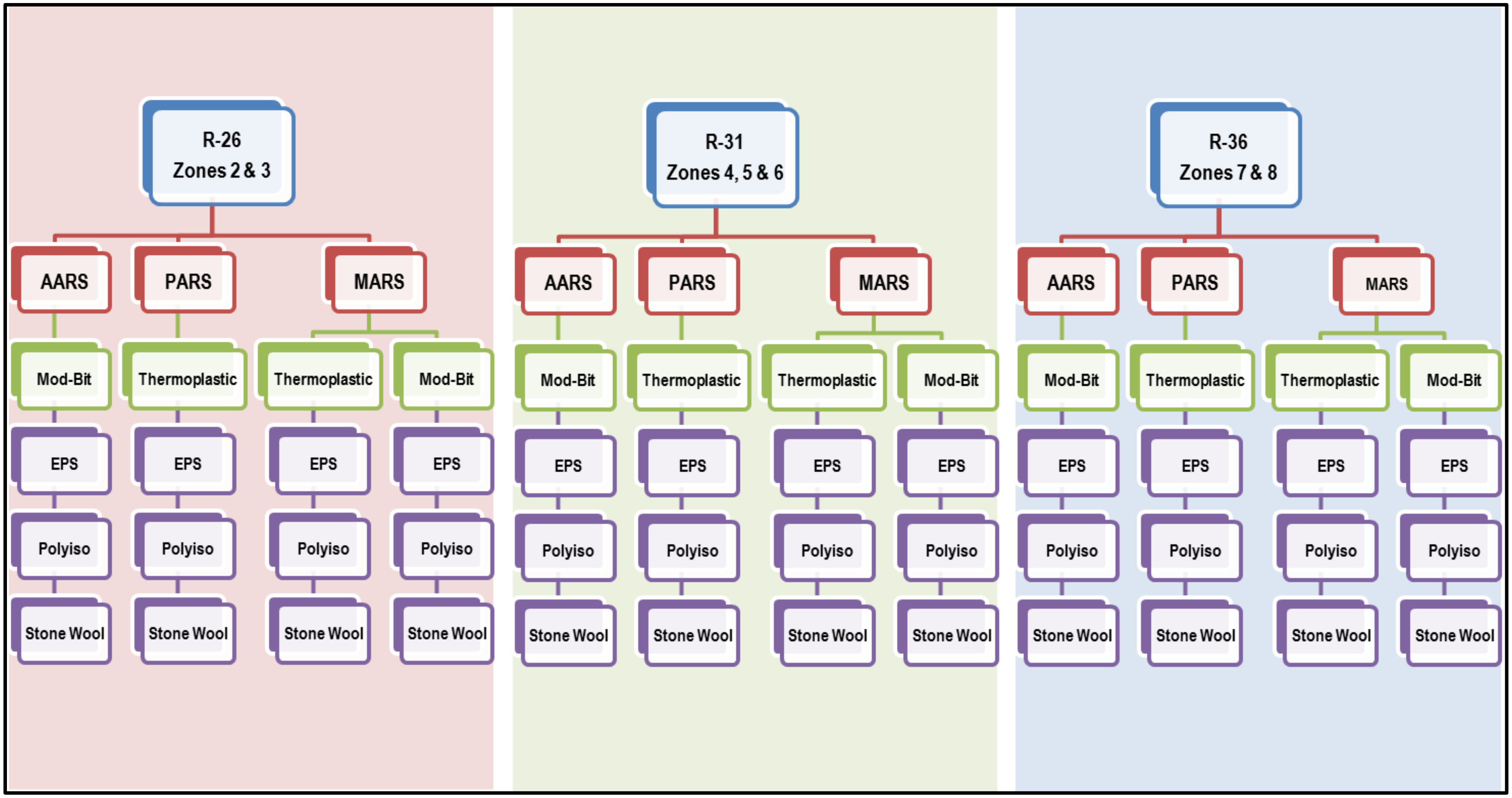

Figure 1-2: Test Matrix Developed by the ERCR Consortium

1.4. Thesis Outline

Chapter 1: Introduction

This chapter provides a brief overview of concepts, scope and objective of this thesis.

Chapter 2: Energy Design of Roofs

This chapter introduces and explains the concepts of low-slope roofing and thermal fundamentals which are the bases for the research. The reader will build an understanding of thermal properties, basic heat flow calculations and thermal impact factors.

Chapter 3: Literature Review

This chapter provides an overview of the most important literature related to the thermal transfer of roof assemblies and the associated effects of thermal impact factors. The goal of this chapter is to introduce the reader to current progress in the field and provide an understanding of the methodologies and experimental approaches.

Chapter 4: Experimental Methodology

This chapter illustrates the experimental methodology used to test and evaluate the thermal performance of roofing components and assemblies, and the associated thermal breaks.

Chapter 5: Experimental Results and Analysis

This chapter summarizes the results from all thermal testing on individual components and assemblies, providing adjustment curves for the thermal impact factors.

Chapter 6: Validation and Codification

This chapter validates and adjustment curves through large scale testing and proposes the codification of the adjustment factors for the energy codes.

Chapter 7: Concluding Remarks

This chapter summarizes the experimental results and the magnitude of the thermal impact factors, and it provides closing remarks and future work.

Chapter 2: Energy Design of Roofs

The following chapter introduces the reader to the most common types of roof assemblies and their typical roofing components. The reader is then given an overview of the fundamental thermal concepts used throughout the thesis.

2.1. Roofing Systems and Components

A roof can be classified in two categories: as a low-slope or steep slope roof. The slope of the roof determines its classification; if the roof's slope is less 14 degrees it is a low-slope roof, and if it is greater than 14 degrees it is a steep slope roof. A low-slope roof is commonly found on commercial and industrial buildings, while steep slope roofs are used for residential houses. A successful roof will perform the following tasks:

- Provide a thermal control system to keep the heat out during the summer and retain heat during the winter;
- Provide a vapour control system that does not allow condensation;
- Provide an air barrier between the inside and outside; and,
- Provide a water management system to keep precipitation out.

A conventional roofing assembly is composed of: a deck, vapour barrier, insulation, protection board, and membrane as shown in Figure 2-1. Each component aids in the performance of a successful roof. The deck is the structural substrate for supporting the roof assembly; the vapour barrier for minimizing moisture intrusion; insulation is the thermal barrier; protection board, as the name suggests, protects the insulation from damage; and lastly, the roofing membrane is the barrier against water entry. The installation of vapour barrier is mandatory in Canada but not in the United States. Protection boards are not mandatory in the design of the roof assembly, but are becoming common practice due to roof add-ons such as photovoltaics (solar panels) and green roofs.

Roofing systems are categorized based on their attachment methods. The roof attachment method is how the roof is secured, and therefore able to resist wind uplift forces. Based on the attachment roofs can be classified as: Built-up roofs (BUR), mechanically attached roofs (MARS), partially adhered roofs (PARS), adhesive attached roofs (AARS), ballasted roofs and protected membrane roofs.

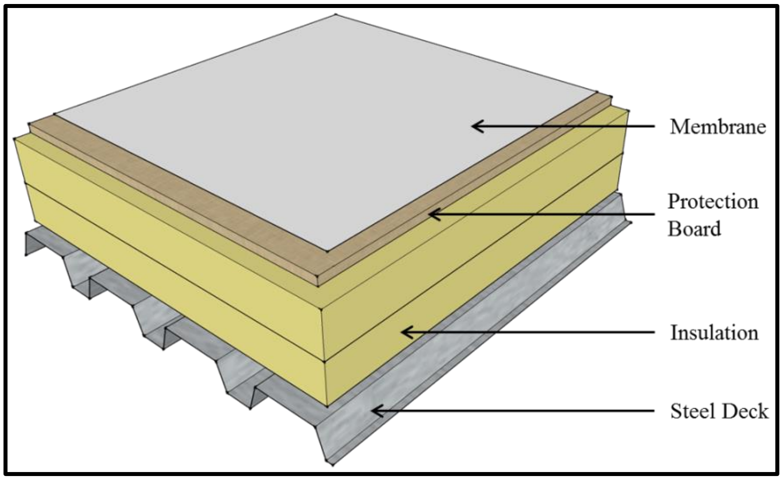

Figure 2-1: Conventional Roof Assembly

2.1.1. Built-Up Roofs (BUR)

A built-up roof was one of the most popular low-slope roof assemblies (Figure 2-2). These are composed of alternating layers of bitumen and reinforcing fabrics typically adhered to each other with hot asphalt that creates a waterproofing membrane. The popularity of these assemblies has declined due to odour issues, intensive labour and material quality. With the advancement in technology, new roofing assemblies have replaced the BUR, and each has benefits and downfalls.

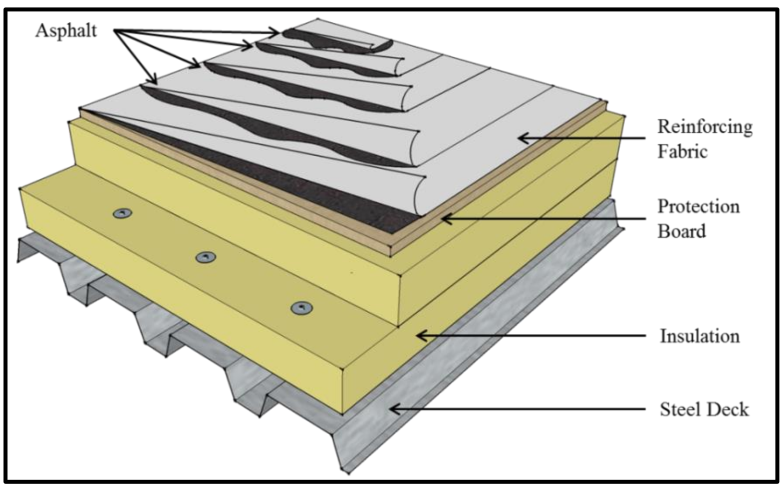

Figure 2-2: Built-Up Roofing System

2.1.2. Mechanically Attached Roofing System (MARS)

When roof components are attached using fasteners to form an assembly, it is classified as a mechanically attached roofing system (MARS). This system includes a membrane, protection board and insulation which are mechanically fastened to the steel deck (Figure 2-3). MARS are by far the most common roof systems due to rapid and low cost of installation, with a well-established wind uplift performance. The disadvantage in thermal resistance of this system is that it uses fasteners, which are thermal bridges and allow thermal energy to bypass the insulation. One layer of fasteners secures the insulation and protection board to the steel deck and second layer of fasteners are used to secure the membrane.

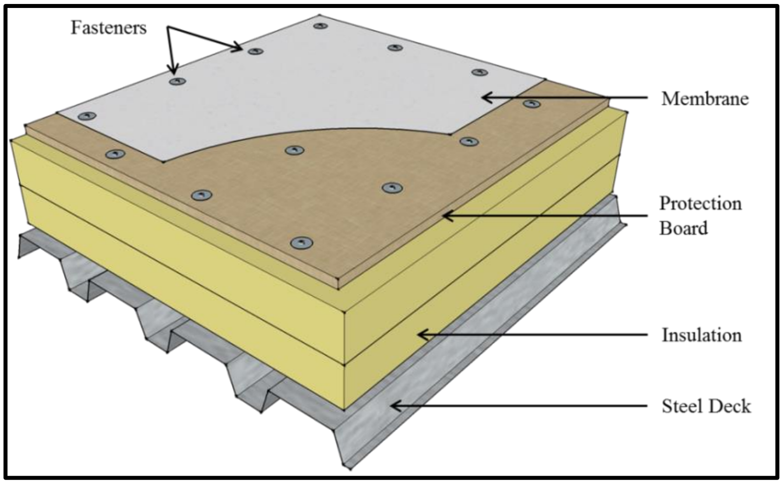

Figure 2-3: Mechanically-Attached Roofing System

2.1.3. Partially Adhered Roofing System (PARS)

Partially adhered roof systems (PARS) are a sub-category of mechanically attached roof systems; this system also uses fasteners to secure the insulation and protection board to the steel deck, except the membrane is adhered (Figure 2-4). This system therefore has a lower number of fasteners resulting in less thermal bridging; however, it is labour intensive due to the application of the adhesive.

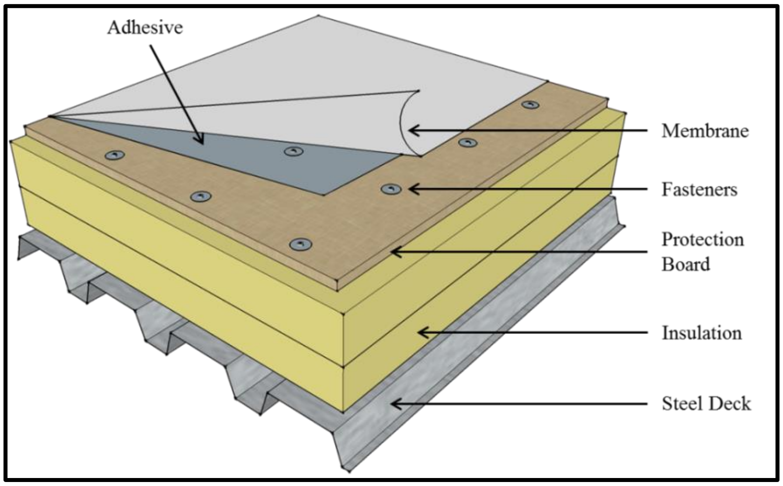

Figure 2-4: Partially Adhered Roofing System

2.1.4. Adhesive Attached Roofing System (AARS)

Adhesive attached roofing systems (AARS) are gaining popularity for low-slope application due to the absence of fasteners. AARS systems do not use fasteners for component attachment but rather integrate them by adhesives (Figure 2-5). Without the use of fasteners AARS offers the advantage of reduction in moisture migration, air leakage and thermal bridging. However, these systems have low wind-uplift performance; the installation is temperature dependant because of the adhesive.

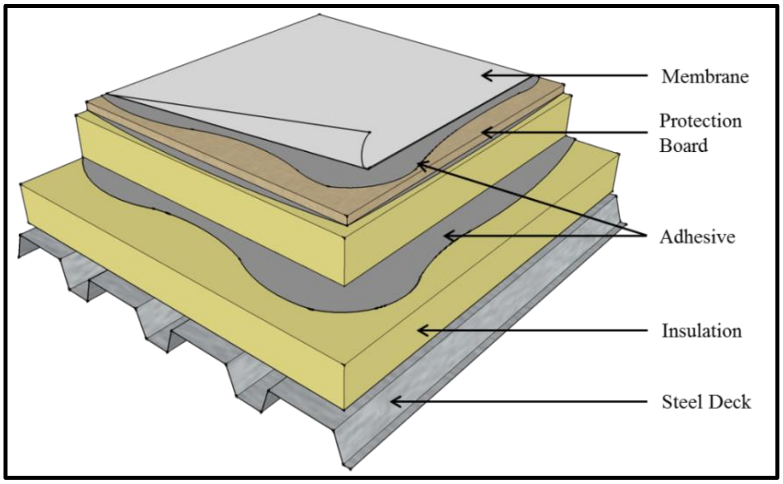

Figure 2-5: Adhesive Attached Roofing System

2.1.5. Ballasted Roof System

A conventional ballasted roof system consists of membrane, substrate and vapour barrier all loose-laid over a deck using a ballast to hold the assembly in place (Figure 2-6). Ballast is a heavy material such as sand, gravel or course stone; ballast stones must be well rounded to not puncture or damage the membrane. The advantage to this system is that it is compatible with most roof insulation materials and it does not incorporate thermal breaks through the use of fasteners. The disadvantages of this system are the low availability and difficulty finding well rounded stone or gravel ballasts; and, the membranes exposure to the ballast may lead to damage such as tearing. Furthermore, the gravel can move, exposing the membrane resulting in low assembly wind-uplift performance. Wind may also lift the ballast and cause it to hit adjacent buildings.

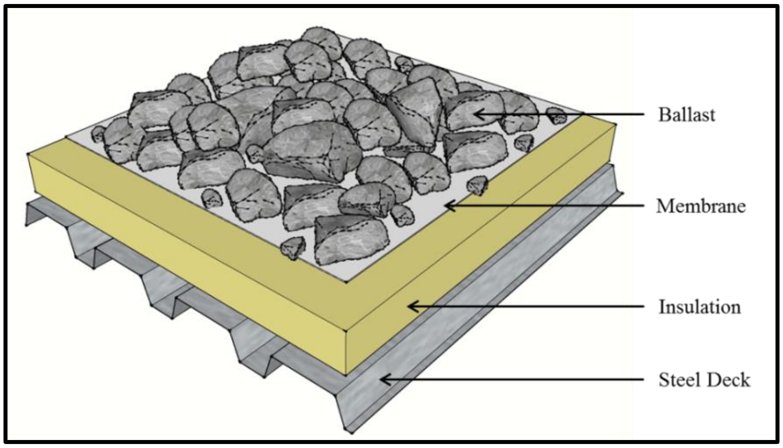

Figure 2-6: Ballasted Roof System

2.1.6. Protected Membrane Roof (PMR)

A protected membrane roof system is similar to a conventional roof system except the membrane is placed below the insulation. Placing the membrane below the insulation protects it against accelerated oxidation, evaporation of volatile oils, ultraviolet degradation and thermal movement (Figure 2-7). Virtually all roof membrane systems may be used in a protected configuration and the advantage is that the membrane serves as a vapour retarder, eliminating the need for an additional vapour barrier. The disadvantage is that the insulation is exposed to the environmental conditions leading to moisture accumulation and decrease in thermal performance.

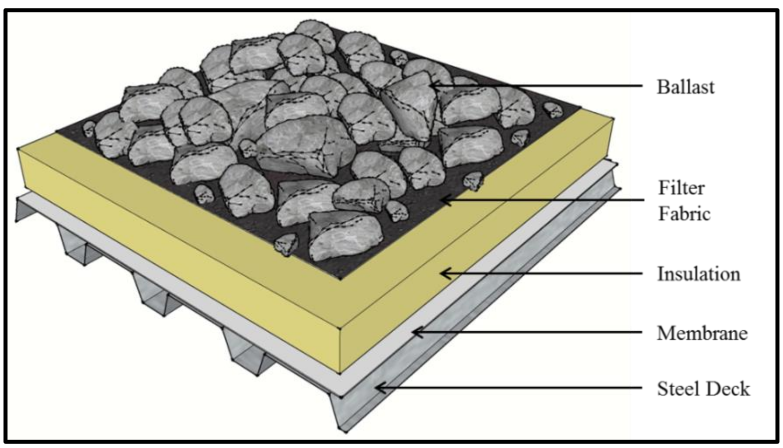

Figure 2-7: Protected Membrane Roof

2.2. Thermal Fundamentals

Thermal resistance is the ability of a material to resist heat flow; this is categorized by an R-value. The R-value is an effective, well-established and widely accepted metric for describing the thermal performance of an insulating material. The greater the capacity an insulating material has to resist heat flow, the higher the R-value rating it is assigned. While an R-value is used to describe the efficiency of an insulating material (just the component of the roof assembly), the thermal transmittance (U-value) is used to describe the overall assembly. Therefore, a high R-value for a system's component alone may not insure the overall system will perform effectively, but rather, the U-value is crucial for defining the thermal efficiency of the assembly as a whole.

2.2.1. Fundamentals of Heat Transfer

Understanding heat transfer and temperature distribution through building materials and assemblies is important for assessing energy use, thermal movement and moisture problems. Heat flow can vary with time or be a steady-state process, meaning that the thermal flow does not vary with time. Typically, assuming steady-state conditions is sufficient to provide accurate predictions for thermal calculations. Heat flow can occur in one, two or three dimensions; in real situations heat flow occurs in three dimensions, though it is acceptable to consider heat flow in one-dimension for simplicity. Heat always flows from hot to cold, and energy efficiency is the ability to slow down the rate of heat transfer. There are three primary mechanisms of heat transfer:

- Conduction: this is the transfer of heat from particle to particle by touch.
- Convection: this is the transfer of thermal energy through movement. Since air density changes with temperature, hot air rises and cold air falls, creating convective heat transfer. In roof assemblies however, the movement of air is a result of air pressure differences due to wind or climatic changes.
- Radiation: this is the transfer of heat from one body to another through space by electromagnetic waves or particles.

An illustration of these principles is shown in Figure 2-8.

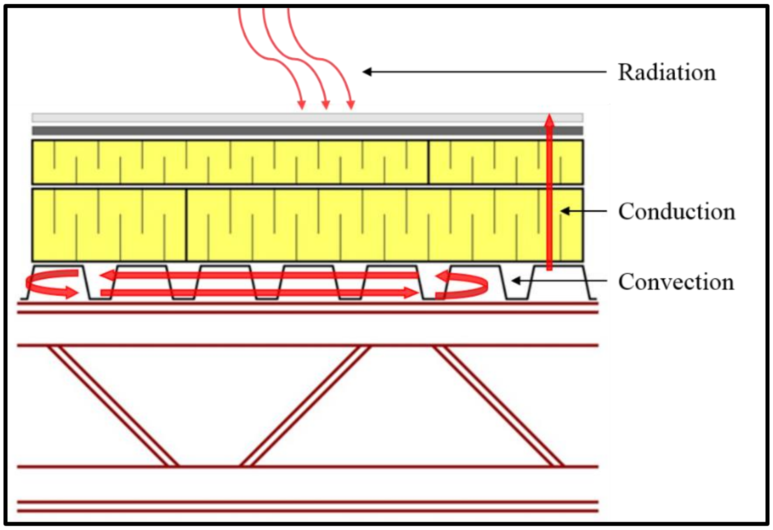

Figure 2-8: Mechanisms of Heat Flow

Since conduction is a major mode of heat transfer and air is a low-cost insulator, insulating materials tend to be high in porosity with large voids. Most materials with high strength have high densities, such as concrete, steel, and wood - in turn they have a reduced capacity for insulation. There is an inverse relationship between the strength of a material and its thermal resistance as highlighted by Straube (2006) in Figure 2-9. Therefore, high-density materials are used for load-bearing functions and low-density materials are used for insulating purposes.

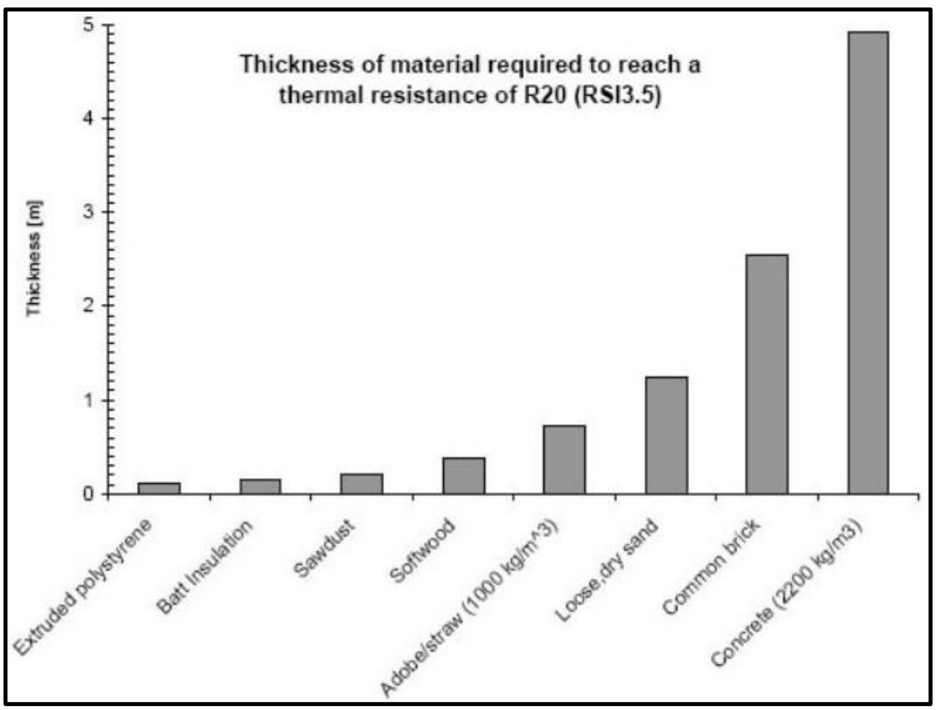

Figure 2-9: Thickness Required to Reach the Equivalent Resistance (retrieved from Straube, 2006)

Important Terms and Factors:

Thermal Conductance (C-Factor): The coefficient of heat transfer through a building component or assembly. This is the measure of heat transfer through a material's entire thickness.

Thermal Conductivity (k-Factor): The coefficient of heat transfer through a building component or assembly. This is the measure of heat transfer through a unit thickness.

Thermal Resistance (R-Value): The measure of resistance to heat flow through a materials entire thickness - calculated by taking the reciprocal of the thermal conductance (Eqn. 2-1).

$$R = \frac{1}{C} \quad \textbf{(Eqn. 2-1)}$$

Thermal Resistivity: The resistance to heat flow through a unit thickness.

Thermal Transmittance (U-Factor): The coefficient of heat transmission; this is the rate of heat transfer through an assembly.

Note: "- ivity" vs. "- ance"

- Conductance/ resistance refer to a material's actual thickness.
- Conductivity/ resistivity refer to a unit thickness.

Apparent R-value: Test measured thermal resistance of a material.

Effective R-value: Test measured thermal resistance of an assembly (steel deck, insulation, cover board, membrane and air films or surface coefficients).

In a building envelope the roof to wall ratio varies depending on the building type, leading people to believe that the roof is not a high priority in the energy efficiency of the envelope. In reality, the roof is the most critical part of a building's envelope with regards to the building thermal efficiency. Roofs are exposed to the sun all day, absorbing heat that is then transferred to the building interior. Similarly, the roof cools overnight and transfers heat from inside the building to the outside. The three most important metrics for energy efficiency in roofing are: reflectivity, emissivity and thermal conductance (Straube, 2006).

Reflectivity is the ability of a surface to reflect (rather than absorb) solar radiation. Dark materials absorb more heat than light ones; similarly, shiny materials reflect more than dull ones.

Emissivity is the ability of a material to release what has been absorbed. If a material has a low emissivity, any insulation or assembly underneath will get hot. Conversely, in very cold climates where heating exceeds cooling, materials with low reflectivity and emissivity would be desired. Therefore, the combination of reflectivity and emissivity are very important for the energy efficiency of the roof envelope.

Another factor that greatly influences energy efficiency is heat capacity. Building materials with heavy, high thermal-masses (like concrete) store heat and radiate it towards the cooler. This is known as the "mass-effect" and is directly affected by the density and thickness of a material. To account for both the radiative and convective heat transfer modes at the exterior and interior surfaces of roofing assemblies, the radiative and convective heat transfer coefficients are used in the form of an *equivalent conductance* or *resistance*. These equivalent coefficients are called surface film coefficients (or air films) and are applied so their effects can be accounted for in heat flow analysis. It is important to note that the resistance to heat flow at a surface is small relative to the resistance to heat flow through an insulator.

The range of temperatures that can occur within a building envelope must be known before it can be properly designed. The building code requires that the assembly has to meet certain minimum R-value requirements to achieve a specific level of efficiency. Climate zones have a large role in determining the type of insulating material and thickness that must be used in order to achieve the minimum R-value for each specific region (Building Science Corporation, 2013). The ASHRAE standard provides a climate zone map for the range of acceptable R-values in each region of North America, as seen in Figure 2-10. Figure 2-11 summarizes the Canadian zones.

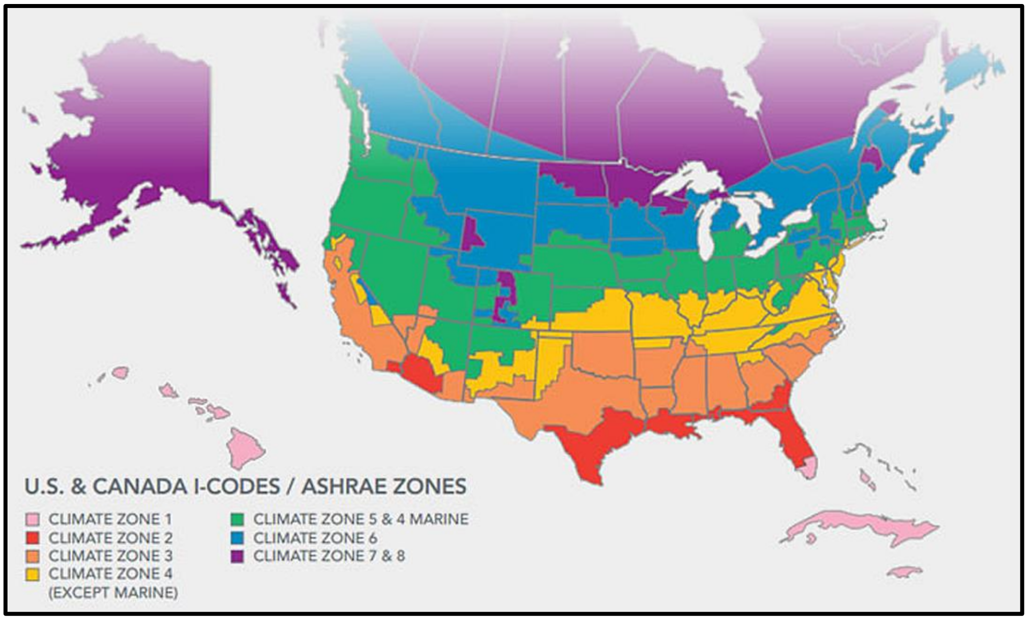

Figure 2-10: ASHRAE: U.S. and Canada Climate Zone Map (retrieved from Green Building Advisor, 2015)

TABLE B1-2 Canadian Climatic Zones

Province City	Zone	Province City	Zone	Province City	Zone	Province City	Zone
Alberta (AB)		(Manitoba cont.)		**Ontario (ON)**		**(Québec cont.)**	
Calgary International A	7	Winnipeg International A	7	Belleville	6	Granby	6
Edmonton International A	7	**New Brunswick (NB)**		Cornwall	6	Montreal Dorval International A	6
Grande Prairie A	7	Chatham A	7	Hamilton RBG	5	Québec City A	7
Jasper	7	Fredericton A	6	Kapuskasing A	7	Rimouski	7
Lethbridge A	6	Moncton A	6	Kenora A	7	Septles A	7
Medicine Hat A	6	Saint John A	6	Kingston A	6	Shawinigan	7
Red Deer A	7	**Newfoundland (NF)**		London A	6	Sherbrooke A	7
British Columbia (BC)		Comer Brook	6	North Bay A	7	St Jean de Cherbourg	7
Dawson Creek A	7	Gander International A	7	Oshawa WPCP	6	St Jerome	7
Fort Nelson A	8	Goose A	7	Ottawa International A	6	Thetford Mines	7
Kamloops	5	St John's A	6	Owen Sound MOE	6	Trois Rivieres	7
Nanaimo A	5	Stephenville A	6	Peterborough	6	Val d'Or A	7
New Westminster BC Pen	5	**Northwest Territories (NW)**		St Catharines	5	Valleyfield	6
Penticton A	5	Fort Smith A	8	Sudbury A	7	**Saskatchewan (SK)**	
Prince George	7	Inuvik A	8	Thunder Bay A	7	Estevan A	7
Prince Rupert A	6	Yellowknife A	8	Timmins A	7	Moose Jaw A	7
Vancouver International A	5	**Nova Scotia (NS)**		Toronto Downsview A	6	North Battleford A	7
Victoria Gonzales Hts	5	Halifax International A	6	Windsor A	5	Prince Albert A	7
Manitoba (MB)		Kentville CDA	6	**Prince Edward Island (PE)**		Regina A	7
Brandon CDA	7	Sydney A	6	Charlottetown A	6	Saskatoon A	7
Churchill A	8	Truro	6	Summerside A	6	Swift Current A	7
Dauphin A	7	Yarmouth A	6	**Québec (PQ)**		Yorkton A	7
Flin Flon	7	**Nunavut**		Bagotville A	7	**Yukon Territory (YT)**	
Portage La Prairie A	7	Resolute A	8	Drummondville	6	Whitehorse A	8
The Pas A	7						

Figure 2-11: Canadian Climatic Zones (retrieved from ASHRAE 90.1 pg.182, 2013)

In Canada, the National Energy Code for Buildings provides the minimum design energy specifications for the six climatic zones shown Figure 2-12; similarly, ASHRAE provides the minimum thermal design specifications for the eight North American climatic zones shown in Figure 2-13. Table 2-1 and Table 2-2 summarize all of the NECB and ASHRAE climatic zones minimum thermal resistance requirements.

Table 3.2.2.2.
Overall Thermal Transmittance of Above-ground Opaque Building Assemblies
Forming Part of Sentences 3.2.2.2.(1) and (2)

Above-ground *Opaque Building Assembly*	Heating Degree-Days of *Building* Location,(1) in Celsius Degree-Days					
	Zone 4:(2) < 3000	Zone 5:(2) 3000 to 3999	Zone 6:(2) 4000 to 4999	Zone 7A:(2) 5000 to 5999	Zone 7B:(2) 6000 to 6999	Zone 8:(2) ≥ 7000
	Maximum *Overall Thermal Transmittance*, in W/(m²·K)					
Walls	0.315	0.278	0.247	0.210	0.210	0.183
Roofs	0.227	0.183	0.183	0.162	0.162	0.142
Floors	0.227	0.183	0.183	0.162	0.162	0.142

Figure 2-12: Building Envelope Requirements (retrieved from NECB Division B pg.3-5, 2015)

Table 5.5-6 Building Envelope Requirements for Climate Zone 6 (A,B)*

Opaque Elements	Nonresidential		Residential		Semiheated	
	Assembly Maximum	Insulation Min. R-Value	Assembly Maximum	Insulation Min. R-Value	Assembly Maximum	Insulation Min. R-Value
Roofs						
Insulation Entirely above Deck	U-0.184	R-5.3 c.i.	U-0.184	R-5.3 c.i.	U-0.360	R-2.6 c.i.
Metal Building[a]	U-0.175	R-4.4 + R-1.9 Ls	U-0.163	R-5.3 + R-1.9 Ls	U-0.341	R-3.3 + R-3.3
Attic and Other	U-0.119	R-8.6	U-0.119	R-8.6	U-0.192	R-5.3

Figure 2-13: Building Envelope Requirements for Zone 6 (retrieved from ASHRAE 90.1 pg.27, 2013)

Table 2-1: Summary of all NECB Zone Thermal Requirements

NECB Zones	Roof Assembly Minimum Effective R-Value	
	Metric $(m^2 \cdot °K/W)$	Imperial $(ft^2 \cdot °F \cdot hr/Btu)$
4	R-4.4	R-25
5	R-5.5	R-31
6	R-6.2	R-35
7A & 7B	R-6.2	R-35
8	R-7.1	R-40

Note: the conversion from metric to imperial units for R-value is 5.67446.

Table 2-2: Summary of all ASHRAE Zone Thermal Requirements

ASHRAE Zones	Roof Assembly Minimum Effective R-Value Metric ($m^2 \cdot °K/W$)	Imperial ($ft^2 \cdot °F \cdot hr/Btu$)
1	R-3.5	R-20
2 & 3	R-4.4	R-25
4 & 5 & 6	R-5.3	R-30
7 & 8	R-6.2	R-35

Note: the conversion from metric to imperial units for R-value is 5.67446.

2.2.2. Fundamental Calculations of Heat Transfer

Thermal conductivity is the basis for most heat flow calculation methods in the building industry. One-dimensional steady-state conductive heat flow through a homogeneous material can be described using Fourier's Law (Eqn. 2-2), where the heat flow, Q, is dependent on the material's dimensions (cross-section, A and thickness, t), the temperature difference across the material, ΔT, and the material's specific conductivity (K-factor).

$$Q = \frac{k \cdot A \cdot \Delta T}{t} \quad \textbf{(Eqn. 2-2)}$$

or

$$k = \frac{Q \cdot t}{A \cdot \Delta T} \quad \textbf{(Eqn. 2-3)}$$

Calculating a materials conductivity using Fourier's Law is then used to calculate the conductance of the material by dividing the conductivity by the thickness (Eqn. 2-4).

$$C = \frac{k}{t} \quad \textbf{(Eqn. 2-4)}$$

The measure of resistance to heat flow, a material's R-value, is calculated by taking the reciprocal of the thermal conductance (Eqn. 2-5). Calculating the assembly's overall thermal transmittance, the U-value, is the addition of all component R-values in the assembly (Eqn. 2-6) and taking the reciprocal (Eqn. 2-7).

$$R = \frac{1}{C} \quad \textbf{(Eqn. 2-5)}$$

and

$$R_T = R_{si} + R_1 + R_2 + \cdots R_n + R_{se} \quad \textbf{(Eqn. 2-6)}$$

where

$$U = \frac{1}{R_T} \quad \textbf{(Eqn. 2-7)}$$

2.3. Thermal Transmittance of a Roof Assembly - Design Example

The following design example, in Figure 2-14, is retrieved from the National Energy Code of Canada (NECB-2014). The purpose of this example is to introduce the reader to the current national regulations and requirements for the design of roofing assemblies. The assembly in the example is a simple built-up roof in NECB zone 5. The respective thermal resistance of each component in the assembly is listed and considered in the design of the roof. By adding the individual thermal resistance of the different components, including the surface film coefficients, the effective design value is determined to be $5.45\, m^2 \cdot K/W$. In order to meet the design requirements, insulation with a thermal resistance of $4.85\, m^2 \cdot K/W$ is required.

Example 3-2 – Roof: Flat Roof (4-ply built-up roofing (BUR) and steel deck)

Figure A shows a roofing assembly with 4-ply BUR and a steel deck.

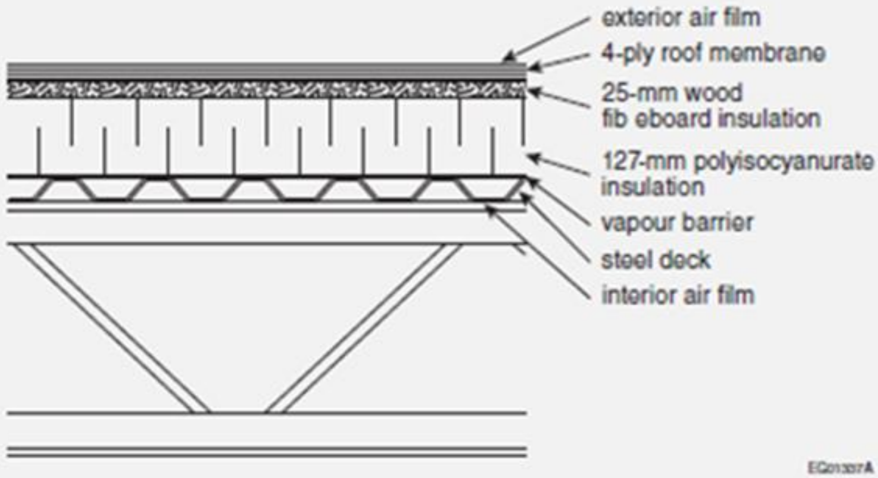

Assembly Components	RSI, $(m^2 \cdot K)/W$
Exterior air film	0.03
4-ply roof membrane (built-up roofing, 10 mm)	0.06
25-mm wood fibreboard insulation (insulating fibreboard)	0.40
127-mm polyisocyanurate insulation	4.85
Vapour barrier	0.00
Steel deck	0.00
Interior air film	0.11
RSI_T	5.45
$U_T = 1/RSI_T$	0.183

Figure 2-14: NECB Design Example (retrieved from NECB pg.6, 2014)

Since the roof assembly is designed with polyiso insulation, the thickness required to reach the desired thermal resistance is 127 mm (or 5”) as shown in Figure 2-15. If the designer used XPS insulation, a thickness between 127 mm and 152 mm would be required to meet the same resistance. Through interpolation, it is calculated that 138.5 mm (or 5.45”) of XPS would achieve the same resistance. This is the current procedure for designing a roof assembly; the values used in the design are all under ideal conditions found through laboratory testing. The effects of mean operating temperatures of the roofs and thermal impact factors are not considered in the design process. These thermal impact factors have significant implications and must be considered in the energy codes.

Table 3-5
Thermal Resistance Values of Common Insulation Materials: Insulation Boards, Slabs and Sheathing

Insulation Materials	RSI/mm	RSI Values for Thickness of Insulation Board, Slab and Sheathing Materials											
		Material Thickness, mm											
		13	16	19	25	38	51	64	76	89	101	127	152
Expanded polystyrene (EPS)													
Type 1	0.026	0.34	0.42	0.49	0.65	0.99	1.33	1.66	1.98	2.31	2.63	3.30	3.95
Type 2	0.028	0.36	0.45	0.53	0.71	1.06	1.43	1.79	2.13	2.49	2.83	3.56	4.26
Type 3	0.030	0.39	0.48	0.57	0.76	1.14	1.53	1.92	2.28	2.67	3.03	3.81	4.56
Extruded polystyrene (XPS), Types 2, 3, 4	0.035	0.46	0.56	0.67	0.88	1.33	1.79	2.24	2.66	3.12	3.54	4.45	5.32
Semi-rigid mineral fibre(1)	0.0298	0.39	0.48	0.57	0.75	1.13	1.52	1.91	2.26	2.65	3.01	3.78	4.53
Insulating fibreboard	0.016	0.21	0.26	0.30	0.40	0.61	0.82	1.02	1.22	1.42	1.62	2.03	2.43
Polyisocyanurate/polyurethane – permeably faced, Types 1, 2, 3	0.03818	0.50	0.61	0.73	0.97	1.45	1.90	2.44	2.90	3.40	3.86	4.85	5.80
Polyisocyanurate/polyurethane – impermeably faced, Types 1, 2, 3	0.03937	0.51	0.63	0.75	0.98	1.50	2.00	2.52	2.99	3.50	3.98	5.00	5.98
Gypsum sheathing	0.0063	0.082	0.101	0.120	0.158	0.239	0.321	0.403	0.479	0.561	0.636	0.800	0.958
Particleboard – low density (593 kg/m³ = 37 lbs/ft³)	0.0098	0.127	0.157	0.186	–	–	–	–	–	–	–	–	–
Particleboard – medium density (800 kg/m³ = 50 lbs/ft³)	0.0077	0.100	0.123	0.146	–	–	–	–	–	–	–	–	–
Particleboard – high density (993 kg/m³ = 62 lbs/ft³)	0.0059	0.077	0.094	0.112	–	–	–	–	–	–	–	–	–
Plywood – generic softwood	0.0087	0.109	0.135	0.161	–	–	–	–	–	–	–	–	–
Plywood – Douglas fir	0.0111	0.139	0.172	0.205	–	–	–	–	–	–	–	–	–
Waferboard – 705 kg/m³	0.0095	0.124	0.152	0.181	–	–	–	–	–	–	–	–	–
Oriented strandboard (OSB)	0.0098	0.127	0.157	0.186	–	–	–	–	–	–	–	–	–

(1) Semi-rigid mineral fibre includes both glass and rock wool fibre.

Figure 2-15: Thermal Resistance Values of Common Insulation (retrieved from NECB - User’s Guide pg.29, 2011)

2.4. Thermal Impact Factors

2.4.1. Gaps between Insulation Boards

The formation of gaps between insulation boards is inevitable, whether they are existent due to poor installation or unavoidable dimensional changes because of temperature variation. Most common roof assemblies have two layers of insulation placed in a staggered configuration in order to overlap the gaps and limit the potential thermal losses. Although two layers is the recommended practice, it is not uncommon to see single layer installation in some parts of North America with milder climates. Roof assemblies with a single layer of insulation have the potential for a through gap formation at every insulation joint; this is the worst-case scenario for thermal resistance due to a direct path for heat flow. The three possible gap types in roof assemblies are shown in Figure 2-16.

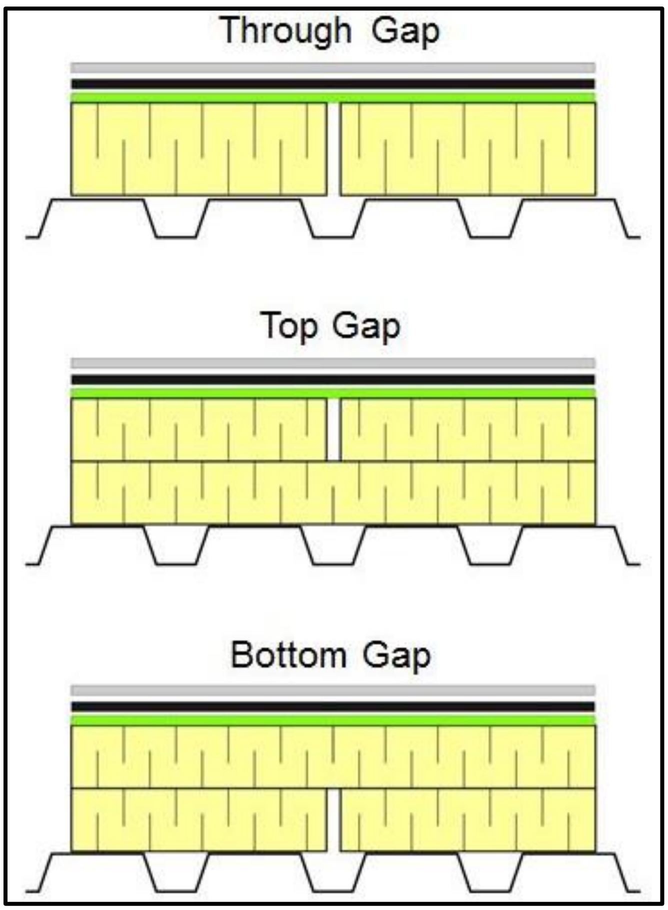

Figure 2-16: Insulation Gaps

It is important to differentiate between “joints” and “gaps”. A joint is the joining or contact between two insulation boards; gaps are the spaces that can form in-between the joints. Figure 2-17 shows the three types of joints manufactured for insulation boards: butt joint, ship-lapped joint, and tongue and groove joint. Figure 2-18 shows the formation of a gap between a butt joint.

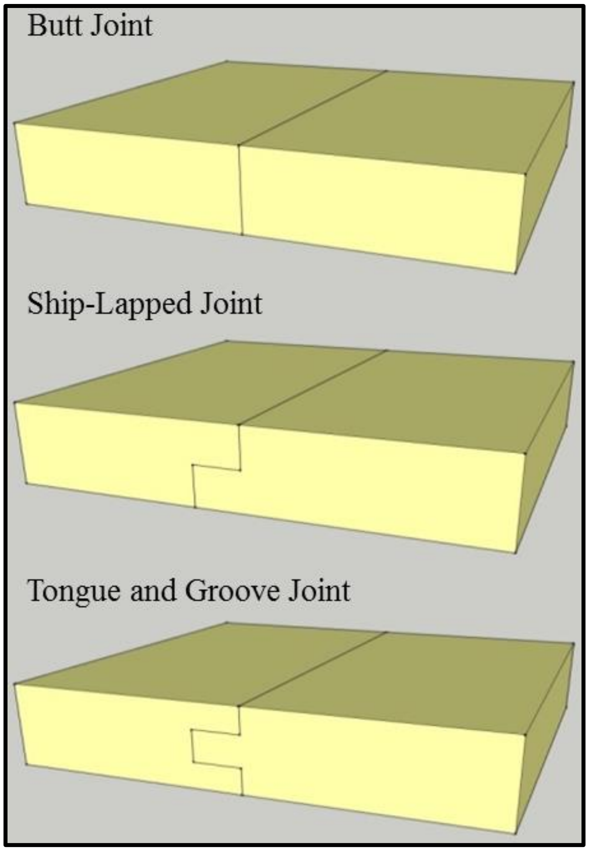

Figure 2-17: Insulation Joints

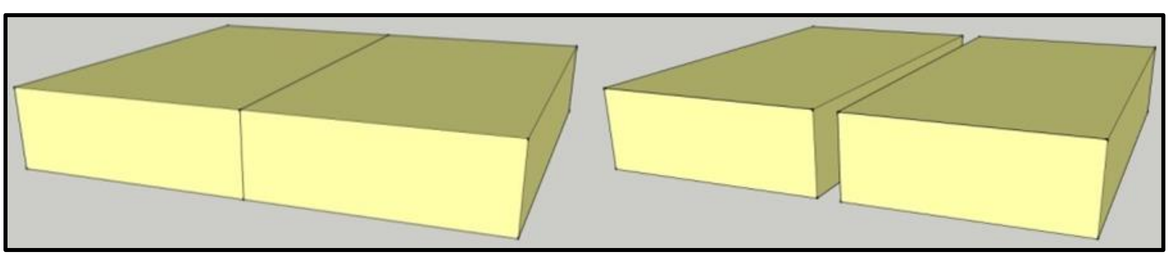

Figure 2-18: Insulation Gap Formation

The three sources that contribute to the formation of gaps are depicted in Figure 2-19. The effect of each contributor must be considered and tested to study the extent of its impact. Once the magnitude of the impact of each factor is determined, tests can be run under those conditions.

1. Gaps as a result of installation are a potential source for the presence of gaps between the insulation boards. Even with careful installation practice, gaps between boards are inevitable. Improper installation compounded by improperly manufactured boards (Figure 2-20) can cause wide gaps.
2. Within a roof assembly insulation boards are subjected to temperature variations, whether from day to night or summer to winter. These boards will expand or contract under temperature variations; the degree of change with respect to the materials' original length is its coefficient of expansion. The effect of linear expansion is not permanent as the insulation material will expand and contract but return to its initial dimension when returned to the initial conditions.
3. The last major contributor to gap formation is the dimensional stability of the insulation boards. This is the degree to which a material maintains its original dimensions when subjected to changes in temperature and humidity. Unlike the coefficient of linear expansion, this is a permanent deformation.

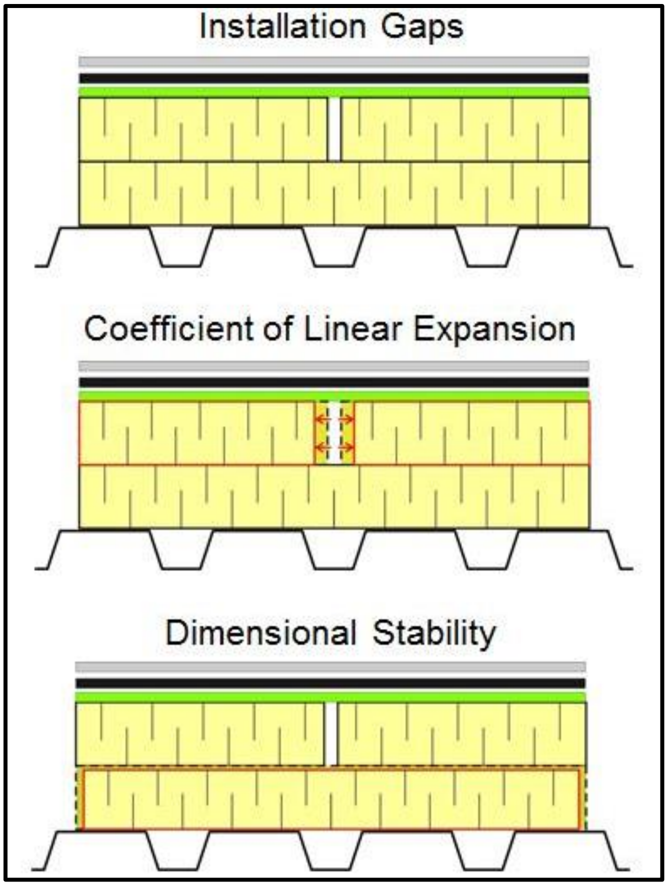

Figure 2-19: Cause of Gap Formation

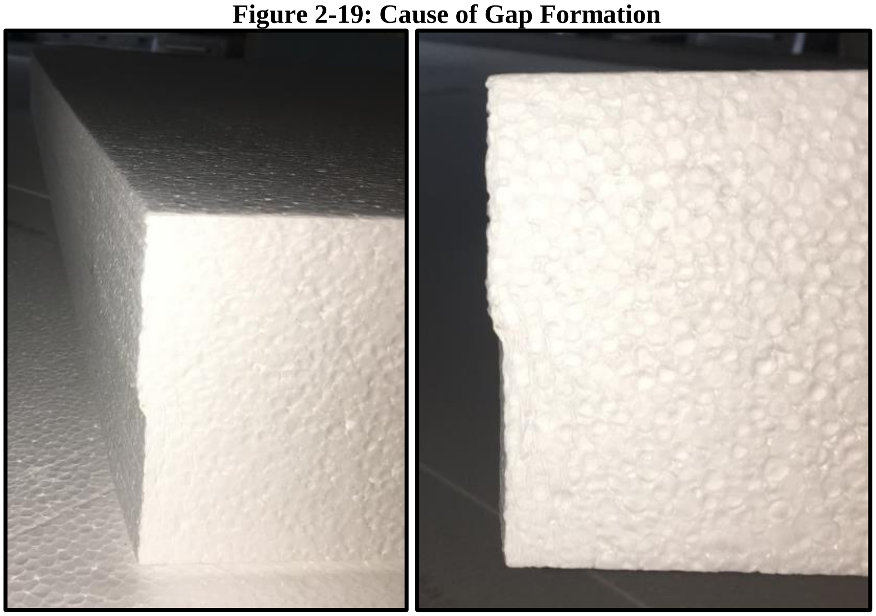

Figure 2-20: Insulation Defect

Results from literature on the thermal impact of gaps concluded that gaps have a significant impact on the thermal performance of roof assemblies. Lewis (1979) investigated the effects of gaps between insulation boards on the heat transfer coefficient and concluded that a one percent gap (one percent relating to the overall board dimensions) can lead to a 3% to 9% increase in thermal transmittance, depending on the insulation thickness. Hedlin (1985) conducted tests on gaps varying from $2.5\ mm$ to $25.4\ mm$ ($1/10$ " to 1") in size and found that the increase in heat loss ranged from 4% to 35%. Finally, Petrie et al. (2000) investigated the effect of a one-inch gap on single and double layer for insulation. Petrie concluded that two layers of insulation have a 15% decrease in thermal resistance while single layer insulation has a 17% reduction in thermal resistance.

The presence of gaps in roofing assemblies, especially gaps in the range of an inch or greater may seem far-fetched, but the reality is that these gaps exist. Regardless of whether gaps are formed due to improper installation, panel defects for dimensional changes, it is certain that gaps are present in the majority of low-slope roofs. Figure 2-21 and Figure 2-22 further emphasise the importance of considering gaps in the thermal design of roofs, showing in-situ examples of the extent of gap formation.

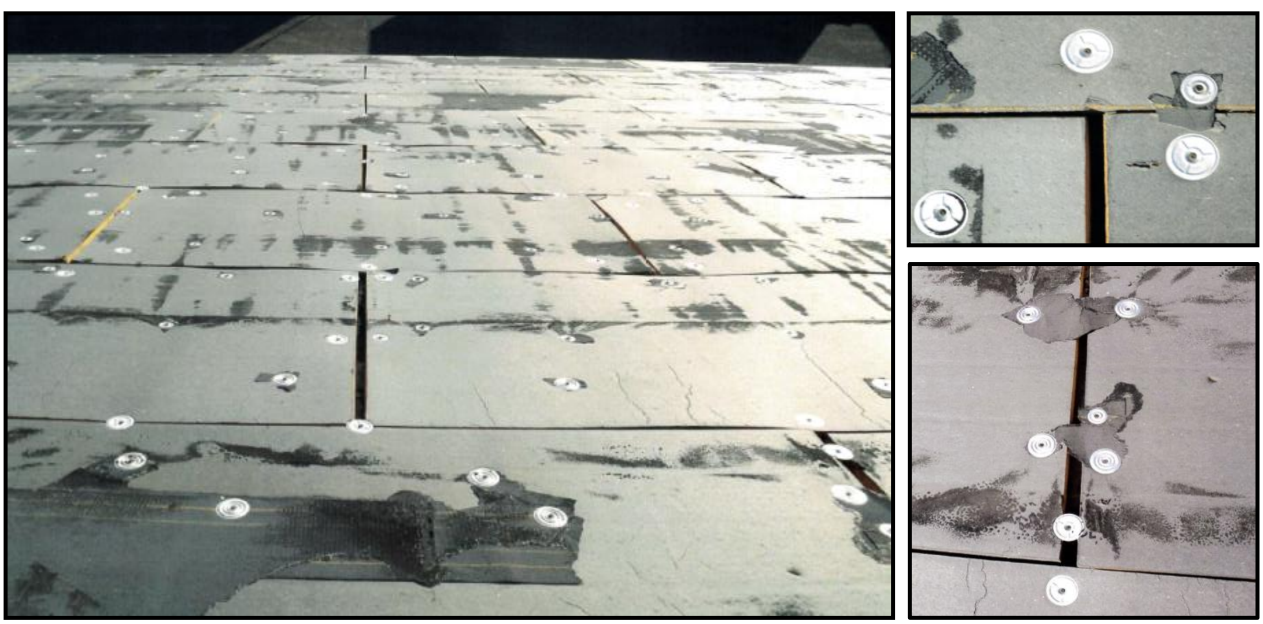

Figure 2-21: In-situ Insulation Gaps #1 (retrieved from the Canadian Roofing Contractors Association, 2016)

Figure 2-22: In-situ Insulation Gaps #2 (retrieved from the Canadian Roofing Contractors Association, 2016)

2.4.2. Mechanical Fasteners

Fasteners are used in the majority of roofing systems to secure the individual components and provide resistance against wind uplift forces. The fasteners create a thermal bridge through which thermal energy may easily bypass the roof insulation (Figure 2-23). The larger number of fasteners used to secure an assembly, the higher the thermal bridging effect. In other words, the greater the fastener density in an assembly, the more thermal losses the system will experience.

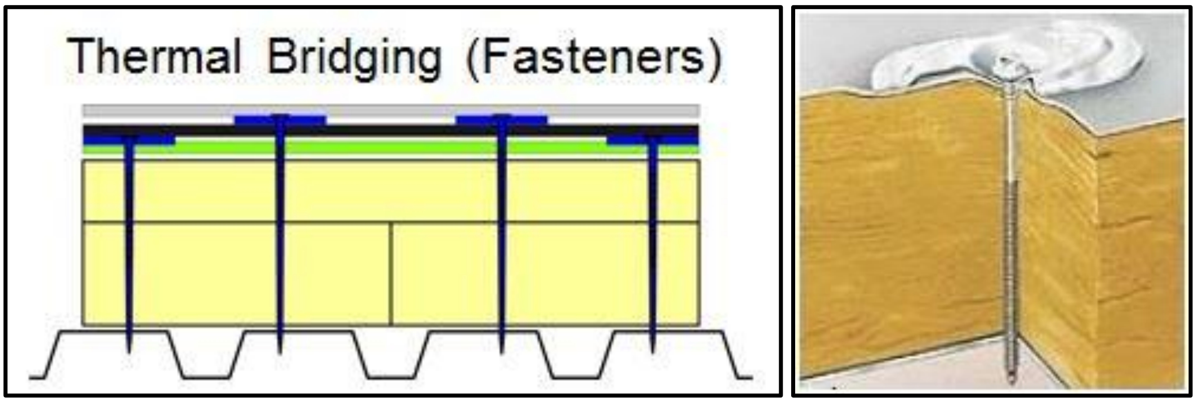

Figure 2-23: Fasteners (right: retrieved from Wieland, 2006)

The fastener density depends on the type of roof assembly, the type of membrane, insulation layout and the location of the roof. A partially adhered roof system (PARS) uses fasteners to secure all components except the membrane, for which an adhesive is used (Figure 2-24a). An identical roof system that is comprised of a mechanically attached assembly (MARS) will have a greater fastener density due to the extra layer of fasteners used to secure that membrane (Figure 2-24b). The fastener density of MARS assembly may further increase based on the type of membrane used, membrane sheet width or fastener row (FR), fastener spacing (FS) along the seam. Figure 2-25 show two MARS assemblies with different membrane layout.

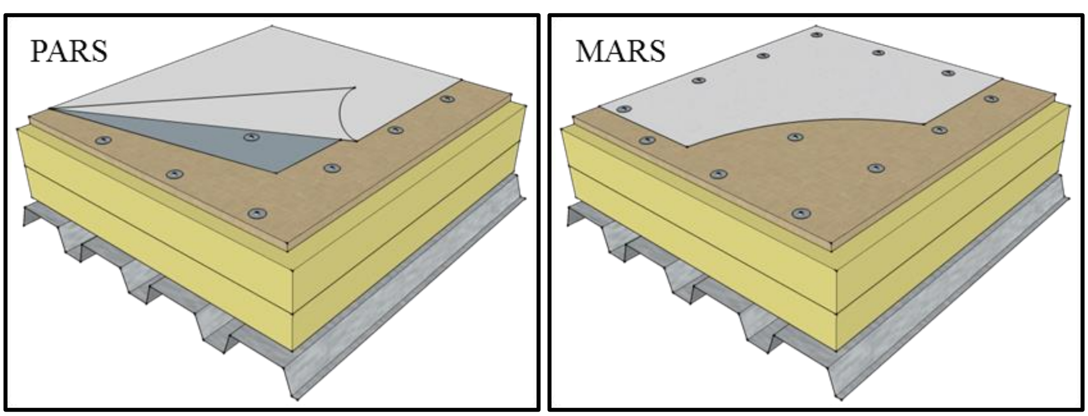

Figure 2-24: PARS vs. MARS Roof Assemblies

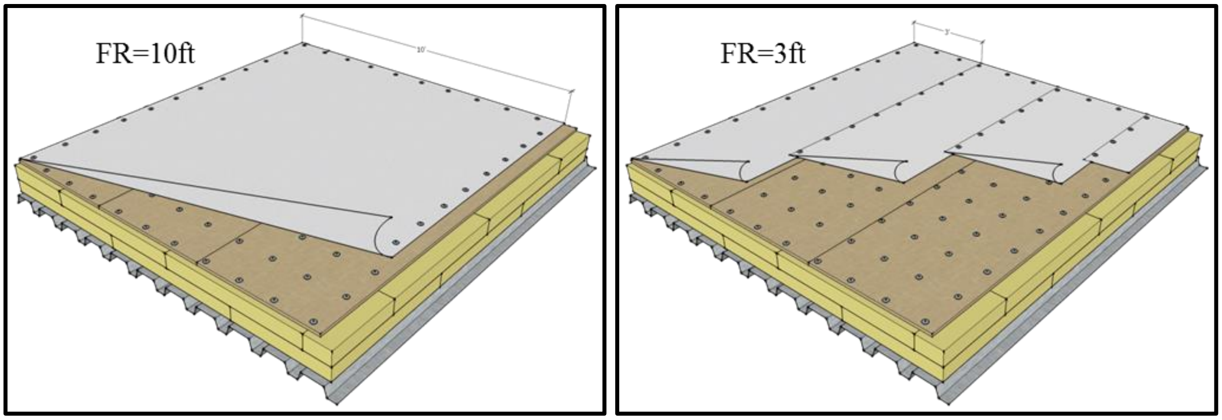

Figure 2-25: Effect of Membrane on Fastener Density

Although the fastener density of a roof is influenced by the type of assembly, membrane and location; the fastener density is selected based on the designer's discretion. The designer will select the fastener types, lengths, plates and choose from one of the fastener densities in Figure 2-26.

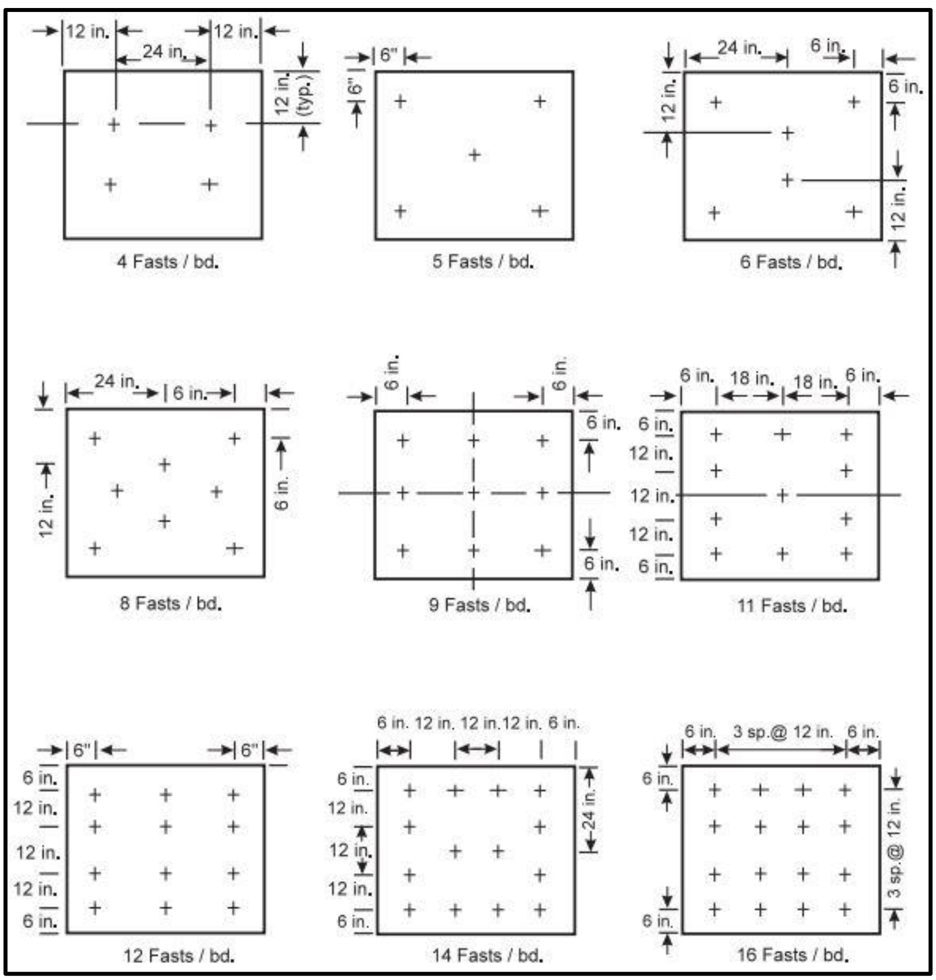

Figure 2-26: Industry Fastener Densities (retrieved from FM Global, 2016)

Results from literature on the thermal impact of fasteners concluded that thermal bridging has a high impact on the thermal performance of roof assemblies. Burch, Shoback, and Cavanaugh (1986) studied the effect of fasteners on the thermal resistance of low-sloped roofs through numerical modeling, and concluded that a fastener density of 5.4 fasteners/m^2 will reduce the overall thermal resistance in metal-deck roofs by 3 to 8%. Wieland (1988) reported a 3.3% decrease in thermal resistance from a fastener density of 3.3 fasteners/m^2. Petrie et al. (2000) reported a 12% decrease in thermal resistance from a fastener density of 5.4 fasteners/m^2, and O'Brien (2006) reported a 15% decrease in thermal resistance from a fastener density of 10 fasteners/m^2.

Current energy codes do not consider the effect of fasteners on the thermal resistance of roofing assemblies. It is evidently crucial to study and quantify the impact of fasteners on the thermal performance of low-slope roof assemblies, as studies have shown their impact can result in a 15% decrease in thermal resistance. Figure 2-27 is a perfect example of thermal bridging due to fasteners; the roof is covered in a layer of snow that has melted over each fastener which has provided a path for heat flow.

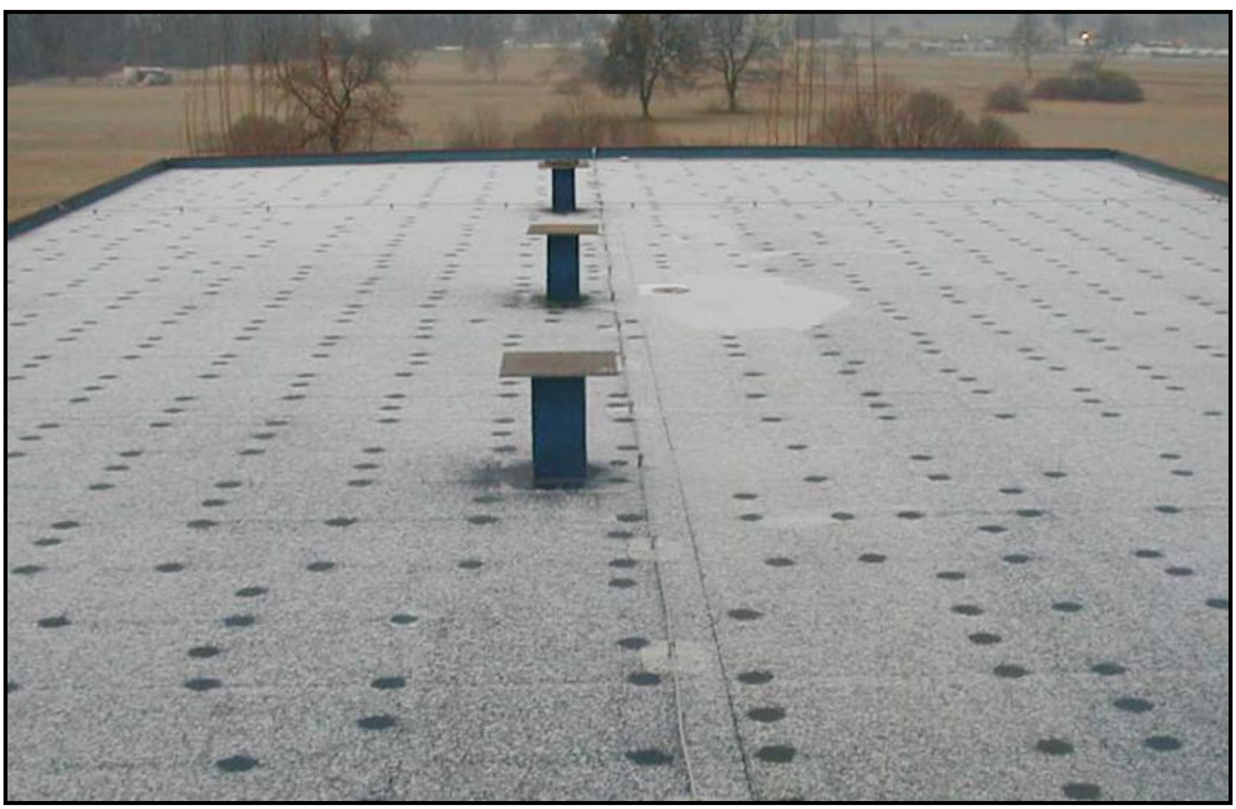

Figure 2-27: In-situ Fastener Thermal Impact (retrieved from Wieland, 2006)

2.4.3. Air Intrusion and Moisture

Moisture and airflow are the third mode of thermal losses in roofing assemblies; these mechanisms are outside the scope of this thesis and will not be tested - however, a brief overview of their impact is done to express their significance and outline the future work for this topic.

One of the largest concerns in the roofing industry is the air intrusion into the roof assembly (Baskaran and Molleti 2009). This air intrusion can carry moisture that can have a significant impact on the durability and energy efficiency of roofing assemblies. Controlling air intrusion is critical to ensuring good roofing system performance, because if left unchecked, it can have effects on wind uplift resistance, moisture accumulation, and thermal resistance (Figure 2-28). This intruded air is a binary mixture of dry air and water vapor. Thus air intrusion becomes one of the major driving forces for the movement of moisture in the form of water vapor into mechanically attached roofing systems. Moisture can also migrate into the roofing system by means of water vapor diffusion during the winter season. All previous studies focussed only on the diffusion process, which has often been blamed for condensation problems that might have been due to mass air movement by the air intrusion process. If moist air from the building interior can intrude into the mechanically attached system, where it will be cooled, condensation can occur in the same way it does from diffusion of water vapor. The difference is that the quantities involved from air intrusion are likely to be much greater than from diffusion; also, the moisture movement is much faster by air intrusion than by diffusion. As of today, MARS have not been fully evaluated with regard to their moisture performance, particularly from the air intrusion process. This will be the third impact factor that will be evaluated as part of the ERCR project.

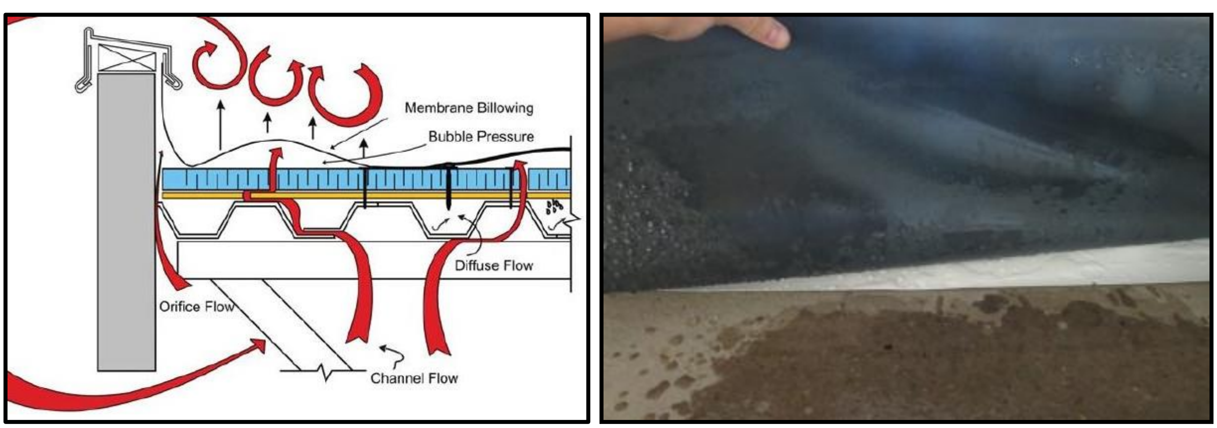

Figure 2-28: Air Intrusion Impact on Roofing Assemblies (retrieved from Baskaran and Molleti, 2009)

2.4.4. Thermal drift

Insulation boards such and polyisocyanurate (polyiso), expanded polystyrene insulation (EPS), and extruded polystyrene (XPS) are made from foam. In order to turn the foam into a rigid structure, a hardening phase is undergone through the use of blowing agents. A blowing agent is applied at the liquid stage, resulting in a chemical reaction which increases the stiffness of the material and fills the porous foam with gas – this gas has a lower vapour conductivity than air (Holladay 2016). Though the blowing agents have a lower conductivity and therefore provide a greater material thermal resistance, over time the gases dissipate. As the gases diffuse through the rigid foam, they are replaced by air; this process of gradual reduction in the foam's thermal resistance is referred to as "thermal drift". The blowing agents used to make EPS and XPS are replaced by air very rapidly after manufacturing. The thermal resistance is measured after the blowing agent have dissipated, making the thermal resistance values of EPS and XPS stable for the life of the insulation (Holladay 2016). The dissipation of gases from polyiso insulation on the other hand takes several years (Holladay 2015), therefore the insulations performance will diminish over time.

2.4.5. Reporting Mean Temperatures

All commonly used insulating materials exhibit a change in their thermal conductivity over a range of temperatures. Since all building properties are reported at 24℃ (75°F), the temperatures are not representative of typical in-service conditions. Grin, Schumacher, and Smegal (2014) took a closer look at the performance of polyiso insulation during winter conditions in all climatic zones. They found that the insulation allows a significantly greater heat flow during colder and warmer weather and concluded that the reporting of common building insulation thermal properties at 24℃ is not representative of in-service conditions. The Building Science Corporation (2013) also carried out experiments on polyiso insulation over four mean temperatures and reported that the insulation boards behave differently at different mean temperatures (Figure 2-29). Courville et al. (1989) investigated the temperature variation on the thermal resistance of EPS, fiber-glass and phenolic foam insulation and similarly concluded that there is variation of thermal resistance with temperature. It can be concluded that the reporting mean temperature of insulation properties is not representative of the behaviour at various temperatures.

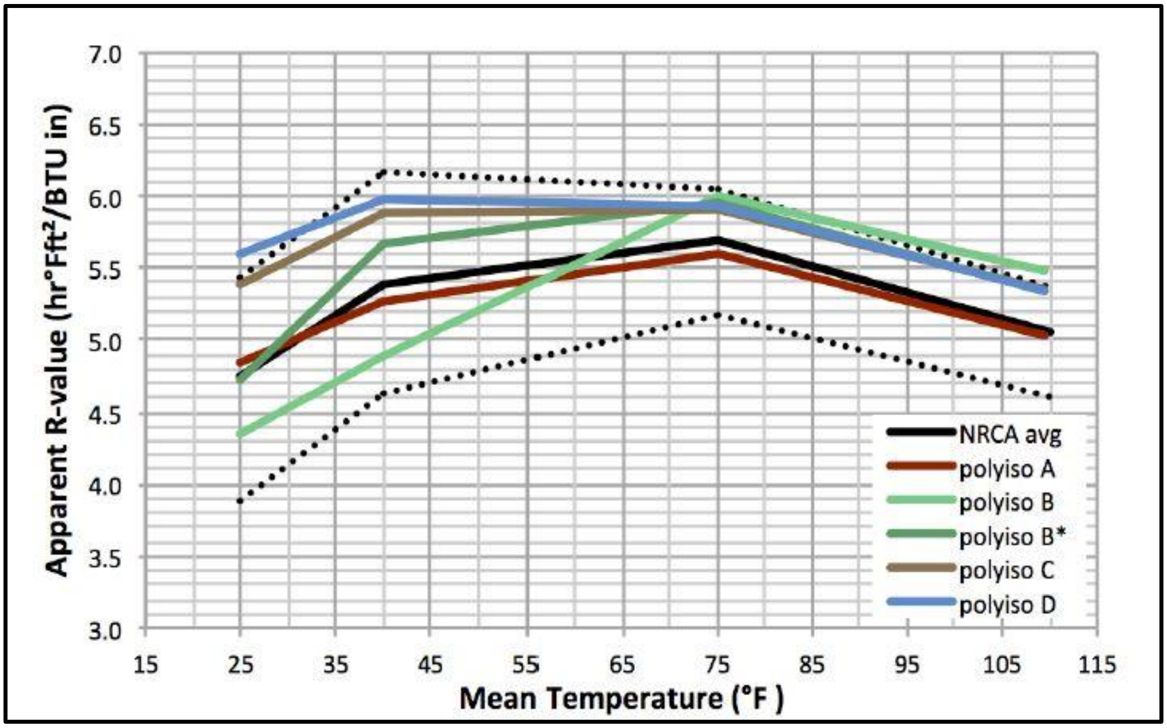

Figure 2-29: Insulation Behaviour over Ranging Mean Temperature (Building Science Corporation, 2013)

2.5. Concluding Remarks

It can be concluded that many factors have an impact on the thermal performance of roofing assemblies. These factors range from the method of manufacturing insulation over its lifetime, which can result in thermal drift and decrease of the thermal efficiency of the insulation; to the standard of reporting thermal properties at a given temperature. Of these different influencing factors, two factors namely the thermal bridging of fasteners, and gaps between insulation boards are considered to have a significant impact on the thermal performance of the roof assemblies. This research study quantifies these factors to understand the magnitude of their impact in the energy design of roofs.

Chapter 3: Literature Review

This chapter provides an overview of the most important literature related to the thermal performance of roofing systems and the associated effects of thermal impact factors. This chapter is divided in three sections. First, a discussion of the standard test methods used in determining thermal transmission in materials and assemblies, and their significance in attaining accurate and comparable results, is introduced. Second, the chapter reviews numerical studies conducted to predict the thermal performance of roofing systems and thermal impact factors. The final section is a review of the experimental testing done to quantify the impact of thermal impact factors on roofing assembly's thermal performance. The goal of this chapter is to introduce the reader to current progress in the field, provide an understanding of the methodologies, experimental and theoretical approach, and identify the knowledge and test gaps thereby justifying the need for this research.

When tests are carried out, whether they are numerical models or experimental tests, a test standard is required to provide standard properties, information and values to obtain comparative results. For example, testing material properties under different conditions will yield different results. Therefore, standards are used to ensure designers, manufacturers and users can evaluate materials at comparable values. There are a variety of standards that are available specific to industry specifications and regulations of a country, group of countries or the international community. The organizations and standards used in the following literature review are:

- American Society for Testing and Materials (**ASTM International**) is an international standard development organization for creating test methods, specifications, classifications, guides and procedures.
- American National Standards Institute (**ANSI**) facilities the development of American Nation Standards by accrediting the procedures of standards developing organizations.
- American Society of Heating, Refrigerating, and Air Conditioning Engineering (**ASHRAE**) focuses on sustainability and improvement of building systems, energy efficiency, air quality and refrigeration.
- International Organization for Standardization (**ISO**) is an international standard organization for the development of internationally accepted standards.

3.1. Standard Test Methods

3.1.1. Steady-State Heat Flux Measurements of Thermal Transmission Properties by Means of Guarded-Hot-Plate Apparatus (ASTM C177-10)

This test method measures the steady-state heat flow through a homogeneous flat material. Two materials selected with properties (thickness, areas, density, etc.) as similar as possible are placed on either side of the guarded hot plate and between cold plates (Figure 3-1). The apparatus measures the thermal resistance of the two test specimens and records the mean value. The average value from two specimens increases the confidence of the apparatus results due to the decreased probability of property deviation. The properties of a material with an irregularity would have less significance on the final mean result. This apparatus can only test components, as inhomogeneous specimens (assemblies including the steel structural deck or fasteners) will cause a non-unidirectional and non-uniform thermal flux both within the specimen and over the metered area. This apparatus has heat flux and temperature sensors in one axis therefore thermal field distortions will give rise to serious errors.

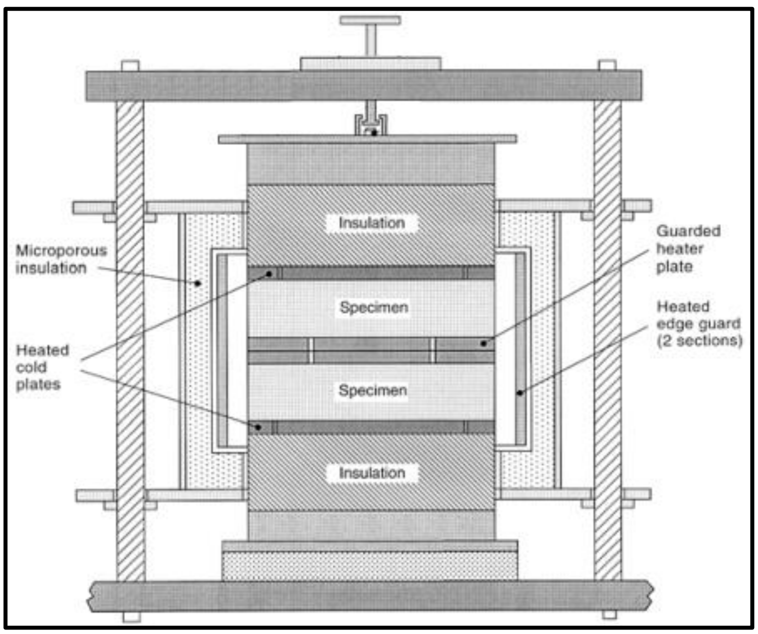

Figure 3-1: Guarded-Hot-Plate Apparatus (reproduced from ASTM C177, 2010)

Limitations:

- Test apparatus only capable of testing components but not assemblies;
- Specimen maximum thickness is one-third the dimension of the metering section;
- Cannot test thermal impact factors (gaps, fasteners, moisture and airflow).

3.1.2. Steady-State Thermal Transmission by Heat Flow Meter Apparatus (ASTM C518-10)

The heat flow meter measures fast and accurate thermal properties under one-dimensional steady-state conditions through a flat specimen placed between a hot and a cold plate (Figure 3-2). The heat flow meter has similar capabilities and limitations as the guarded hot plate apparatus but tests single samples. Only homogeneous components may be tested as assemblies will result in thermal distortions. This test method has a precision and repeatability of 1% so it is used to provide baseline thermal properties for calibration of other thermal chambers such as the guarded hot box.

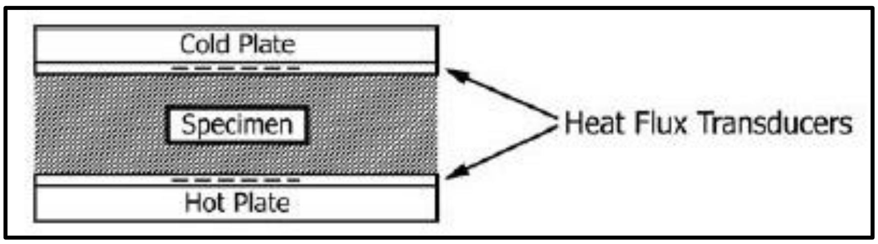

Figure 3-2: Heat Flow Meter Apparatus (retrieved from ASTM C518, 2010)

The procedure for data analysis of the heat flow meter is as outlined in section 2.2.2, using (Eqn. 2-3), (Eqn. 2-4) and (Eqn. 2-5) to calculate the thermal conductivity, conductance and resistance. The dimensions of the test specimen are measured; thermocouples measure the temperature of both plates, and heat flux sensors in measure the heat flow.

Limitations:

- Test apparatus only capable of testing components but not assemblies;
- Specimen maximum thickness is one-third the dimension of the metering section;
- Cannot test thermal impact factors (gaps, fasteners, moisture and airflow).

3.1.3. Thermal Performance of Building Materials and Envelope Assemblies by Hot Box Apparatus (ASTM C1363-11)

The hot box apparatus measures thermal properties of an assembly under controlled air temperature, velocity, radiation and moisture conditions (Figure 3-3). This apparatus is used to determine the thermal resistance and transmittance of large non-homogeneous systems such as building structures and composite assemblies.

Calibration:

Maintaining a perfectly guarded metering area during testing is not possible - therefore corrections are needed to characterize all heat flow paths and losses from the chamber. Tests results must be compared with a specimen of known thermal properties; it is therefore required that this test apparatus is run in conjunction with ASTM C177-10 or ASTM C518-10 to compare the standard thermal properties of a homogenous specimen for the calibration of the guarded hot box. The calibration of a new guarded hot box is very crucial for the accuracy and precision of the apparatus, therefore an in-depth analysis and overview of the procedure is done in section 4.5.2.

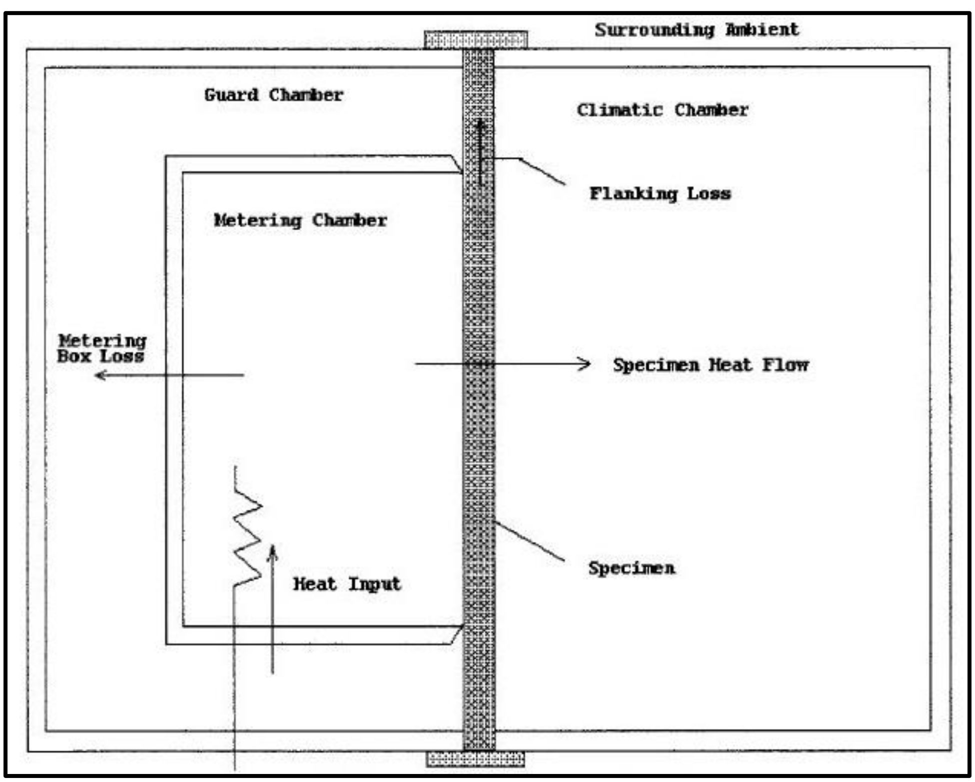

Figure 3-3: Typical Guarded Hot Box Schematic (retrieved from ASTM C1363, 2011)

Measurements:

At steady-state conditions, the thermal resistance through the specimen is calculated based on the power usage of the heater and fans - corrected for the heat passing through the chamber walls and heat flanking the specimen. Therefore properties measured before and during testing include:

- Cross-sectional area and thickness of the specimen;
- The temperature of each chamber and specimen, measured by a minimum of five thermocouples per chamber;
- The power usage of the heater, used for the calculation of the heat flow.

Chamber Requirements:

There must be a minimum of 5 differential thermocouple pairs per m^2 of metering box wall. The climatic chamber must be capable of providing controlled conditions associated with normal outdoor settings - must be able to measure air temperature and velocity in order to maintain desired surface heat transfer coefficients. Air circulation: when running forced convection, velocity shall be less than $0.5\,m/s$ if natural convective air conditions are to be simulated. Velocities greater than $1\,m/s$ are permissible when the effect of heat transfer is to be determined.

Reproducibility:

The reproducibility of the apparatus must be in the range stated in Figure 3-4.

TABLE 2 Reproducibility Test Results—Homogeneous Specimens—ASTM Hot Box Round Robin (19)

Mean Temperature (°C)	Reproducibility Interval (%)		Difference in Resistance (m^2K/W)
	Calibrated	Guarded	
4	13.6	14.6	± 0.22
24	14.4	15.6	± 0.22
43	15.4	17.2	± 0.22

Figure 3-4: Guarded Hot Box Reproducibility (retrieved from ASTM C1363, 2011)

3.1.4. Response of Rigid Cellular Plastics to Thermal Aging (ASTM D2126-09)

Due to the wide variety of potential uses of rigid cellular plastics[1], lab exposure is conducted to estimate the 'effective behavior' of the material. The effective behavior of a material (or its dimensional stability) is the degree to which a material maintains its original dimensions when subjected to changes in temperature and humidity. This test standard covers the procedures for the thermal and humid exposure of rigid cellular plastics in order to determine the dimensional stability and possible material exposure conditions.

Apparatus

- Oven, circulating-air, capable of holding the required temperature (± 2℃).
- Cold box, capable of maintaining required temperature (± 3℃).
- Balance, capable of weighing 0.05% accuracy.
- Digital caliper ruler, measurements to the nearest $\pm 0.1\%$.

Samples

- Sample minimum dimensions of $100 \times 100mm$ $(4 \times 4in)$.
- Minimum two specimens must be tested.

Exposure

- 1 day, 1 week, 2 weeks

Procedure

After exposure, allow the specimens to come to room temperature for two hours before measuring dimensions. Appropriate exposure conditions can be selected from Figure 3-5.

Temperature, °C (°F)	Relative Humidity, %
−73 ± 3 (−100 ± 6)	ambient
−40 ± 3 (−40 ± 6)	ambient
70 ± 2 (158 ± 4)	ambient
100 ± 2 (212 ± 4)	ambient
150 ± 2 (302 ± 4)	ambient
23 ± 2 (73 ± 4)	50 ± 5
38 ± 2 (100.0 ± 4)	97 ± 3
70 ± 2 (158 ± 4)	97 ± 3
other temperatures and humidities selected for individual needs	

Figure 3-5: Temperature Conditions for Aging (retrieved from ASTM D2126, 2009)

Calculations

[1] Definition available on page ix.

The percent change in dimensions will be calculated using (Eqn. 3-1) and (Eqn. 3-2).

$$Change, \%\, Mass = (\frac{m_f - m_o}{m_o}) \times 100 \quad \textbf{(Eqn. 3-1)}$$

$$Change, \%\, Dimension = (\frac{L_f - L_o}{L_o}) \times 100 \quad \textbf{(Eqn. 3-2)}$$

where

$$m_o / \, L_o = mass/\, length\ Initial \quad \textbf{(Eqn. 3-3)}$$

$$m_f / \, L_f = mass/\, length\ final \quad \textbf{(Eqn. 3-4)}$$

Table 3-1: Summary of Dimensional Stability Test Requirements

Sample minimum dimensions	$100 \times 100\ mm$
Minimum test samples	2 samples
Exposure duration	1 day, 1 week, 2 weeks
Room temperature duration	2 hours
Temperature	• Max: 70℃ • Min: −73℃

3.1.5. Selecting Temperatures for Evaluation and Reporting Thermal Properties of Thermal Insulation (ASTM C1058-10)

Thermal properties of a material can change under high varying mean temperatures. Data and information at standard temperatures are necessary for valid comparison of thermal properties. Mean temperatures selected for testing must be based on the materials intended use. Since all of the tests in this thesis are run under steady-state conditions, Figure 3-6 presents the experimental temperature set-points for the thermal transmittance evaluation of specimen with both surfaces exposed to fixed temperatures.

Temperature, ° C[B]			Temperature, [° F][B]		
Mean	Hot Ambient[C]	Cold Ambient[C]	Mean	Hot Ambient[C]	Cold Ambient[C]
−4	24 ± 5	−32± 5	[25]	[75 ± 9]	[−25 ± 9]
4	24 ± 5	−15± 5	[40]	[75 ± 9]	[5 ± 9]
10	24 ± 5	−4 ± 5	[50]	[75 ± 9]	[25 ± 9]
24	38 ± 5	10 ± 5	[75]	[100 ± 9]	[50 ± 9]
38	52 ± 5	24 ± 5	[100]	[125 ± 9]	[75 ± 9]
43	63 ± 5	24 ± 5	[110]	[145 ± 9]	[75 ± 9]

Figure 3-6: Standard Temperatures for Thermal Testing (retrieved from ASTM C1058, 2010)

3.2. Thermal Analysis via Numerical Modeling

The following studies are the most relevant to this research and are organized in chronological order to show the progression of the numerical models, their accuracy and significance to this field.

3.2.1. Lewis (1979)

Lewis (1979) investigated the effect of gaps between insulation boards on the heat transfer values. The study was done to quantify the heat loss due to gaps through analytical modeling and validation through experimental testing. There are three types of gaps investigated by Lewis: an upper gap, lower gap, and a through gap, also known as a total gap (Figure 3-7). Though the focus of the study was the most critical gap (the through gap), tests were done on all three gap scenarios. Since most roofs are unique, a generalized built-up roof assembly was selected for testing based on the most commonly used industry roof components. The assembly includes: a steel deck, a double-layer of fiberglass insulation and a three-ply fiberglass membrane with an asphalt coating.

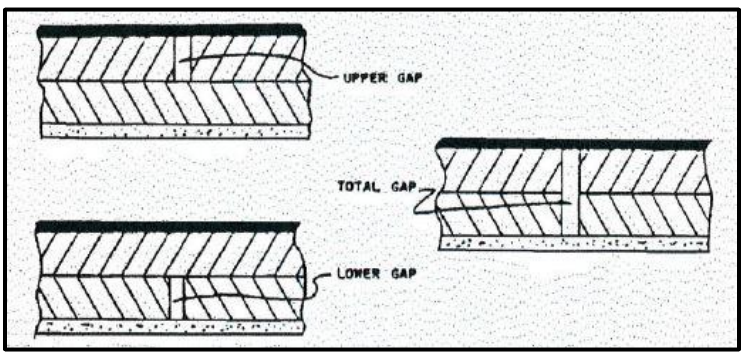

Figure 3-7: Adjacent Insulation Gaps (retrieved from Lewis, 1979)

The gaps widths tested were selected based on commonly found gaps due to improper installation, compounded by the effect of thermal contraction after installation. It was found that even with careful installation, insulation gaps range from $1.6\,mm$ to $7\,mm$ (1/16" to 5/16"). For the study, a typical gap is considered to be $4.8\,mm$ (3/16") and is the main test case for the numerical model. The overall thermal transmittance was measured for an assembly with and without the presence of an insulation gap; this is done to provide baseline conditions for the comparison of the percent decrease in thermal transmittance. Lewis concluded that the effects of the gap diminish $150\,mm$ (6") away from the gap. The through gap had the most critical effect on the system, followed by the upper gap and the lower gap having the least impact, as seen in Figure 3-8.

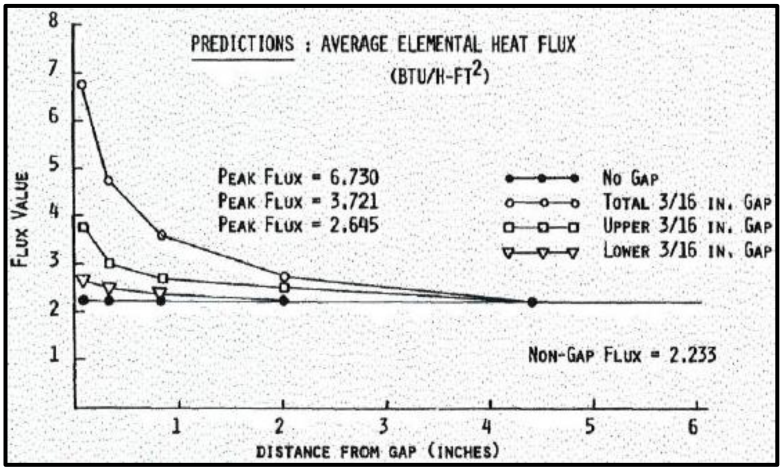

Figure 3-8: Thermal Transmittance due to Gaps (retrieved from Lewis, 1979)

Experimental testing was done to validate the numerical model results; the test was done in accordance to ASTM C236 (guarded hot box). Thermocouples were installed along the gap and the mid-width of the insulation board (Figure 3-9) to monitor the dissipation of the incluence of the gap. The tests were conducted in two laboratories to compare the independent results; one test was done on insulation boards with dimensions of $500\,mm \times 500\,mm$ $(20" \times 20")$, while the other test are done on insulation boards with dimension of $1524\,mm \times 1524\,mm$ $(5ft \times 5\,ft)$. Only one mean temperature was tested, 24°C (75°F), at a temperature difference of 22.2°C (40°F). Unlike the numerical model, four gap widths were tested: $0\,mm$, $4.8\,mm$, $15.9\,mm$ and $19\,mm$ (0", 3/16", 5/8" and ¾"). All values were found to be within 8% of the numerical model.

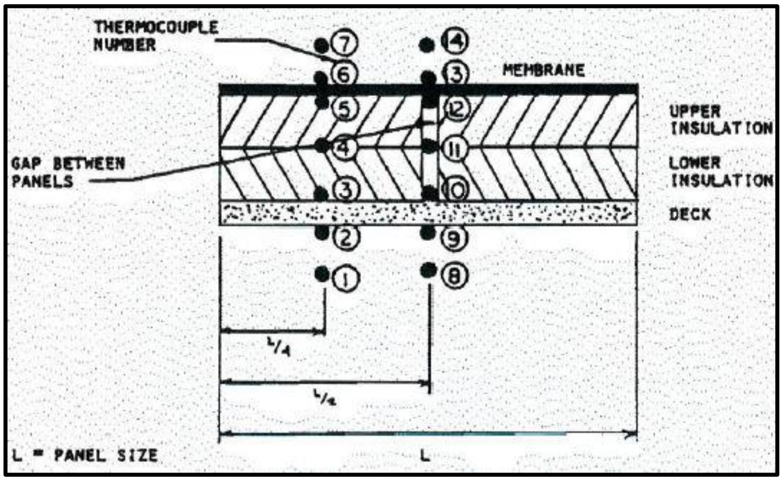

Figure 3-9: Thermocouple Locations (retrieved from Lewis, 1979)

It was previously believed that a 1% increase in gap area is equal to 1% increase in heat loss, but Lewis determined that it is much greater than that. Lewis concluded that a 1% gap can result in 3%-9% increase in thermal transmittance depending on the insulation thickness. A relation is made for gap width and percent increase in thermal transmittance shown in Figure 3-10. This is for two layered insulation with a through gap, but a factor of 0.19 can be applied to convert the values for a staggered joint configuration. It is concluded that a 57 mm (2.25") thick insulation board with a 25.4 mm (1") through gap will result in a thermal transmittance increase of 25% to 30%. The thermal transmittance is approximately 19% less for a staggered gap formation.

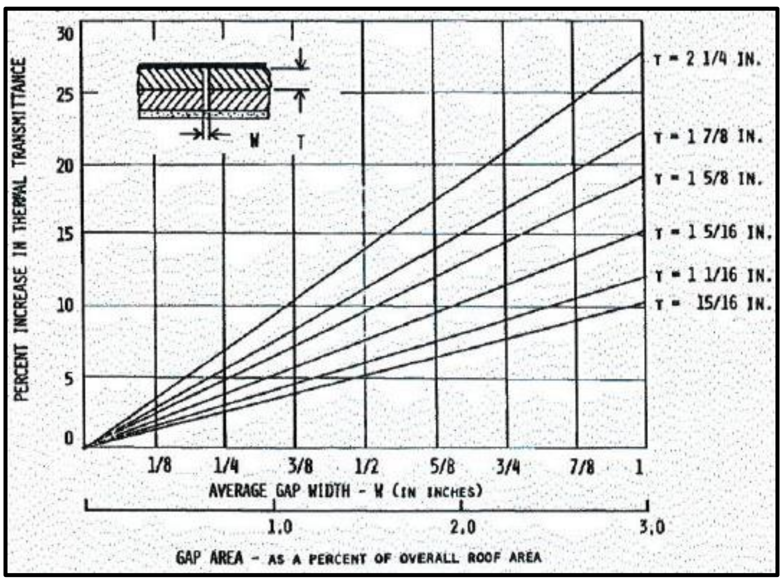

Figure 3-10: Percent Increase in Thermal Transmittance (retrieved from Lewis, 1979)

Limitations:

- The tests were conducted on only one type of insulation (fiberglass insulation); therefore the effect of insulation type on thermal properties cannot be observed.
- One insulation thickness was experimentally tested;
- The staggered joint layout was not experimentally tested to validate the model.
- Results only applicable to a staggered gap in one layer of insulation and not both.
- Considers equal thickness for both layers of insulation which is not always representative of field application.

3.2.2. Burch, Shoback, and Cavanaugh (1987)

Metal fasteners are used to secure built-up roof assemblies from wind-induced uplift pressure. The fasteners create a thermal bridge through which thermal energy may bypass the roof insulation. Burch, Shoback, and Cavanaugh (1986) studied the effect of metal fasteners on the overall thermal resistance of low-sloped roofs. Both metal and wooden decks were considered in the model along with metal fasteners with and without a plastic cap. The plastic cap was tested to study the reduction in thermal transmittance. The tests were run using indoor and outdoor temperatures of 21℃ and -18℃, respectively. The tests were run for two scenarios: the fastener penetrates the bottom insulation layer of insulation (Figure 3-11a), and the fastener penetrates the entire insulation (Figure 3-11b) for a fastener density of 5.4 fasteners per m^2.

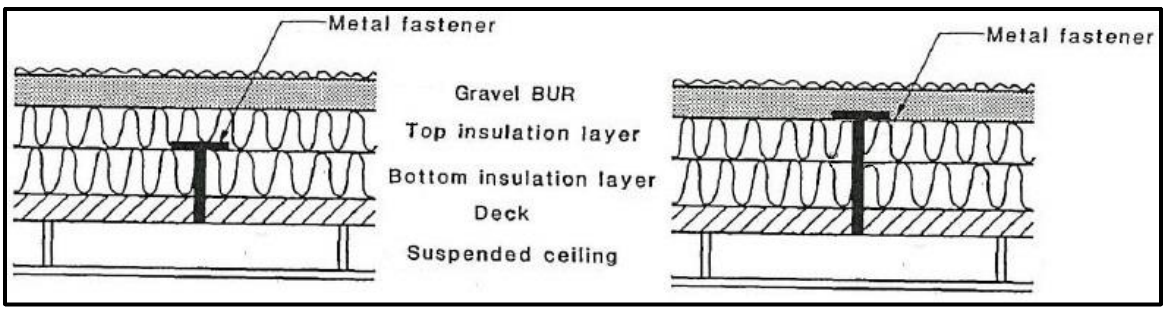

Figure 3-11: Fastener through (a) Bottom Layer of Insulation (b) Entire Insulation (retrieved from Burch, Shoback, and Cavanaugh, 1987)

Burch, Shoback and Cavanaugh concluded that the fasteners reduced the overall thermal resistance of metal-deck roofs by 3%-8%. The effect of metal fasteners in a wood-deck assembly was found to have half the effect of metal-deck roofs; this is because the absence of lateral heat conduction in the wood portion of the roof assembly. The use of plastic caps instead of a metal plate for the fasteners reduced the heat transfer by about 44%. Last, the effect of the metal fastener on the overall thermal resistance was reduced by a factor of 3 when used to attach only the bottom layer of insulation.

Limitations:

- No experimental testing was done to validate the model.
- The tests were conducted on one type of insulation (fiberglass insulation); therefore the effect of insulation type on thermal properties cannot be observed.
- A single fastener density was modeled for individual thicknesses; therefore, the results cannot be forecast of greater fastener densities.

3.2.3. Wieland (1988)

Wieland (1988) ran a finite element model in to compare the effects of a carbon steel fastener and plate to that of a carbon steel fastener with a plastic plate (Figure 3-12). The assembly modeled consisted of a $100\ mm$ thick layer of insulation with thermal conductivity of $0.04\ W/m \cdot K$ with a $2\ mm$ PVC roofing membrane and fasteners every $300\ mm$ (therefore a fastener density of $3.3\ m^2$). Wieland concluded that a fully carbon steel fastener and plate increase the thermal conduction by 3.3% (therefore decrease the thermal resistance by 3.3%), while stainless-steel fasteners with a plastic plate result in a 1.1% increase in thermal conduction. The stainless-steel fastener with a plastic plate conducts 3 times less thermal energy because the thermal conductivity of stainless-steel is one-quarter of that of normal alloy steel.

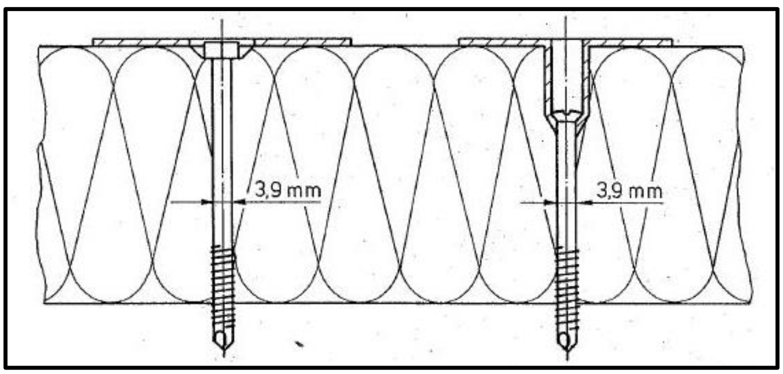

Figure 3-12: System with Carbon Steel Screw (left) and Screw with Plastic Shank (right) (retrieved from Burch, Shoback, and Cavanaugh, 1987)

Limitations:

- No experimental testing was done to validate the modeling.
- A single insulation thickness was modeled, so the effect of insulation thickness cannot be observed.
- A single fastener density was modeled, therefore the effect of fastener density on thermal transmittance cannot be observed.
- The purpose of this study was to show that the fastener material has an impact on the thermal conduction, but an adjustment for this increase in conduction was not done.

3.2.4. Wieland (2006)

Wieland (2006) conducted a more in-depth finite element analysis expanding on his (1988) research. Wieland studied the effects of fasteners and the associated decrease in thermal resistance for three fastener assemblies:

- Solid carbon steel fastener 4.8 mm in diameter with a carbon steel plate (Figure 3-13a);
- A plastic sleeve with a short carbon steel fastener 4.8 mm in diameter (Figure 3-13b);
- A stainless-steel fastener 4.8 mm in diameter with a carbon steel plate.

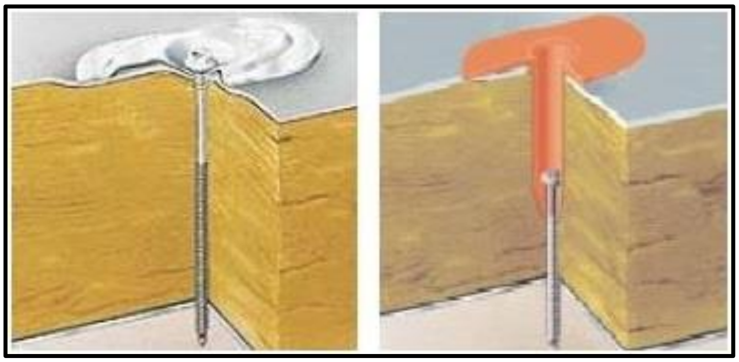

Figure 3-13: (a) Metal Fastener and Plate (b) Plastic Sleeve with Metal Fastener (retrieved from Wieland, 2006)

The results of the model are summarized in Figure 3-14, where the percent increase in thermal loss is modeled for an increasing thickness of insulation. A meter squared area was modeled with four fasteners; Wieland concludes that the value obtained from the figure can be calibrated for any number of fasteners by dividing by four and multiplying by the desired number of fasteners. Wieland (2006) concludes that the thermal bridging effect of mechanical fasteners depends on the material and geometry of the fastener. The thermal losses are highest for carbon steel fasteners with steel plates, then for steel fasteners with plastic sleeves, and the thermal loss is lowest for stainless steel fasteners.

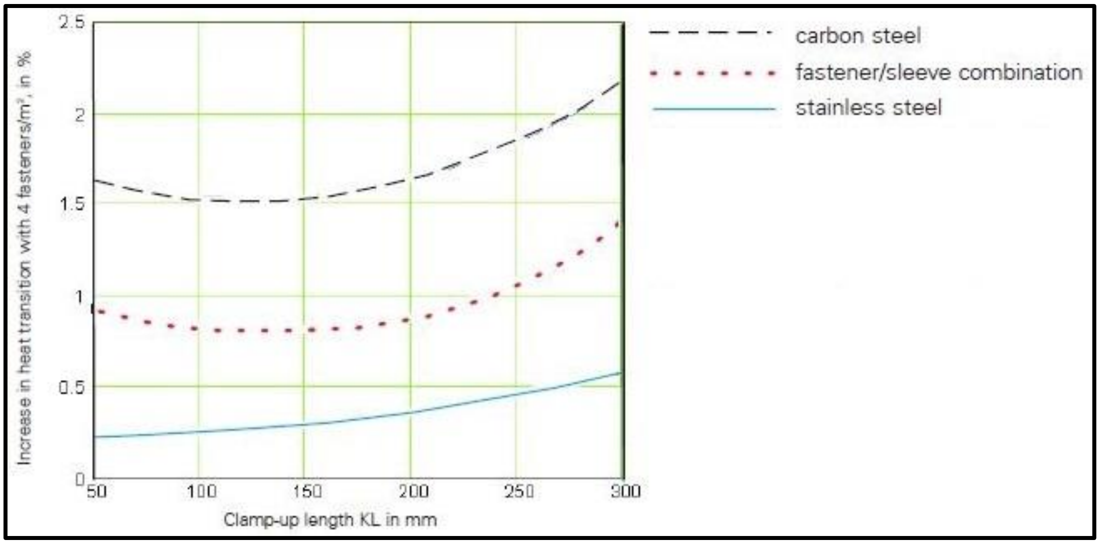

Figure 3-14: Percentage Increase in Heat Loss with 4 Fasteners/m^2
(retrieved from Wieland, 2006)

Limitations:

- The model was run at one mean temperature of 5℃ which is not the standard reporting temperature (24℃) therefore results cannot be compared to other studies.
- No experimental testing was done to validate the modeling.
- A single fastener density was modeled, Wieland assumed that the fastener density can be divided by the number of fasteners used and multiplied by any number of fasteners to achieve the result for that density. This theory was not validated.

3.2.5. O'Brien (2006)

O'Brien (2006) conducted a basic numerical model to study the influence of fasteners on a roof assembly. Based on a three-dimensional thermal model O'Brien considered the impact of a $5\ mm$ (3/16") diameter fastener at a spacing of 10 fasteners per meter squared in an R-20 roof. O'Brien concluded that this fastener density reduces the assembly's thermal resistance by 15%.

Limitations:

- The tests were conducted on one type of insulation (fiberglass insulation); therefore the effect of insulation type on thermal properties cannot be observed.
- A single insulation thickness and a single fastener density were modeled.

3.2.6. Grin, Schumacher, and Smegal (2014)

All commonly used insulating materials exhibit a change in their thermal conductivity over a range of temperatures. Since most building properties are reported at 24℃ (75°F), the temperatures are not representative of typical in-service conditions. In order to assess the impact of temperature-dependent thermal conductivity, Grin, Schumacher, and Smegal (2014) tested and compared the behavior of two insulation types: stone wool and polyiso. The insulation was modeled using manufacture advertised specifications and running it for seven climate zones (zones 1-7). Figure 3-15 shows the requirement for each climate zone and the thickness of insulation used to attain the code required thermal resistance.

Climate Zone	CZ 1	CZ 2	CZ 3	CZ 4	CZ 5	CZ6	CZ7
Location	Miami	Houston	Atlanta	St Louis	Boston	Minneapolis	International Falls
2012 IECC R-Value	R-20 (RSI 3.5)			R-25 (RSI 4.4)		R-30 (RSI 5.3)	R-35 RSI (6.2)
Roxul Thickness (R-3.8/in.)	5.3 in (134mm)			6.6 in (167mm)		7.9 in (201mm)	9.2 in (234mm)
PIC Thickness (Avg. R-6.1/in)	3.3 in (83mm)			4.1 in (104mm)		4.9 in (125mm)	5.7in (146mm)

Figure 3-15: Insulation Requirements and Associated Material Thickness (retrieved from Grin, Schumacher, and Smegal, 2014)

The thickness required for an R30 assembly according to Figure 3-15 would be 125 mm (4.9”) for polyiso and 201 mm (7.1”) for stone wool. Modeling the performance of the insulation over varying mean temperatures, polyiso insulation never meets the advertised performance, where the advertised performance is marked by the red point on Figure 3-16; and the thermal resistance significantly drops in the colder climate. Taking a closer look at the performance of the insulation in the winter climate in all seven zones is shown in Figure 3-17. Polyiso insulation allows a significantly greater heat flow during colder climate zones. Grin, Schumacher, and Smegal conclude that the reporting of common building insulation thermal properties at 24℃ (75°F) is not representative of in-service conditions. It was found that stone wool performs much better, with a total energy flow between 32% and 58% less than polyiso.

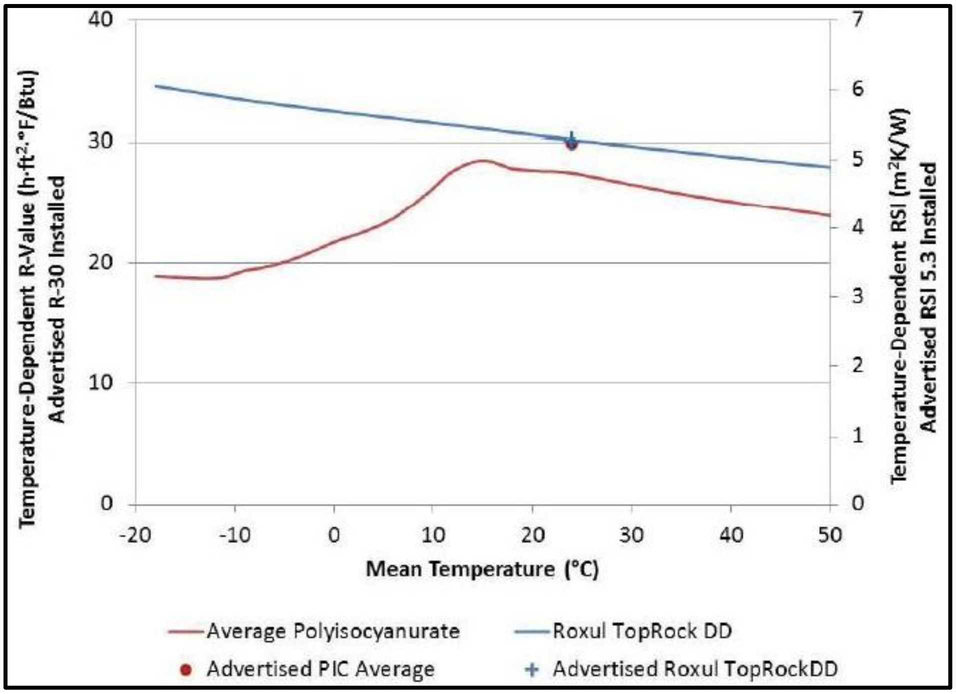

Figure 3-16: Temperature Dependent R-Value for R-30 Insulation (retrieved from Grin, Schumacher, and Smegal, 2014)

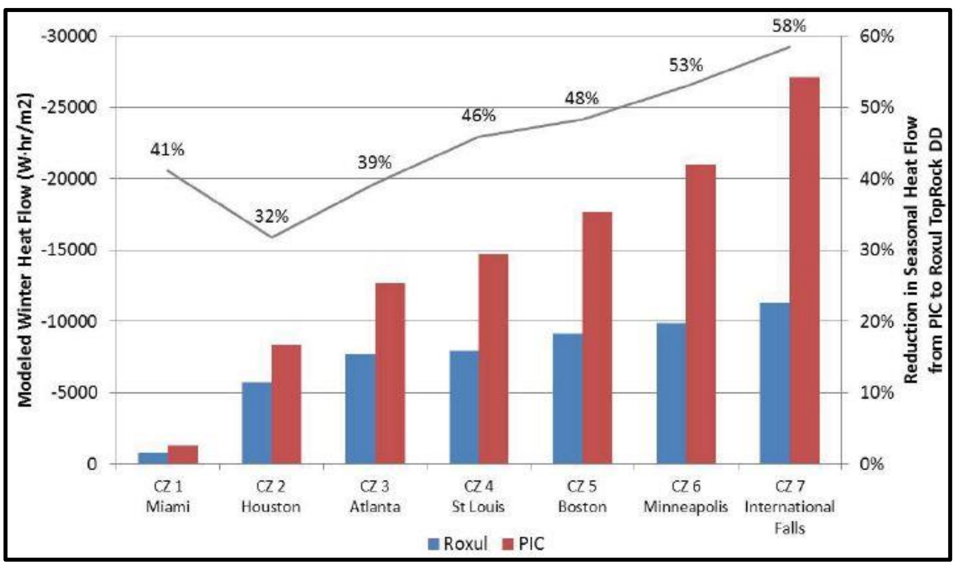

Figure 3-17: Modeled Winter Heat Flow (retrieved from Grin, Schumacher, and Smegal, 2014)

Limitations:

- No experimental testing was done to validate the model.
- This study was done to demonstrate the influence of temperature on the thermal properties of insulation; therefore thermal impact factors were not considered.

3.2.7. Gulati, Suddapalli, and Srinivasan (2016)

Roof fasteners in metal deck roofing systems penetrate through several layers of the assembly in order to secure the system and prevent wind induced uplift forces. In the event of a roof is damaged, the assembly is either replaced or re-covered, which is known as “reroofing” and “re-covering” respectively. Reroofing is the processes of replacing an existing roof cover, while re-covering is the installation of an additional roof cover over an existing one to conceal the damaged substrate. Using the reroofing method to repair a roof system leaves holes in the assembly as a result of the previously installed fasteners, while re-covering leaves existing fasteners in place while additional fasteners are installed to secure a new cover. These additional fasteners result in an increase of fastener density per unit area. Both options leave the roof system more susceptible to thermal losses, as both holes in the substrate and larger fastener density lead to a thermal bridging. Gulati, Suddapalli, and Srinivasan (2016) studied the effects of thermal bridging as a result of re-roofing and recovering and discuss the impact of metal fasteners during those scenarios. The authors modelled and two re-covering assemblies (Figure 3-18) and four reroofing assemblies (Figure 3-19). It is evident that the presence of fastener holes with re-covering (Figure 3-20a) and the additional fasteners with reroofing (Figure 3-20b) had a large influence on the heat flow. Since this is an on-going project, thermal values and conclusions have not yet been stated.

Type	Fastening Pattern	Section
1	Single-ply, mechanically fastened at laps 12 in. o.c.; perimeter mechanically fastened at laps 12 in. o.c. with one additional row of fastening in the center; corner mechanically fastened at laps 12 in. o.c. with two additional rows of fastening.	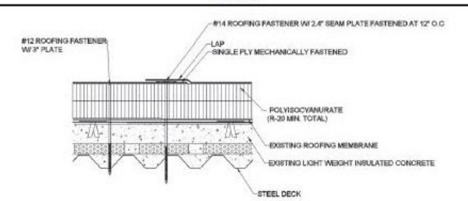
2	Base ply mechanically fastened at laps 12 in. o.c.; perimeter mechanically fastened at laps 12 in. o.c. with one additional row of fastening in the center; corner mechanically fastened at laps 12 in. o.c. with two additional rows of fastening. Insulation and cover board preliminary fastened. Top cap ply adhered.	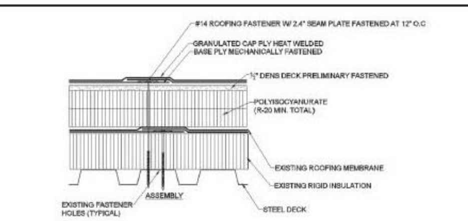

Figure 3-18: Re-Covering Assemblies (retrieved from Gulati, Suddapalli, and Srinivasan, 2016)

Type	Fastening Pattern	Section
1A	Base ply mechanically fastened at laps 6 in. o.c.; perimeter mechanically fastened at laps 6 in. o.c. with one additional row of fastening in the center; corner mechanically fastened at laps 6 in. o.c. with two additional rows of fastening. Insulation and cover board preliminarily fastened. Base ply is mechanically fastened; top cap ply adhered.	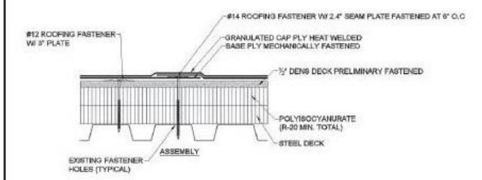
2	Field, one fastener every 4 sq. ft.; perimeter, one fastener every 2 sq. ft.; corner, one fastener every 1 sq. ft.	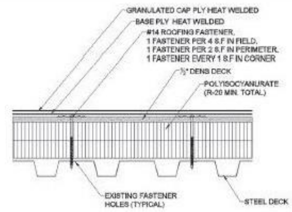
3	Field, one fastener every 4 sq. ft.; perimeter, one fastener every 2 sq. ft.; corner, one fastener every 1 sq. ft.	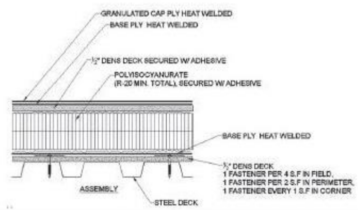
4A	Field, 6 fasteners per board; perimeter, 10 fasteners per board; corner, 15 fasteners per board with single layer of polyisocyanurate insulation.	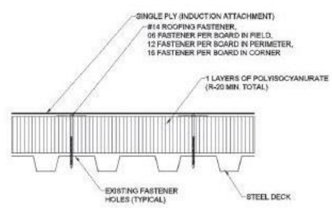

Figure 3-19: Reroofing Assemblies (retrieved from Gulati, Suddapalli, and Srinivasan, 2016)

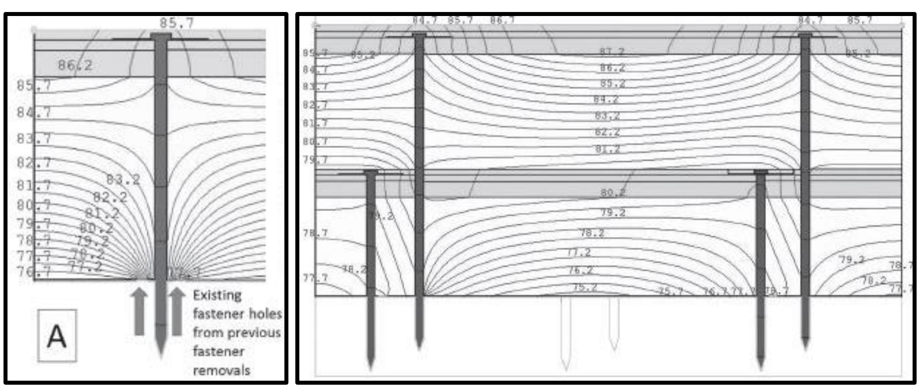

Figure 3-20: (a) Reroofing and (b) Re-Covering Heat Flux Vectors (retrieved from Gulati, Suddapalli, and Srinivasan, 2016)

Limitations:

- The tests were modelled on one type of insulation (polyisocyanurate insulation); therefore the effect of insulation type on thermal properties cannot be determined.
- Experimental testing was not done to validate the modeling.
- A correlation between fastener density and thermal losses is not yet established.

3.3. Thermal Analysis via Experimental Testing

The following studies are the most relevant in terms of experimental literature done in this field. The studies are organized in chronological order to show the progression of experimental testing, their accuracy and significance in this field.

3.3.1. Hedlin (1985)

Hedlin (1985) studied the heat loss for several insulation gaps on extruded polystyrene (EPS) insulation in two roofing configurations: conventional roofing and protected membrane arrangement. Measurements are done on gaps ranging in width from $2.5\,mm$ to $25.4\,mm$. Figure 3-21 displays a generalized roof assembly with a deck, insulation and a heat flow meter sensor to measure the heat flow.

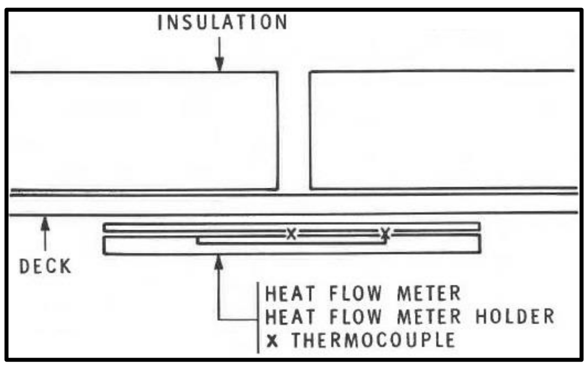

Figure 3-21: System Configuration (retrieved from Hedlin, 1985)

Six heat flow meters are installed along the insulation to monitor the dissipation of heat; each heat flow meter is $50\,mm$ wide measuring the respective area. Figure 3-22 shows the measured data at each heat flow meter. This is an in-situ study which has a lot of limitations do the limited methods of measuring thermal properties of built assemblies.

Hedlin concludes that the heat losses are estimated to range from 4% to 35% for the respective insulation gaps. It is also found that the gaps effect dissipates $100\,mm$ away from the gap edge, as measurements at $125\,mm$ and $300\,mm$ from the edge of the gap are nearly equal. An equation is interpolated from the data to describe the effect of insulation gaps on the heat flow.

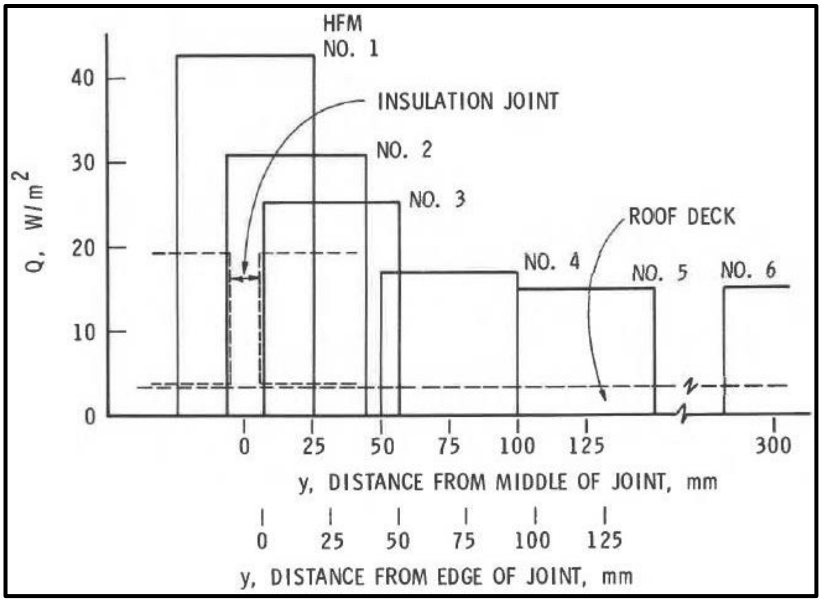

Figure 3-22: Measure Heat Flow along Insulation (retrieved from Hedlin, 1985)

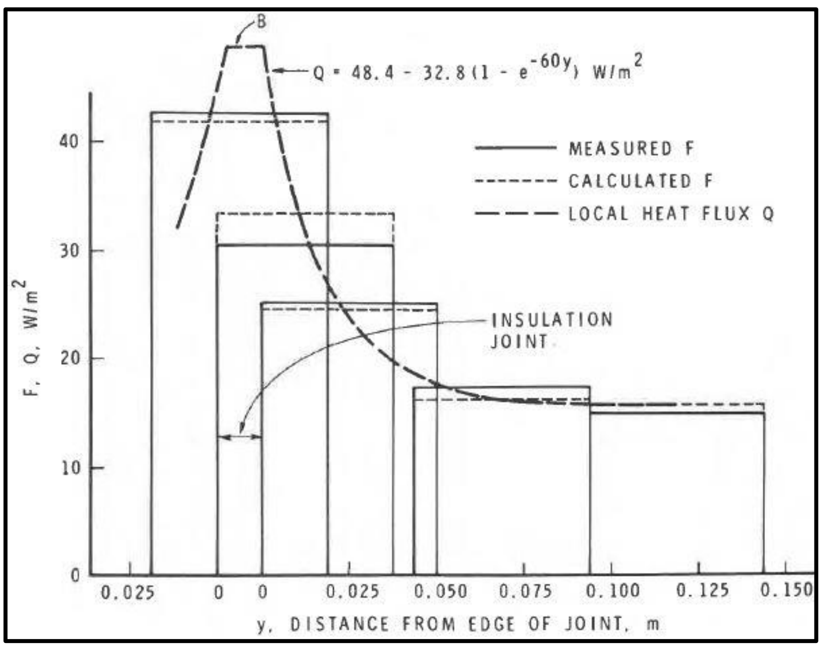

Figure 3-23: Measure and Calculated Heat Flow (retrieved from Hedlin, 1985)

Limitations:

- This is an in-situ study; therefore the only method for measuring thermal properties is by heat flow sensors. The relationship between lateral and vertical heat flow is unknown, therefore it is difficult to characterization the heat flow though the gap.
- Effect of gap width and gap height was not identified.

3.3.2. Petrie et al. (2000)

Petrie et al. (2000) investigated the effects of thermal impact factors on the thermal performance of metal-deck, low-slope roofs with polyiso insulation. Tests were done on single and double layer insulation boards $50.8\,mm$ (2") thick. The tests were run in accordance to the ASTM C1363, using a large-scale climate chamber shown in Figure 3-24, with a test area of $2.44\,m \times 2.44m$ ($8ft \times 8ft$). An array of mean temperatures were tested ranging from $-1℃$ to $51℃$ listed in Figure 3-25.

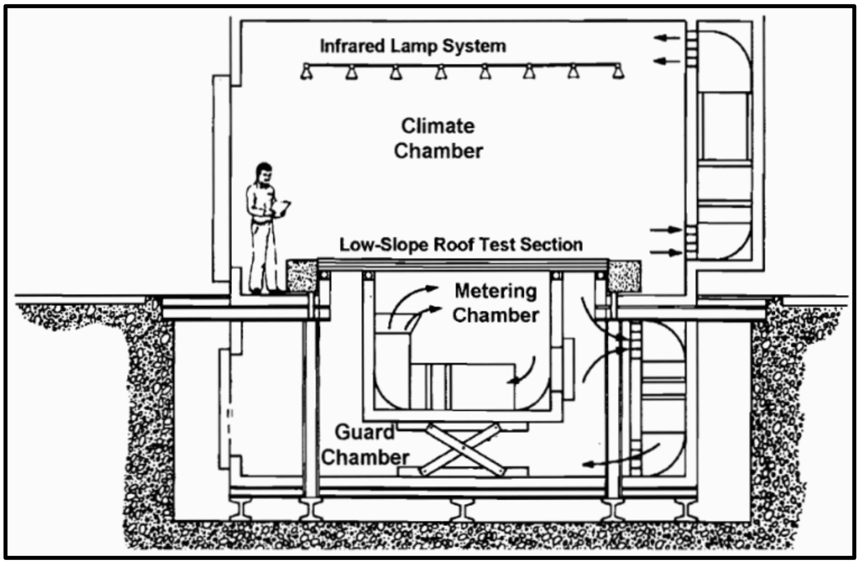

Figure 3-24: Schematic of Large Scale Climate Simulator (retrieved from Petrie et al., 2000)

Tests were first run on opaque assemblies (without fasteners or gaps) to establish a baseline performance, and then tested with fasteners and gaps. Fasteners were test were at a density of 1 fastener per $0.18\,m^2$ ($2ft^2$), totaling 32 fasteners. Gap tests were done with a $25.4\,mm$ (1") gap between the insulation boards.

Table 1. Conditions imposed on the roof assemblies in steady-state tests for the effects of fasteners and gaps on the thermal performance of low-slope roofs. The configurations involved one or two layers of polyisocyanurate insulation, each layer 5.1 cm (2 in.) thick.

Mean Insulation Temperature °C (°F)	Climate Chamber Air Temperature °C (°F)	Meter Chamber Air Temperature °C (°F)	Configurations
–1 (30)	–23 (–10)	21 (70)	One and two layers
10 (50)	–1 (30)	21 (70)	One and two layers
24 (75)	41 (105)	7 (45)	One and two layers
34 (93)	43 (110)	24 (75)	One layer only
37 (98)	66 (150)	7 (45)	One and two layers
51 (123)	91 (195–196)*	7 (45)	Two layers only

Figure 3-25: Conditions Imposed on Roof Assembly (retrieved from Petrie at al., 2000)

Petrie et al. concluded that the use of conventional steel plate fasteners resulted in a thermal resistance loss of 12%, whereas plastic plate fasteners had a thermal resistance loss of 3%. The 25.4 mm gap between insulation boards resulted in 15% loss of thermal resistance for two layers of insulation boards and a 17% loss in single layer tests. The results of the tests are plotted in Figure 3-26, it can be seen the gaps have a most critical effect on the thermal resistance of the insulation; however, 25.4 mm gaps are a very extreme case.

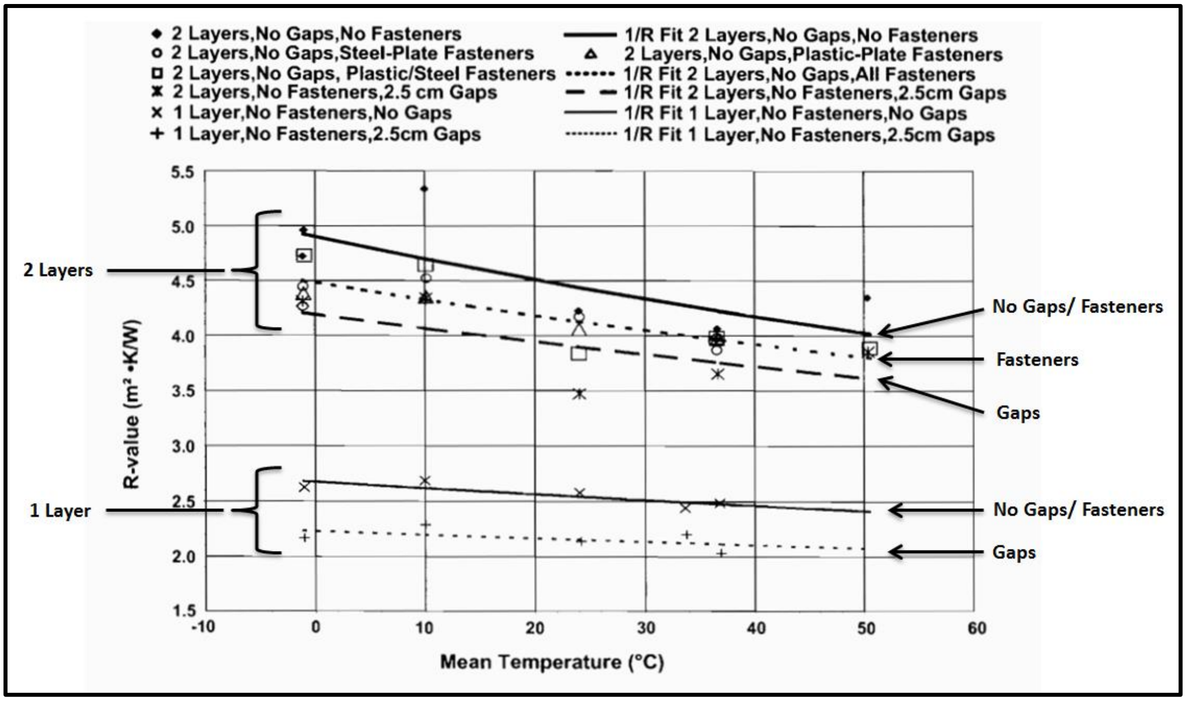

Figure 3-26: R-Values for the Effects of Gaps and Fasteners (retrieved from Petrie et al., 2000)

Limitations:

- The tests were conducted on only one type of insulation; therefore the effect of insulation type on thermal performance of the roof assembly cannot be observed.
- A single fastener density and gap width were tested, therefore their effect on the thermal transmittance of the insulation cannot be observed.
- The relationship between the mean temperature and R-value is not typical for this type of insulation.

3.3.3. Building Science Corporation (2005)

When measuring thermal resistance, testing is done in accordance to the ASTM standard at a mean temperature of 24°C (75°F); however, this temperature does not reflect typical in-service temperature conditions. Polyiso insulation is a popular commercial roof insulation with one of the highest thermal resistance per unit thickness. The Building Science Corporation (2013) has conducted a study to look at performance between different polyiso manufacturers and the variation of thermal resistance in-service conditions. The results from the thermal testing of polyiso insulation is summarized in Figure 3-27, it is obvious that polyiso exhibits undesirable tendencies as temperatures deviate from the reporting temperature. This is a concern that must be addressed as polyiso insulation performs at 80% of the reported value in winter climates.

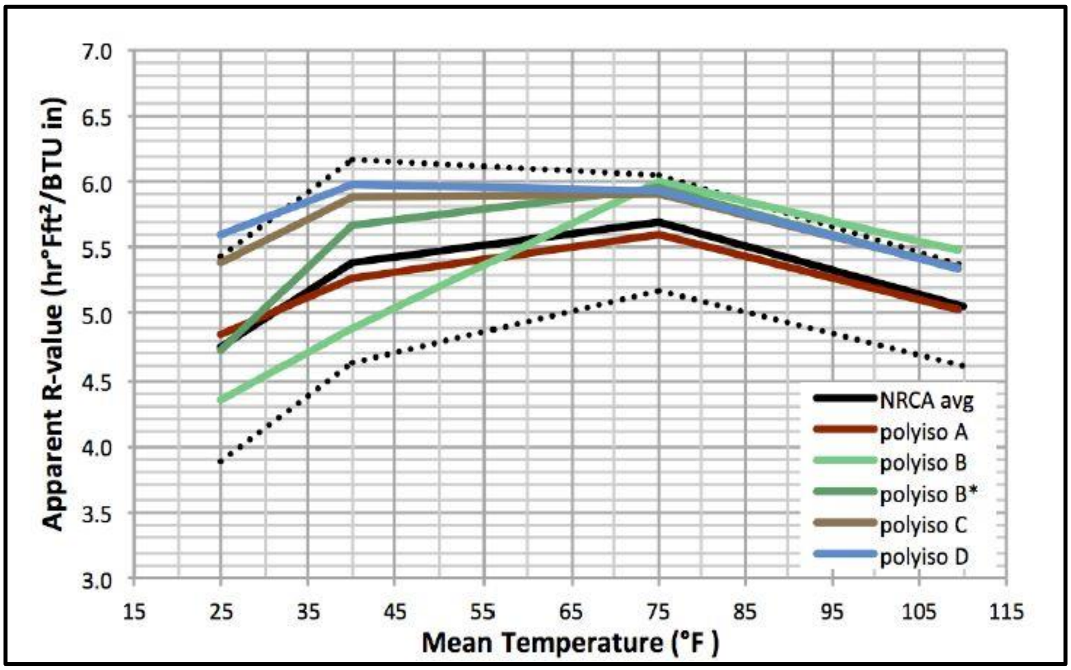

Figure 3-27: Thermal Resistance Variation for Polyiso Insulation (retrieved from the Building Science Corporation, 2005)

Limitations:

- This study was done to demonstrate the influence of temperature on the thermal properties of insulation; thermal impact factors were not considered.

3.4. Concluding Remarks

A review of all applicable literature in this field shows that an array of theoretical and experimental tests has been done on a variety of components and assemblies, studying the effects of thermal impact factors, insulation properties and reporting temperatures. However, the literature is limited to expressing that the thermal performance of roofs is compromised at in-service conditions without appropriate remedies that may be applied to reach the building code design values. The individual effects of fastener types and density, insulation board gaps and thickness, and the effect of temperature variation on the insulation performance have been studied without a solution for appropriate implementation. All literature studies regard the effects of these thermal losses on specific components or assemblies, without generalizing the results for the application of all insulation boards, cross-sections, thicknesses or configurations

Current research done by numerical modelling is accurate in terms methodology, but very limited to its boundaries and parameters as it has never been validated with in-situ monitoring or experimental testing. There is a necessity for experimental testing to provide test parameters and validate all numerical models. With the rising cost of energy and climate change, it has led to the continued increase in requirements for energy efficiency in many new and existing buildings. The studies have shown that thermal impact factors can lead to 20% loss in thermal resistance; building codes require higher levels of thermal control than ever before, and adjustment curves are the next step for increasing the efficiency of the building envelope.

The review of the literature on this topic has shown that thermal impact factors have a clear and significant impact on the thermal performance of roofs. While this conclusion has been stated by all authors, no practical approach has been devised to account for the thermal losses due to these thermal impact factors. All previous literature focused on a single parameter, such as, one insulation type, one insulation thickness, one gap width or one fastener density. These results are therefore not practical for real application, and trends in thermal performance due to the thermal impact factors cannot be conceived. The goal of this research is to quantify the thermal impact factors and devise adjustment curves that are applicable to any roof assembly regardless of insulation type, size, or range of thermal impact factor (gap width or fastener density).

Chapter 4: Experimental Methodology

This chapter illustrates the experimental test setup and methodology used to test and evaluate the thermal performance of roof components and assemblies. The experimental methodology involved measuring thermal transmission properties of the roofing insulation on heat flow meter apparatus (HFM) followed by assembly testing on guarded hot box (GHB). In assembly testing thermal impact factors – fasteners and gap between insulation boards were quantified. The experimental testing also involved measuring the coefficient of expansion and dimensional stability of the roofing insulation to garner data on the potential gap formation. This chapter is in chronological order of tests run.

4.1. Roofing Components

The experimental testing is done on the most commonly used insulation components. This includes three types of insulation boards as illustrated in Figure 4-1.

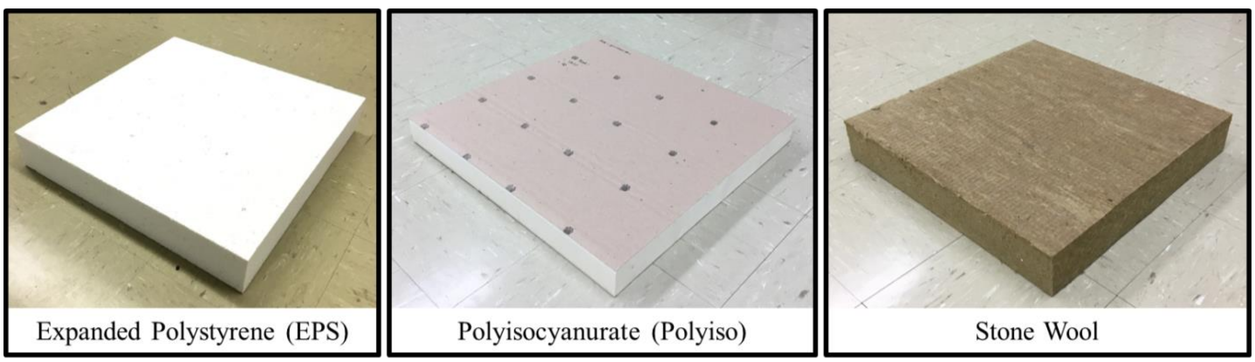

Figure 4-1: Insulation Boards

The manufacturer of each insulation board provided the necessary insulation thicknesses to meet the minimum design requirements for each climatic zone. Table 4-1 lists the thickness for achieving the NECB and ASHRAE specified thermal resistance. The use of two layers of insulation boards is becoming common practice for preventing through gaps; Table 4-2 summarizes the thicknesses of each top and bottom insulation board for achieving the overall thickness to meeting the effective design R-value of each zone.

Table 4-1: Manufacture Provided Thickness for Achieving Respective R-Value

System Thickness	R-26	R-31
Polyisocyanurate (polyiso)	115 mm [4.5”]	135 mm [5.3”]
Expanded Polystyene (EPS)	160 mm [6.25”]	197 mm [7.75”]
Stone Wool	166 mm [6.5”]	203 mm [8”]

Table 4-2: Individual Board Thickness

Board Thickness	R-26	R-31
Polyisocyanurate (polyiso)	$51\,mm + 64\,mm$ [2” + 2.5”]	$51\,mm + 84\,mm$ [2” + 3 1/3”]
Expanded Polystyene (EPS)	$80\,mm + 80\,mm$ [3 1/8” + 3 1/8”]	$98\,mm + 98\,mm$ [3 7/8” + 3 7/8”]
Stone Wool	$64\,mm + 102\,mm$ [2.5” + 4”]	$102\,mm + 102\,mm$ [4” + 4”]

The protection board and membrane do not have a significant thermal performance on roof assemblies; they are used for consistency and to prevent insulation damage from the fastener plate. The protection board and membrane used in the assemblies are Densdeck and PVC membrane respectively shown in Figure 4-2.

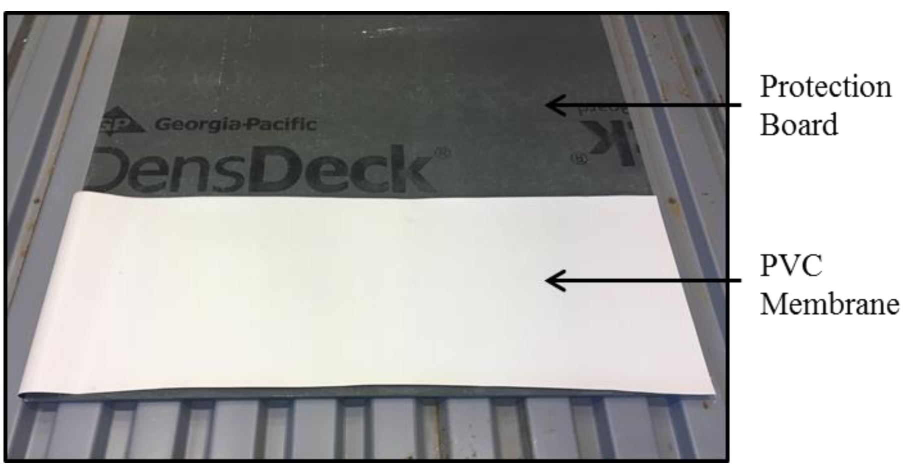

Figure 4-2: DensDeck Protection Board and PVC Membrane

4.2. Heat Flow Meter (HFM)

The heat flow meter (HFM) is used to test the insulation component of the roof assembly. Since the HFM provides fast and reliable properties of thermal insulation, it is an excellent starting point and method for establishing baseline conditions for the thermal insulation. The HFM establishes a steady-state one-dimensional heat flow - meaning thermal properties are assumed under idealized conditions. The HFM measures thermal properties through direct contact of the hot and cold plates with the sample, eliminating the possibility of monitoring the effect of a steel deck, mechanical fasteners or air flow (and therefore surface coefficients). The HFM is used to test opaque components in order to provide baseline conditions and reference values for the calibration of the guarded hot box apparatus; where an Opaque component is insulation without fasteners or gaps. Thermal measurements and calculations for the HFM are done following standard ASTM C518-10 as outlined in section 3.1.2.

Test setup

1. The test specimen is placed on the bottom plate, while the top plate is lowered overtop (Figure 4-3a and Figure 4-3b).
2. An insulation perimeter is placed around the edges of the sample to limit the extraneous and lateral heat losses (Figure 4-3c).
3. The HFM is then covered by an insulated box creating a boundary between room and the test conditions (Figure 4-3d).
4. Compressed air is constantly pumped into the enclosure to lower the relative humidity of the test, since humidity can decrease the thermal resistance of insulation (Figure 4-3e).

Limitations

While the HFM may provide accurate thermal properties for insulation without fasteners and gaps, the apparatus has limitations for the dimensions of test sample. The apparatus allows for the testing of samples 1/3 the thickness of its dimensions. For a $600\,mm$ (24”) wide apparatus, the maximum test sample thickness may be $200\,mm$ (8”); however, with increasing sample thickness an increase in lateral heat flow will occur lowering the accuracy of the apparatus. This concept of lateral heat flow is discussed in the HFM results (section 5.3).

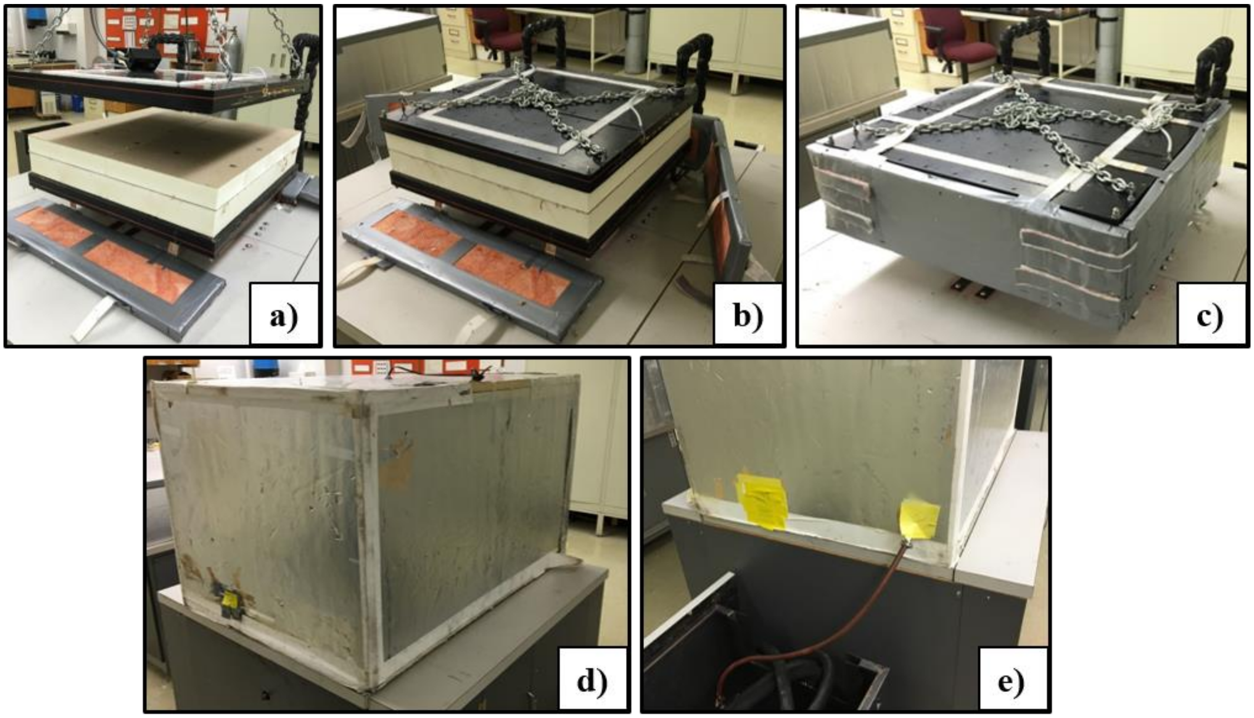

Figure 4-3: Heat Flow Meter Test Setup

Following standard ASTM C1058-10 – Selecting Temperatures for Evaluating Thermal Properties, the HFM tests are run at the mean temperatures listed in

Table 4-3.

Table 4-3: Heat Flow Meter Test Mean Temperatures

Mean Temperature (°C)	Target Top Plate Temperature (°C)	Target Bottom Plate Temperature (°C)	Delta Temperature (°C)
2	-18	22	40
12	-8	32	40
24	4	44	40
42	22	62	40

Note: temperatures are selected with accordance to ASTM C1058-10

The manufacturer provided insulation board thicknesses for achieving the NECB and ASHRAE thermal requirements (listed in Table 4-1) are tested as shown in Figure 4-4 and Figure 4-5.

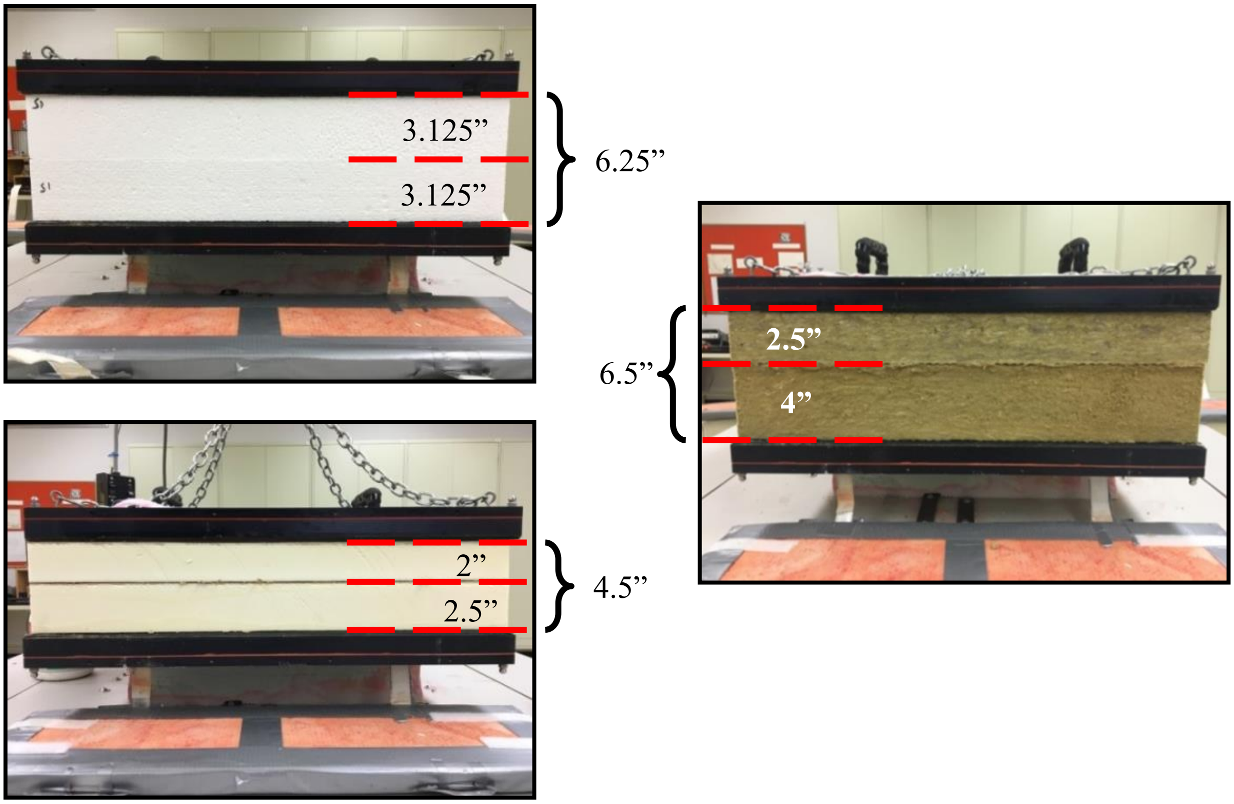

Note: 1” = 25.4mm

Figure 4-4: Manufacturer Provided Thickness for Achieving Design R26

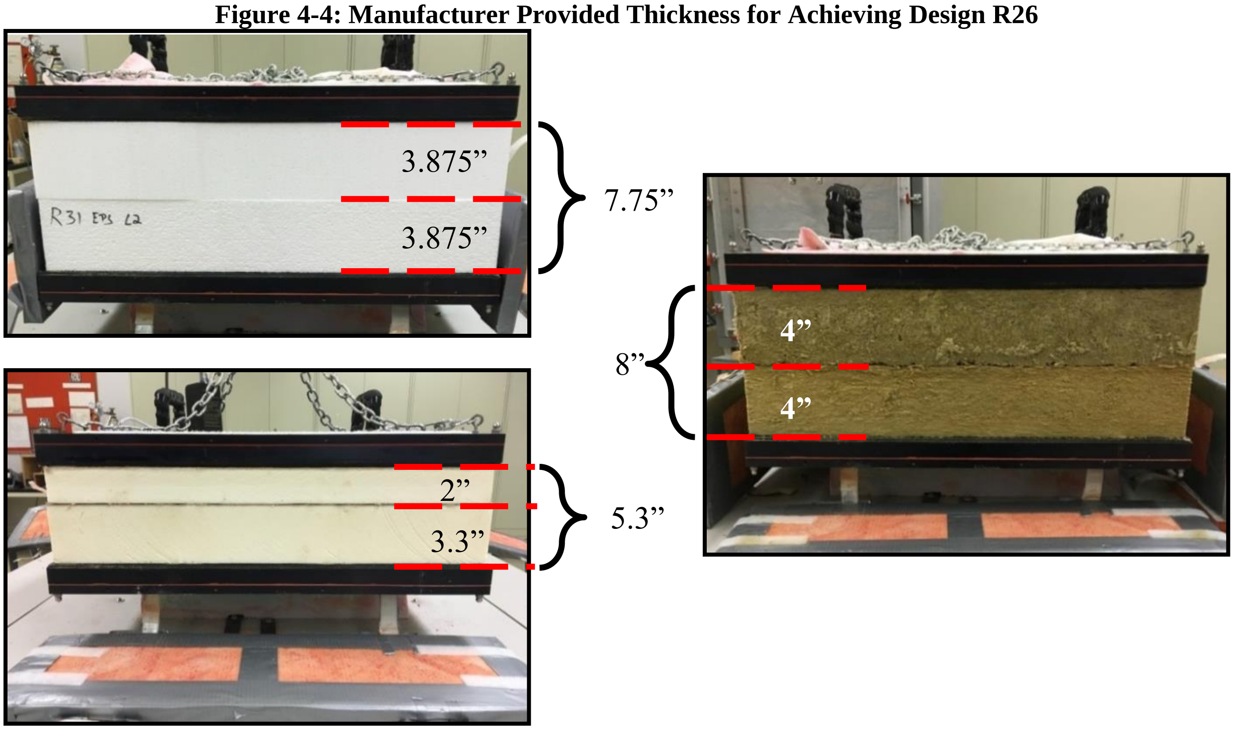

Note: 1” = 25.4mm

Figure 4-5: Manufacturer Provided Thickness for Achieving Design R31

4.3. Coefficient of Linear Expansion

The purpose of the coefficient of linear expansion testing is to determine the dimensional changes insulating materials undergo during heating or cooling conditions; such as summer and winter climates. The measured dimensional changes from this experiment will be used in the identification of the possible size of gap formation between insulation boards. The results, along with the results from the dimensional stability testing will be used to validate the appropriate insulation gap test parameters for the guarded hot box testing.

The coefficient of linear expansion is tested by using linear variable displacement transformers (LVDTs). An LVDT (Figure 4-6) is an electromechanical transducer that can measure the one-dimensional motion of an object. These sensors are installed in the insulation boards to monitor change in dimension over time due to different temperature exposures.

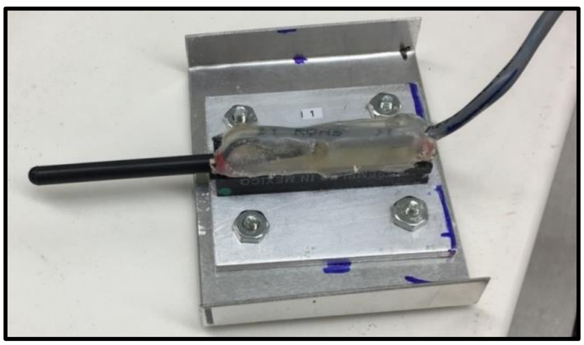

Figure 4-6: Linear Variable Displacement Transformers

Test Setup

1. A steel deck, vapour barrier and Plexiglas are installed to provide a base for the assembly and a rigid flush surface for the exterior facing LVDT (Figure 4-7a).
2. The first layer of insulation is placed and adhered to one side, so the dimensional changes occur only at the LVDT (Figure 4-7b).
3. The second layer of insulation is place with the gap in the center for a staggered configuration with two LVDTs in the center (Figure 4-7c).
4. Thermocouples are placed between each layer to monitor the rate of heat flow through the system (Figure 4-7b and Figure 4-7c).
5. The assembly is covered by a climatic chamber with temperature capabilities of $-10°C$ to $60°C$ for simulating outdoor conditions; the bottom of the chamber is at room temperature simulating indoor conditions (Figure 4-8).

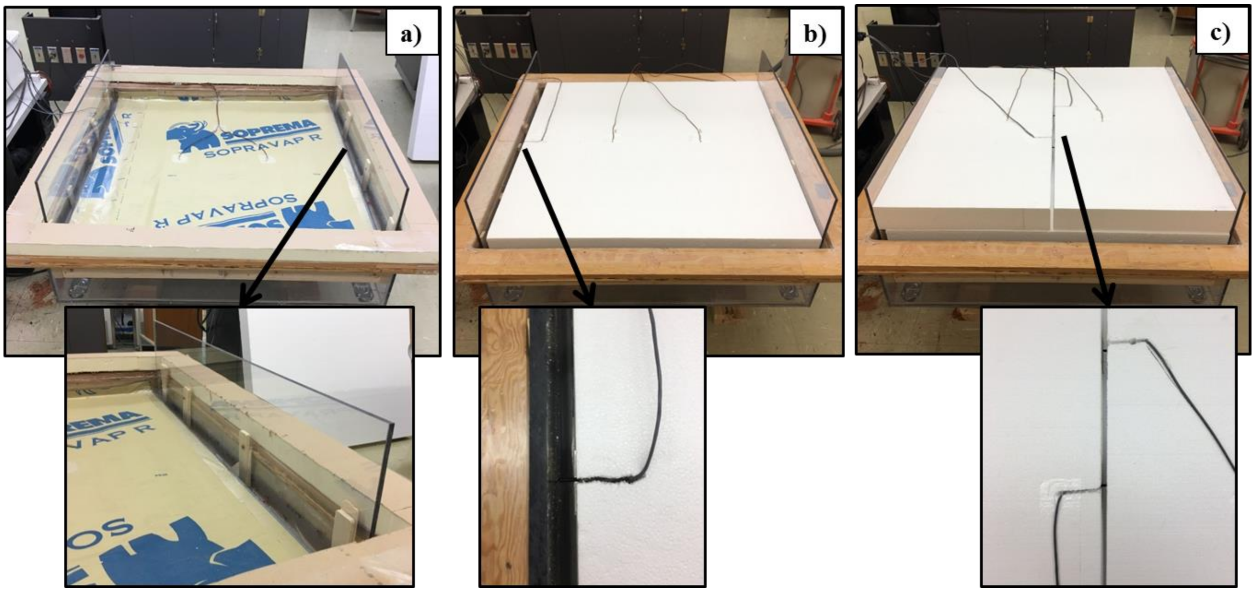

Figure 4-7: Test Configuration and LVDT Location

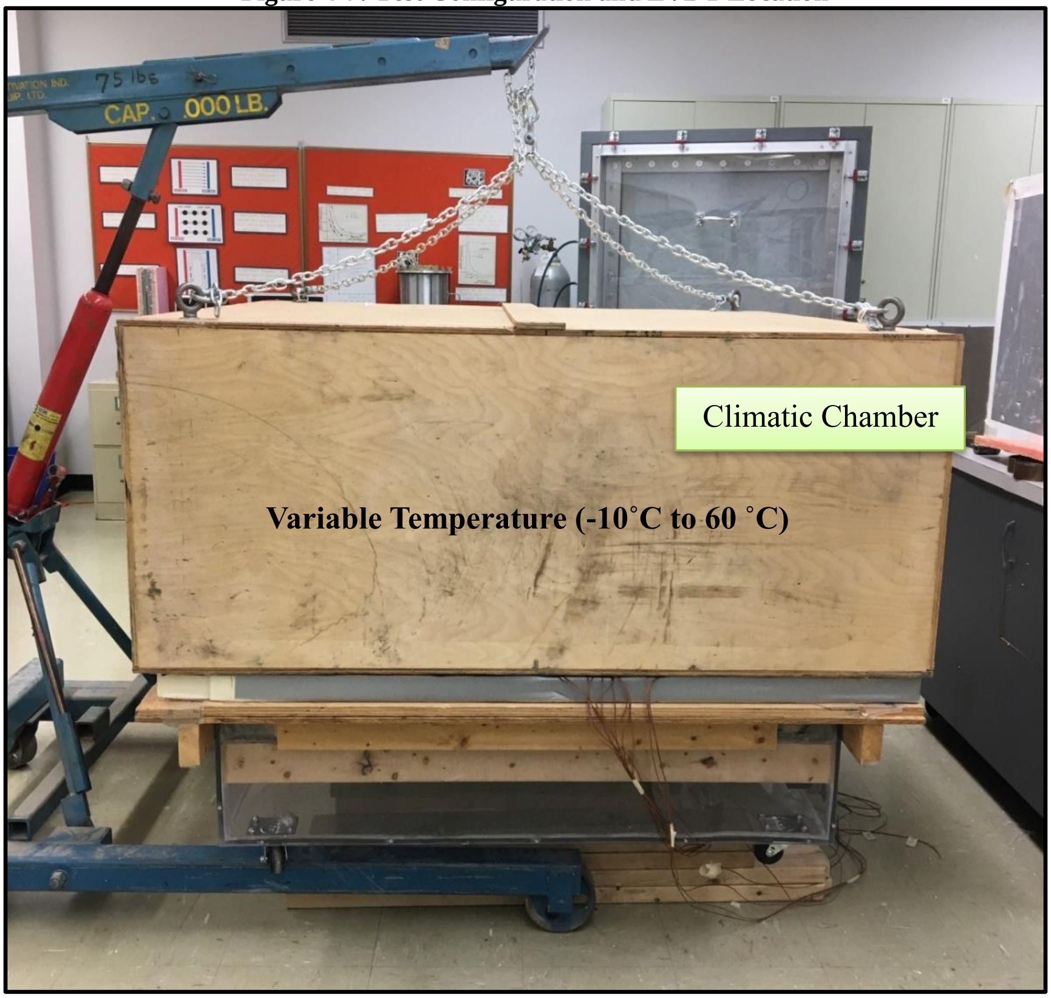

Figure 4-8: Coefficient of Linear Expansion Test Apparatus

4.4. Dimensional Stability

The purpose of the dimensional stability testing is to determine the permanent dimensional changes insulating materials undergo during heating or cooling conditions, such as summer and winter climates. The measured dimensional changes from this experiment will be use in the identification of the possible gap formation between insulation boards. The results, along with the results from the coefficient of linear expansion testing will be used to validate the appropriate insulation gap test parameters for the guarded hot box testing.

The procedure for testing the dimensional stability of a rigid cellular plastic[2] is to expose the samples to extreme conditions, following standard ASTM D2126-09 outlined in section 3.1.4. The insulation samples are placed in a heating (Figure 4-11) and cooling (Figure 4-12) chamber and subjected to the temperatures and conditions outlined in the test standard. After exposure, the samples are left in room temperature conditions for two hours before measuring the dimensions (Figure 4-10).

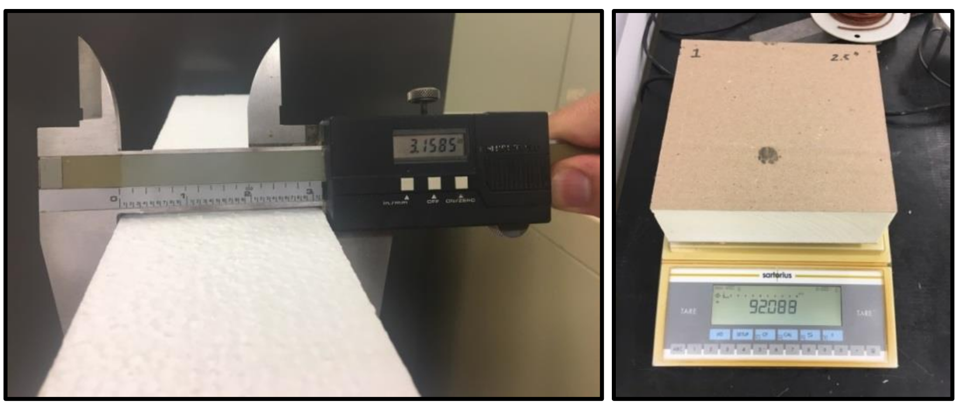

Figure 4-9: Dimensional Stability Measurement Tools

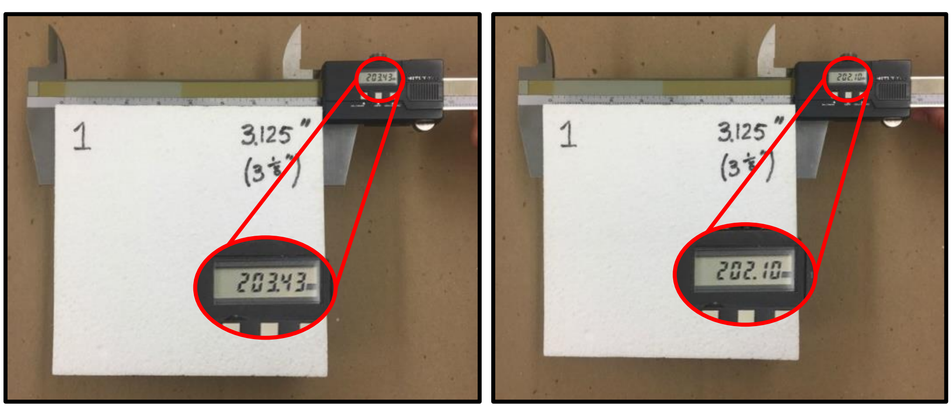

Figure 4-10: Board Dimensions Before and After Dimensional Stability Test

[2] Definition available on page ix

Figure 4-11: Dimensional Stability – Heating Chamber

Figure 4-12: Dimensional Stability – Cooling Chamber

Table 4-4 is a summary of all insulation test standards for the dimensional stability of insulating materials. Each test method has a dimensional limit; the associated dimensions have been calculated from an industry typical insulation board.

Table 4-4: Dimensional Stability Limits of Different Insulation from Test Standards

Material	Standard		Test Method	Limits (based on 4'x4' board)
	Designation	Title		
EPS	CAN/ULC S701-11	Thermal Insulation, Polystyrene, Boards and Pipe Covering	ASTM D2126	1.5% (3/4")
	ASTM C578-12	Standard Specification for Rigid, Cellular Polystyrene Thermal Insulation	ASTM D2126	2% (1")
Polyiso	CAN/ULC S704-11	Standard for Thermal Insulation, Polyurethane and Polyisocyanurate Boards, Faced	ASTM D2126	2% (1")
	ASTM C1289-13	Standard Specification for Faced Rigid Cellular Polyisocyanurate Thermal Insulation Board	ASTM D2126	2% (1")
Stone Wool	CAN/ULC-S702.1-14-AMD1	Standard for Mineral Fiber Thermal Insulation for Buildings	NO Requirements	N/A
	ASTM C726-12	Standard Specification for Mineral Wool Roof Insulation Board	ASTM D2126	1% (1/2")

4.5. Guarded Hot Box Apparatus (GHB)

The guarded hot box (GHB) is used to measure the thermal resistance and transmittance properties of roofing components and assemblies. Using this apparatus, thermal impact factors such as mechanical fasteners and insulation gaps can be accurately tested and their influence quantified.

Figure 4-13 illustrates the different components of the GHB, the guard chamber, the metering chamber and the climatic chamber. The metering and climatic chambers create the temperature test parameters and measure the heat flow through the test assembly. The purpose of a guard chamber is to prevent any thermal losses through the metering chamber walls to the environment.

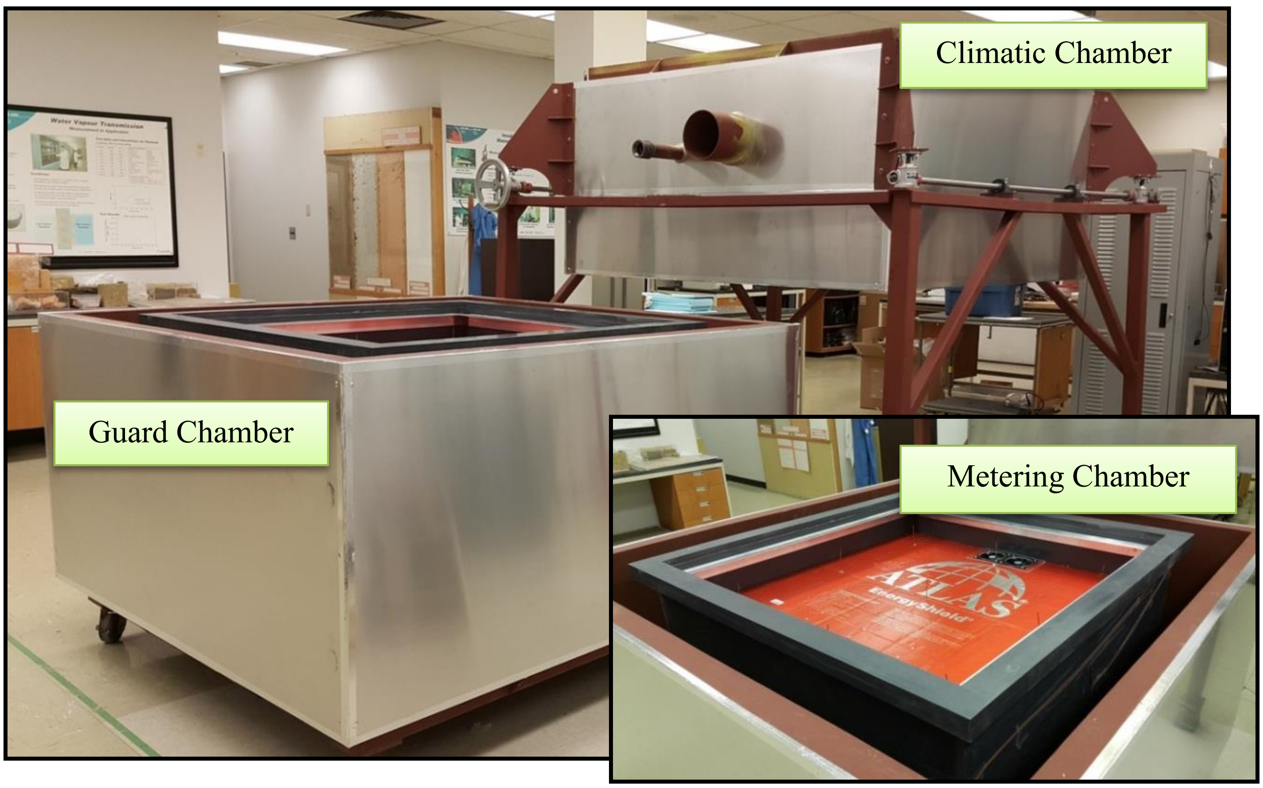

Figure 4-13: Guarded Hot Box Chambers

Figure 4-14 shows a schematic of the GHB, the test results are obtained by measuring the heat flow from the metering chamber through the test assembly to the climatic chamber. In this chamber configuration the temperature of the metering chamber and guard chamber are kept equal. Any heat lost through the guard chamber to the environment is replenished by a separate heater; the energy consumption of this heater is not measured, turning on when the temperature of the chamber lowers maintaining a constant temperature. With equal temperatures between both chambers, heat loss from the metering chamber to the guard chamber is prevented, leaving a path of heat flow only through the assembly into the climatic chamber.

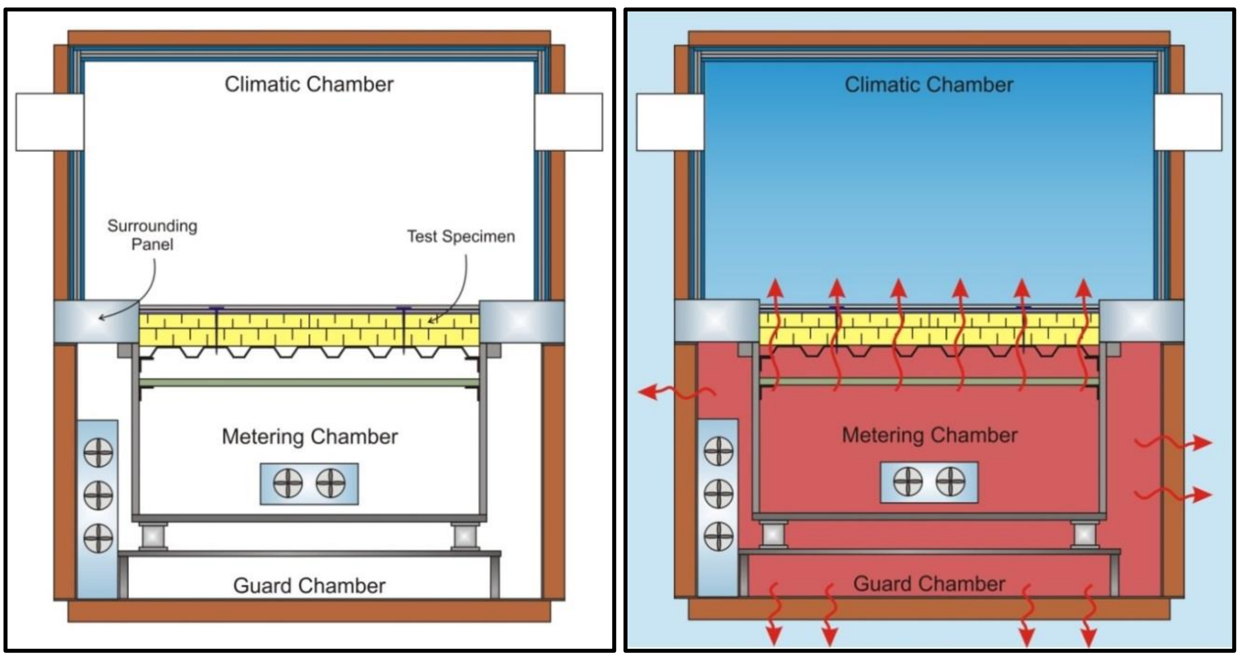

Figure 4-14: Guarded Hot Box Apparatus

4.5.1. Construction of the Guarded Hot Box

The following is the procedure for the construction of the GHB:

1. The main structure of the GHB is made from steel. All the walls of the test chamber are insulated with spray foam on the exterior side and outfitted with stainless steel sheets (Figure 4-15).

Figure 4-15: Insulating the Exterior Walls of the GHB

2. The interior walls of the test chamber are well insulated with a thermal resistance of R40 (Figure 4-16). In order to ensure an air tight chamber, any openings or joints are spray foamed, silicone topped and finally covered using air and moisture resistant tape (Figure 4-17).

Figure 4-16: Insulating the Walls of the Guard Chamber

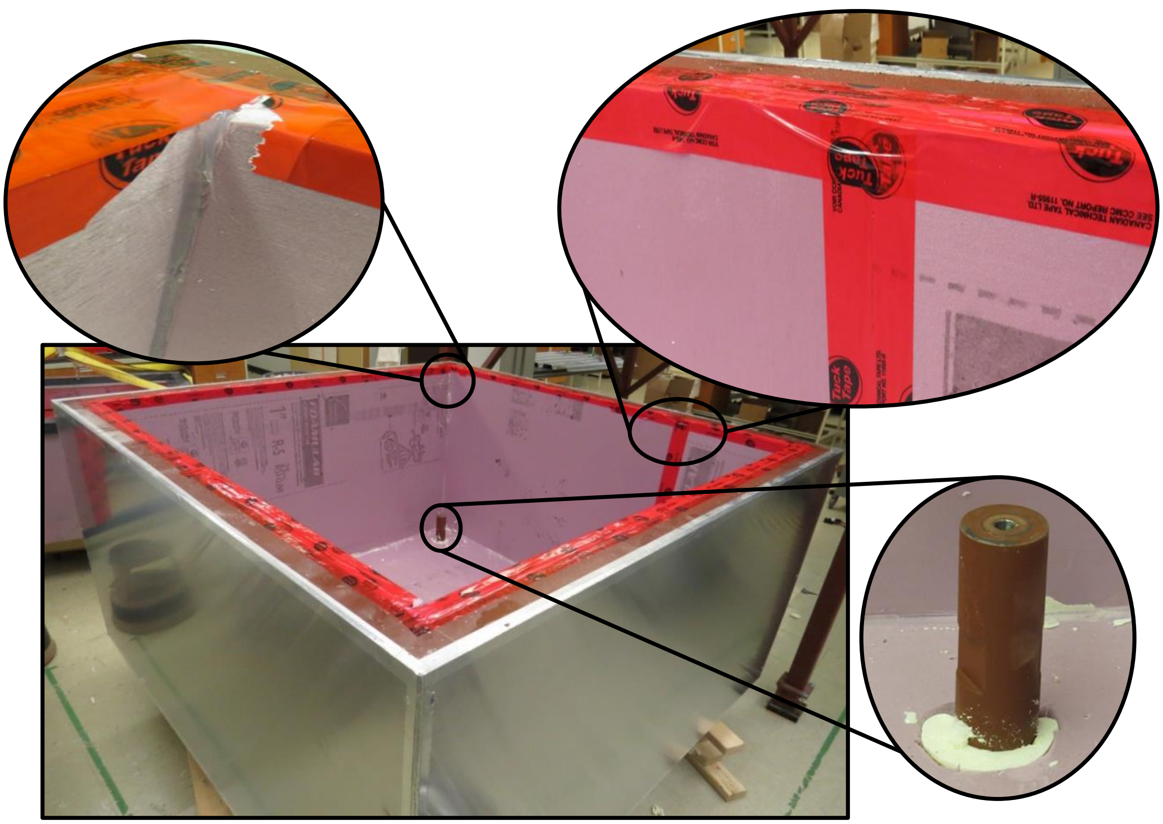

Figure 4-17: Air and Moisture Proofing the Chamber

3. Next, the metering chamber, made from PVC, is insulated using the same procedure as the guard chamber. Thermal couples are placed on the surface and extending from the surface of the metering chamber as required by standard ASTM C1363-11 (Figure 4-18).

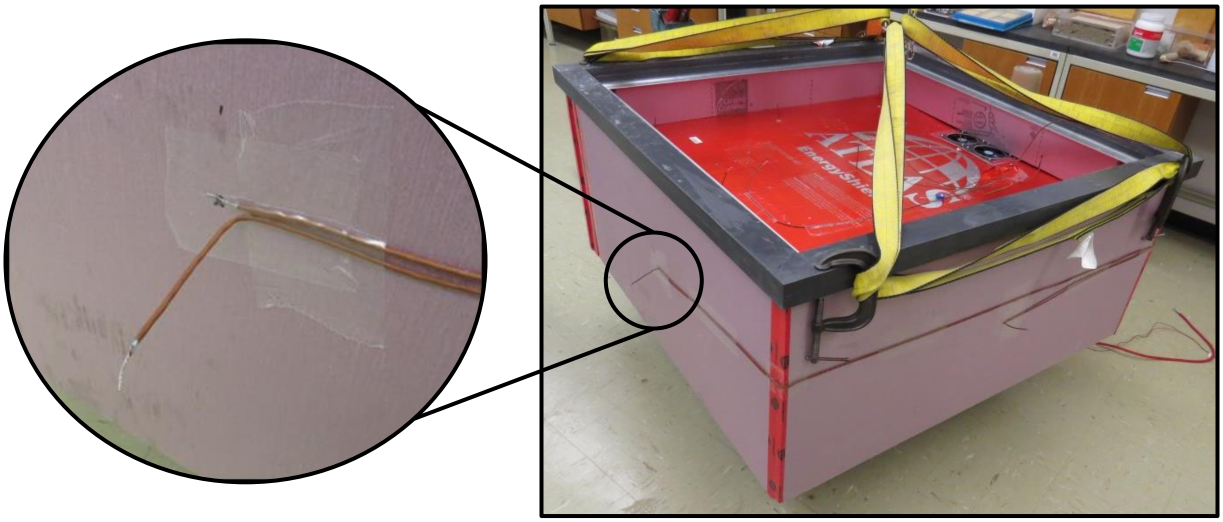

Figure 4-18: Insulated Metering Chamber and Thermal Couple Installation

4. The metering chamber is then placed inside of the guard chamber, and an air barrier is installed to prevent any air or moisture migration between the two chambers (Figure 4-19).

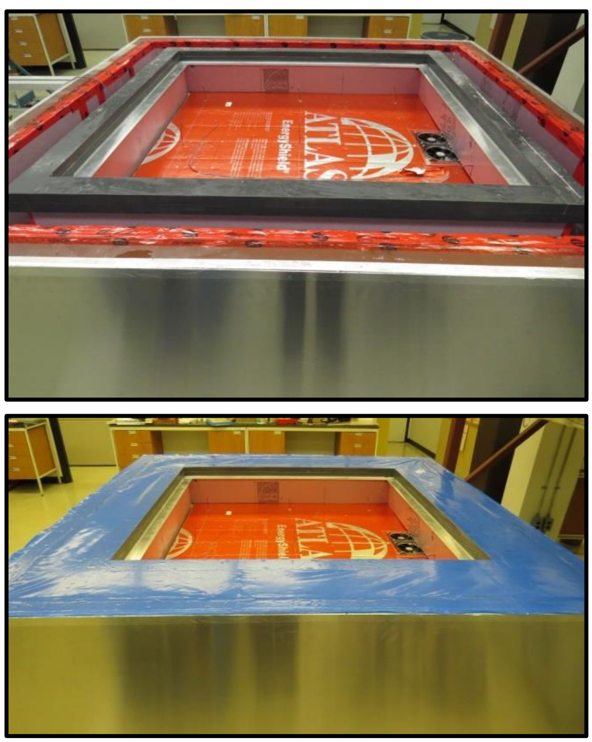

Figure 4-19: Assembled Guarded Hot Box

5. The climatic chamber (Figure 4-20) is insulated similarly to the guard and metering chambers. The measured thermal losses are only recorded for the metering chamber. The climatic chamber is only used to create a temperature gradient[3], any losses that are replenished by the cooling unit do not bring errors into the measured data.

Figure 4-20: Climatic Chamber

Figure 4-21 is the completed GHB and a test schematic.

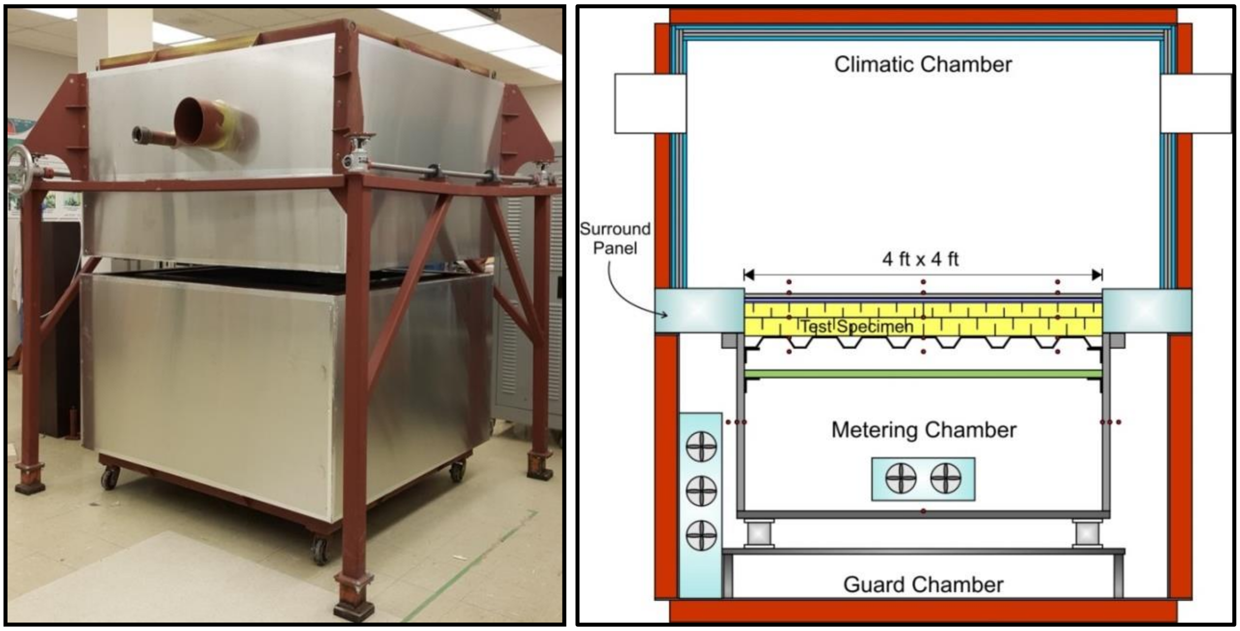

Figure 4-21: Completed Guarded Hot Box Apparatus

[3] Definition available on page ix.

4.5.2. Calibration

This section covers the measurements and theory involved in calibrating the new GHB apparatus. In order to properly calibrate a test apparatus, there must be an understanding of what the accuracy and precision of measurements are.

Accuracy refers to the proximity of a measured value to a standard or known value. If a 10 kg mass is weighed on a scale and the scale reading is 6.5 kg, the measurement is not accurate.

Precision (or repeatability) is the variation in measurements recorded by an instrument or apparatus under the same conditions. Using the example above, if a 10 kg mass is weighed five times and the scale reads 9.9 kg each time, the apparatus is very precise.

Understanding accuracy and precision is important for calibration, because if an apparatus is not accurate, an offset can be applied to the measured value to account for the difference in measured data. If an apparatus is not precise, a single offset will not be applicable to the results, therefore the measurements will be inconsistent, and the data will be incomparable.

Calibration of the GHB followed the test standard "ASTM C1363-11: Thermal Performance of Building Materials and Envelope Assemblies by Means of a Hot Box Apparatus". The significant requirements and limitations for calibration are summarized:

- To gain confidence in the test result of the hot box apparatus, it is necessary to compare the measurements to those of homogenous boards whose thermal properties are uniform and predictable. These boards have their thermal performance measured on a device that yields results to a national standards laboratory, for example test method ASTM C518: Steady-State Thermal Transmission Properties by Means of the Heat Flow Meter Apparatus (ASTM C1363 Cl.1.3.2. pg.1).
- In an ideal hot box test, there is no temperature difference that would drive heat across the boundary of the metering chamber walls. However, since maintaining a perfect guard is not possible, small corrections are needed to accurately characterize the heat flow. At steady state conditions, the heat transfer through the specimen equals the electrical power to the heater and fans, corrected for the heat passing through the chamber walls and flanking the specimen (ASTM C1363 Cl.1.3.1. pg.1).

- The metering wall losses must be less than 10% of the specimen heat transfer (ASTM C1363 Cl.6.5.3.2. pg.9).
- For uniform test results, the maximum point to point air temperature variation across the test board (perpendicular to the airflow direction) shall be less than 2% of the overall air to air temperature difference (ASTM C1363 Cl.6.8.6. pg.10).
- The precision for the apparatus is based on an experiment done during the 1980's, where 21 laboratories with a hot box apparatus were sent homogenous specimens from a controlled batch ensuring a uniform product. The thermal properties were measured and compared at a mean temperature of 24℃. The reproducibility intervals based upon these tests are presented in Figure 4-22 (ASTM C1363 Cl.13.2.1. pg.20-21).

TABLE 2 Reproducibility Test Results—Homogeneous Specimens—ASTM Hot Box Round Robin (19)

Mean Temperature (°C)	Reproducibility Interval (%)		Difference in Resistance (m^2K/W)
	Calibrated	Guarded	
4	13.6	14.6	± 0.22
24	14.4	15.6	± 0.22
43	15.4	17.2	± 0.22

Figure 4-22: Guarded Hot Box Precision Interval

These five GHB calibration criteria are to be met to insure the accuracy and validity of the results.

4.5.3. Temperature Offset

In an ideal situation the guard and metering chambers would be at the exact same temperature; any thermal losses to the environment would come from the guard chamber and the metering chamber would not have any thermal losses (Figure 4-23). The heat lost from the guard chamber would be restored by the heater in the chamber, which would turn on as necessary. This would prevent any losses from the metering chamber and maintain a constant heat flow only through the test assembly. Since maintaining two identical temperatures between the metering and guard chambers is not possible, small corrections for the heat passing through the chamber walls are required as outlined by ASTM1363-11 Cl.1.3.1.

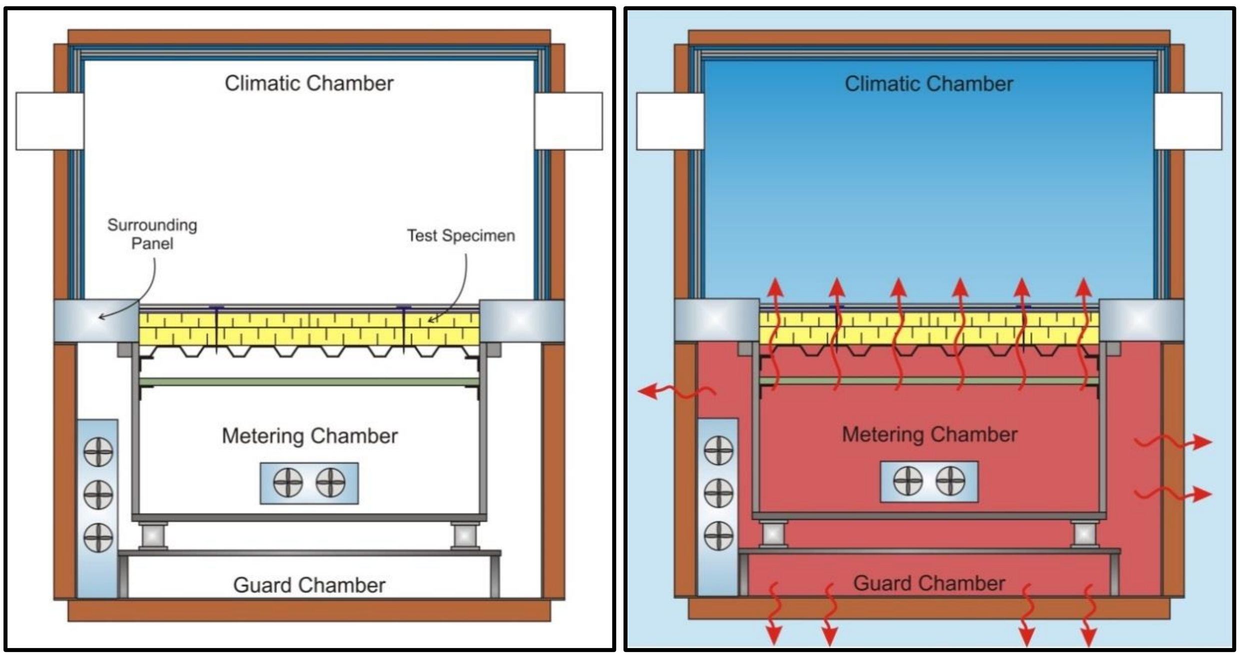

Figure 4-23: Ideal Guarded Hot box

In practice, there are two possible temperature scenarios:

a) The temperature is higher in the guard chamber (Figure 4-24a), simulating higher performance for the assembly. This is because the heat lost through the insulation will be restored in the metering chamber by the heat flowing inward from the guard chamber. Since all the heat lost through the assembly will be restored, measurements will show that the assembly is not allowing any thermal losses.

b) The temperature is lower in the guard chamber (Figure 4-24b); this would result in heat flowing out of the metering chamber into the guard chamber. This will simulate a worse assembly performance, since a larger quantity of heat is lost.

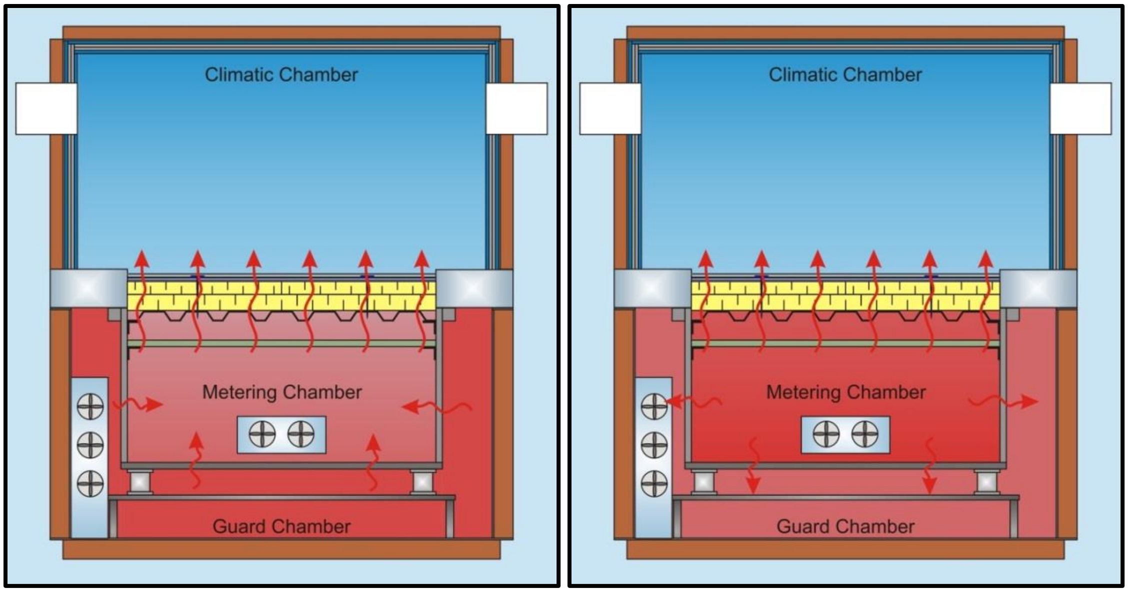

Figure 4-24: Chamber Temperature Scenarios

It is important to determine the offset associated with both situations to account for these losses as they occur during testing. In order to characterize the thermal loss between the metering and guard chambers, the temperatures of the metering and climatic chambers are set equal to each other, to eliminate (or at least significantly limit) any heat flow through the assembly (Figure 4-25). Under this condition the only heat flow will be through the chamber wall, measuring the associated loss. Iterations can be run, increasing the temperature difference between the metering and guard chambers to provide a temperature offset curve.

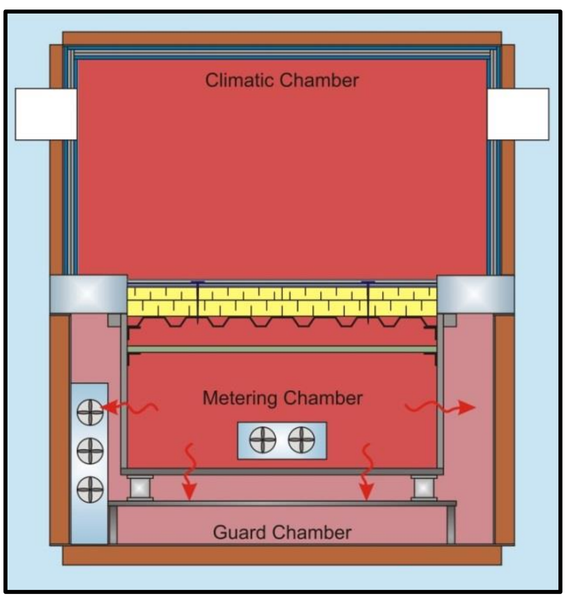

Figure 4-25: Temperature Offset Calibration

(Eqn. 4-1) is used to calculate the energy required to raise the temperature of a chamber based on its volume, specific heat capacity, density of air, and temperature difference between chambers.

$$Q = m \cdot c_p \cdot (T_1 - T_2) \quad \textbf{(Eqn. 4-1)}$$

and

$$m = \rho \cdot V \quad \textbf{(Eqn. 4-2)}$$

where

Q is heat flow $[Watts]$

m is the mass of air $[kg/cu.ft.]$

c_p is the specific heat capacity of air $[KJ/kg℃]$

ρ is the density of air$[kg/cu.ft.]$

V is the volume of air in metering chamber $[cu.ft.]$

Calculating the theoretical temperature offset for heat transfer through the chamber wall is:

$$Q = (0.036 \times 46.85)(1.006)(\Delta T)$$
$$Q = 1.744 \times \Delta T \quad \textbf{(Eqn. 4-3)}$$

ASTM C1363 Cl.6.5.3.2 states that the metering wall losses must be less than 10%. The lowest measured wattage for an opaque system is 10.5 watts, therefore the maximum offset may be 1.05 watts. (Eqn. 4-3) is used to calculate the maximum allowable temperature difference between the metering and guard chambers. The results from the calculation are summarized in Table 4-5, where the maximum temperature offset for 1.05 watts is 0.6℃. Therefore, the largest allowable temperature gradient between the two chambers is 0.6℃.

Table 4-5: Calculated Temperature Offset

ΔT	Watts
0.0	0.000
0.05	0.087
0.10	0.174
0.15	0.262
0.20	0.349
0.25	0.436
0.30	0.523
0.35	0.610
0.40	0.698
0.45	0.785
0.50	0.872
0.55	0.959
0.60	1.046
0.65	1.134

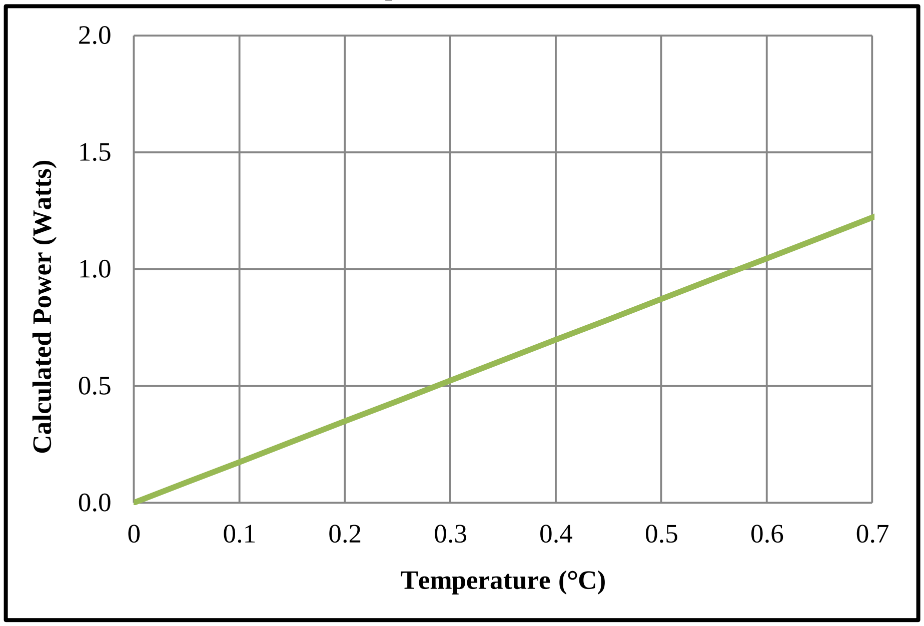

The final temperature offset that must be considered in calibrating the GHB is due to the fans. The purpose of the fans in the metering chamber is to circulate the air, so the hot air does not remain stagnant. Since the fans are constantly on, irrespective of the heater, a significant amount of heat is emitted. The energy emitted by the fans can be calculated using (Eqn. 4-4), where the current and voltage of the fans is measured using an ammeter. There are five fans, three in the guard chamber and two in the metering chamber, the calculation needs to reflect only two fans.

$$W = A \times V \qquad \textbf{(Eqn. 4-4)}$$

where

W is Power ($Watts$)

V is Voltage ($Volts$)

A is Current ($Amps$)

$$W = (0.794) \times (11.894) \times \frac{1\, metering\, fan}{5\, total\, fans}$$

$$W = 1.889\, watts$$

It is important to note that this calibration factor is only applied when the chamber is brought to a temperature below room temperature. When heating the metering chamber, the heater turns on less frequently due to the extra thermal radiations from the fans; the watts used to power the fans are measured and therefore accounted for. However, when the metering chamber is cooled, the cooling unit will expend more energy cooling the chamber due to the added heat from the fans; it is in this case that the fans need to be considered.

4.5.4. Thermocouples

Thermocouples are sensors that are used to measure temperature during tests. A thermocouple consists of two wire conductors that when saturated together form a junction. The temperature can be calculated through the voltage measured. Figure 4-26 shows the process of making a thermocouple as outlined by standard ASTM C1363-11. The thermocouple must be stripped, the wires must be twisted at-least 6 times to prevent separation and sauntered.

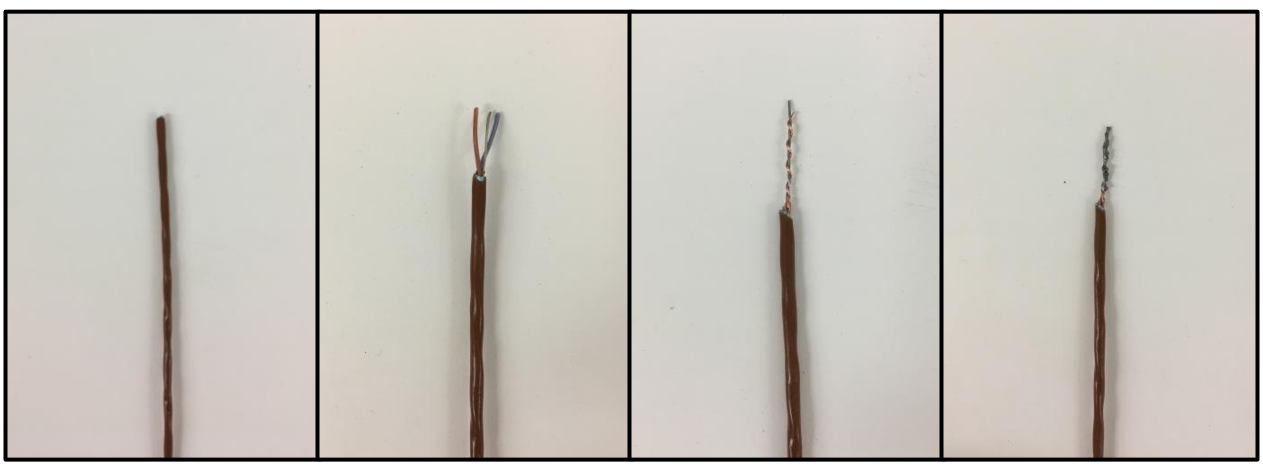

Figure 4-26: Thermocouple

4.5.5. Specimen Installation

The following are the steps for installing a roof assembly in the GHB:

1. The steel deck and thermocouples are placed (Figure 4-27b).
2. The first layer of insulation is placed on top of the steel deck (Figure 4-27c) and silicon is applied around the edge to prevent any air or moisture migration (Figure 4-27d).
3. The second layer of insulation is placed (Figure 4-27e) with another layer of thermocouples and a heat flux sensor, which is used as a reference for the data (Figure 4-27f).
4. A perimeter is installed around the assembly to prevent any lateral heat flow (Figure 4-27f).
5. The protection board and membrane are then placed last (Figure 4-27g and Figure 4-27h).

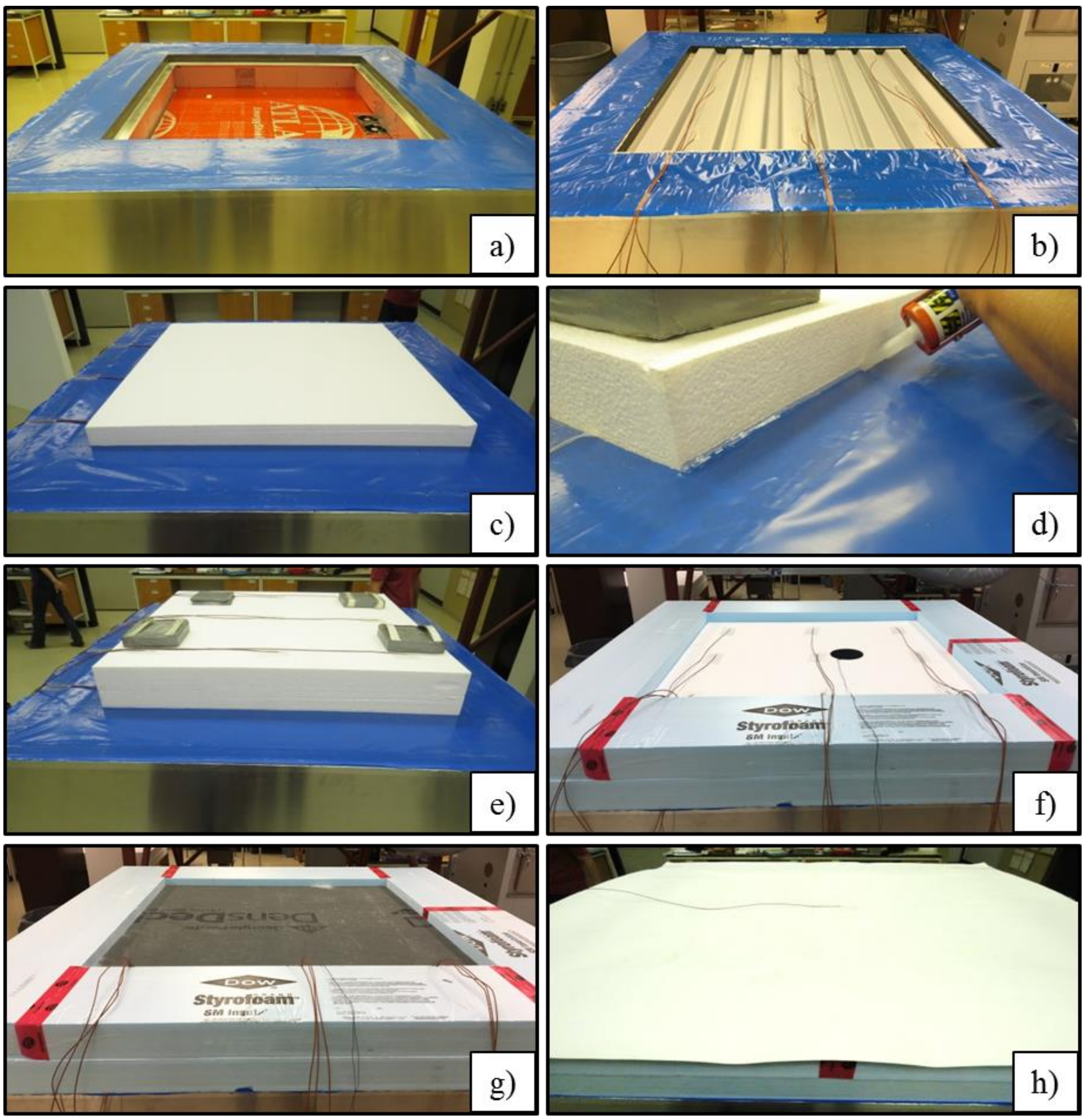

Figure 4-27: Opaque Assembly Installation

4.5.6. Fastener Installation

Roof fastener densities are dependent on the type of roof system, location of the roof and the designer selected fastener configuration from Figure 2-26. The typical fastener densities per meter squared and per $1.2\ m \times 1.2\ m$ ($4ft \times 4ft$) insulation board that will be tested are shown in Table 4-6 and Figure 4-28. These test parameters were decided by the ERCR consortium based on the wide-spread use of these fastener configurations and field experience.

Table 4-6: Typical Fastener Density

Roof System – Membrane	Fastener Density per m^2	Fastener Density per Insulation Board
PARS – PVC	2.70	4
MARS – PVC	4.00	6
MARS – MB	6.75	10

Note: Insulation Board dimensions are $1.2\ m \times 1.2\ m$ ($4ft \times 4ft$)

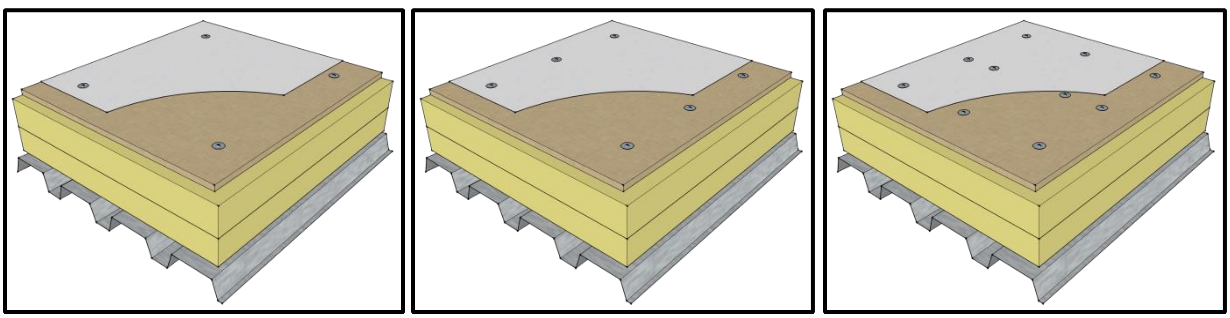

Figure 4-28: Fastener Densities

The installation of an assembly with fasteners follows the same steps as the opaque system installation but, the respective fastener density is installed after placing the protection board - securing the components together. It is important to note that in a real situation the membrane would also be fastened, since the GHB does not exert any uplift forces it is not required to secure the membrane.

Figure 4-29 shows the GHB installed fastener densities. The length of fastener required to fasten each assembly depends on the thickness of the assembly. The fasteners must puncture $25.4\ mm$ (1") into the steel deck; therefore, a five-inch system must have six inch fasteners. The assembly thicknesses (as seen in Table 4-1) range from $115\ mm$ to $203\ mm$ (4.5" to 8"); fasteners used must range from $152\ mm$ to $228\ mm$ (6" to 9") (Figure 4-30).

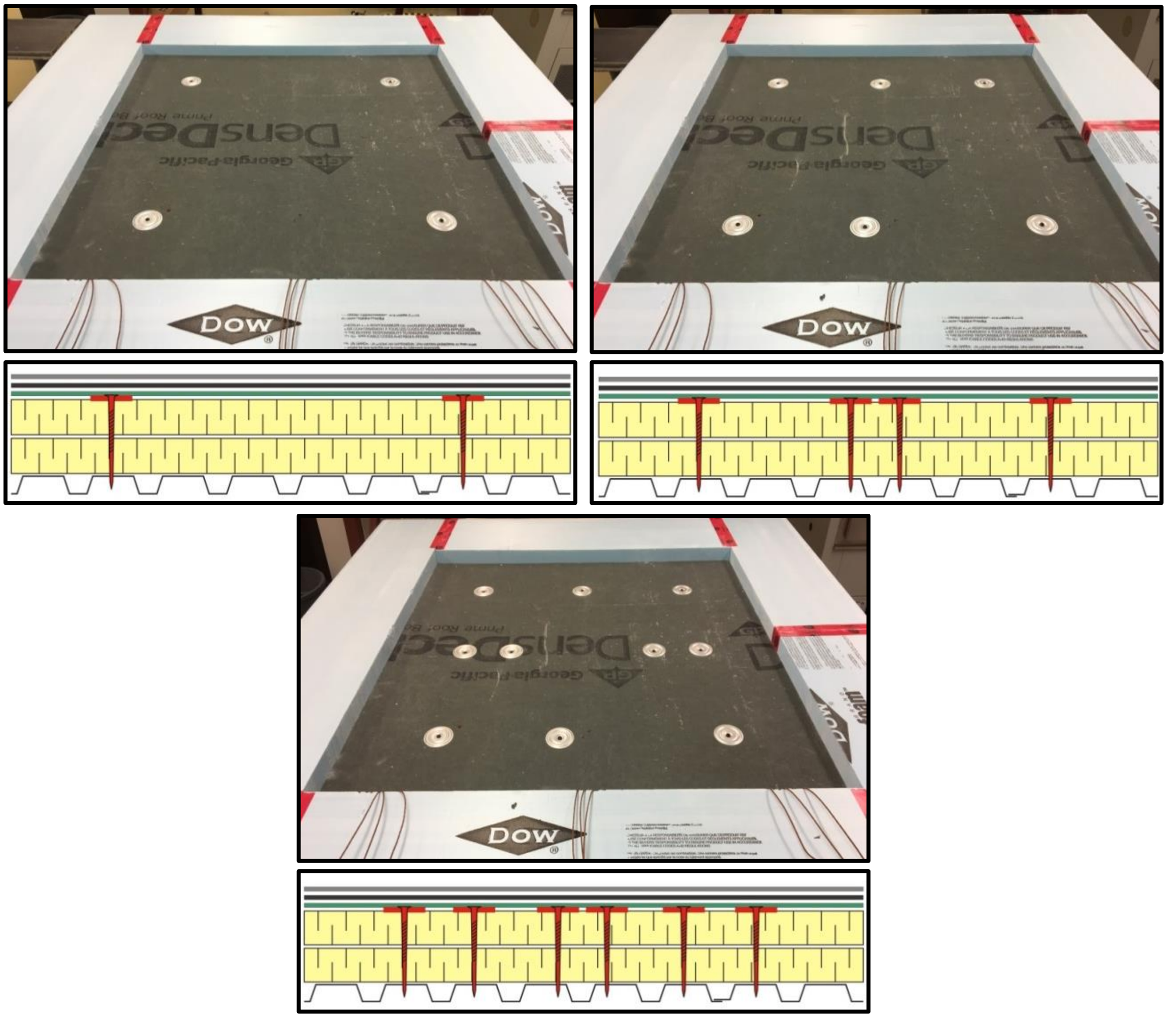

Figure 4-29: Fastener Assembly Installation

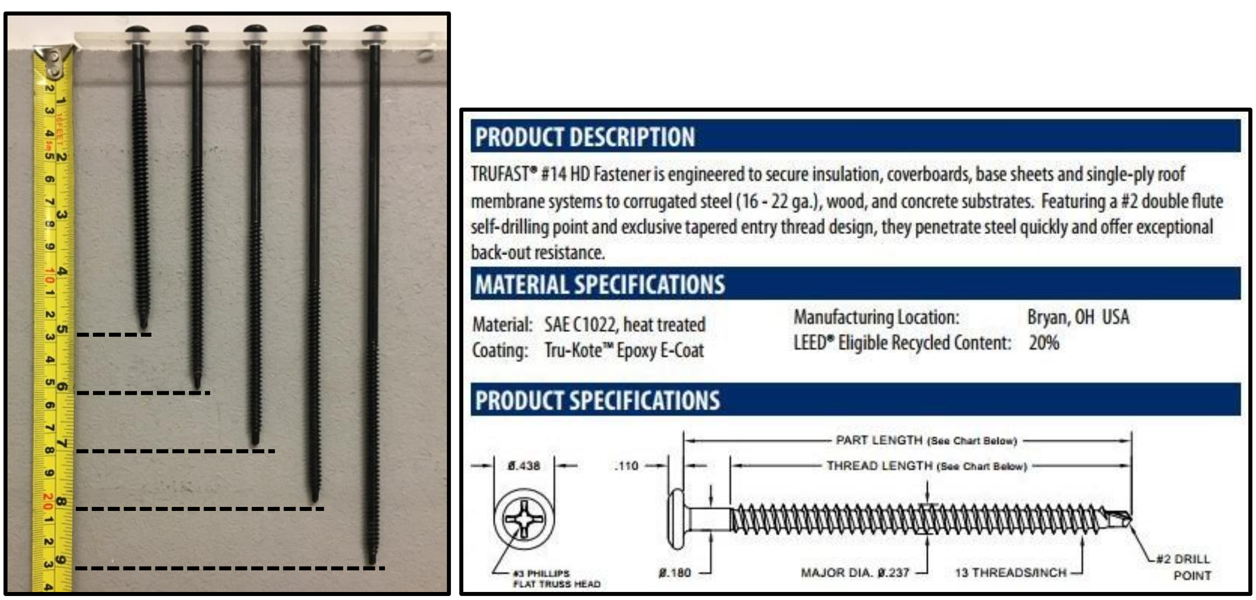

Figure 4-30: Fastener Lengths and Specifications

4.5.7. Gap Installation

The gaps tested on the GHB are based on all possible joint configurations encountered in a typical roof cross-section that have the potential to become gaps. The three possible joint scenarios are shown in Figure 4-31 which are: a single top joint, a single bottom joint and a staggered top and bottom joint. A 6.4 mm and 12.7 mm (1/4" and ½") wide gaps will be tested; decided by the ERCR consortium based on the commonly observed formed gaps from field experience.

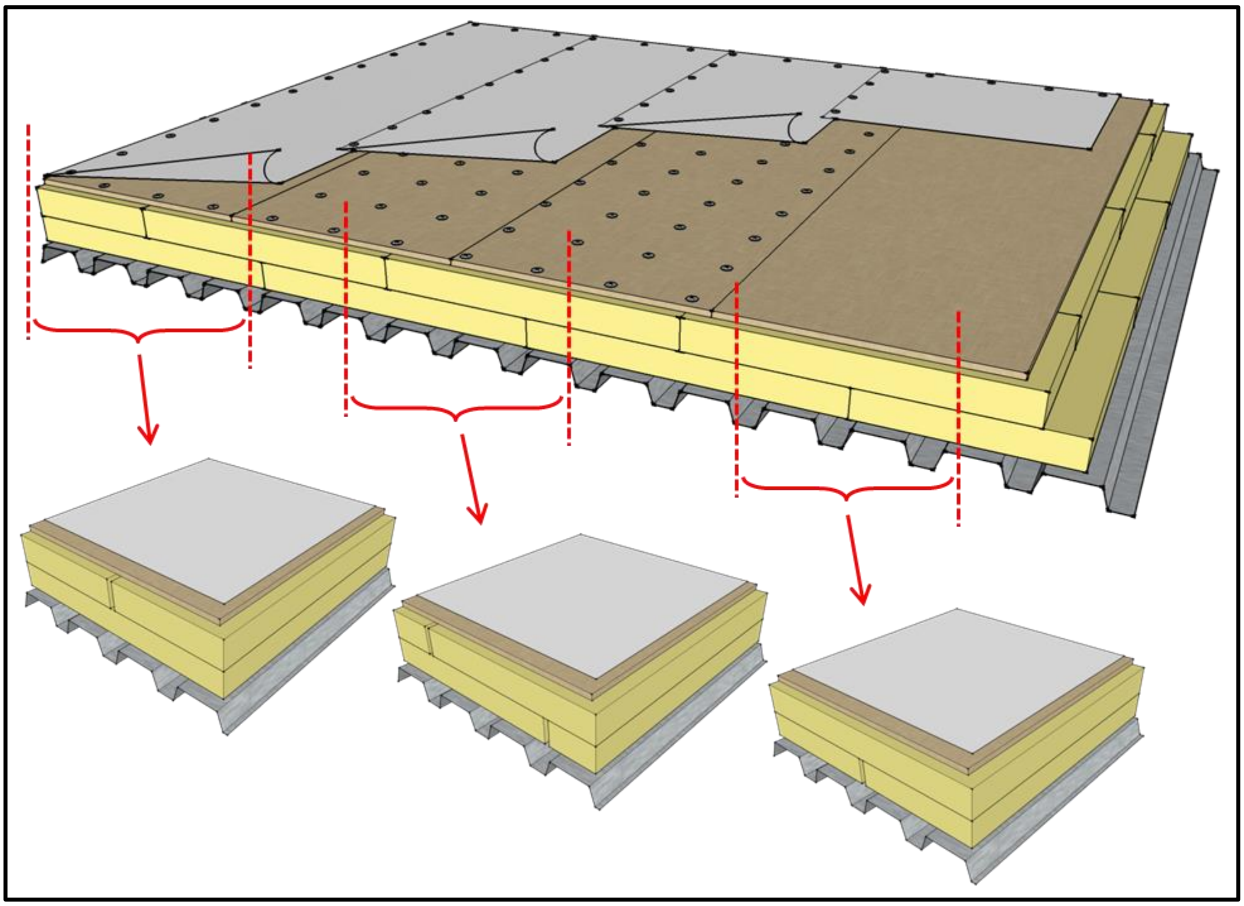

Figure 4-31: All Possible Joint Configurations in 4 Foot Cross-Section

The installation of an assembly with gaps follows the steps as the opaque system installation but, the insulation boards are cut on a table saw to simulate the presence of gaps. The boards are cut and then placed using spacers to insure the gap size does not change. The three joint scenarios for which gaps are created are: a top joint (Figure 4-32) a bottom joint (Figure 4-33) and staggered joints (Figure 4-34).

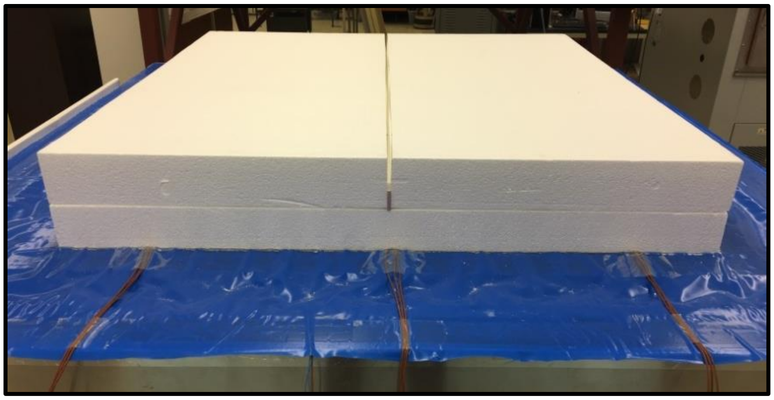

Figure 4-32: Top Joint

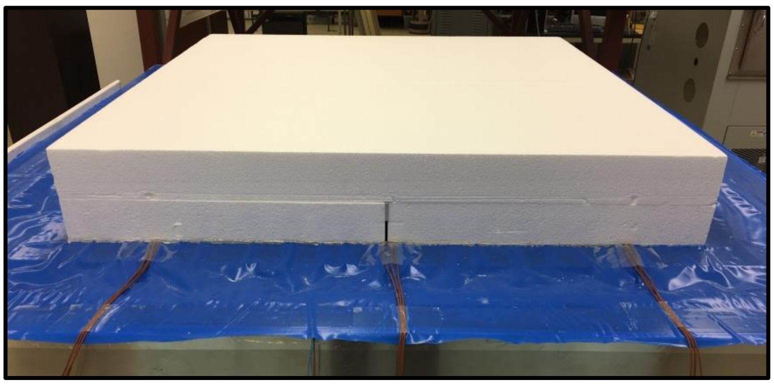

Figure 4-33: Bottom Joint

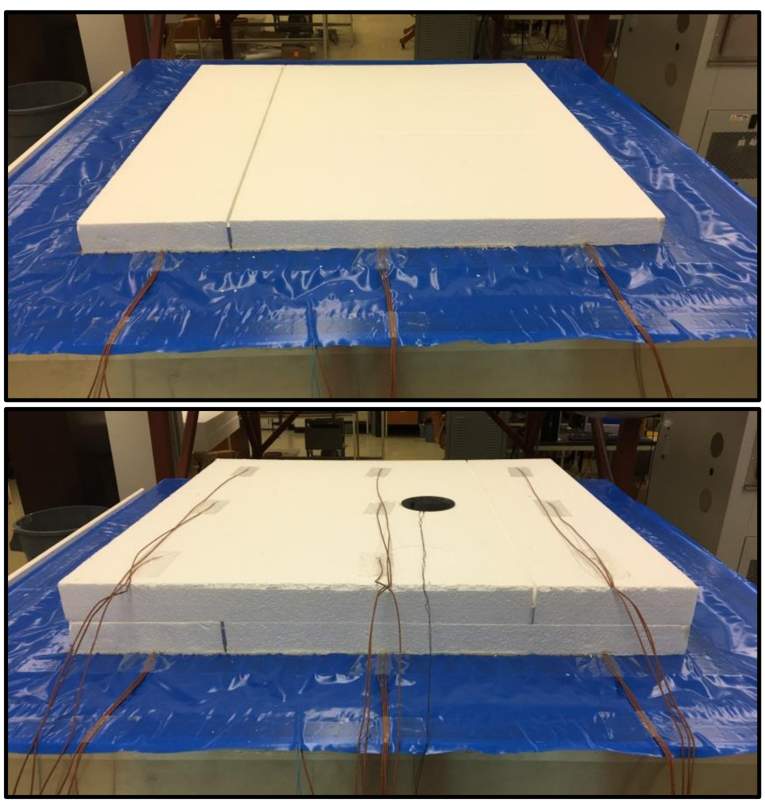

Figure 4-34: Staggered Joints

Chapter 5: Experimental Results and Analysis

This chapter summarizes and discusses the results from all the tests overviewed in Chapter 4: Experimental Methodology. The chapter begins by analyzing the results for the coefficient of linear expansion and dimensional stability tests, as they rationalize the parameters for the testing of gaps between insulation boards on the GHB. The thermal transmission properties of the different insulations tested on the HFM are discussed next, as they provide the benchmarking data towards the calibration and validation of the GHB. Lastly, the thermal impact factors quantified from the GHB testing are presented and implemented in the development of adjustment factors that can potentially be applicable toward the energy design of commercial roofs.

5.1. Coefficient of Linear Expansion

The coefficient of linear expansion testing follows the parameters outlined in the experimental methodology. The results for the tests are summarized in Figure 5-1 and Figure 5-2. The LVDTs are installed as shown in Figure 4-7, where LVDT 3 is located at the end of the bottom insulation board, while LVDT 1 and LVDT 2 are between the top two insulation boards. Although the tests were exposed to the test conditions for upward of a month, the majority of the dimensional changes took place in the first week; therefore, the focus is on that timeframe. Figure 5-1 shows the dimensional changes of the assembly's boards during exposure to the summer cycle, while Figure 5-2 shows the dimensional changes during the winter cycle. It can be concluded that the dimensional changes are more prominent during exposure to heat - as evaporation of moisture results in the loss of mass and dimensions. This concept is further discussed and confirmed by the dimension stability results in the following section. The maximum dimensional change for the assembly is summarized in Table 5-1; although 1.5 mm (1/16") may seem as negligible dimensional change, compounded over a hundred insulation boards for an entire roof, the gaps become significant.

Table 5-1: Coefficient of Linear Expansion Results

	Maximum Linear Dimensional Change, mm [in]		
	LVDT 1	**LVDT 2**	**LVDT 3**
Hot Cycle	1.59 mm [1/16"]	1.50 mm [~1/16"]	1.40 mm [~1/16"]
Cold Cycle	0.30 mm [~1/64"]	0.29 mm [~1/64"]	N.A.

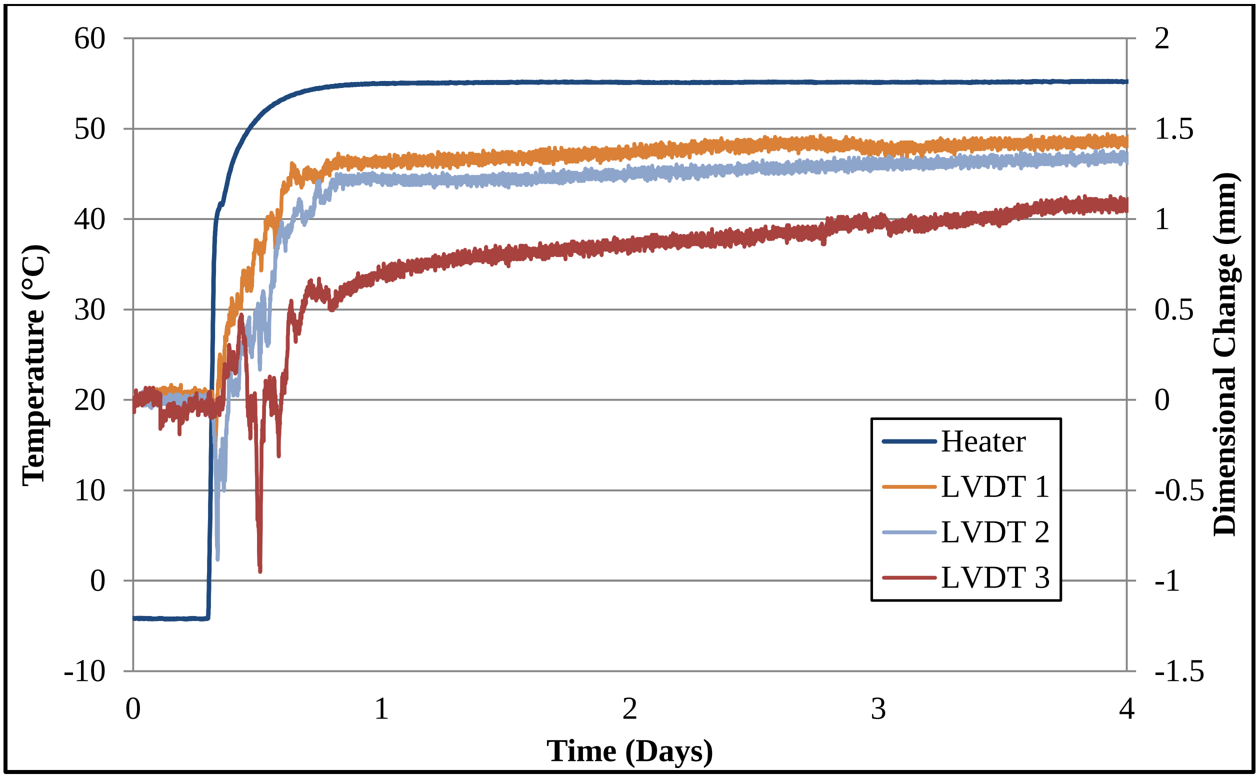

Figure 5-1: Coefficient of Linear Expansion, Heating Cycle

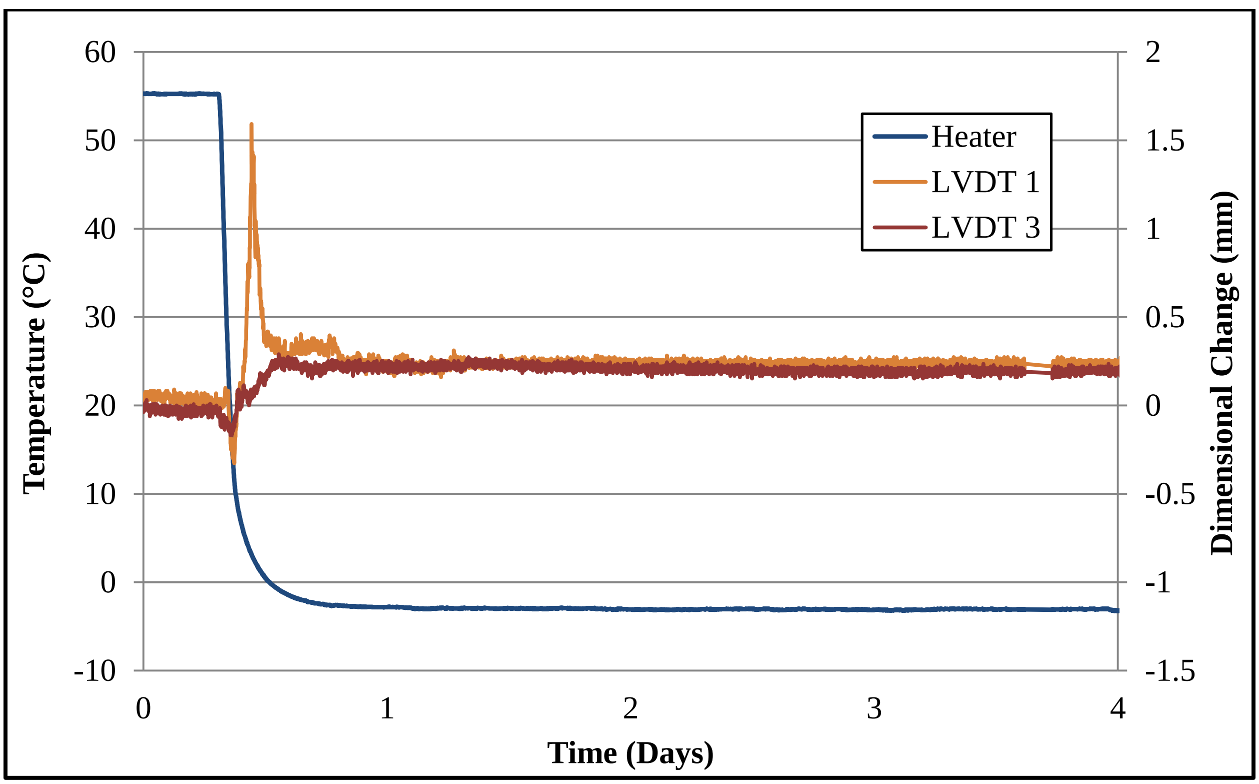

Figure 5-2: Coefficient of Linear Expansion, Cooling Cycle

5.2. Dimensional Stability Results

The results of the dimensional stability tests are summarized following standards ASTM D2126-09 outlined in the experimental methodology. The results of EPS insulation are used to demonstrate the effect of dimensional stability on insulation boards; the results for the other insulations are summarized in Appendix B: Dimensional Stability Results.

Three insulation boards of each thickness (thicknesses shown in Table 5-2) were exposed to the standard stated heating and cooling conditions. The dimensional change for the EPS 80 mm and 98 mm (3 1/8" and 3 7/8") thick insulation boards are shown in Figure 5-3 and Figure 5-4, respectively. The average values for each thickness and exposure condition are summarized in Figure 5-5.

Table 5-2: Insulation Thicknesses Tested

EPS	Polyiso	Stone Wool
80 mm [3.125"]	51 mm [2"]	64 mm [2.5"]
98 mm [3.825"]	64 mm [2.5"]	102 mm [4"]
-	84 mm [3.3"]	-

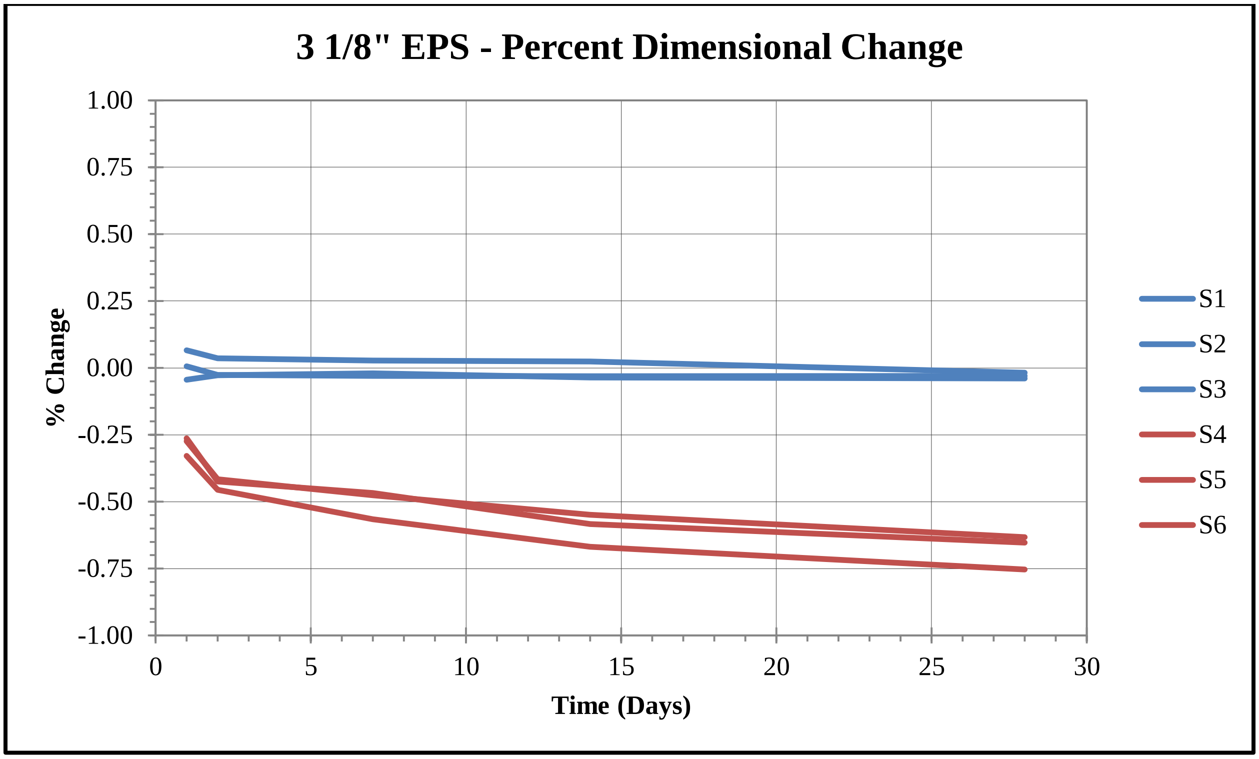

Notes: Blue lines (S1-S3) represent exposure to cold and red lines (S4-S6) represent exposure to heat.

Figure 5-3: Dimensional Stability of 3 1/8" EPS Boards

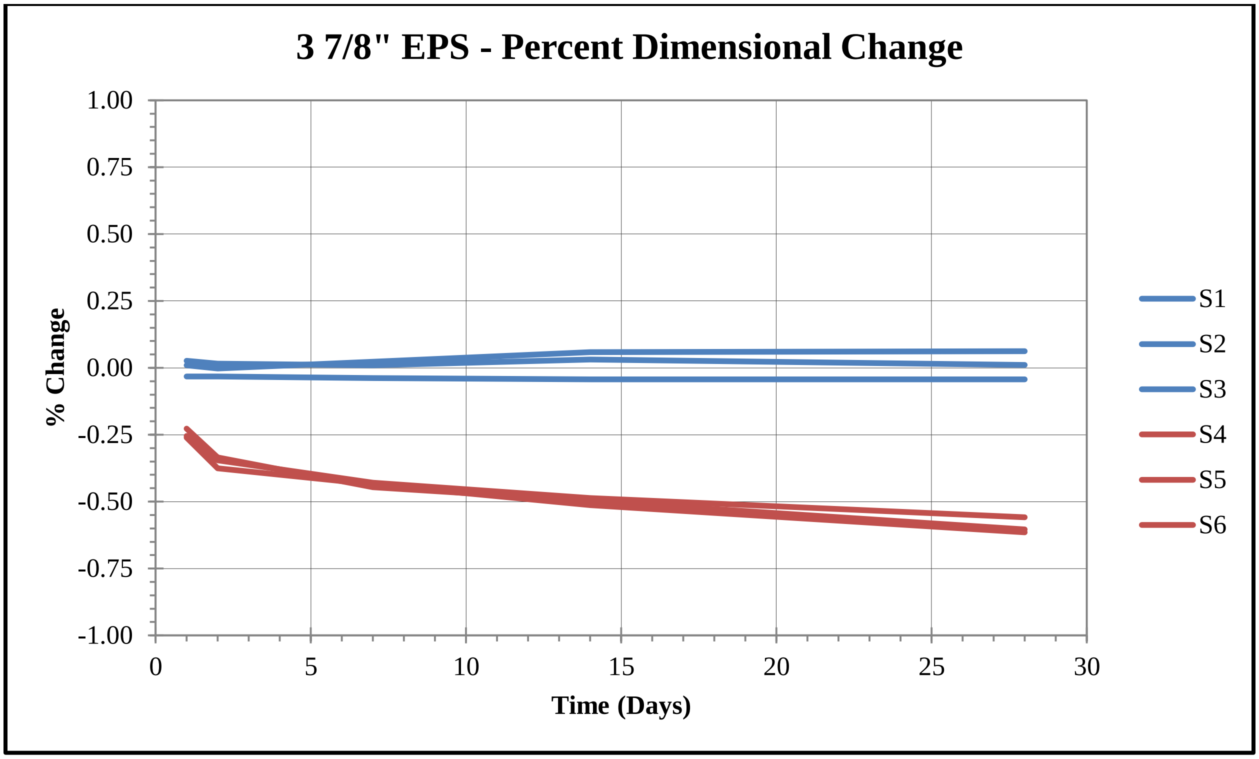

Notes: Blue lines (S1-S3) represent exposure to cold and red lines (S4-S6) represent exposure to heat.

Figure 5-4: Dimensional Stability of 3 7/8” EPS Boards

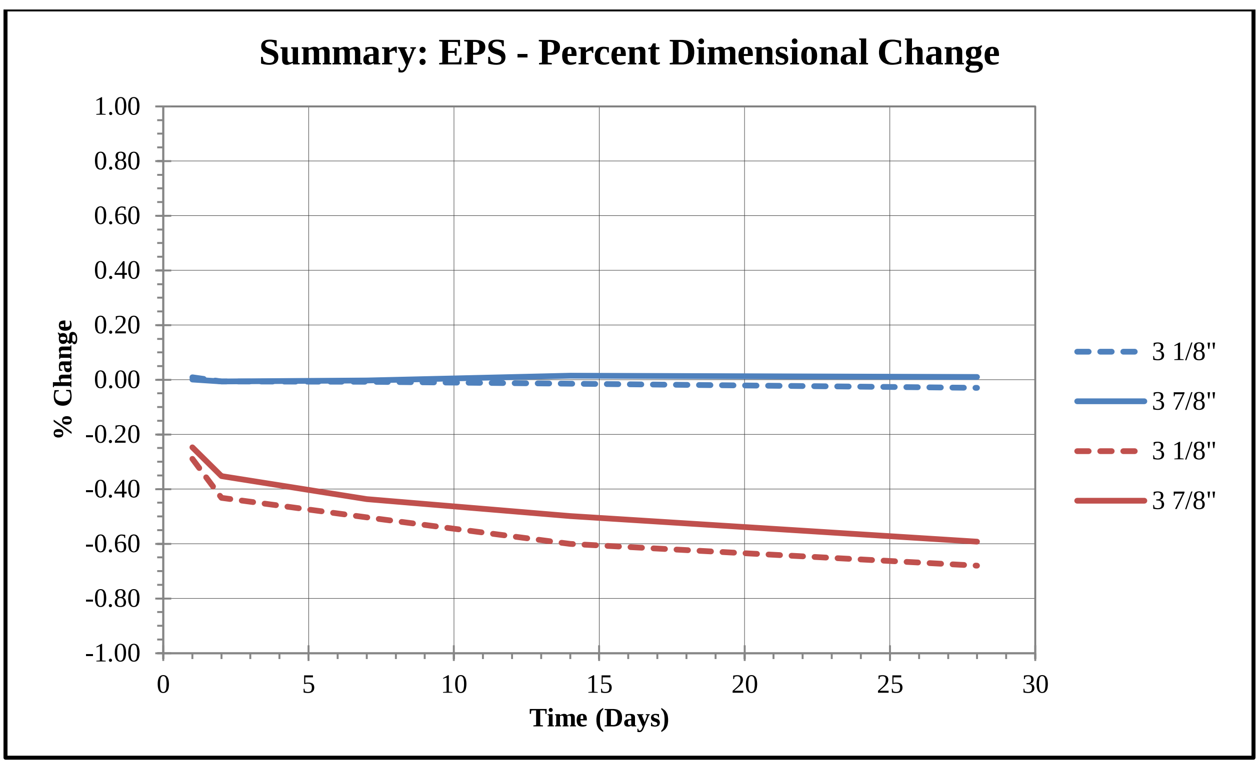

Notes: Blue lines represent exposure to cold and red lines represent exposure to heat.

Figure 5-5: Summary of Dimensional Changes of EPS Boards

It can be concluded that the dimensional changes are more prominent during exposure to heat, as evaporation of moisture within the insulation boards results in the loss of mass and dimensions. Table 5-3 summarizes the average change in mass of the EPS samples over the four-week exposure. When the specimens are exposed to heating, evaporation of the moisture in the specimen leads to a decrease in dimensions and weight. On the other hand, the samples exposed to cooling conditions gained mass, which can be attributed to condensation. The standard for testing the dimensional stability of insulating materials requires the specimen to be left at room temperature for two hours after exposure, before taking measurements; during this time, condensation occurs on the cooled samples leading to an increase in mass from the relative humidity of the lab.

Table 5-4 summarizes the recorded maximum dimensional changes of each insulation type. It can be seen the permanent deformation on a $200\ mm$ (8”) EPS sample after 28 days of testing is 0.75% (or $8.5\ mm$). Since insulation boards are most commonly $1.2\ m \times 1.2\ m$ ($4ft \times 4ft$) in dimension, this could correlate to a deformation six times greater than that of the test specimen. However, this conclusion would have to be verified and tested.

Table 5-3: Percent Change in Mass

% Change in Mass	
Heating	Cooling
-0.21%	0.23%

Table 5-4: Dimensional Stability Results

	Dimensional Stability, % [in]		
	EPS	**Polyiso**	**Stone Wool**
Heating	-0.75% [~1/3”]	-0.22% [~1/10”]	-0.09% [~0”]
Cooling	0.07% [~0”]	0.08% [~0”]	0.04% [~0”]

Note: The associated dimensional change in inches corresponds to a typical 4’ by 4’ board.

Table 4-4 summarizes the standard allowable dimensional changes for each insulation type; the standards allow for a much greater deformation than produced in lab conditions to account for a wide variety of insulation uses - this provides a tolerance for the insulation.

5.3. Heat Flow Meter Results

As described in Chapter 4, the HFM is used to provide fast and reliable thermal properties of thermal insulation. The purpose of the HFM testing is to obtain calibration data for benchmarking the GHB, as required by standard ASTM C1363-11. It is important to understand the difference between the thermal values measured on each apparatus; the HFM measures the R-value, while the GHB measures the effective R-value. The effective R-value is the resistance of the entire assembly, which includes surface coefficients (or air films). The thermal resistance of the surface coefficients is $R0.79\ ft^2 \cdot {}^{\circ}\mathrm{F} \cdot h/Btu$. Due to the contact of the hot and cold plates with the test specimen during HFM testing, the surface coefficients are not present. Therefore, a component designed to reach an effective R-value of R26 will have an R-value of R25.21.

5.3.1. Thermal Transmission Properties of Thermal Insulation

The resistivity and resistance of thermal insulation is compared to check the accuracy of the apparatus. Insulation boards from each design category (R25.21 and R30.21) are tested individually and then as an assembly of boards (Figure 5-6). The resistivity of the insulation is calculated based on the test results of the single boards and compared to the measured resistance of the overall assembly. Measuring the resistivity of the single boards will ensure a higher accuracy due to the lower possibility of lateral heat flow. Although heat flow through the HFM is idealized as vertical and one-dimensional, there is lateral heat flow escaping the system. Figure 5-7 shows how most of heat flow is vertical with a smaller insulation thickness; if the thickness was increased, the amount of lateral heat flow and therefore heat loss through the perimeter would increase (Figure 5-8). The resistivity of two insulation boards of the same material should have the same value; therefore, multiplying the resistivity of a thin component by the thickness of another should yield the same resistance. However, a discrepancy between the measured and calculated values due to the losses associated with lateral heat flow and the increasing thickness of a component are seen in the results. To account for this deviation, a normalization of the data is necessary. To determine values for normalization, tests were done at four mean temperatures to develop the trend line. Once the data points were fitted to a regression line, the thermal resistance of the insulation at the specific testing mean temperatures was determined.

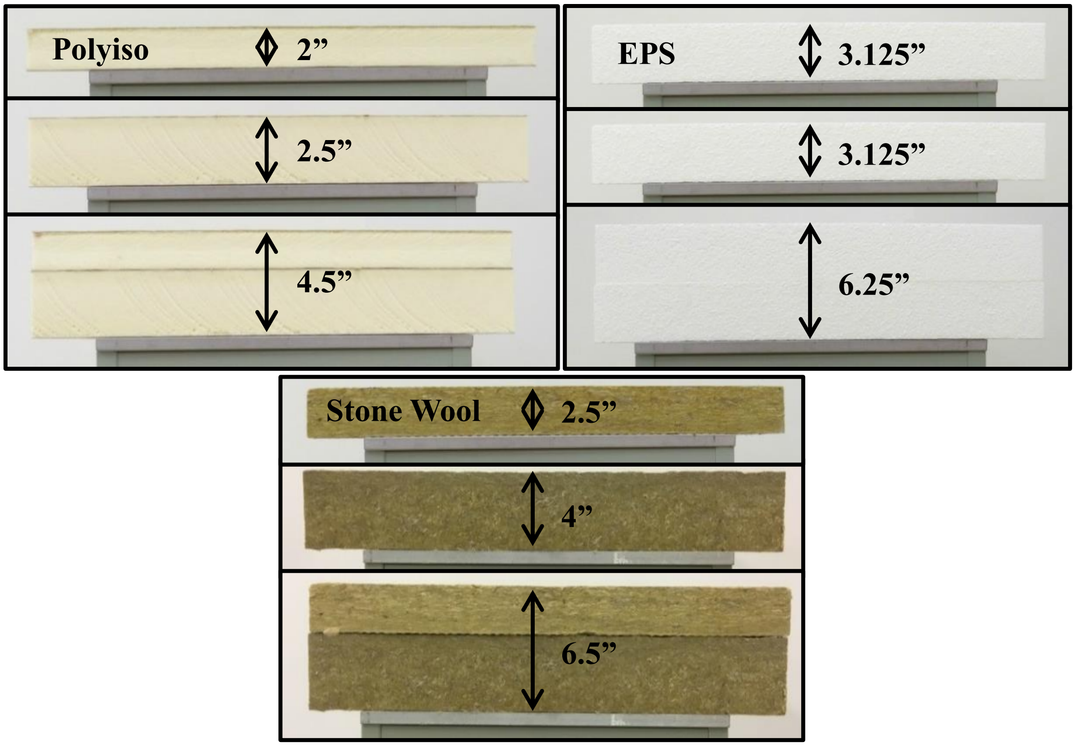

Figure 5-6: R26 Components and Assembly

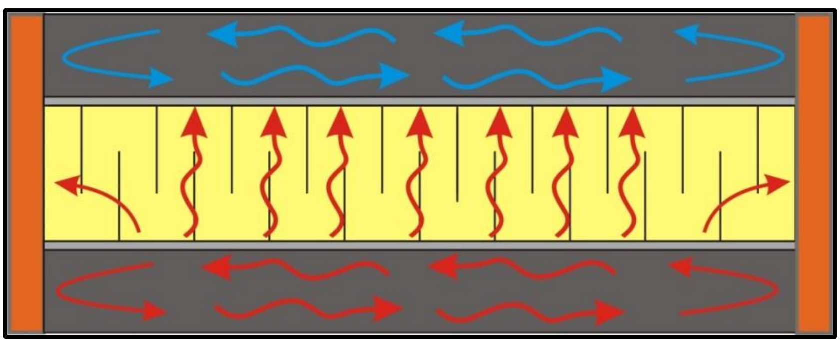
Figure 5-7: Heat Flow through Thin Insulation

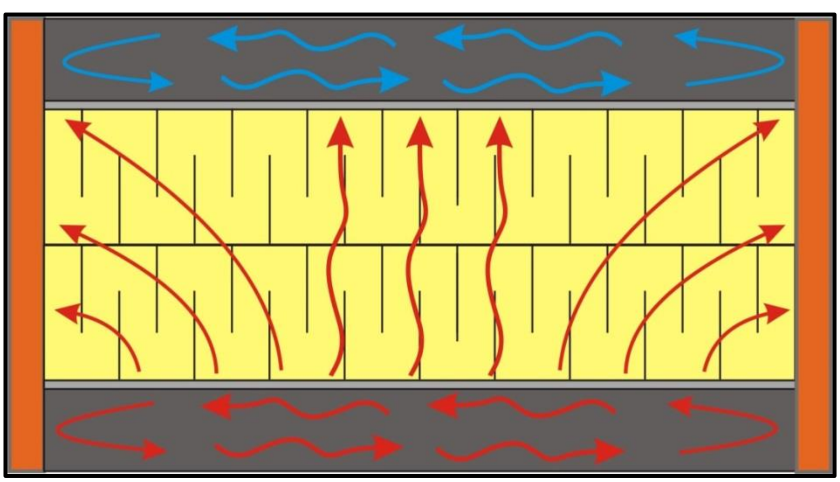
Figure 5-8: Heat Flow through Thick Insulation

Figure 5-9 demonstrates the deviation of measured test results from the set points (where the dotted lines represent the set points) due to the lateral heat flow losses. In order to adequately compare results from multiple tests, they must be normalized using a trend line developed from multiple tests done on an insulation board with a high confidence interval. The trend line is developed from the results of the thinnest available insulation board to limit the lateral heat flow. In the case of EPS insulation, the 80 mm (3.125”) boards are used to create the trend line due to its high repeatability. Figure 5-10 demonstrates how the offset is applied to the measured values.

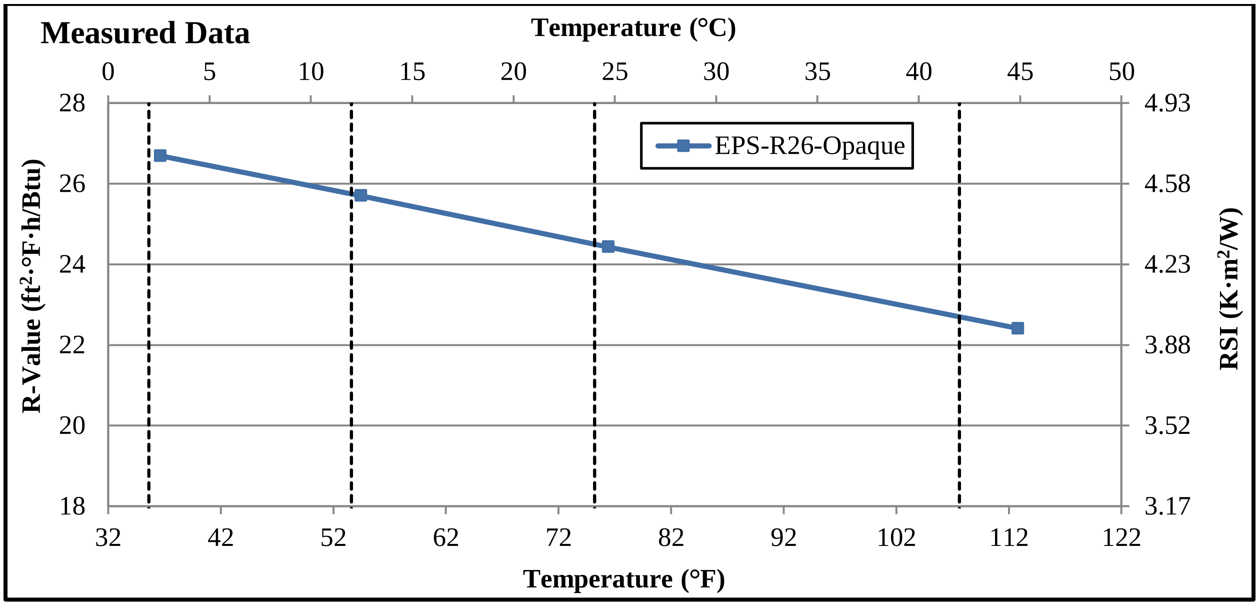

Figure 5-9: Typical Measured Data

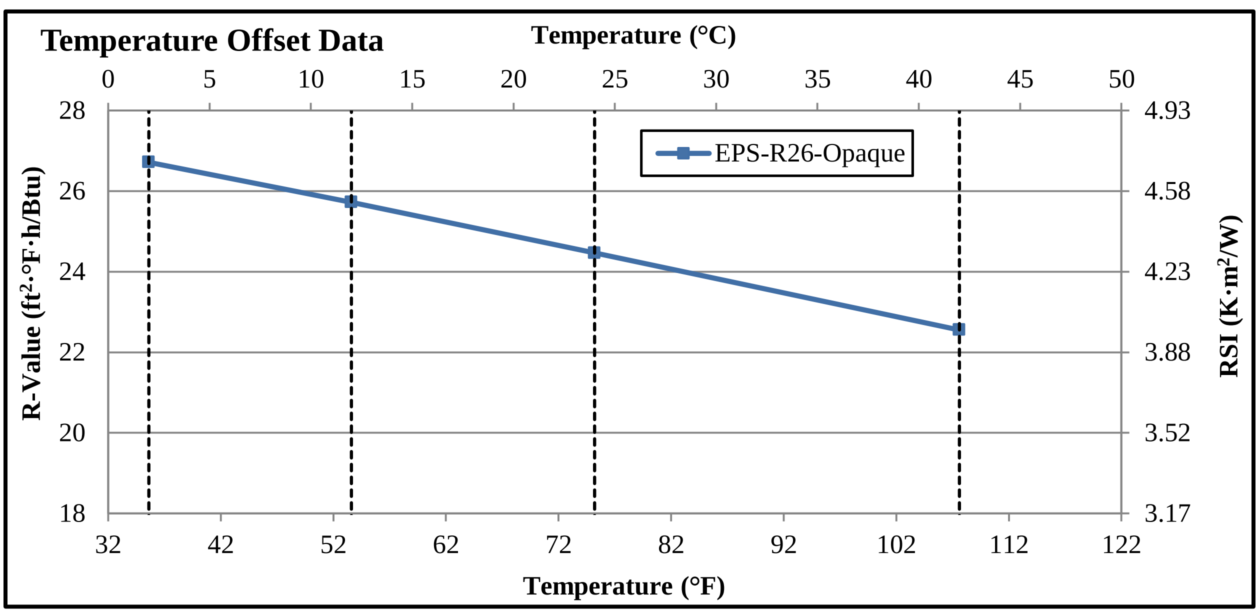

Figure 5-10: Normalized Data

Figure 5-11 shows the measured thermal resistance of a single layer of EPS insulation obtained from three test specimens. The average data of the three EPS samples are summarized in Table 5-5; the maximum deviation is less than half a percent, providing a high confidence interval and therefore justifying the data for a trend line used to normalize the measured values. It is important to note that each insulation type will have its own respective trend line for normalizing the data. The three main points to take away from the single layer of EPS insulation test results is that thermal resistance decreases with increasing mean temperature, the data follows a linear trend, and the repeatability of thinner insulation is very high.

Table 5-5: Average R-Value and Standard Deviation of 3.125" EPS Insulation

Mean Temperature		Average R-Value	Standard Deviation	Error
(°C)	(°F)	$(ft^2 \cdot °F \cdot h/Btu)$	$(ft^2 \cdot °F \cdot h/Btu)$	(%)
2	36	13.22	0.029	0.22
12	54	12.75	0.017	0.13
24	75	12.25	0.022	0.18
42	108	11.54	0.044	0.38

Figure 5-12 shows the two-layer EPS insulation assembly tests. It is seen that there is a discrepancy between the test results, confirming that an increase in thickness gives rise to error due to the lateral heat flow.

Comparing the results from the single layer testing and two-layer testing, the resistivity of EPS insulation is calculated from the average resistance of the single board test data (Figure 5-13). The resistivity is used to calculate the resistance of EPS for an R25.21 system, which is compared to the average measured data. Figure 5-14 shows the comparison between calculated and measured data showing the difference, and therefore potential error, between the two tests. The difference between the measured and calculated thermal resistance is fairly small, but this is because the thickness of the EPS R25.21 is within the tolerance of the HFM (where the HFM can test a thickness of 1/3 of its dimensions – therefore $203\,mm$ or 8"). As the thickness of the assemblies increase, the quantity of error will increase. Figure 5-15 shows the measured and calculated results for the EPS R30.21 system, and the increase in error is evident. It is therefore concluded that the resistivity results from the single layer testing will be used as the calibration data for the GHB.

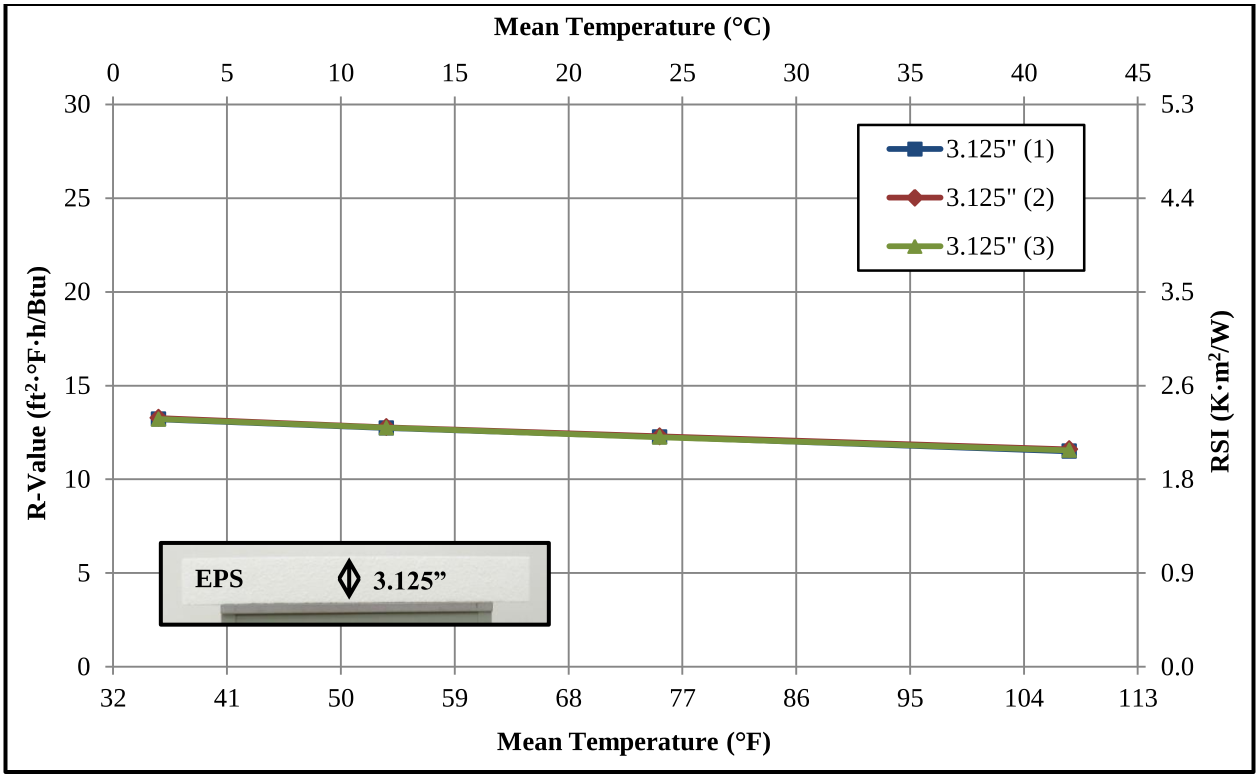

Figure 5-11: EPS - R25.21 Single Layer Repeatability

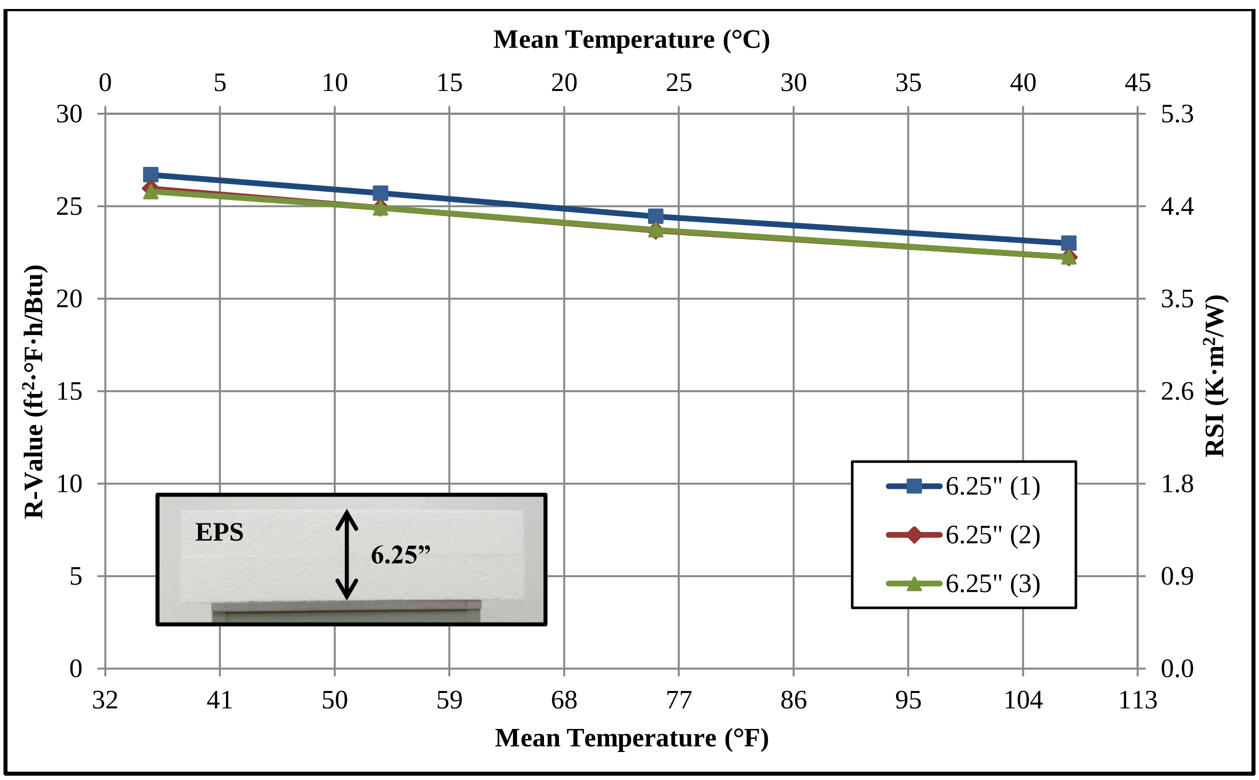

Figure 5-12: EPS - R25.21 Two Layer Repeatability

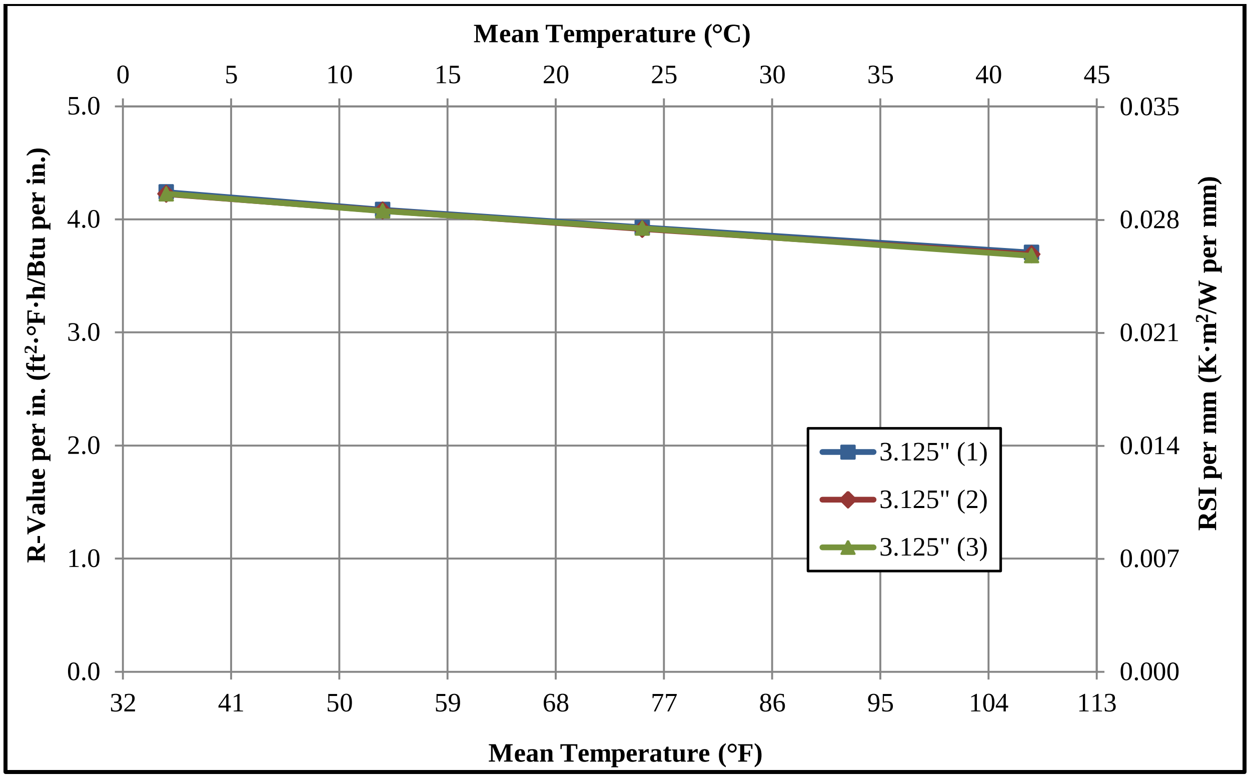

Figure 5-13: EPS - Thermal Resistivity

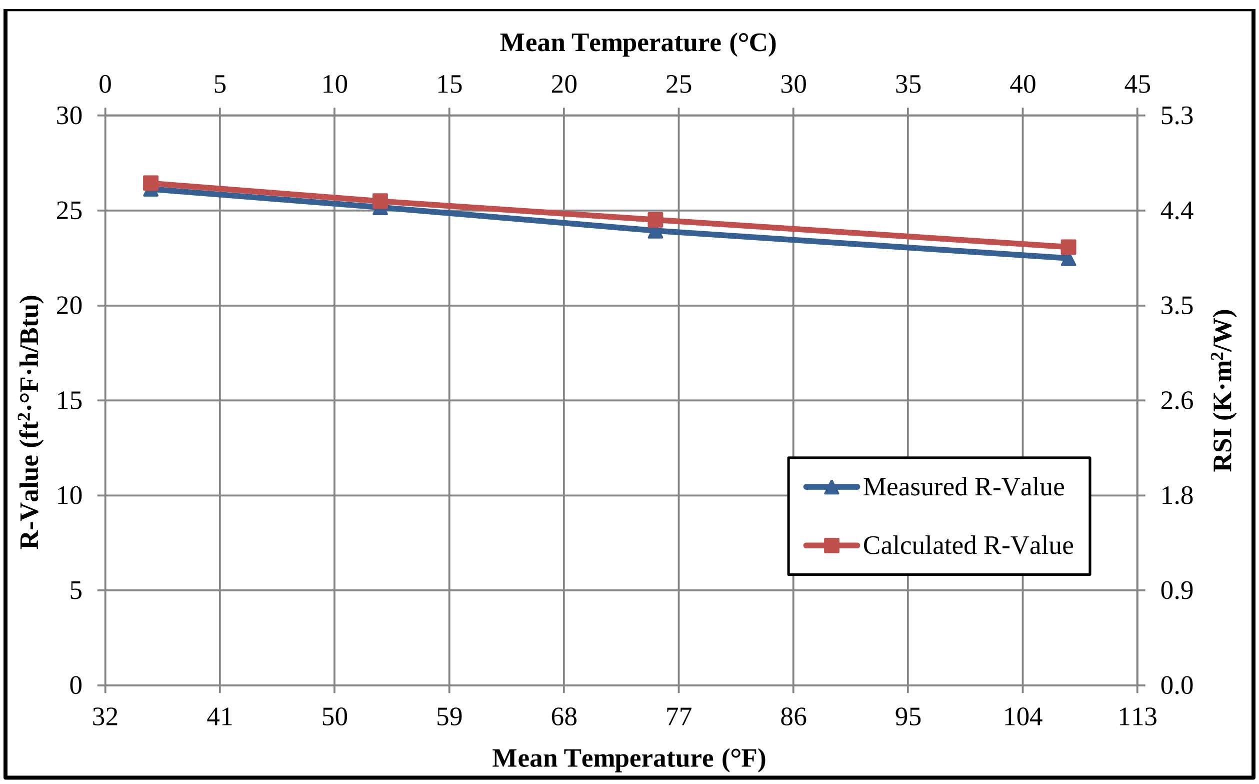

Figure 5-14: Measured vs. Calculated Thermal Resistance for EPS R25.21

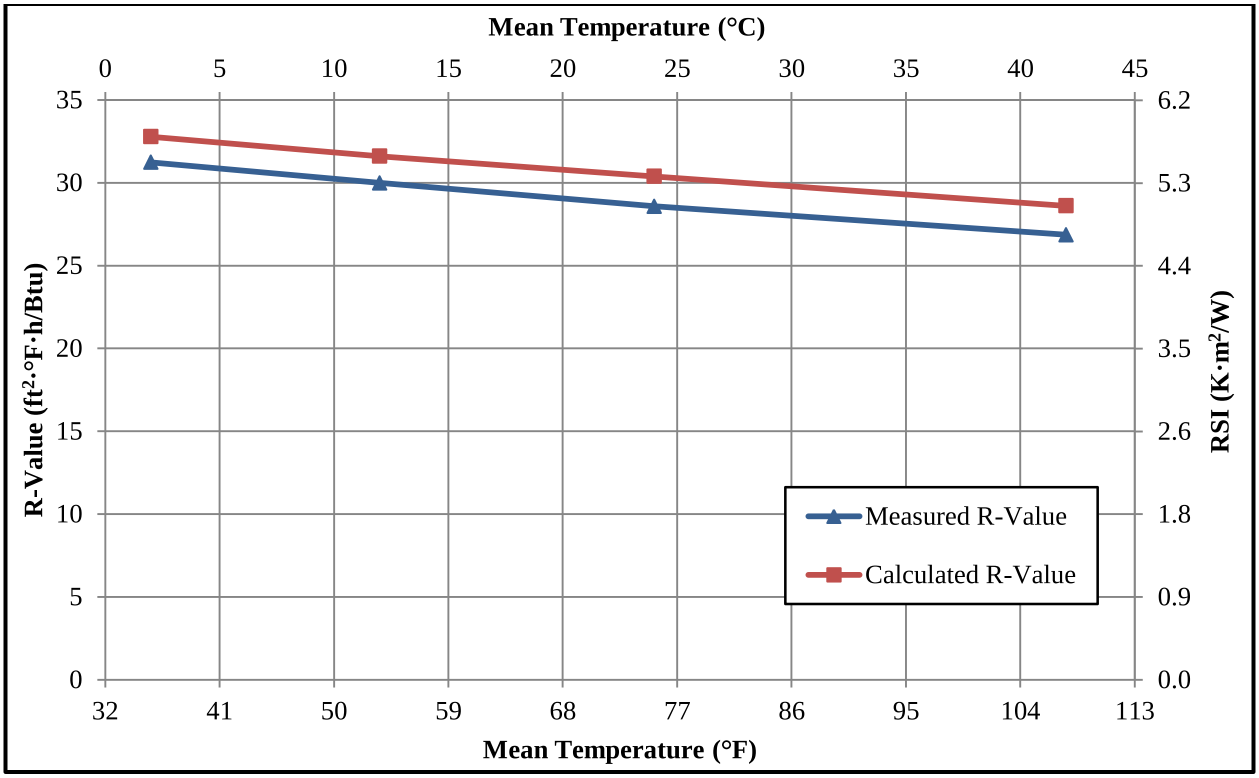

Figure 5-15: Measured vs. Calculated Resistance for EPS R30.21 Insulation

The results for the other insulations can be found in Appendix C: Heat Flow Meter Results.

5.3.2. Effect of Adhesive

Mechanically attached roof systems are secured by fasteners and do not use any adhesive; adhered and partially-adhered roof systems, however, use adhesive or a combination of fasteners and adhesive. In order to measure the decrease in thermal performance of an assembly with gaps, an opaque system must first be tested; the insulation boards are then cut to simulate gaps between the boards, and then retested. The use of adhesive would require multiple different insulation boards be tested, since adhered boards cannot be separated to create the gap. This would require testing multiple different insulation boards, with any imperfections or differences between the boards resulting in inconsistencies in the data. Therefore validation is needed on whether adhesive has an impact on the thermal resistance of the assembly, or if it can be omitted.

Tests are done on the HFM on two adhesive configurations to verify the effect on thermal properties. The first configuration and typical industry standard method for adhering boards is shown in Figure 5-16. The adhesive is applied in an 'S' pattern, where the strips are spaced at $305\,mm$ (12") apart. The second configuration (Figure 5-17) is an extreme case, where the adhesive is applied to cover the entire surface of the board. The results from the tests are shown in Figure 5-18, from which it can be concluded that adhesive does not influence an assembly's thermal properties, and it is not a necessary component in AARS or PARS testing.

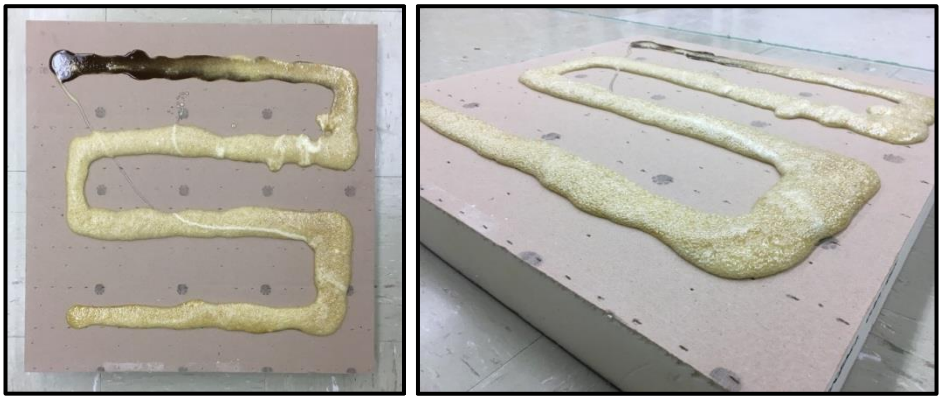

Figure 5-16: Strip Applied Adhesive

Figure 5-17: Spread Applied Adhesive

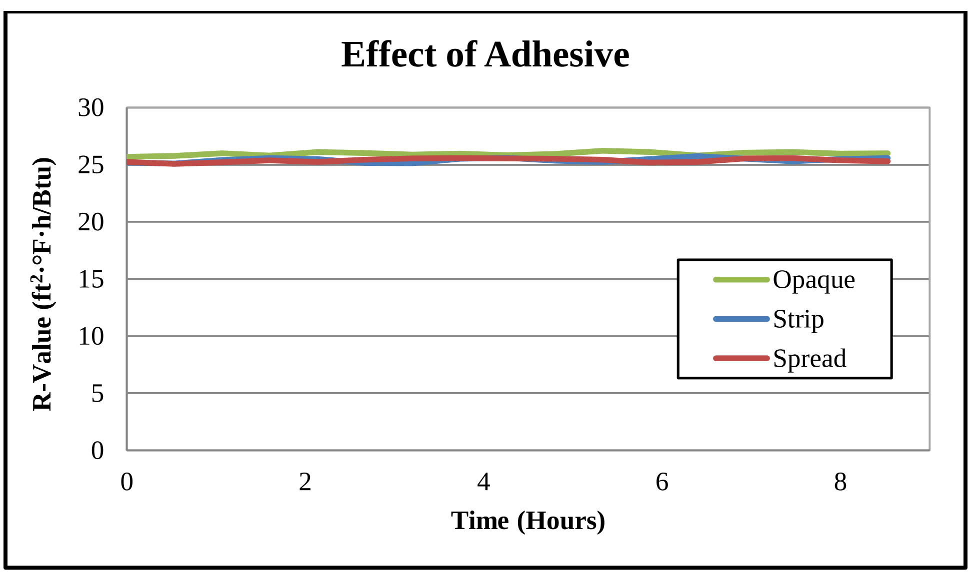

Average R-Value	
Opaque	25.9
Strip	25.5
Spread	25.4

Note: R-value = 5.67446 RSI

Figure 5-18: Effect of Adhesive on R-Value

5.4. Guarded Hot Box Results

This section provides the results for the GHB testing. It is split into three parts:

1. Data analysis and validation,
2. Test results: Development of adjustment factors, and
3. Validation of adjustment factors.

5.4.1. Data Analysis and Validation

The data acquisition for the GHB is based on three parameters which are measured and recorded: the temperature across the assembly, the voltage, and current used to power the heater. The thermal resistance of the assembly is calculated by dividing the change in temperature across the assembly by the heat flow (Eqn. 5-1).

$$RSI = \frac{\Delta T_{assmbly}}{Q} \quad \textbf{(Eqn. 5-1)}$$

The heat flow, Q, is watts per meter squared (Eqn. 5-2), where the watts are calculated from the measured volts and amps of the heater (Eqn. 5-3). The watts calculated in (Eqn. 5-3) are for the whole area of the GHB, which is $1.2\,m \times 1.2\,m$ or $1.48\,m^2$ ($4ft \times 4ft$ or $16ft^2$); this area is normalized to a meter squared (Eqn. 5-4).

$$Q = W/m^2 \quad \textbf{(Eqn. 5-2)}$$

$$W = V \times A \quad \textbf{(Eqn. 5-3)}$$

where

W is Power ($Watts$)

V is Voltage ($Volts$)

A is Current ($Amps$)

$$16ft^2 \times \frac{0.0929m^2}{ft^2} = 1.48645m^2 \quad \textbf{(Eqn. 5-4)}$$

Once the watts are normalized to a meter squared, the thermal resistance of the assembly is calculated according to (Eqn. 5-1). The thermal resistance or RSI (metric unit for thermal resistance) can be converted to an R-Value (imperial unit for thermal resistance) by multiplying the RSI value by 5.67446.

The GHB tests are run for 24 hours to establish uniform steady-state conditions. According to ASTM C1363-11 CL 6.8.6, for uniform steady-state conditions, the maximum point to point air temperature variation across the test board, perpendicular to the air flow direction at the center of the board, shall be less than 2% of the overall air to air temperature difference or 2℃, whichever is greater.

Figure 5-19 to Figure 5-23 show the typical temperature data for each test chamber and across the test specimen - shown for an EPS R26 opaque assembly. The value corresponding to the requirements of CL 6.8.6 is the “Max Offset” in the upper right of Figure 5-19 to Figure 5-23; this is the maximum difference in temperatures between all thermocouples. The “Offset” below each individual thermocouple corresponds to the maximum deviation in temperature for that single thermocouple over the test duration.

The maximum offset within the metering, guard and climatic chamber is 0.45℃, 1.38℃ and 0.23℃, respectively. The top and bottom test specimen have a maximum offset of 0.72℃ and 1.2℃, respectively, which is within the limit of 2℃ as per the ASTM C1363-11 requirement. Similar temperature offsets are measured for all tested assemblies, and it is determined that they all meet the ASTM C1363-11 requirements.

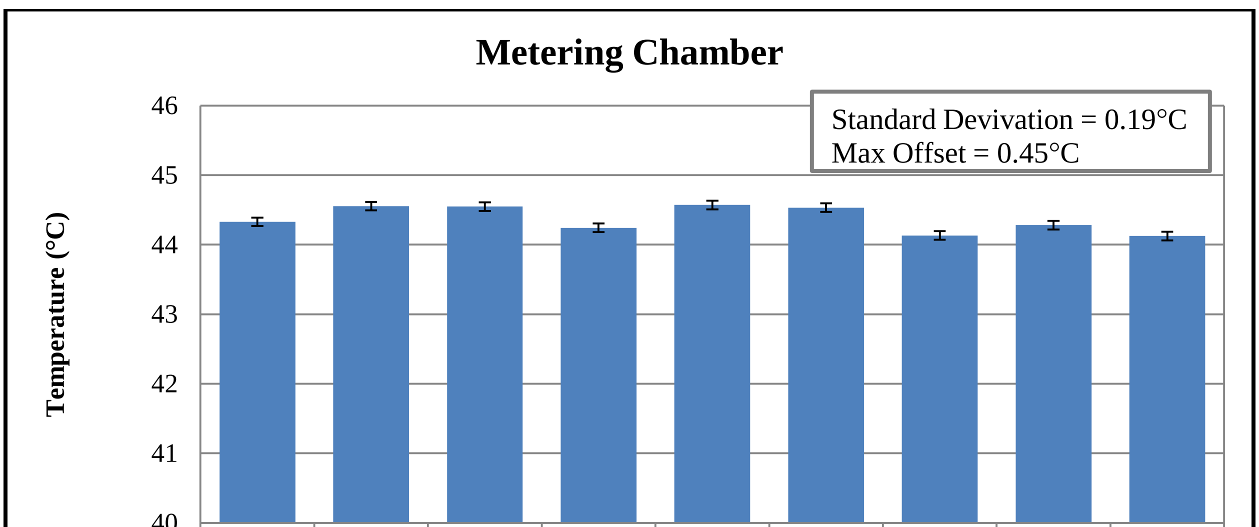

	Metering Air 1	Metering Air 2	Metering Air 3	Metering Air 4	Metering Air 5	Metering Air 6	Metering Air 7	Metering Air 8	Metering Air 9
Temp (°C)	44.33	44.55	44.55	44.24	44.57	44.53	44.13	44.28	44.13
Offset	0.11	0.13	0.10	0.10	0.11	0.10	0.11	0.12	0.09

Figure 5-19: Metering Chamber Temperature

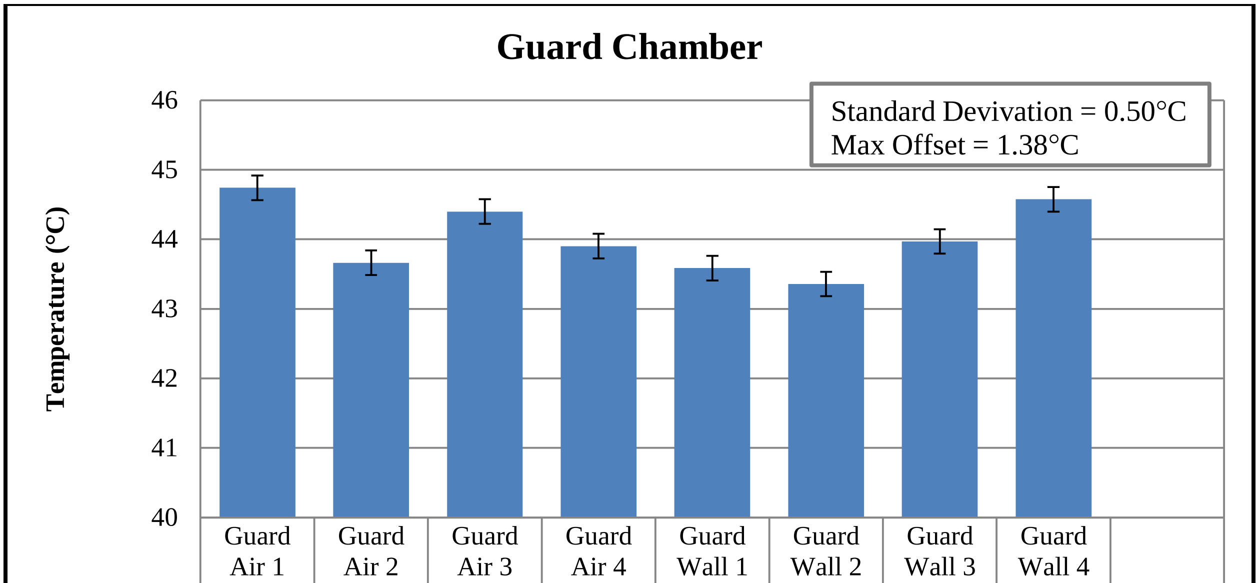

	Guard Air 1	Guard Air 2	Guard Air 3	Guard Air 4	Guard Wall 1	Guard Wall 2	Guard Wall 3	Guard Wall 4
Temp (°C)	44.74	43.66	44.40	43.90	43.59	43.36	43.97	44.58
Offset	1.21	0.60	0.89	0.25	0.35	0.18	0.25	0.37

Figure 5-20: Guard Chamber Temperature

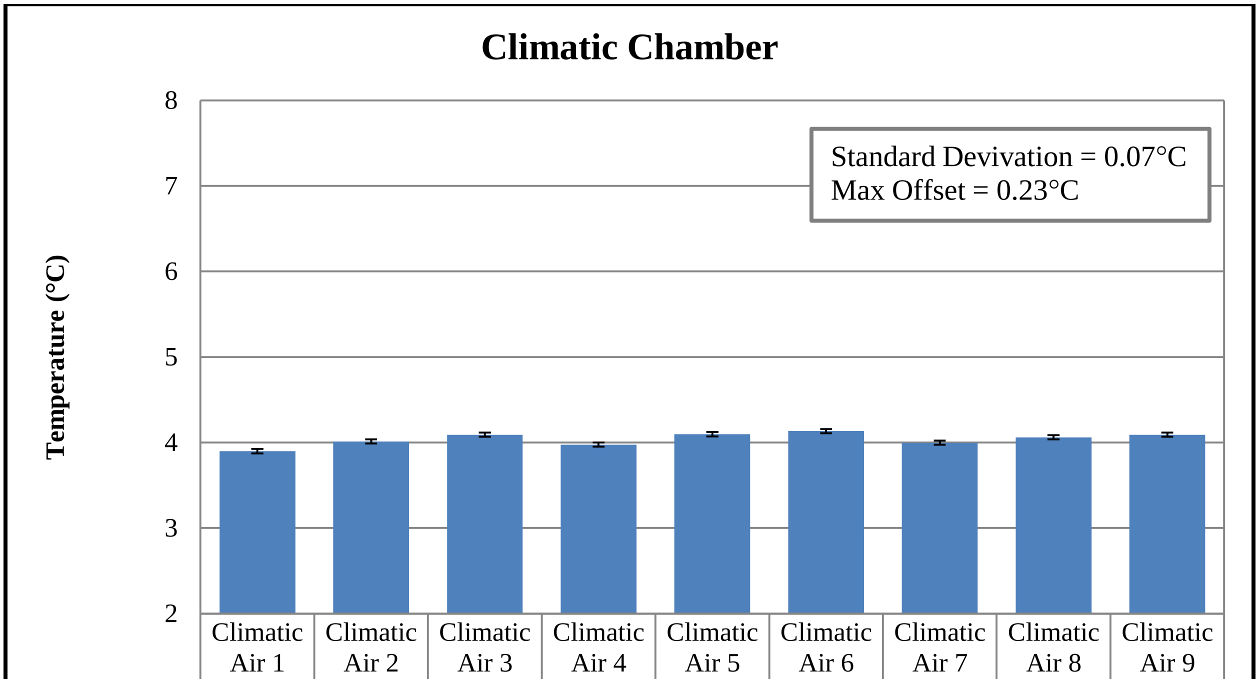

	Climatic Air 1	Climatic Air 2	Climatic Air 3	Climatic Air 4	Climatic Air 5	Climatic Air 6	Climatic Air 7	Climatic Air 8	Climatic Air 9
Temp (°C)	3.90	4.01	4.09	3.97	4.10	4.13	4.00	4.06	4.09
Offset	1.77	1.92	1.80	2.04	1.82	1.88	2.21	1.92	2.02

Figure 5-21: Climatic Chamber Temperature

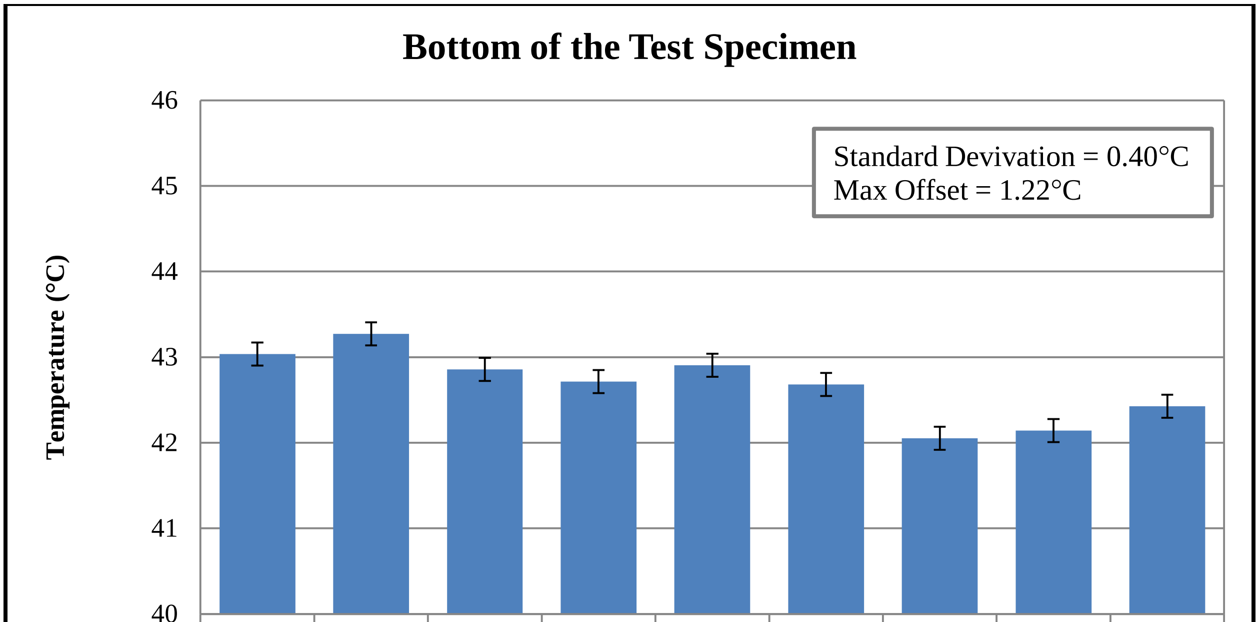

	Bottom Spec. 1	Bottom Spec. 2	Bottom Spec. 3	Bottom Spec. 4	Bottom Spec. 5	Bottom Spec. 6	Bottom Spec. 7	Bottom Spec. 8	Bottom Spec. 9
Temp (°C)	43.04	43.27	42.86	42.72	42.91	42.68	42.05	42.14	42.43
Offset	0.07	0.07	0.05	0.05	0.06	0.06	0.09	0.07	0.07

Figure 5-22: Bottom Specimen Temperature

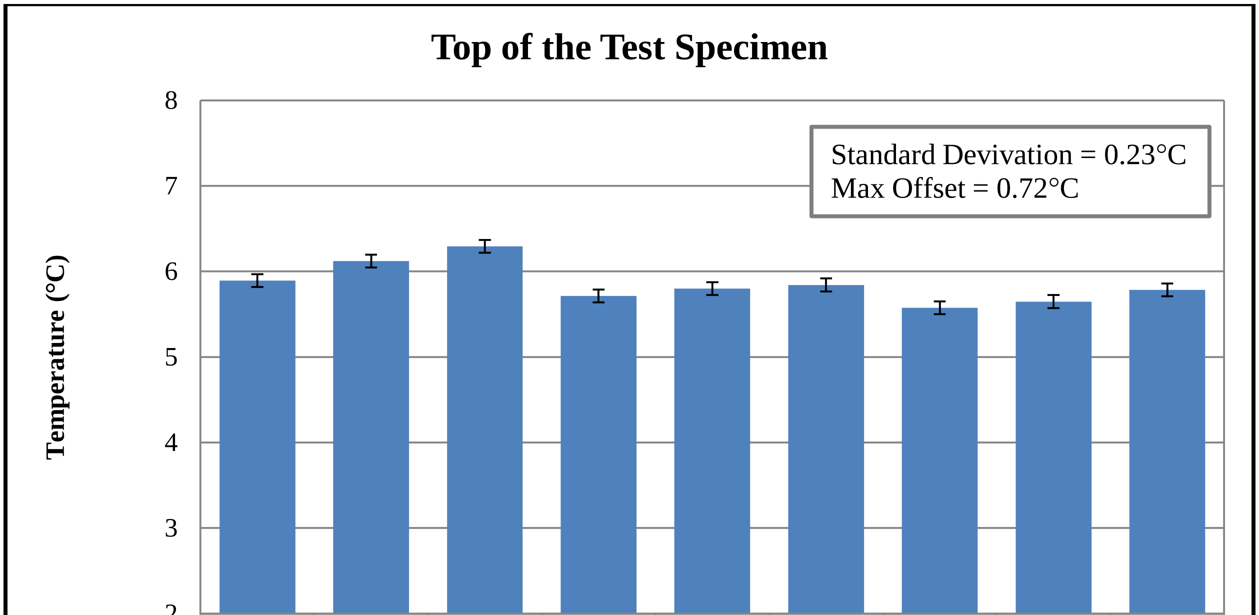

	Top Spec. 1	Top Spec. 2	Top Spec. 3	Top Spec. 4	Top Spec. 5	Top Spec. 6	Top Spec. 7	Top Spec. 8	Top Spec. 9
Temp (°C)	5.89	6.12	6.29	5.71	5.80	5.84	5.58	5.65	5.78
Offset	0.58	0.43	0.48	0.46	0.44	0.48	0.50	0.49	0.57

Figure 5-23: Top Specimen Temperature

Figure 5-24 shows the typical temperature profile of an EPS R26 opaque assembly, measured over a testing period of 24 hours. As shown in the figure, the metering and guard chambers reached a uniform condition at the set target temperature of 44°C, while the climatic chamber reached a uniform condition at the set target temperature of 4°C. When the temperatures have stabilized and reached steady-state conditions, the temperature and heat flow data (Figure 5-25) from the last 12 hours is analyzed to determine the effective R-value of the assembly.

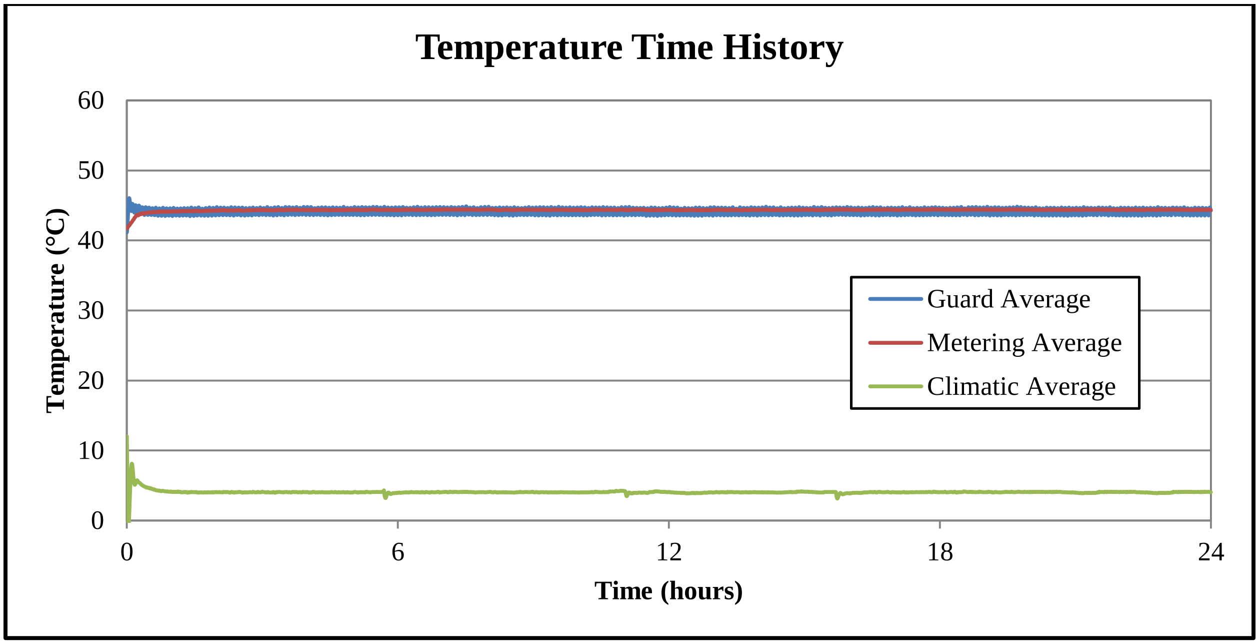

Figure 5-24: Typical GHB Temperature Time History

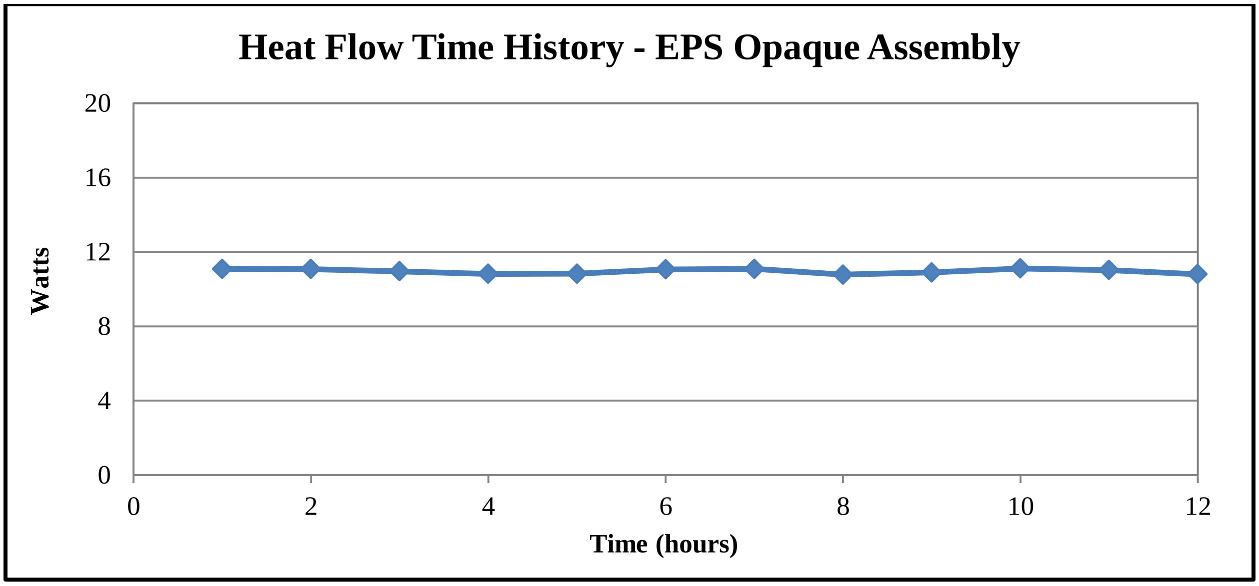

Figure 5-25: Typical GHB Heat Flow Time History

According to ASTM C1363-11 CL 1.3.2, the benchmarking specimens are homogeneous panels whose thermal properties are uniform. These panels have their thermal performance measured on other devices such as the Heat Flow Meter. Following the discussed data analysis procedure, the R-value of the EPS R26 opaque assembly was quantified at 4 different mean temperatures (2℃, 12℃, 24℃ and 42℃) and compared with the HFM testing data and a $2.4\ m \times 6.1\ m$ $(8ft \times 20ft)$ calibrated thermal chamber (CTC), as shown in Figure 5-26. It should be noted that this validation is done on insulation boards from the same manufactured batch. The proximity of results for the three thermal chambers validates the accuracy and precision of the GHB. The aforementioned calibrated thermal chamber will be discussed in the validation of the results obtained from the GHB.

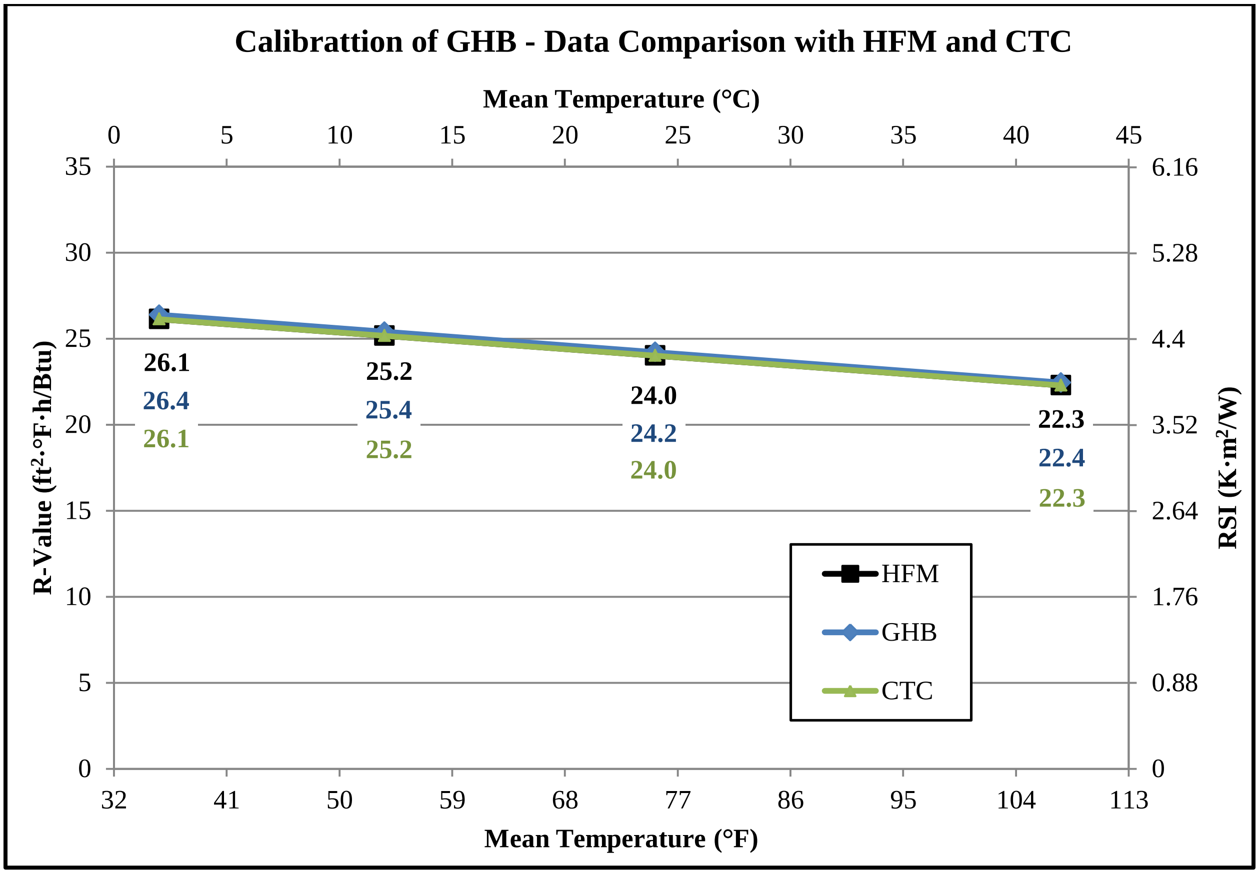

Figure 5-26: Calibration of GHB – Data Comparison with HFM and CTC

The repeatability of the GHB is established by running the same assembly three times. This is done on the polyiso R26 and R31 opaque assemblies as shown in Figure 5-27 and Table 5-6. The data indicates that the maximum deviation between opaque test results is $0.62\ ft^2 \cdot °F \cdot h/Btu$ ($0.11\ m^2 \cdot K/W$) which is less than 2.5%. Standard ASTM C1363-11 (CL.13.2.3) allows for a reproducibility difference of $1.25\ ft^2 \cdot °F \cdot h/Btu$ ($0.22\ m^2 \cdot K/W$), as shown in Figure 3-4. Therefore, the reproducibility of the GHB is well in the range of the standard.

Table 5-6: GHB Repeatability

Assembly	R26 ($ft^2 \cdot °F \cdot h/Btu$)	R31 ($ft^2 \cdot °F \cdot h/Btu$)
1	25.50	31.28
2	25.15	31.13
3	25.76	31.08
Stand. Dev.	0.31	0.11
Max. Offset	0.62	0.20

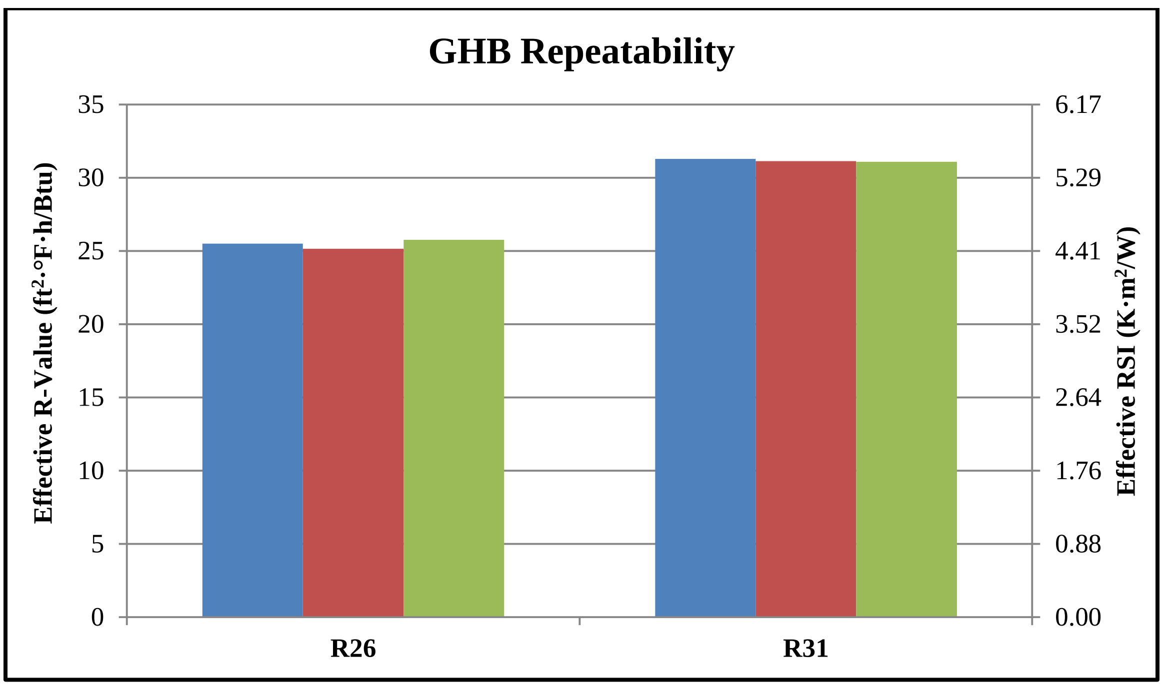

Figure 5-27: GHB Repeatability Test Data of Polyiso Opaque Assembly

5.4.2. Development of Adjustment Factors

5.4.2.1. Effect of Fasteners

As discussed in the experimental methodology, 4, 6 and 10 fasteners per insulation board are tested to quantify the impact of fasteners on the effective R-value of the assembly. The effects of fasteners are shown for each type of insulation and then cumulatively summarized and used to create a fastener density adjustment curve.

Figure 5-28 shows a typical heat flow time history for an EPS R31 assembly with and without fasteners. The data shows that the presence of fasteners increases the heat flow leading to thermal bridging in the assembly. Figure 5-29 to Figure 5-31 show the relation between fastener density and the effective R-value for the R26 and R31 assemblies; Table 5-7 to Table 5-12 show the associated thermal values. The plotted data clearly identifies that an increase in fastener density results in a decrease in the effective R-value in the roof assemblies. It is also observed that the percent decrease in R-value per fastener slightly decreases with increasing fastener density; this can be seen in Table 5-7 to Table 5-12. This suggests that there is a potential diminishing effect of the influence of each fastener as the density is increased. This diminishing effect will be further discussed in the validation of the results.

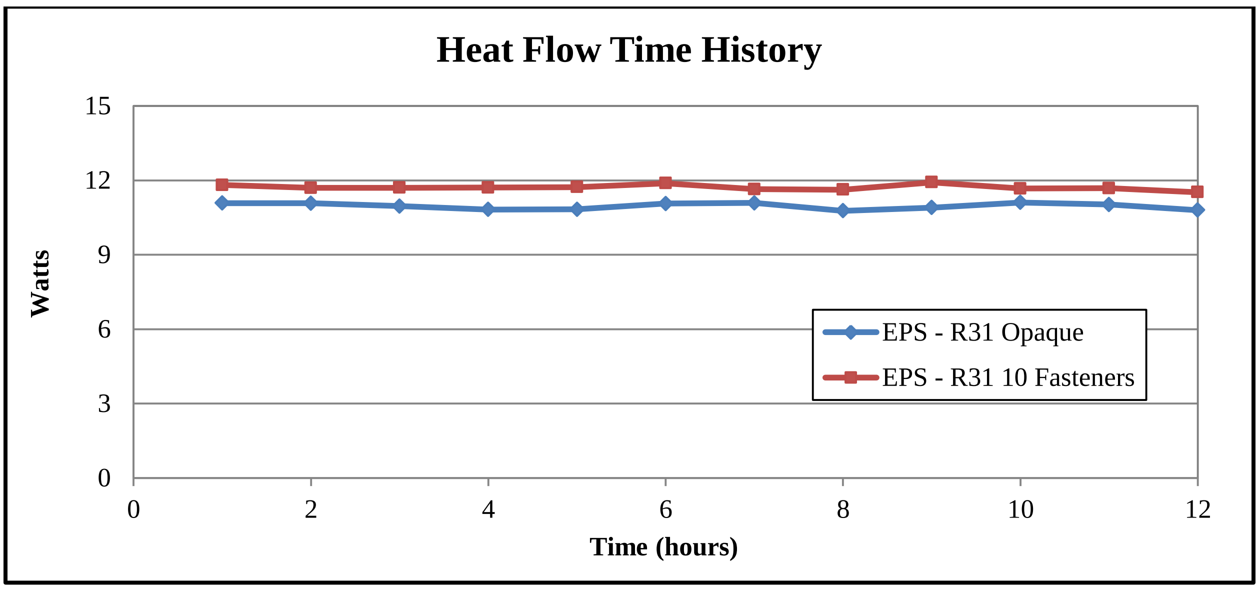

Figure 5-28: Opaque vs. Fastener Assembly – Heat Flow Time History

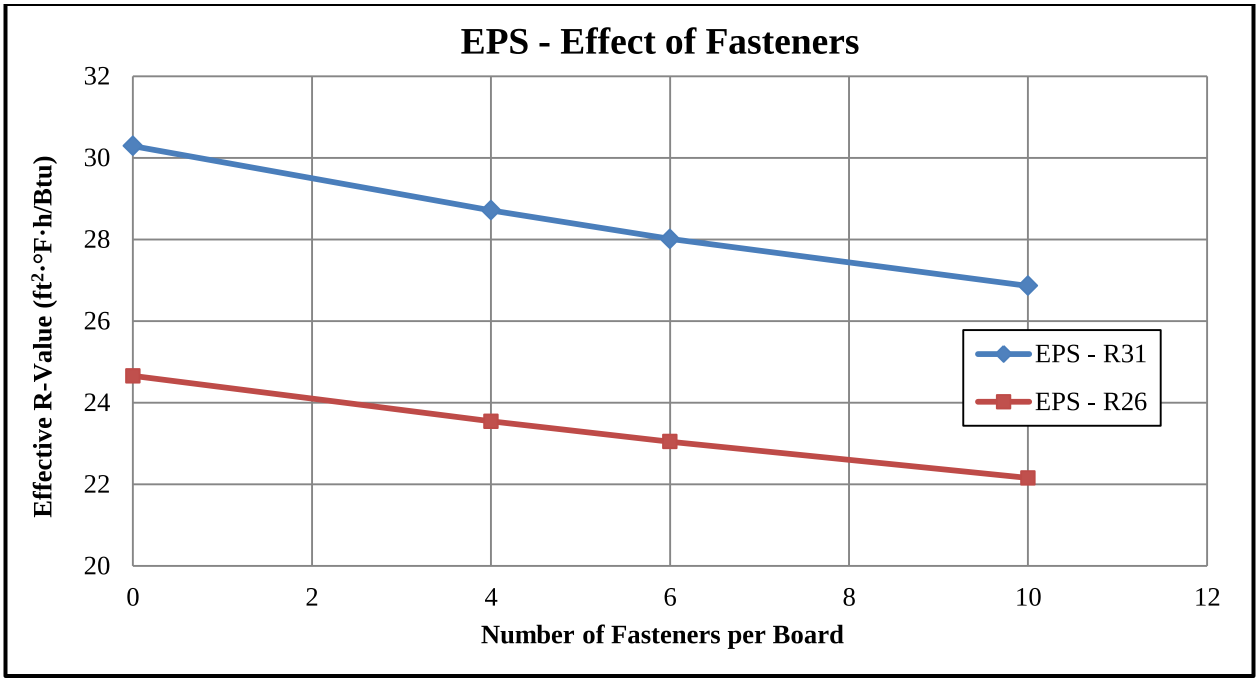

Figure 5-29: EPS – Effect of Fasteners

Table 5-7: EPS – R26 – Fastener Results

EPS - R26		**Effective R-Value (ft^2 °F h/Btu)**	**% Decrease in R-Value**	**% Decrease/ Fastener**
Fasteners	0	24.65	-	-
	4	23.54	4.51	1.13
	6	23.04	6.53	1.09
	10	22.15	10.14	1.01

Table 5-8: EPS – R31 – Fastener Results

EPS - R31		**Effective R-Value (ft^2 °F h/Btu)**	**% Decrease in R-Value**	**% Decrease/ Fastener**
Fasteners	0	30.29	-	-
	4	28.72	5.20	1.30
	6	28.01	7.53	1.25
	10	26.87	11.31	1.13

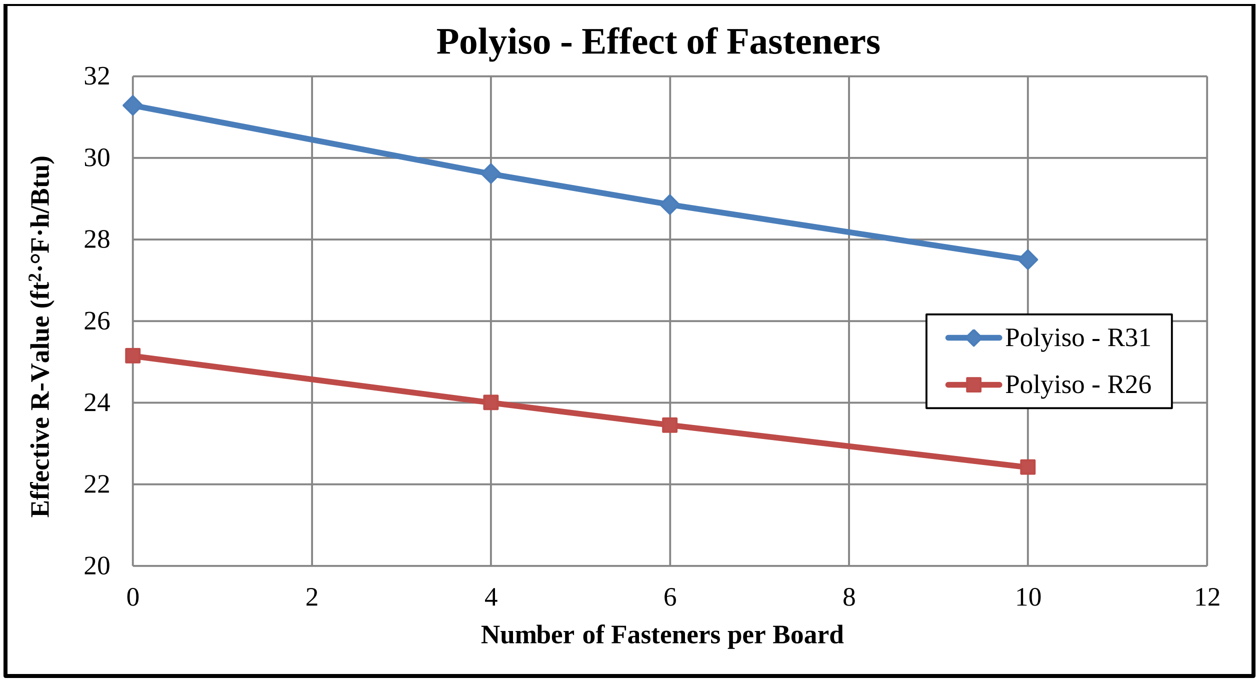

Figure 5-30: ISO – Effect of Fasteners

Table 5-9: Polyiso – R26 – Fastener Results

Polyiso - R26		**Effective R-Value** ft^2 °F h/Btu	**% Decrease in R-Value**	**% Decrease/ Fastener**
Fasteners	0	25.15	-	-
	4	24.00	4.56	1.14
	6	23.45	6.75	1.12
	10	22.42	10.86	1.09

Table 5-10: Polyiso – R31 – Fastener Results

Polyiso - R31		**Effective R-Value** ft^2 °F h/Btu	**% Decrease in R-Value**	**% Decrease/ Fastener**
Fasteners	0	31.28	-	-
	4	29.61	5.35	1.34
	6	28.85	7.77	1.29
	10	27.50	12.08	1.21

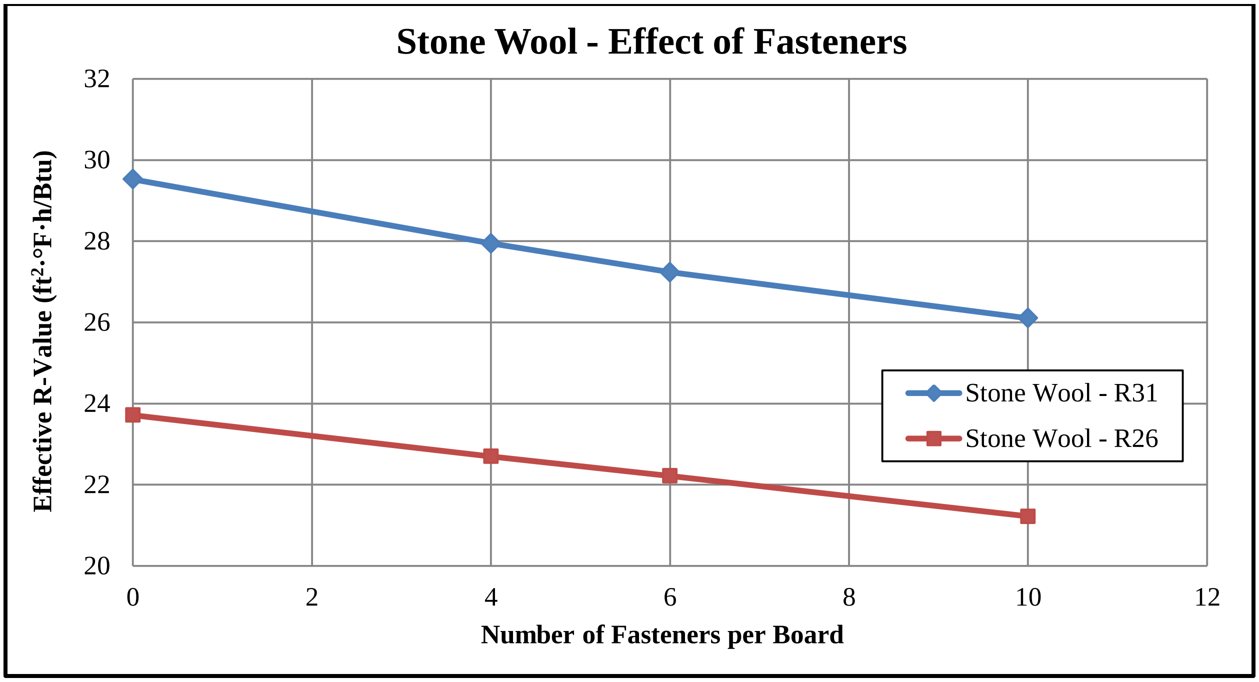

Figure 5-31: Stone Wool – Effect of Fasteners

Table 5-11: Stone Wool – R26 – Fastener Results

Stone Wool - R26		Effective R-Value ft² °F h/Btu	% Decrease in R-Value	% Decrease/ Fastener
Fasteners	0	23.72	-	-
	4	22.70	4.28	1.07
	6	22.22	6.32	1.05
	10	21.22	10.52	1.05

Table 5-12: Stone Wool – R31 – Fastener Results

Stone Wool – R31		Effective R-Value ft² °F h/Btu	% Decrease in R-Value	% Decrease/ Fastener
Fasteners	0	29.53	-	-
	4	27.95	5.34	1.34
	6	27.24	7.76	1.29
	10	26.10	11.58	1.16

Figure 5-32 summarizes the results of the fastener tests and shows the relation between fastener density per meter squared and effective thermal resistance of the tested assemblies. Comparing the different insulations, they all follow the same trend; the decrease in thermal resistance is consistent irrespective of insulation type. This conclusion is significant as it validates that the adjustment curve will be applicable to all assemblies irrespective of insulation type.

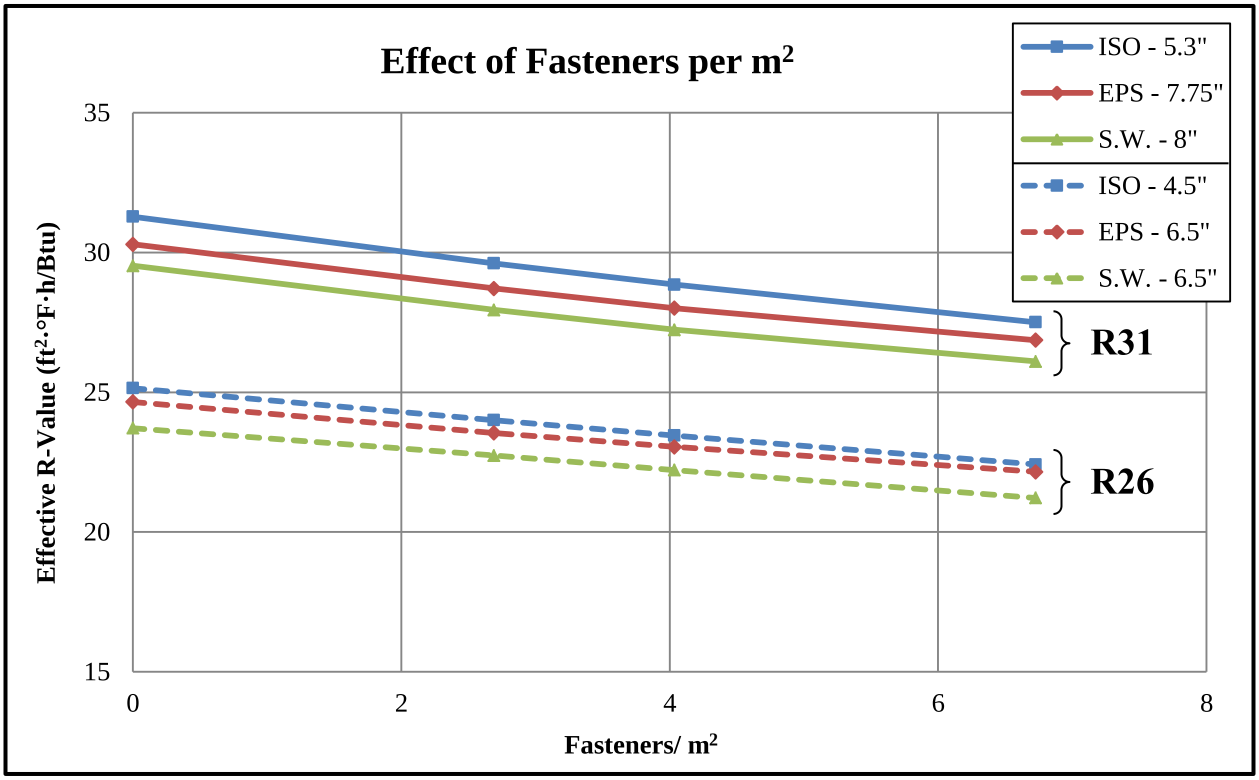

Figure 5-32: Fastener Density per m^2 vs. Effective R-Value

Figure 5-33 shows the results based on the percent decrease in effective thermal resistance. In this data arrangement, it is seen that the decrease in effective thermal resistance is influenced by the thermal resistance of the insulation, where design zone R31 has a greater impact compared to design zone R26. Towards developing the fastener adjustment factor, the measured data is fitted with a trend line which allows the designer to predict losses for larger fastener densities. Table 5-13 summarizes the numerical results for the adjustment curve. The trend line fitted with a polynomial curve which better describes the data as it considers the influence of the diminishing effect of the fasteners. As shown in Figure 2-26, fastener densities can increase to 16 fasteners per $1.2\,m \times 1.2\,m$ $(4ft \times 4ft)$ insulation board or 10.75 fasteners per meter squared. Since the fastener densities tested only reached 10 fasteners per insulation board, interpolation of the results must be done to predict the thermal decrease in effective resistance for higher fastener densities. The interpolated results are considered accurate due to the consistent trends by the results; these values however would require validation.

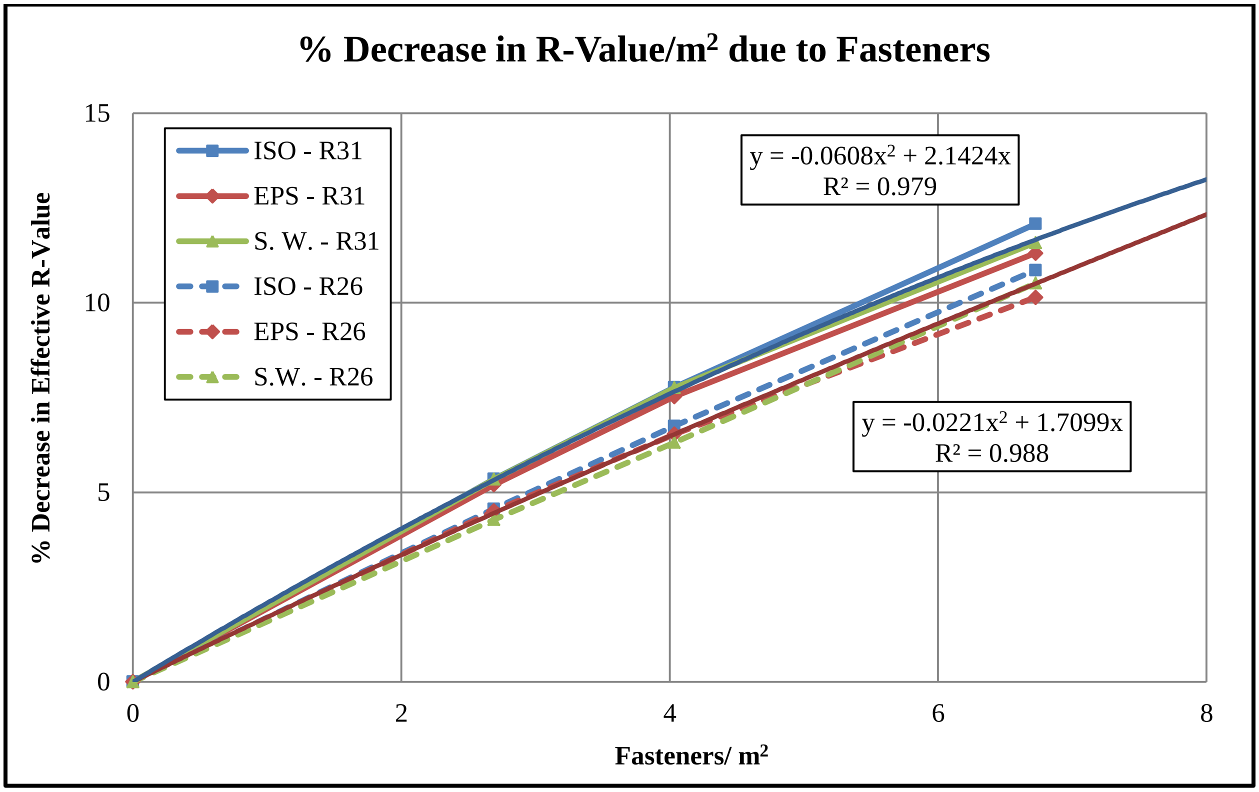

Figure 5-33: Percent Decrease in Thermal Resistance due to Fasteners

Table 5-13: Fastener Density Adjustment Factors

% Decrease in R-Value		
Fasteners/ m^2	**R26**	**R31**
0	0.0	0.0
1	1.7	2.1
2	3.3	4.0
3	4.9	5.9
4	6.5	7.6
5	8.0	9.2
6	9.5	10.7
7	10.9	12.0
8	12.3	13.2
9	13.7	14.4
10	15.0	15.3

Note: values beyond 7 fasteners/m^2 are extrapolated

5.4.2.2.Effect of Gaps

As previously discussed, commercial roofing insulation boards can be installed in a single or double layer configuration. Although two layers is the recommended practice, it is not uncommon to see single layer installation in some parts of North America with milder climates. The gap testing first begins by establishing the impact of the one-layer insulation with a through joint, followed by two layers of insulation arranged in a staggered formation. Figure 5-34 shows a typical heat flow time history for an EPS R31 assembly with and without gaps. The data shows that the presence of gaps increases the heat flow leading to thermal bridging in the assembly.

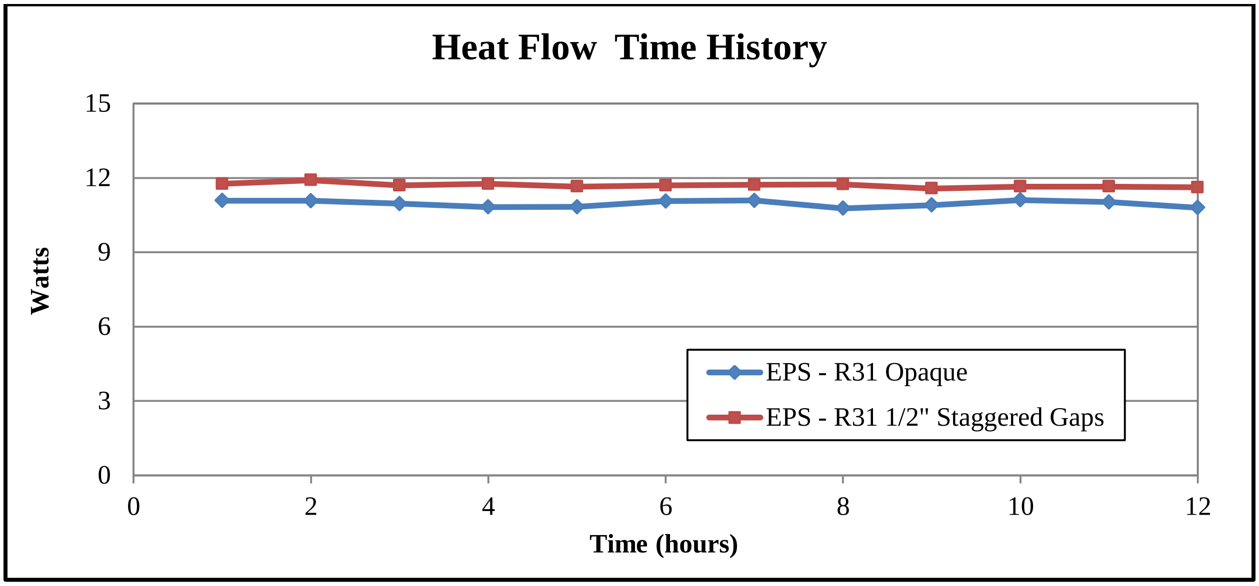

Figure 5-34: Opaque vs. Gap Assembly – Heat Flow Time History

Roof assemblies with a single layer of insulation have the potential of through gap formation at every insulation joint; this is the most critical scenario for the effect of gaps, so it is used to provide a maximum thermal loss value. Tests are carried out on a single layer, 84 mm (3.3”) thick polyiso insulation to understand how critical a through gap is compared to a staggered gap. Figure 5-35 presents the comparison between the two insulation layouts; the data shows a through gap leads to over 13% decrease in the effective thermal resistance of the roof assembly. By staggering the gap, the impact is lowered to a 6% decrease in the effective thermal resistance.

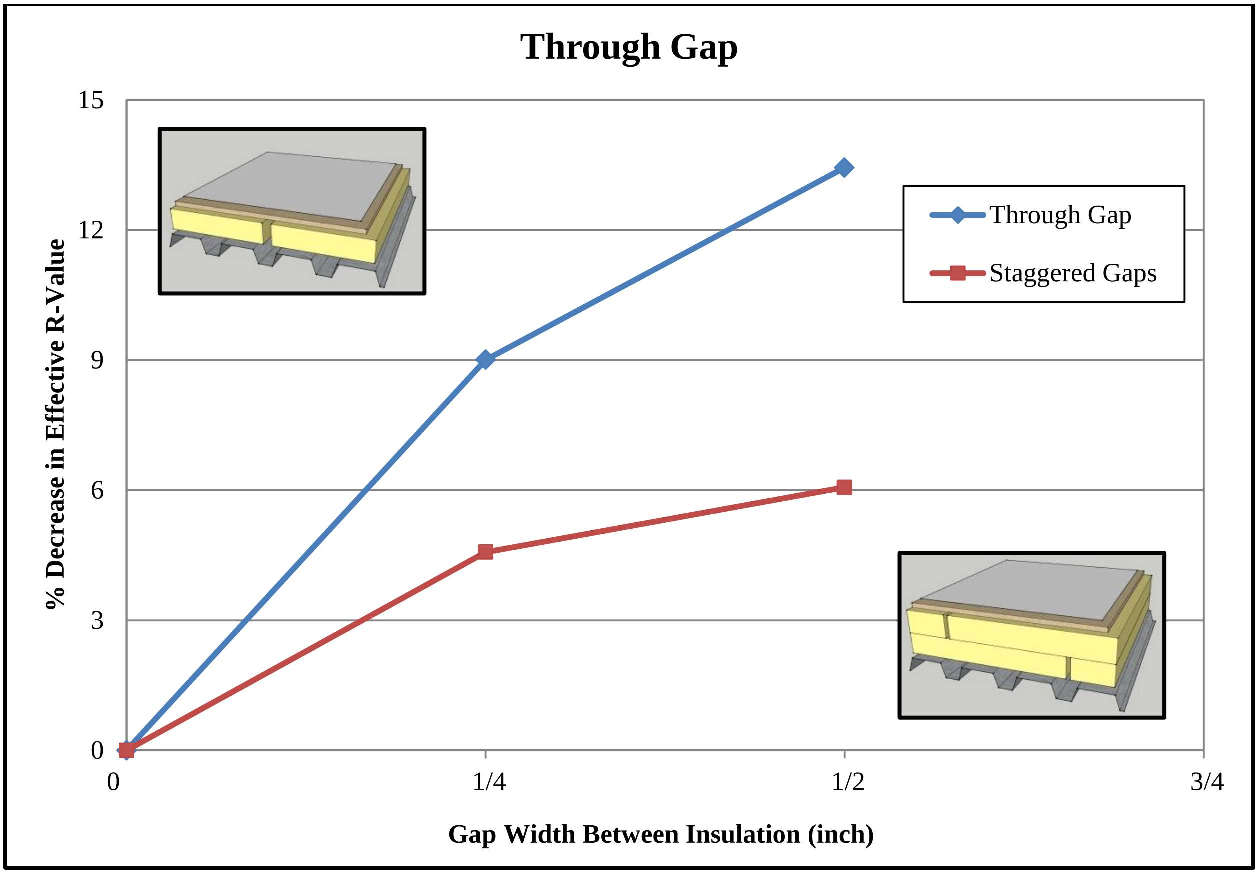

Figure 5-35: Through Gap Results (1" =25.4mm)

Figure 5-36 shows the three gap configurations tested in the two-layer insulation layout. As an example, Figure 5-37 shows the measured effective thermal resistance of an EPS R26 assembly which highlights the impact of the gaps between the insulation boards. The results show that the presence of gaps reduce the effective thermal resistance of EPS from 3% to 7% depending on the gap.

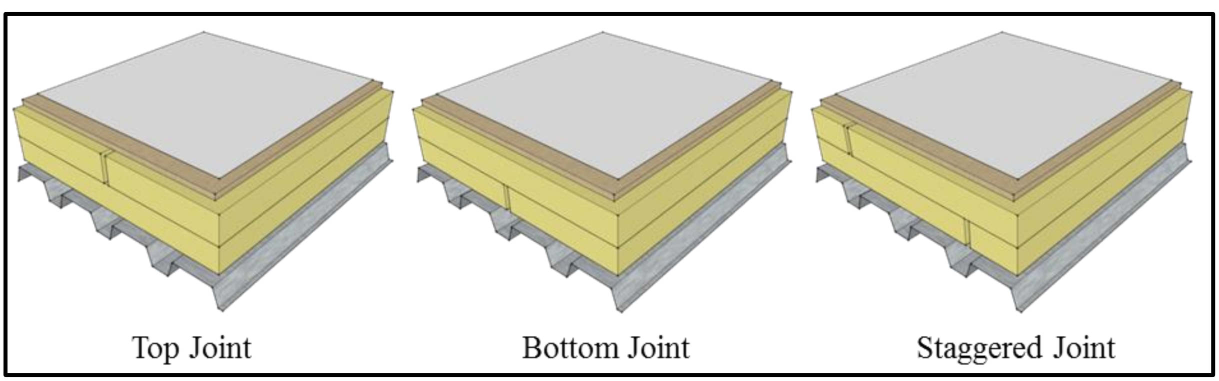

Figure 5-36: Gap Test Configurations

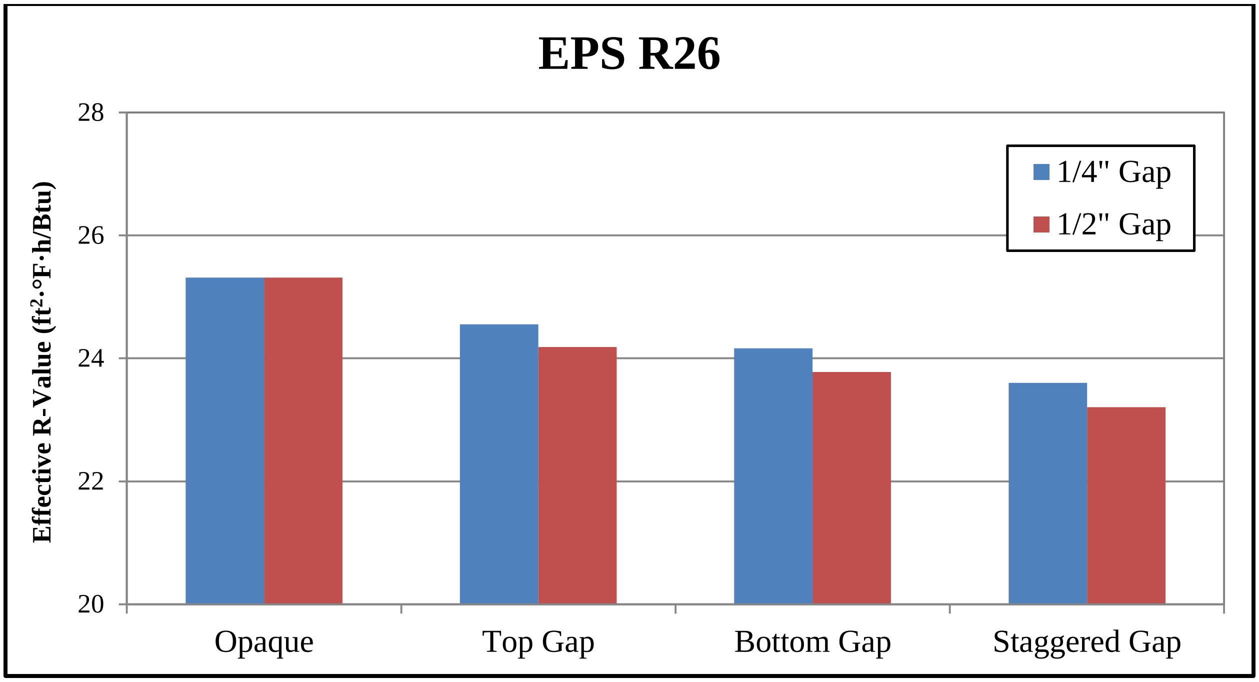

Figure 5-37: Effect of Gap Type on the Effective Thermal Resistance

Figure 5-38 and Figure 5-39 show the relation between gap size and insulation thickness on the effective R-value for the R26 and R31 assemblies; Table 5-14 and Table 5-15 show the associated values for the decrease in the effective thermal resistance. The results are presented by gap type (top and bottom then staggered) to observe the effect and trends of each gap on the effective R-value.

A summary of the gap test show:

1. The decrease in effective R-value of the assembly is found to be linear;
2. Irrespective of the gap position, with increase in insulation thickness (or gap height) there is a decrease in the effective R-value of the assembly;
3. The decrease in effective thermal resistance is consistent irrespective of insulation type;
4. With an increase in gap width, there is a decrease in the effective R-value of the assembly;
5. For staggered gaps, the total gap height is equal to the thickness of the insulation; the data trend remains the same - with increased gap width and height, there is an increase in effective thermal losses.

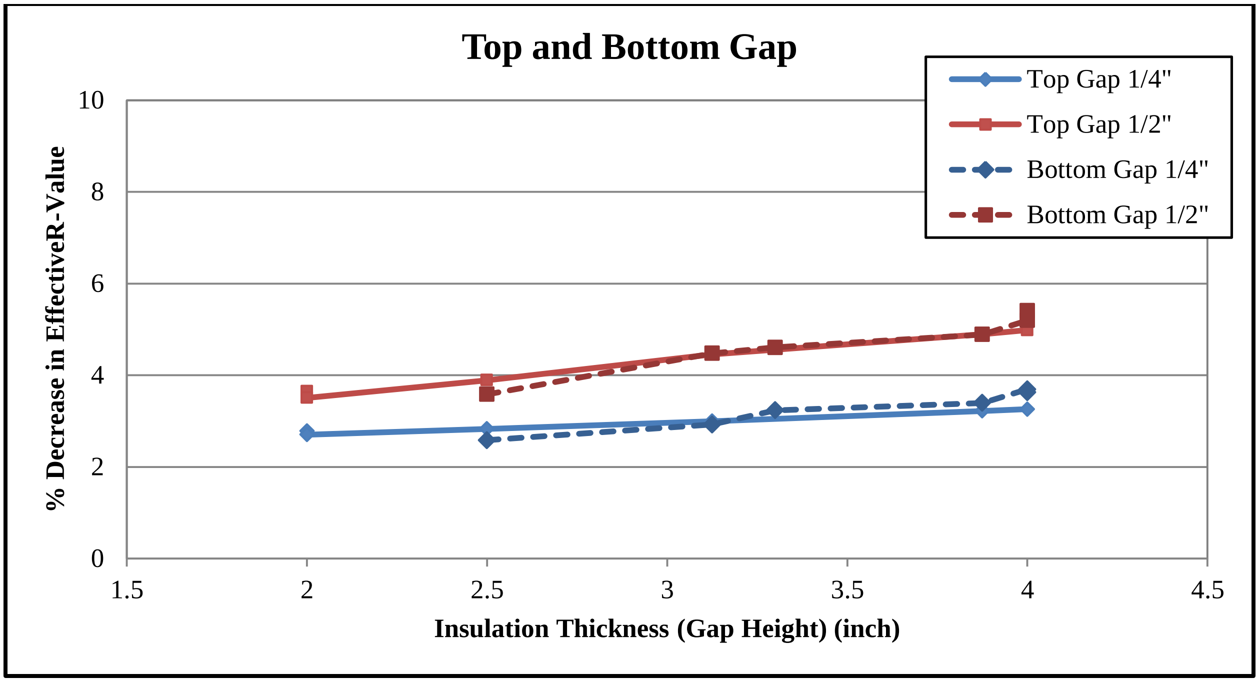

Figure 5-38: Top and Bottom Gap Results

Table 5-14: Top and Bottom Gap Results

Top Joint					
Insulation	**Zone**	**Total Thickness (in)**	**Gap Height (in)**	**% Decrease in Effective R-Value**	
				1/4"	**1/2"**
Polyiso	R26	4.5	2	2.78	3.65
Polyiso	R31	5.3	2	2.71	3.51
Stone Wool	R26	6.5	2.5	2.83	3.89
EPS	R26	6.25	3.125	3.00	4.46
EPS	R31	7.75	3.875	3.22	4.90
Stone Wool	R31	8	4	3.26	4.98
Bottom Joint					
Insulation	**Zone**	**Total Thickness (in)**	**Joint Thickness (in)**	**1/4"**	**1/2"**
Polyiso	R26	4.5	2.5	2.58	3.58
EPS	R26	6.25	3.125	2.93	4.48
Polyiso	R31	5.3	3.3	3.24	4.61
EPS	R31	7.75	3.875	3.39	4.89
Stone Wool	R26	6.5	4	3.69	5.20
Stone Wool	R31	8	4	3.63	5.41

Note: 1”=25.4mm

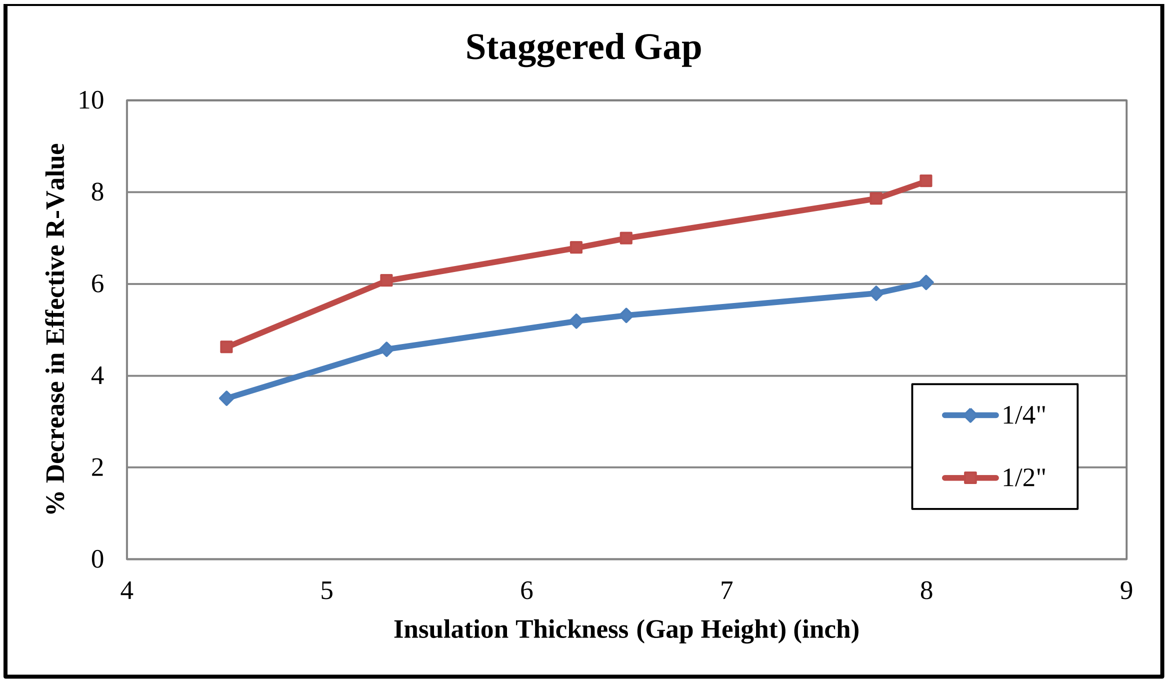

Figure 5-39: Staggered Gap Results

Table 5-15: Staggered Gap Results

Staggered Joints					
Insulation	**Zone**	**Total Thickness (in)**	**Gap Height (in)**	**% Decrease in Effective R-Value**	
				1/4"	**1/2"**
Polyiso	R26	4.5	4.5	3.51	4.62
Polyiso	R31	5.3	5.3	4.57	6.07
EPS	R26	6.25	6.25	5.19	6.79
Stone Wool	R26	6.5	6.5	5.31	6.99
EPS	R31	7.75	7.75	5.79	7.86
Stone Wool	R31	8	8	6.03	8.24

Note: 1”=25.4mm

The measured data from Table 5-14 and Table 5-15 are combined and generalized to obtain the gap adjustment curve shown in Figure 5-40. This gap adjustment curve is applicable for any insulation layouts, with gaps in a single layer of the insulation or arranged in a staggered configuration. The adjustment curve is also applicable for any insulation type. Figure 5-40 has a regression line fitted through the data for each design zone (R26 and R31). The R^2 values for each curve show that the curves fit the data very well, with results following the same trend regardless of gap location, gap size or insulation type.

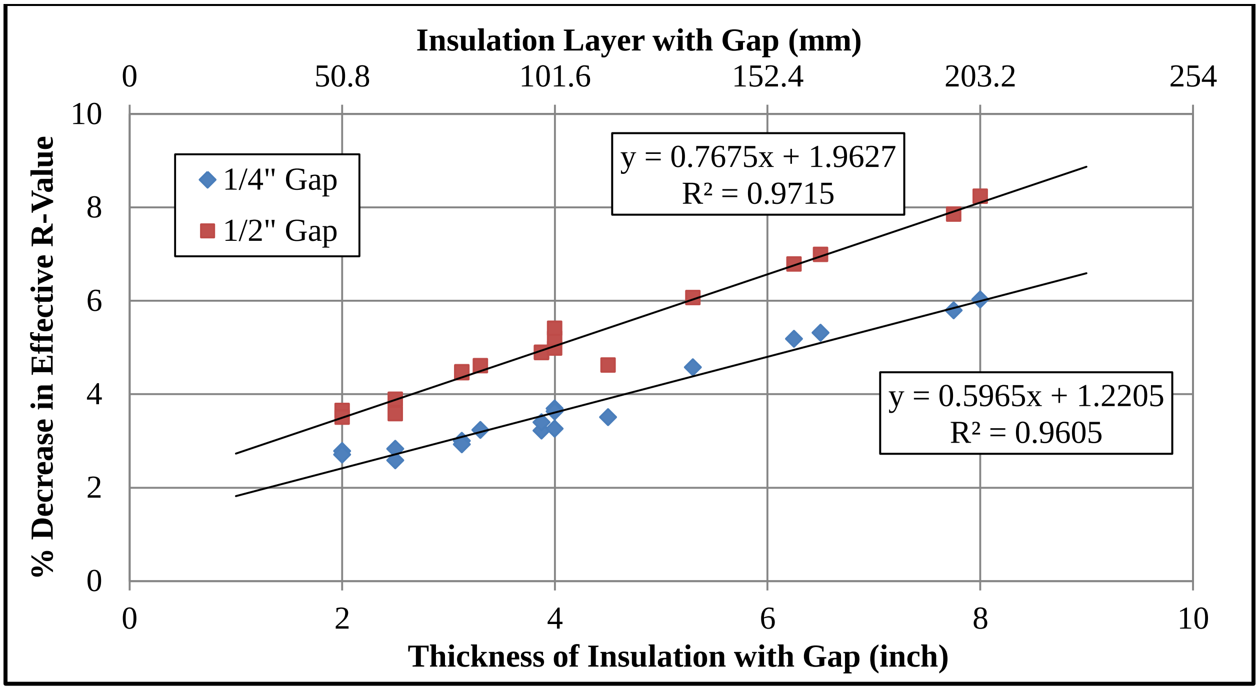

Note: The x-axis refers to the thickness of the insulation layer with a gap. Example: If an assembly has 6" of insulation, 2" top layer and 4" bottom layer, and a gap is in the bottom layer, the "thickness of insulation with gap" is 4". If there are gaps in both layers, then the value will be 6".

Figure 5-40: Gap Adjustment Curve

5.4.3. Combined Fastener and Gap Test Results

To verify the combined effect of fasteners and gaps on the effective R-value of the roof assemblies, R31 designed roof assemblies with three insulation types are tested for a combination of fasteners (10 per board) and staggered gaps (12.7 mm or 1/2"). The design effective R-value is adjusted for the thermal impact factors using (Eqn. 5-5) and (Eqn. 5-6). The results from Table 5-16 validate the developed adjustment factors, full scale validation of these factors will be discussed in following section.

$$R_{effective} = R_{Opaque} - \Delta R \qquad \textbf{(Eqn. 5-5)}$$

where,

$$\Delta R = (\%\ Decrease_{gap} \times R_{opaque}) + (\%\ Decrease_{fastener} \times R_{Opaque}) \qquad \textbf{(Eqn. 5-6)}$$

Table 5-16: Fastener and Gap Combined Test Results

Assembly (R31)	R_{opaque}	$\%Decrease_{gap}$ (a)	$\%Decrease_{fast}$ (b)	Cumulative Effect (a+b)	ΔR	$R_{effective}$	Measured cumulative effect	$R_{effective}$
Polyiso	31.08	6.07	12.08	18.15	5.64	25.44	18.40	25.36
EPS	30.29	7.86	11.31	19.17	5.81	24.49	19.29	24.45
Stone Wool	29.14	8.24	11.58	19.82	5.78	23.36	18.43	23.77

Chapter 6: Data Validation and Codification

To check the validity, accuracy and application of the GHB results, validation tests are run on a large scale calibrated thermal chamber (CTC). The chamber has dimensions of $2.4\,m \times 6\,m$ ($8ft \times 20ft$) shown in Figure 6-1, and it is capable of inducing moisture and airflow mimicking in-situ conditions closely. Tests are run to validate the worst-case scenarios: $12.7\,mm$ (1/2") gaps and 10 fasteners per insulation board (or 7 fasteners per m^2).

Figure 6-1: Thermal Chamber

6.1. Joint Validation

The insulation tested on the large scale CTC is an R31 design polyiso insulation; an opaque system is first tested to provide a reference value, followed by a $12.7\,mm$ (1/2") gap configuration, shown in Figure 6-2 and Figure 6-3 respectively.

Figure 6-2: Calibrated Thermal Chamber – Polyiso R31 System – No Gaps

Figure 6-3: Calibrated Thermal Chamber – Polyiso R31 System – ½” Gaps

To validate the GHB results and adjustment curves, the data must adequately predict the losses associated with the thermal impact factors. In order to predict the losses from the CTC, a scaling factor must be applied to the GHB data. It can be seen from Figure 6-5 that the CTC is 10 times larger than the GHB, but the calculation of thermal loss depends on the number of joints in the system. Figure 6-4 shows that the insulation configuration in the GHB has four linear feet of gaps between the insulation boards on both the top and bottom layers. The CTC on the other hand is 10 times larger but has more than 15 times the length of gaps. This can be seen in Figure 6-6 and in calculation in Table 6-1. Therefore, in order to adequately compare the two systems, a scaling factor must be applied on the linear feet of joints per layer of each system.

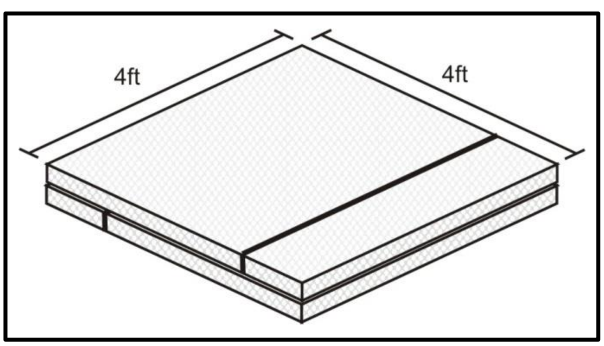

Figure 6-4: GHB Insulation Dimensions

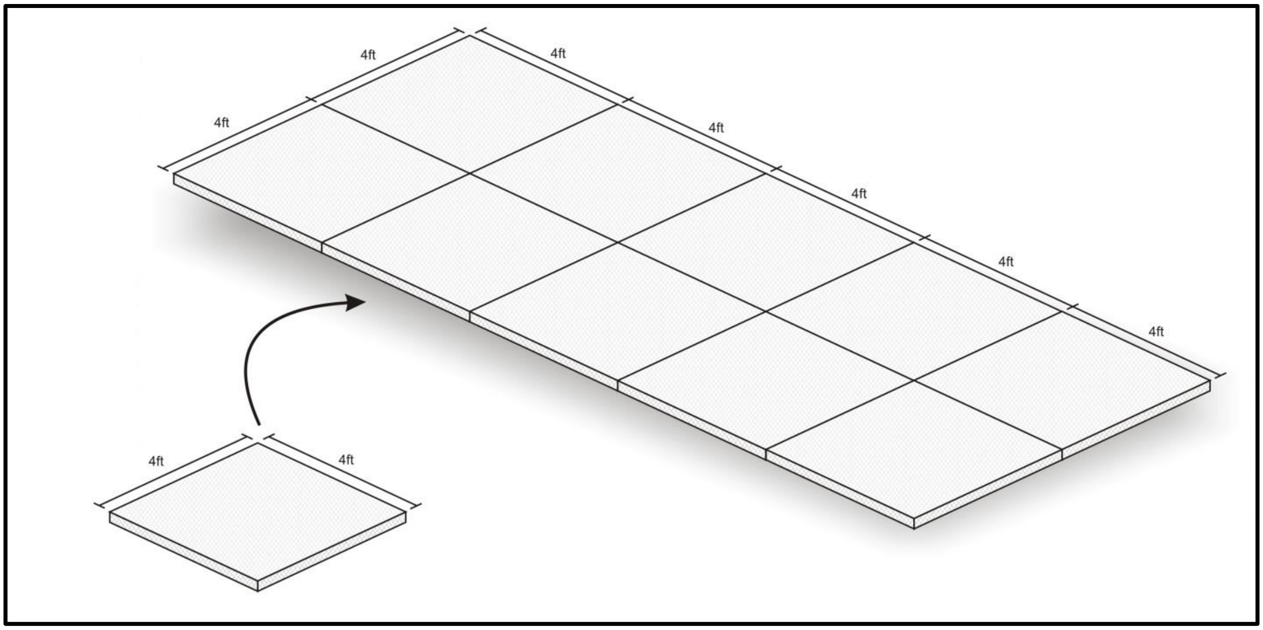

Figure 6-5: GHB vs. CTC Dimensions

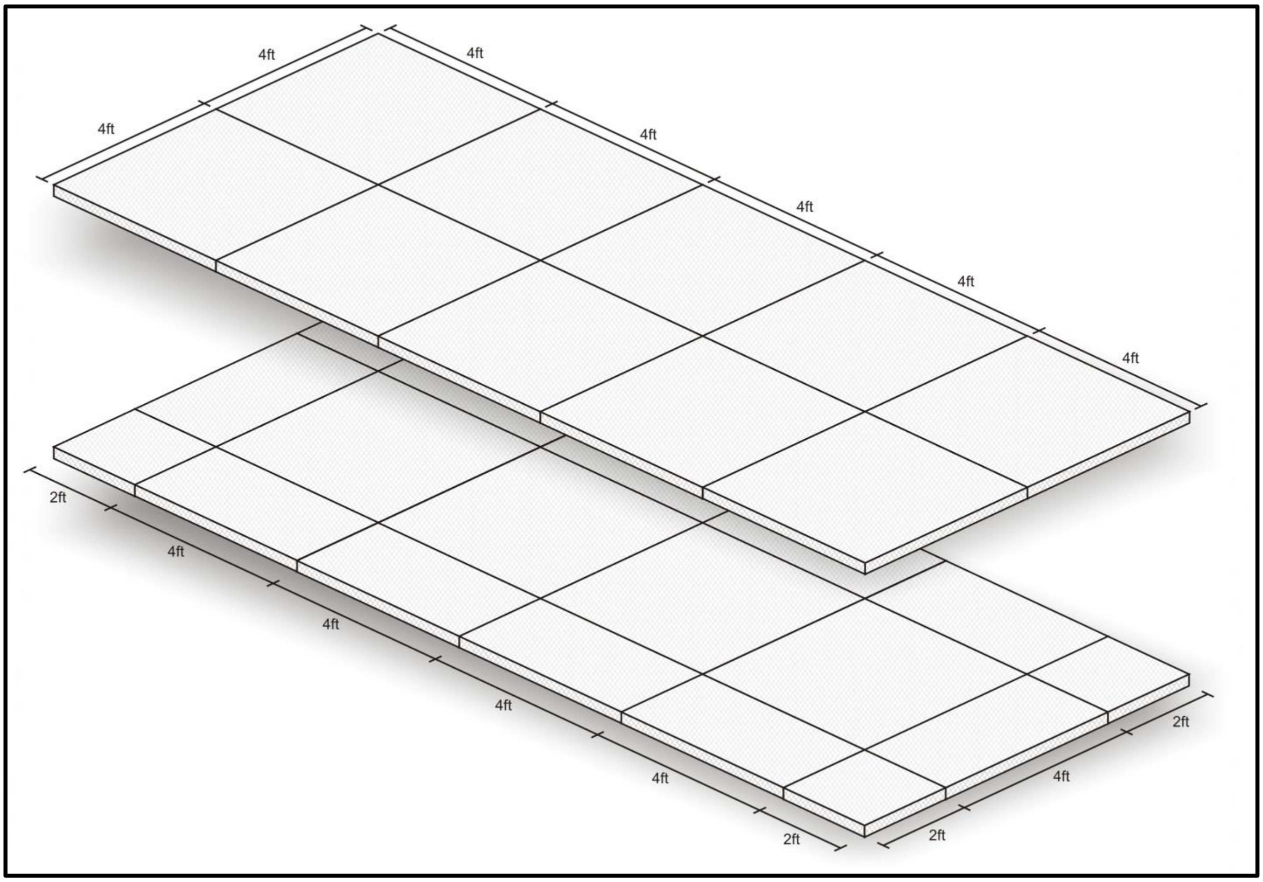

Note: This is the typical in-situ insulation configuration to prevent through gaps.

Figure 6-6: CTC Insulation Dimensions

Although the CTC has a dimension of $2.4\,m \times 6\,m$ ($8ft \times 20ft$), the climatic chamber is placed on top of the test specimen covering $76\,mm$ (3”) of the test perimeter. This gives the CTC a metering dimension of $2.29\,m \times 5.94\,m$ ($7.5ft \times 19.5ft$). In order to use the gap adjustment curve, the ratio of area for the GHB and CTC needs to be equal to the ratio of linear feet of gaps. Table 6-1 shows the calculated linear feet of gaps for both chambers; the values are used in (Eqn. 6-3) to determine the ratio of gaps between chambers. The ratio of test assembly area is then calculated in (Eqn. 6-2).

Table 6-1: Length of Gaps per Chamber

	Guarded Hot Box	Calibrated Thermal Chamber
Top Insulation Layer	$4\,L.F.$	$4 \times 7.5ft = 30\,L.F.$ $1 \times 19.5ft = 19.5\,L.F.$ $Total = 49.5\,L.F.$
Bottom Insulation Layer	$4\,L.F.$	$5 \times 7.5ft = 37.5\,L.F.$ $2 \times 19.5ft = 39\,L.F.$ $Total = 76.5\,L.F.$
Total Gap Length	$8\,L.F.$	$126\,L.F.$

Note: L.F. = Linear Feet

$$\frac{CTC\ Gap\ Area}{GHB\ Gap\ Area} = \frac{126' \times 1/2"}{8' \times 1/2"} = 15.75 \qquad \textbf{(Eqn. 6-1)}$$

$$\frac{CTC\ Area}{GHB\ Area} = \frac{7.5' \times 19.5'}{4' \times 4'} = \frac{146.25ft^2}{16ft^2} = 9.141 \qquad \textbf{(Eqn. 6-2)}$$

Since the two ratios are not a 1:1, a scaling factor needs to be applied to the gap adjustment curve to normalize the data for the CTC test assembly.

$$Scaling\ Factor = \frac{Gap\ Area\ Ratio}{Area\ Ratio} = \frac{15.75}{9.141} = 1.723 \qquad \textbf{(Eqn. 6-3)}$$

From the GHB test results, an R31 designed polyiso assembly with staggered ½”-gap layout will have a decrease in effective thermal resistance of 6.07% (Table 5-15). Therefore, calculating the decrease in effective thermal resistance for the CTC test assembly with ½” staggered gaps yields a 10.46% decrease (Eqn. 6-4).

$$\%\ Decrease\ in\ R-Value = \ Adjustment\ Factor \times Scaling\ Factor \qquad \textbf{(Eqn. 6-4)}$$

$$\%\ Decrease\ in\ Effective\ R-Value = \ 6.07\% \times 1.723$$

$$\%\ Decrease\ in\ Effective\ R-Value = \ 10.46\%$$

The results from the CTC gap test are summarized in Table 6-2, where the decrease in the assembly’s effective thermal resistance due to ½” gaps is 11.82%. There is a slight deviation in the predicted thermal loss, 10.46%, and the actual thermal loss, 11.82%, which can be attributed to the presence of cross-joints in the CTC. Cross-joints, shown in Figure 6-7, results in a gap that bypasses both layers of insulation. The effect of the cross-joint is outside the scope of this thesis but is a parameter that must be quantified. The presence of multiple cross-joints in the CTC (Figure 6-8) is attributed for the 1.36% difference between results.

Table 6-2: CTC Joint Test Results

Calibrated Thermal Chamber - Polyiso R31 - 1/2" Gap		
Assembly	**Effective R-Value**	**% Decrease in R-Value**
	ft^2 °F h/Btu	**%**
Opaque	28.83	-
½” Gap	25.42	11.82

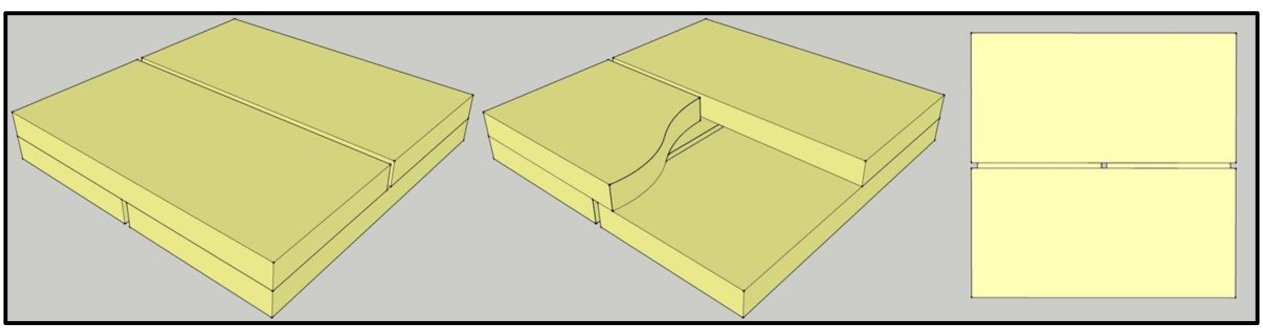

Figure 6-7: Cross-Joint

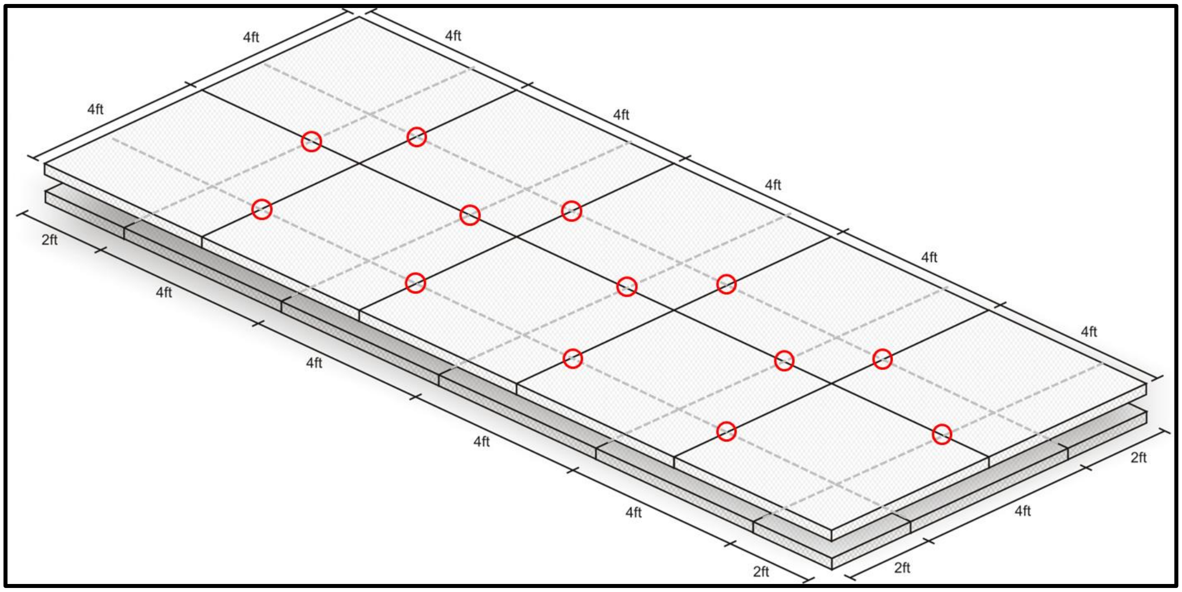

Figure 6-8: CTC Cross-Joints

6.2. Fastener Validation

Similar to the gap data validation, the fastener data is validated through comparison of the GHB data to the CTC results. Figure 6-9 shows the CTC polyiso R26 fastener assembly. No scaling factors are required for the fastener adjustment curves, as they are already normalized for fasteners per m^2.

Figure 6-9: Calibrated Thermal Chamber – Polyiso R31 System - Fasteners

Figure 6-10 shows the fastener densities tested on the GHB

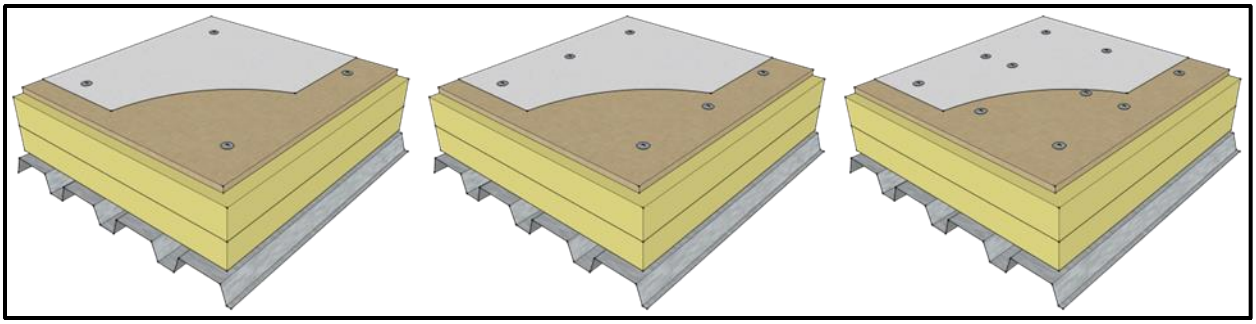

Figure 6-10: GHB Tested Fastener Densities

The CTC assembly tested has 96 fasteners or 7.07 fasteners per m^2. Using the fastener adjustment curve in Figure 5-33 (or Table 5-13 for the exact values), the decrease in the effective thermal resistance due to the fasteners is 11.0%. Table 6-3 presents the results for the CTC fastener test; the decrease in effective thermal resistance is 10%. This result is slightly lower than the predicted values. As previously mentioned, as the fastener density increases, the decrease in thermal resistance becomes slightly lower due to a diminishing effect on the impact factors. This accounts for the discrepancies between the predicted decrease in effective thermal resistance of 11.0% to the CTC measured decrease in effective thermal resistance of 10%.

Table 6-3: Calibrated Thermal Chamber Fastener Test Results

Calibrated Thermal Chamber - Polyiso R31 - Fasteners			
Fasteners	Fasteners /m^2	Effective R-Value	% Decrease in R-Value
		ft^2 °F h/Btu	%
0	0	31.90	-
96	7.07	28.72	9.99

6.3. Codification

Current design in the building code does not account for the impact of fasteners and gaps on the thermal performance of roof assemblies. Based on the findings from this study, the National Energy Code of Canada can be updated to adequately account for the thermal impact factors present in roof assemblies. The new design change proposed for the building code will incorporate these effects through adjustment factors using (Eqn. 5-5) and (Eqn. 5-6). The results for the thermal impact factors have been summarized in adjustment curves that are applicable for all roofing assemblies. The adjustment curves proposed for the NECB are shown in Table 6-4 and Figure 6-11 for fasteners and Figure 6-12 for gaps.

Table 6-4: Fastener Adjustment Factors

Zone		**1**	**2**	**3**	**4**	**5**	**6**	**7**	**8**
Effective Thermal Resistance		21	26	26	31	31	31	36	36
Fasteners/ ft^2	**Fasteners/ m^2**	% Decrease in Effective Thermal Resistance							
0.250	**2.69**	-	6.5	6.5	7.6	7.6	7.6	TBD	TBD
0.375	**4.04**	-	9.5	9.5	10.7	10.7	10.7	TBD	TBD
0.625	**6.73**	-	15.0	15.0	15.3	15.3	15.3	TBD	TBD

Note: Thermal Resistance = 5.67446 RSI

TBD = To Be Decided (Testing in progress)

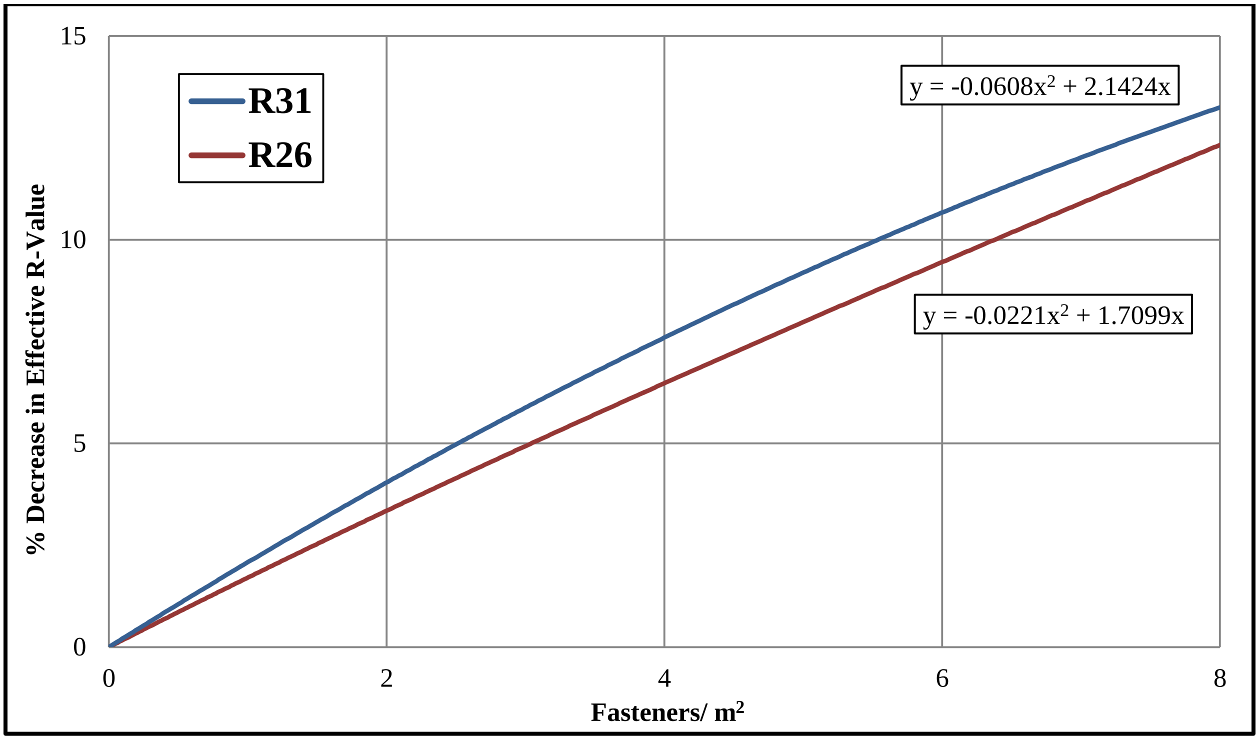

Figure 6-11: Fastener Adjustment Curve

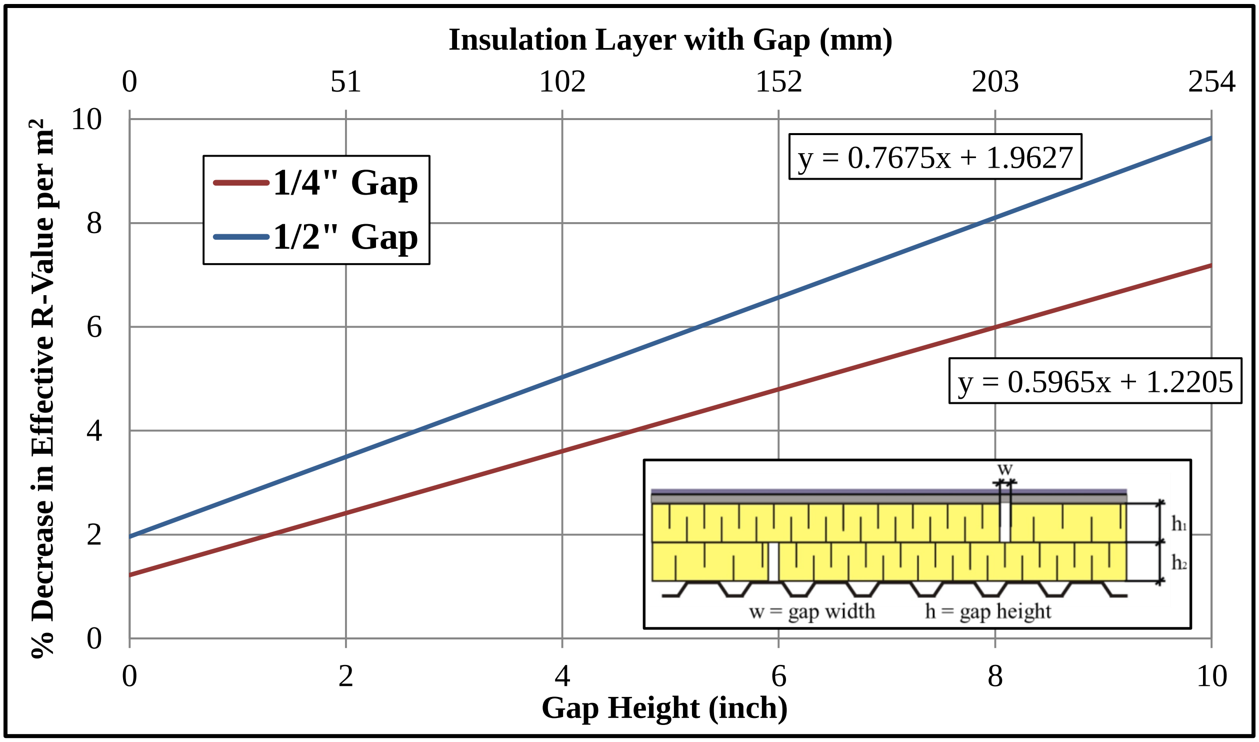

Figure 6-12: Gap Adjustment Curve

The following is a design example showcasing the current roof energy design method and the proposed design method. In the example, a designer designs a MARS roof assembly with the assumption of ½” gaps between the insulation boards. This roof assembly is designed in NECB zone 5 (ASHRAE zone 6) with polyiso insulation; therefore, the assembly must be designed for an effective R-value of R31. As indicated in Table 6-5 the effective R-value was achieved through adding the R-value of opaque components and air films without considering the fasteners and gaps.

Using the proposed design method, the designer would apply the developed adjustment factors to the calculated R-value, to determine the potential decrease in the thermal performance of MARS due to the thermal impact factors.

Table 6-5: Adjustment Factor Implementation Example

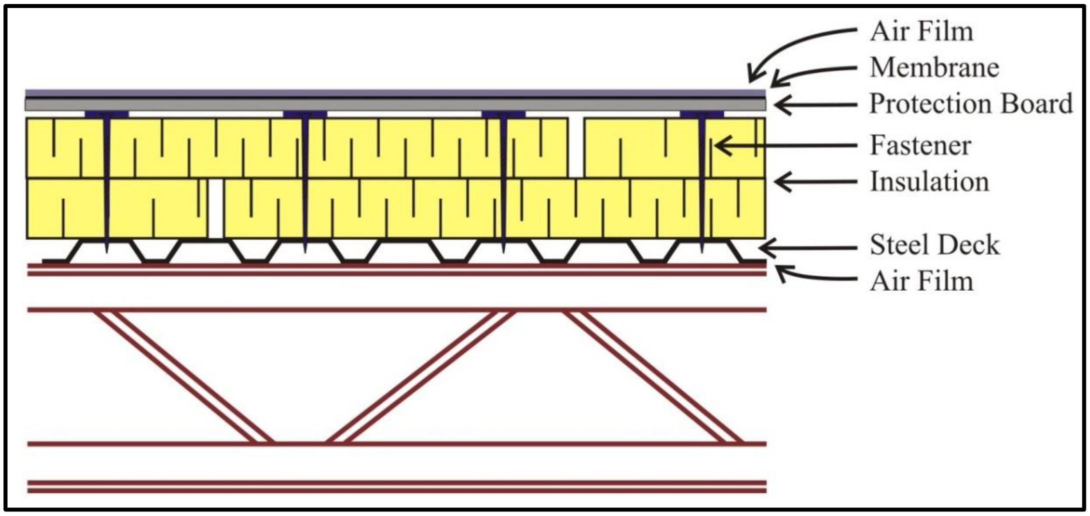

Current Design (does not consider thermal impact factors)

Assembly Components	**R-Value ($ft^2 \cdot$°F$\cdot hr/Btu$)**	**RSI ($m^2 \cdot$°K/W)**
Exterior air film	0.17	0.03
Membrane	0.34	0.06
Protection board	2.30	0.40
Insulation (5" polyiso)	27.52	4.85
Steel Deck	0.00	0.00
Interior air film	0.62	0.11
Total R-value	**30.95**	5.45
U=1/R	0.0323	0.183

Proposed Design (with thermal impact factors)

$$R_{effective} = R_{Opaque} - \Delta R$$
$$R_{Opaque} = 30.95$$

$$\Delta R = \left(\%\, Decrease_{gap} \times R_{opaque}\right) + \left(\%\, Decrease_{fastener} \times R_{Opaque}\right)$$
$$\Delta R = (5.8\% \times 30.95) + (12.4\% \times 30.95)$$
$$\Delta R = 5.63\ \frac{ft^2 \cdot \text{°F} \cdot hr}{Btu}$$

where

$$R_{effective} = 30.95 - 5.63$$
$$\boldsymbol{R_{effective} = 25.32\ \frac{ft^2 \cdot \text{°F} \cdot hr}{Btu}}$$

and

$$U = \frac{1}{R_{effective}} = \frac{1}{25.32} = 0.0395\ \frac{Btu}{ft^2 \cdot \text{°F} \cdot hr}$$

For 5-inch thick insulation, the thermal impact due to gaps is 5.8% (retrieved from Figure 6-12). The fastener configuration for the roof assembly, selected from Figure 2-26, is 12 fasteners per insulation board (or 8.07 fasteners per m^2), the associated thermal decrease is 12.4% (retrieved from Figure 6-11).

By considering the effect of the thermal impact factors, the roof assembly will perform as an R25 roof instead of the required R31. This is a 20% decrease in the roofs' thermal efficiency due to the thermal impact factors, which are not considered in current design practice. An update to the current code will entail the inclusion of Figure 6-11 and Figure 6-12 to allow designers to apply the corresponding factors in the thermal resistance calculation of roof assemblies.

Chapter 7: Concluding Remarks

7.1. Conclusions

Previous work has concluded that many factors have an impact on the thermal performance of insulating materials. These factors range from the method of manufacturing insulation, which can result in thermal drift and therefore decrease the thermal efficiency of insulation over its life time, to the standard of reporting thermal properties at a given temperature. Current energy codes disregard the effect of components that lead to thermal bridging, such as such as fasteners and gaps. Studies previously done have shown the significance and impact of these factors on the effect of roof assemblies, but due to limitations, tests were done on specific assemblies and components which are not generalized or applicable to the current energy design of roofs. Current research done by numerical modelling is accurate in terms of factors and methodology, but very limited to its boundaries and parameters; it has not been validated with experimental testing or in-situ monitoring. The need for experimental testing is crucial for justifying and validating all numerical models and providing test parameters. Up to now, no adequate studies that considered and analyzed the thermal losses of roofing assemblies due to these thermal impact factors had been conducted. The goal this research was to quantify the magnitude of these thermal impact factors and provide thermal adjustment factors that are universally applicable, irrespective of roof type or configuration.

The effect of the thermal impact factors have been quantified and expressed as simple adjustment curves that can be implemented in the design standard alongside the current design procedure. The conclusions from the experimental testing conducted in this research are:

1. An increase in fastener density decreases the effective thermal resistance of the assembly.
2. The decrease in effective thermal resistance in roof assemblies with fasteners is found to be consistent irrespective of insulation type having an equivalent thermal resistance.
3. The decrease in effective thermal resistance of the assembly, due to gaps, is found to be linear.
4. Gap height and gap width were identified to have an impact on the thermal performance of the roof assembly. Irrespective of the gap position (top layer or bottom layer), with increasing insulation thickness (or gap height) there is a decrease in the effective thermal

resistance of the assembly. Similarly, with an increase in gap width, there is a decrease in the effective thermal resistance. For staggered gaps, the total gap height is equal to the thickness of the insulation; the data trend remains the same - increased gap width and height result in a decrease in effective thermal resistance.

5. A through gap is the worst-case scenario for insulation gaps. It was found that there is a 13.44% decrease in effective thermal resistance. It must be noted that this value is specific to a 3.3”-thick gap height, and with increasing gap height there is potential for higher thermal losses. Staggering this gap will reduce its effect by 3% to 7% depending on the gap width.
6. The influence of a ¼” and ½” gap for insulation thicknesses ranging from 2” to 8” have an decrease of 2.6%-8.3% on the thermal performance of the assemblies.
7. The influence of fasteners results in a 12% decrease in the thermal resistance with 10 fasteners per insulation board (6.75 fasteners per m^2), with a potential of 16% decrease for the highest fastener density configuration currently followed in the industry.
8. The combined effect of the thermal impact factors is found to have 18%-20% decrease in the thermal efficiency of roof assemblies.

The results from the GHB tests were validated by comparing the sum of individual thermal impact factor tests to the combined thermal impact factor tests. The results were then used to predict the losses on an assembly built on a large scale thermal chamber. The adjustment curves were able to predict the losses within 2%, validating the accuracy of the adjustment curves. An update to the current code will entail the inclusion of the proposed adjustment curves to allow designers to apply the corresponding factors in the thermal resistance calculation of roof assemblies.

7.2. Future Work

As part of the ERCR project led by the National Research Council of Canada, the next steps for completing this project is to run the fastener and gap thermal impact factors on the design R36 zone. Next, an adjustment curve must be created for the third thermal impact factor, which is moisture and air intrusion.

Beyond the scope of the ERCR project, tests need to be run to validate some parameters observed from the test results. Testing must be done to quantify the influence of cross-joints on the thermal resistance of roof assemblies. Numerical modeling can be used to validate the adjustment curves for the values forecast past the maximum fastener density tested, and the effect of the diminishing effect of the thermal impact factors. Numerical modeling may also be done to accurately map the temperature gradient throughout the insulation boards and the convective flow in gaps between the insulation boards to more accurately measure that change in temperature across the assembly.

References

Baskaran, Bas, and Suda Molleti. 2009. "Air Intrusion vs. Air Leakage: The Dilemma for Low-Sloped, Mechanically Attached Membrane Roofs," 7.

Building Engineering Limited, RDH. 2010. "ASHRAE 90.1 - Requirements for the Building Enclosure: Understanding the Compliance Path for Multi-Unit Residential Buildings." *Builder Insight*.

Building Science Corporation, (BSC). 2013. "Understanding the Temperature Dependence of R-Values for Polyisocyanurate Roof Insulation." *Building Science Information: Sheet 502*.

Burch, Douglas, Paul Shoback, and Kevin Cavanaugh. 1986. "A Heat Transfer Analysis of Metal Fasteners in Low-Slope Roofs." *Roofing Reseach and Standards Developement*, no. ASTM Special Technical Publication 959: 10–20.

"Climate Zone Map." 2015. *Green Building Advisor*. http://www.greenbuildingadvisor.com/climate-zone-map-including-canada.

Courville, G., T. Petrie, P. Shipp, and P. Childs. 1989. "Comparison of the Dynamic Thermal Performance of Insulated Roof Systems.pdf."

Global, Factory Mutual. 2016. "Roof Deck Securement and Above-Deck Foor Componenets." *Property Loss Prevention Data Sheets*.

Grin, Aaron, Chris Schumacher, and Jonathan Smegal. 2014. "The Implications of Thermal Conductivity for Commercial Roof Systems." *Building Science Consulting Inc.*

Gulati, Rupesh, Sasikant Suddapalli, and Ravi Srinivasan. 2016. "Roof Fasteners for Metal Deck Roofing Systems : Energy Impact on Reroofing and Recover Scenarios." In *31st Roof Construction Institute (RCI) International Convention and Trade Show*.

Hedlin, C.P. 1985. "Effect of Insulation Joints on Heat Loss through Flat Roofs Reprinted from." *ASHRAE Transactions* 91 (2B): 608–22.

Holladay, Martin. 2015. "Cold-Weather Performance of Polyisocyanurate." *Green Building Advisor*. http://www.greenbuildingadvisor.com/articles/dept/musings/cold-weather-performance-polyisocyanurate.

2016. "Thermal Drift of Polyiso and XPS." *Green Building Advisor*. http://www.greenbuildingadvisor.com/articles/dept/musings/thermal-drift-polyiso-and-xps.

Kumaran, M. K., and J. C. Haysom. 2000. "Low-Permeance Materials in Building Envelopes." *National Research Council of Canada*, 1–6.

Lewis, James E. 1979. "Thermal Evaluation of the Effects of Gaps Between Adjacent Roof Insulation Panels.pdf." *Thermal Insulation* 3: 80–103.

Lstiburek, Joseph. 2004. "Insulations , Sheathings and Vapor Retarders."

O'Brien, Sean. 2006. "Thermal Bridging in the Building Envelope: Maximizing Insulation Effectivenss Through Careful Design.pdf." *The Construction Specifier*, 62–79.

Petrie, Thomas, Jerald Atchley, Andre Desjarlais, and Jeffrey Christian. 2000. "Effects of Mechanical Fasteners and Gaps between Insulation Boards on Thermal Performance of Low-Sloped Roofs.pdf." *Thermal Envelope & Building Science* 23: 292–317.

Straube, John. 2006. "Thermal Control in Buildings." *Building Science Digest*, no. 11: 1–12.

2007. "Thermal Metrics for High Performance Enclosure Walls: The Limitations of R-Value." *Building Science Corporation, Research Report–0901*.

"User's Guide - National Energy Code of Canada for Buildings." 2011.

Wieland, Heinz. 1988. "Heat Conduction and Condensation by Fastners of Metal or Plastics in Non-Ventilated Roof Assemblies."

2006. "Heat Losses Through Flat Roof Fasteners."

Standards

ASHRAE 90.1, 2013. "Energy Standard for Building Except Low-Rise Residential Buildings"

ASTM C177, 2010. "Steady-State Heat Flux Measurements of Thermal Transmission Properties by Means of Guarded-Hot-Plate Apparatus"

ASTM C518, 2010. "Steady-State Thermal Transmission by Heat Flow Meter Apparatus"

ASTM C1058, 2010. "Selecting Temperatures for Evaluation and Reporting Thermal Properties of Thermal Insulation"

ASTM C1363, 2011. "Standard Test Method for Thermal Performance of Building Materials and Envelope Assemblies by Means of a Hot Box Apparatus"

ASTM D2126, 2009. "Response of rigid Cellular Plastic to Thermal Aging"

NECB, 2015. "National Energy Code of Canada for Buildings"

Appendices

Appendix A: Summary of Literature Results

Table A-1: Summary of Literature (Lewis, 1979)

Test Properties	
Test	Numerical Model
Insulation	Fiberglass
Thickness	1 7/8 inch
Temperature	Mean: 24℃ (75°F)
Gaps	¾, 3/16 and 5/8 inch
Fasteners	N.A.
Findings	• Effects of gaps dissipate 6-10 inches away from gap. • 1% gap can lead to 3-9% increase in thermal transmittance when previously believed 1% gap is equal to 1% increase in thermal transmittance.

Table A-2: Summary of Literature (Burch, Shoback, and Cavanaugh, 1987)

Test Properties	
Testing	Numerical Model
Insulation	Fiberglass
Thickness	1-6 inch
Temperature	Mean: 1.5℃
Gaps	N.A.
Fasteners	5.4 fasteners/m^2
Findings	• Metal fasteners reduce the overall thermal resistance by 3-8% in steel deck assemblies. • Plastic caps reduce thermal bridging by 44% for metal deck systems.

Table A-3: Summary of Literature (Wiedland, 1988)

Test Properties	
Testing	Numerical Model
Insulation	No specific insulation, modeled for an insulating material with thermal conductivity of $0.04\ W/m \cdot °K$.
Thickness	$100\ mm$
Temperature	Mean:
Gaps	N.A.
Fasteners	3.3 fasteners/m^2
Findings	• Carbon steel fasteners and plates increase the thermal conduction by 3.3%, while fasteners with a plastic plate and entirely stainless-steel fasteners conduct an increase of 1.1% more thermal energy.

Table A-4: Summary of Literature (Wieland, 2006)

Test Properties	
Testing	Numerical Model (HEAT3)
Insulation	No specific insulation, modeled for an insulating material with thermal conductivity of 0.04 $W/m \cdot °K$.
Thickness	$50 - 300mm$
Temperature	Mean: 5℃
Gaps	N.A.
Fasteners	4 fasteners/m^2
Findings	• The thermal bridge effects are highest for carbon steel fasteners with steel plates, the heat transfer decreases for steel fasteners with plastic sleeves, and the heat transfer is minimal for stainless steel fastener.

Table A-5: Summary of Literature (O'Brian, 2006)

Test Properties	
Testing	Numerical Model (HEAT 3D)
Insulation	• Fiberglass insulation (0.25 $W/m^2 \cdot °K$)
Thickness	R-20 Roof
Temperature	N.A.
Gaps	N.A.
Fasteners	10 fasteners/m^2
Findings	• 10 fasteners/m^2 on a R-20 roof reduces the assembly's thermal insulation by 15%. • Basic study, purpose was to who that fasteners have a significant effect.

Table A-6: Summary of Literature (Grin, Schumacher, and Smegal, 2014)

Test Properties	
Testing	Numerical Model
Insulation	• Polyisocyanurate • Stone Wool
Thickness	Polyisocyanurate (4.9 in) Stone Wool (7.9 in)
Temperature	Mean: -20℃ to 50℃
Gaps	N.A.
Fasteners	N.A.
Findings	• Reporting of common building insulation thermal properties at 24℃ is not representative of in-service conditions. • Stone wool performs better, with a total energy flow between 32% and 58% less than polyisocyanurate.

Experimental Testing

Table A-7: Summary of Literature (Hedlin, 1985)

Test Properties	
Testing	Experimental testing
Insulation	Extruded polystyrene (EPS)
Thickness	51mm and 76mm (2 and 3”)
Temperature	Mean: 0℃ (20℃ inside, −20℃outside) Difference: 40℃
Gaps	2.5mm to 25mm
Fasteners	N.A.
Findings	• Heat loss increases were estimated to range from 4% to 35% for insulation 610x1219mm (2’x4’). • Joint effect dissipated 100mm from the edge

Table A-8: Summary of Literature (Courville et al., 1989)

Test Properties	
Testing	Experimental testing
Insulation	• Fiberglass • Expanded polystyrene (EPS) • Phenolic foam board
Thickness	4.5”
Temperature	Mean: 15, 40, 75, 110 and 135°F
Gaps	N.A.
Fasteners	N.A.
Findings	• For EPS and fiberglass, the R-values increased with decreasing temperature, which is true for most insulating materials. Phenolic foam had an opposite effect, which can be attributed to the condensation of the chlorofluorocarbon gas in the cell structure.

Table A-9: Summary of Literature (Petrie et al., 2000)

Test Properties	
Testing	Experimental testing
Insulation	Polyisocyanurate
Thickness	2" (single and double layer tested)
Temperature	Mean: $-1, 10, 24, 34, 37$ and $51°C$
Gaps	1 inch
Fasteners	0.5 fasteners/ft^2 (5.4 fasteners/m^2)
Findings	• Fasteners reduced the thermal resistance of the assemblies with two layers of insulation by 7%. • The use of conventional steel plate fasteners resulted in a greater thermal resistance reduction of 12%, whereas plastic plate fasteners had a thermal resistance reduction of only 3%. • The one-inch gap between boards resulted in 15% reduction of thermal resistance for two layers of insulation board and 17% reduction in single layer tests.

Table A-10: Summary of Literature (Building Science Corporation, 2005)

Test Properties	
Testing	Experimental testing
Insulation	• Polyisocyanurate
Thickness	2" and 4"
Temperature	Mean: 2, 12, 32 and 42°C
Gaps	N.A.
Fasteners	N.A.
Findings	• Some insulation materials exhibit better thermal performance as temperature gets cold and vice versa; polyisocyanurate however exhibits undesirable tendencies. It was found that polyisocyanurate insulation exhibit worse thermal performance as temperatures become lower. • The purpose of this study was to show that the reporting temperature has an influence on the insulation R-value.

Appendix B: Dimensional Stability Results

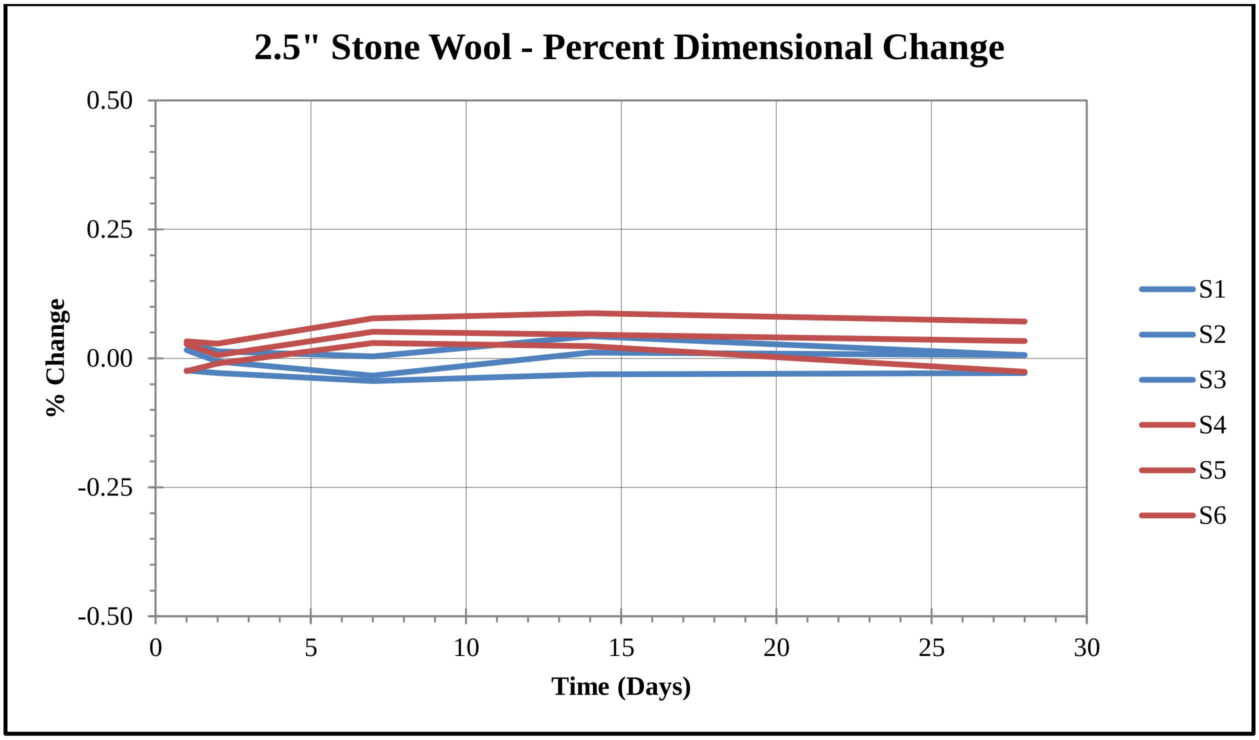

Notes: Blue lines (S1-S3) represent exposure to cold and red lines (S4-S6) represent exposure to heat.

Figure B-1: Dimensional Stability: 2.5" Stone Wool Insulation

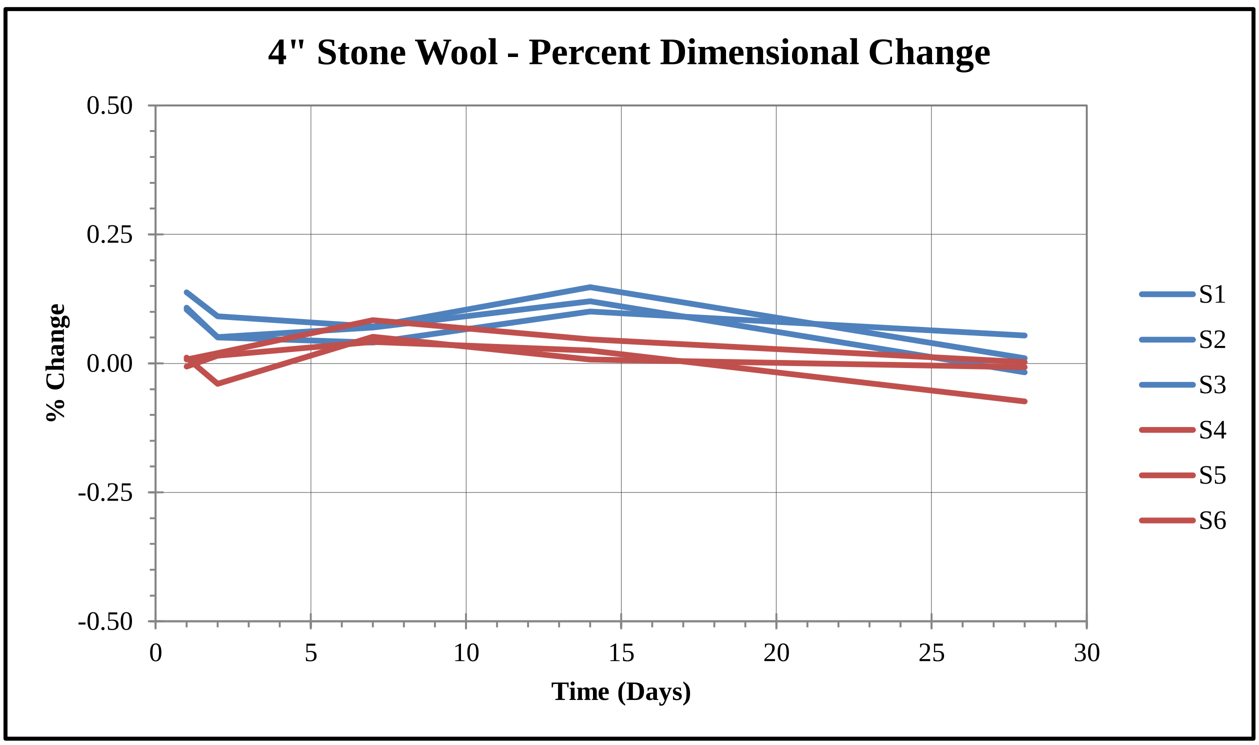

Notes: Blue lines (S1-S3) represent exposure to cold and red lines (S4-S6) represent exposure to heat.

Figure B-2: Dimensional Stability: 4" Stone Wool Insulation

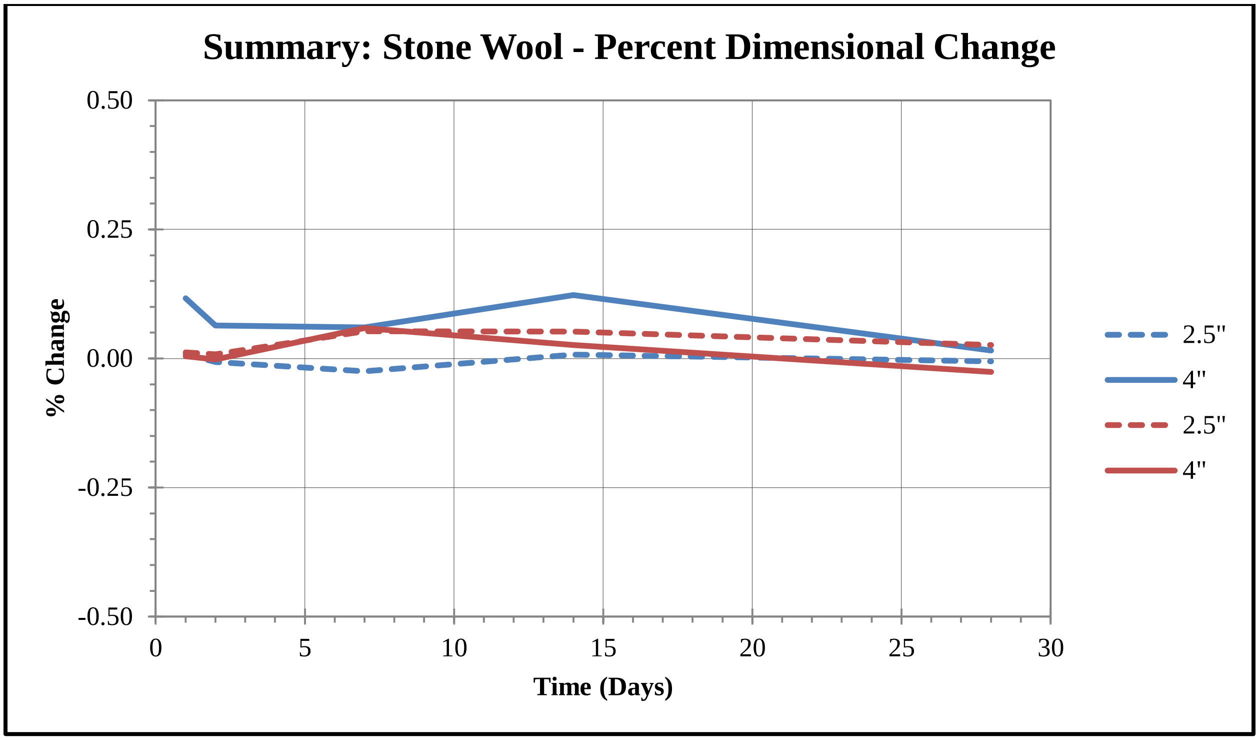

Notes: Blue lines represent exposure to cold and red lines represent exposure to heat.

Figure B-3: Dimensional Stability: Stone Wool Summary

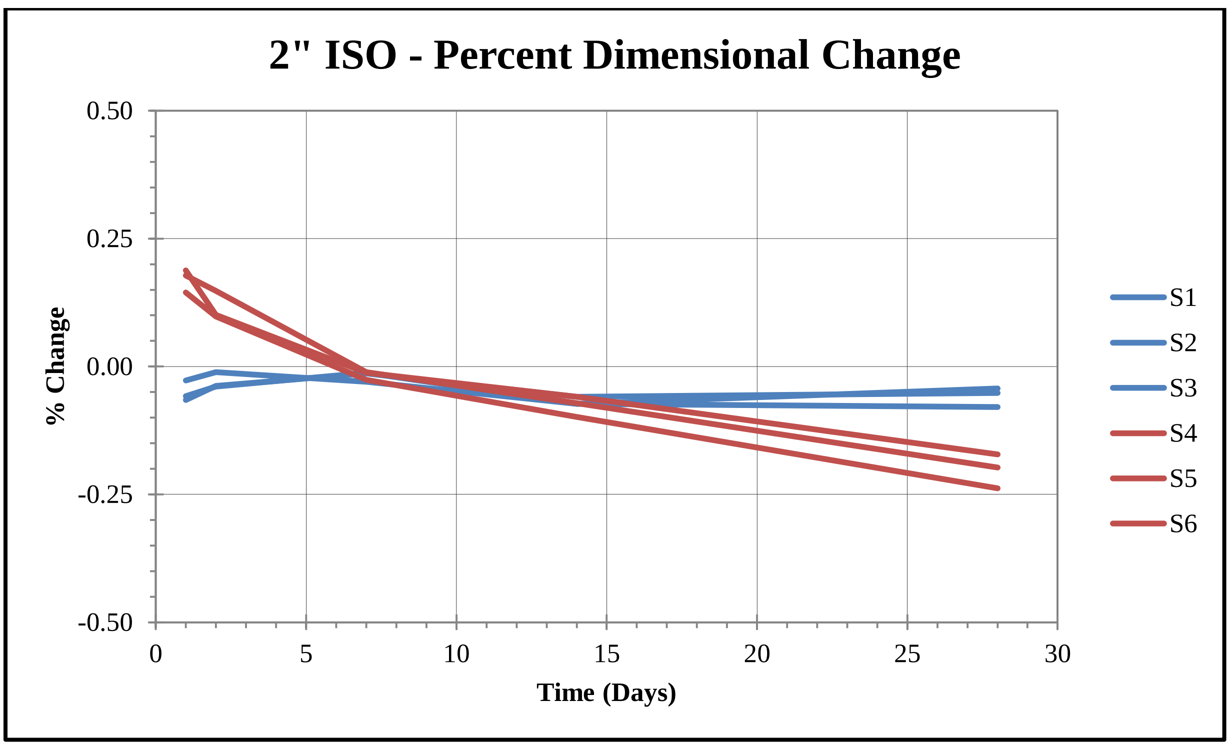

Notes: Blue lines (S1-S3) represent exposure to cold and red lines (S4-S6) represent exposure to heat.

Figure B-4: Dimensional Stability: 2” Polyiso Insulation

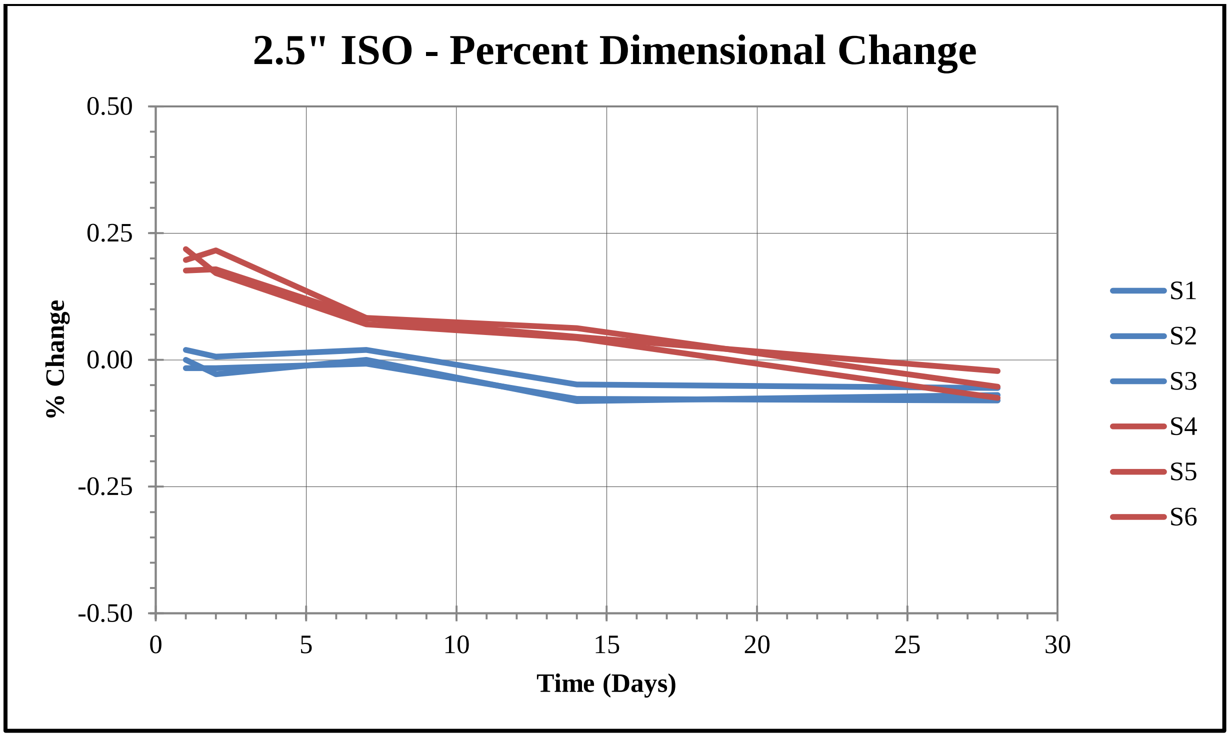

Notes: Blue lines (S1-S3) represent exposure to cold and red lines (S4-S6) represent exposure to heat.

Figure B-5: Dimensional Stability: 2.5" Polyiso Insulation

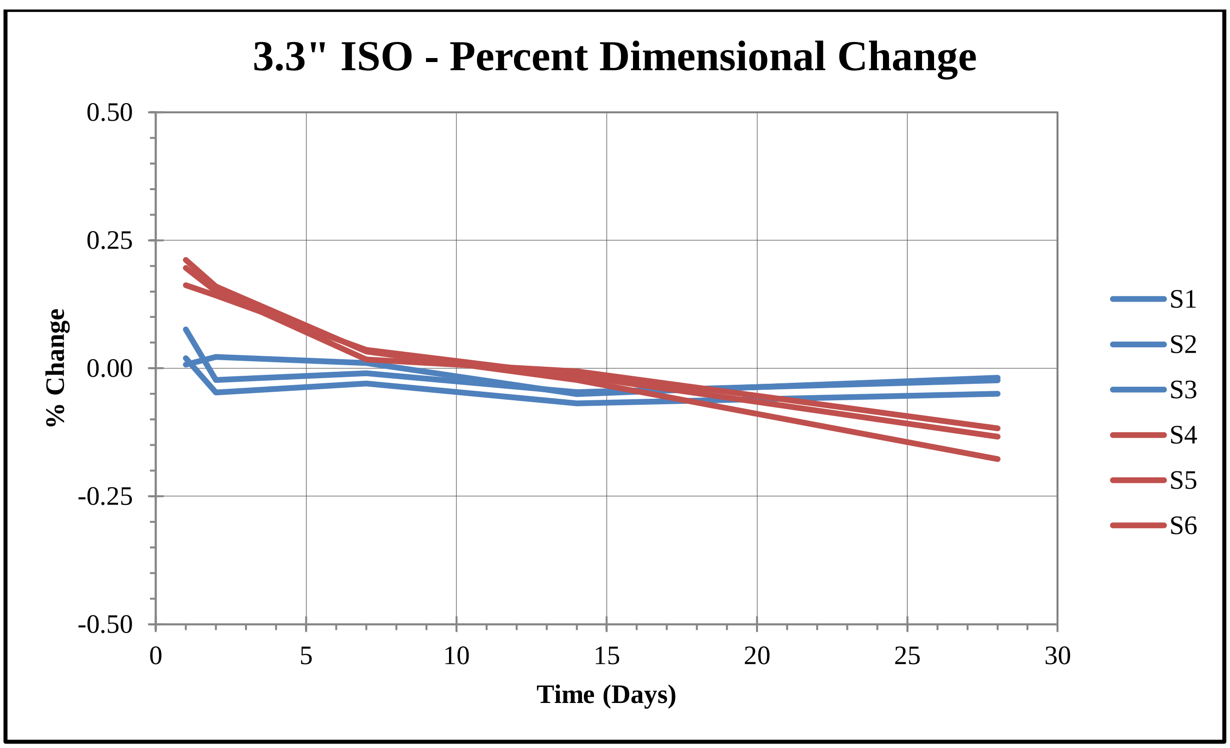

Notes: Blue lines (S1-S3) represent exposure to cold and red lines (S4-S6) represent exposure to heat.

Figure B-6: Dimensional Stability: 3.3" Polyiso Insulation

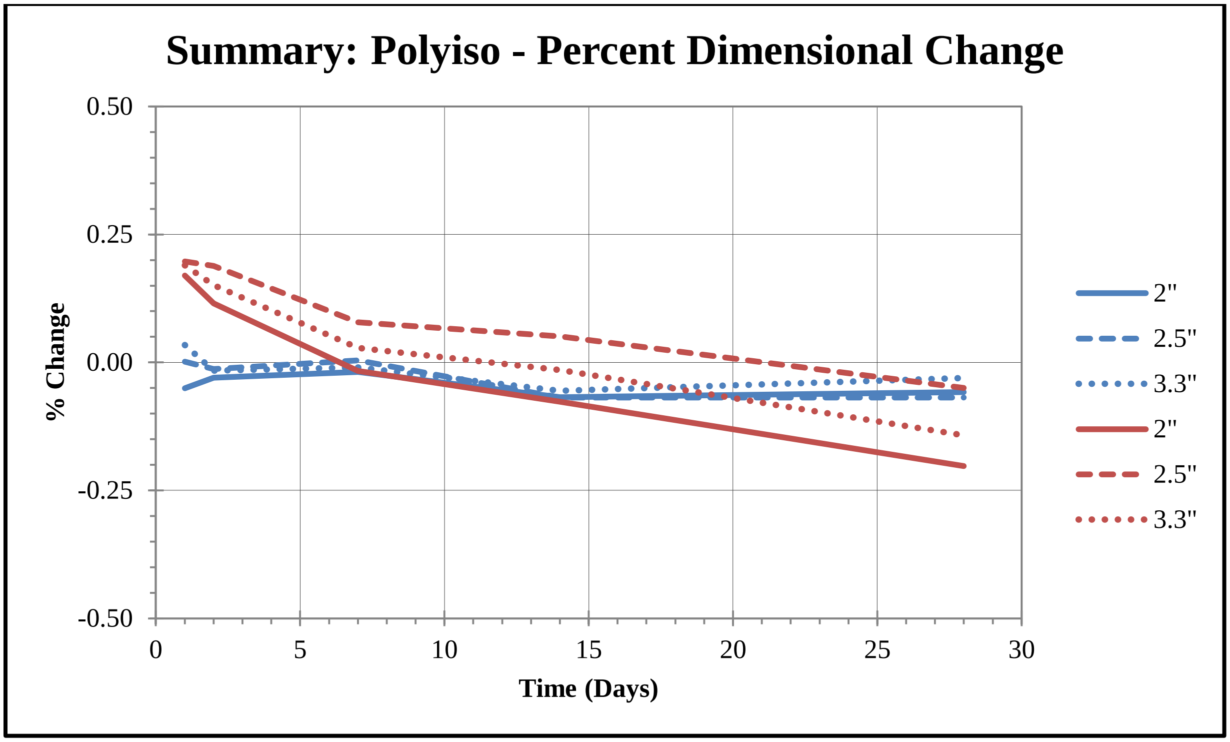

Notes: Blue lines represent exposure to cold and red lines represent exposure to heat.

Figure B-7: Dimensional Stability: Polyiso Summary

Appendix C: Heat Flow Meter Results

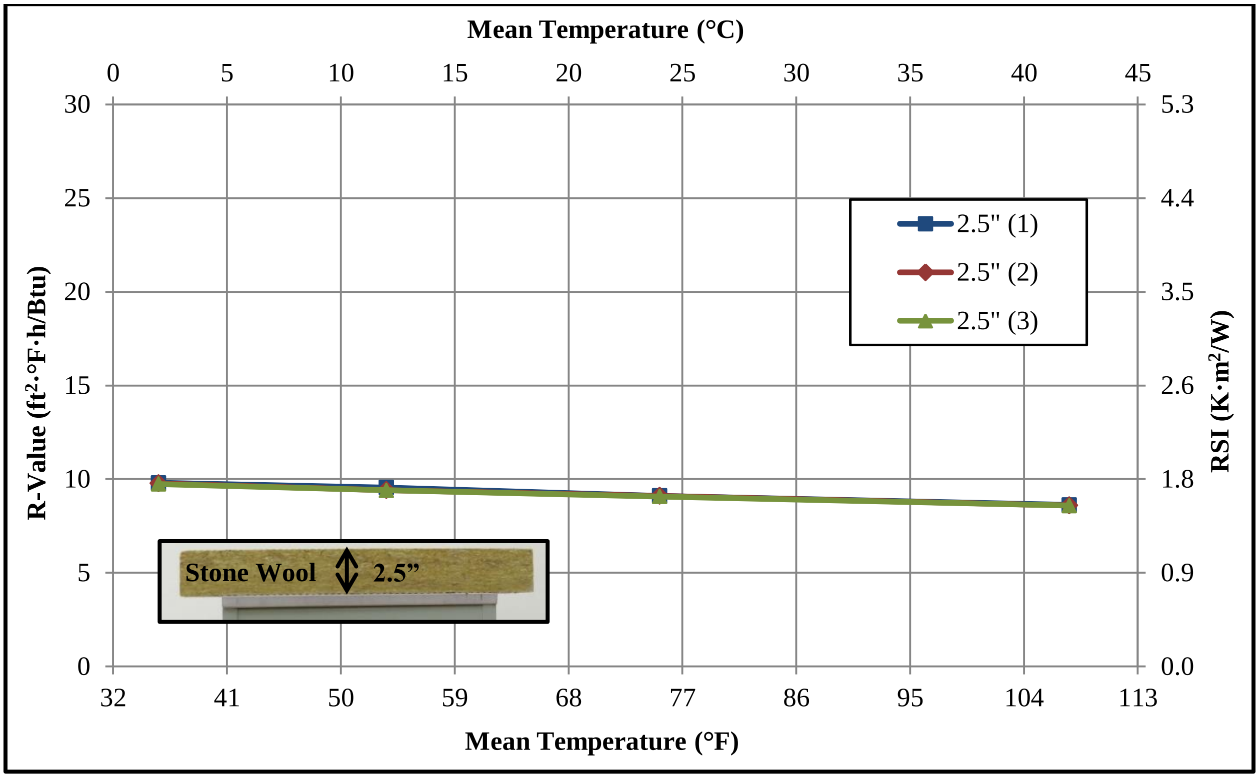

Figure C-1: Stone Wool – R25.21 Single Layer Repeatability

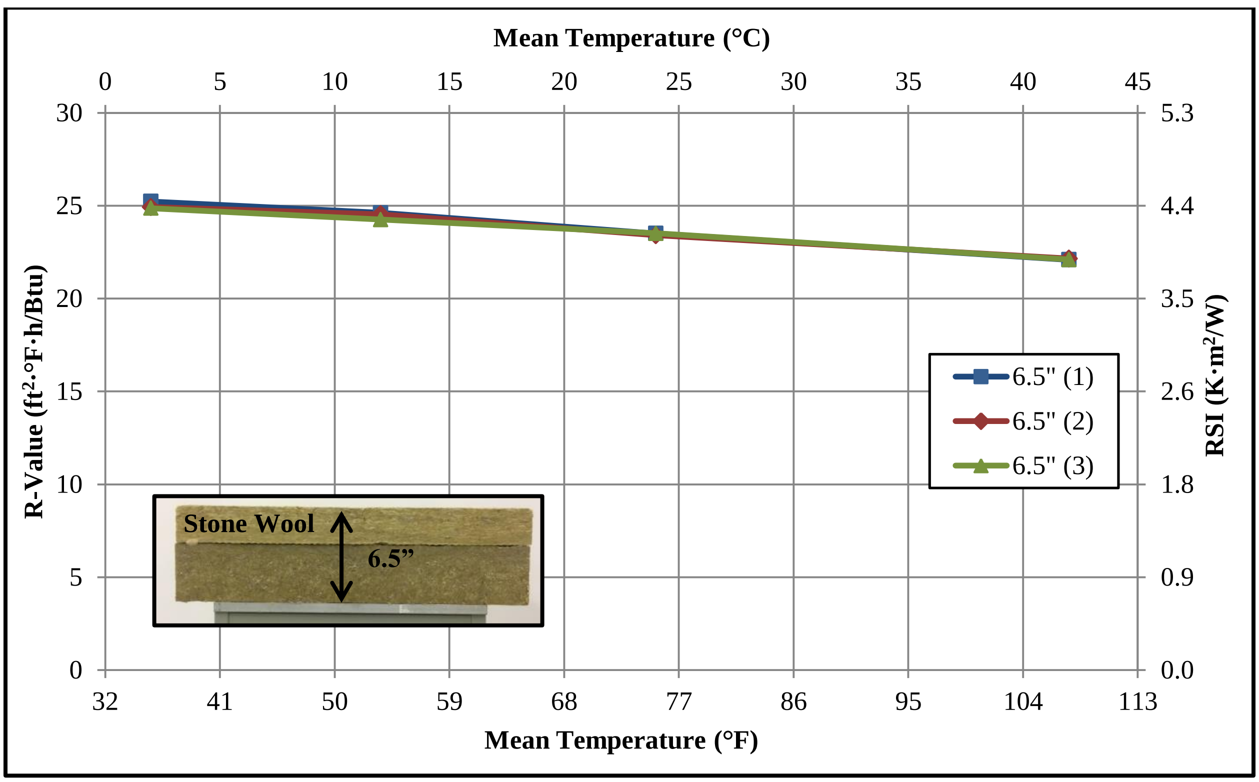

Figure C-2: Stone Wool – R25.21 Two Layer Repeatability

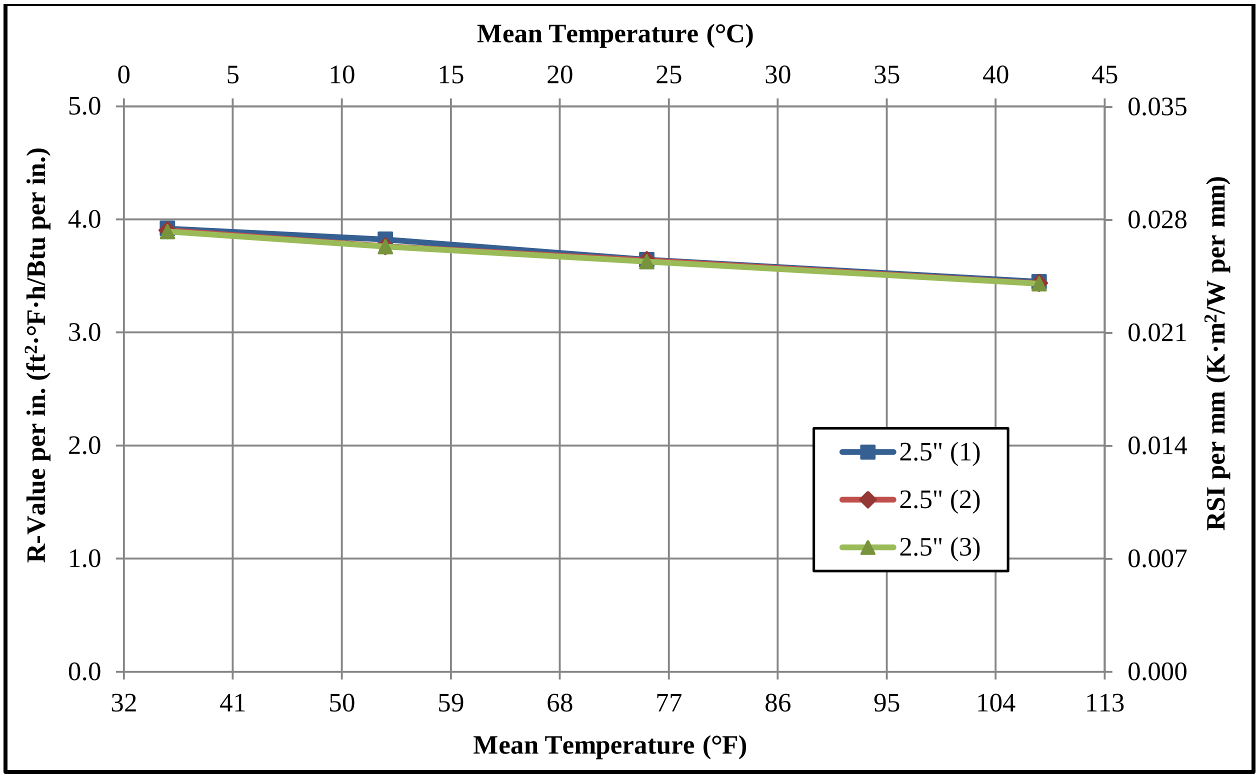

Figure C-3: Stone-Wool Thermal Resistivity

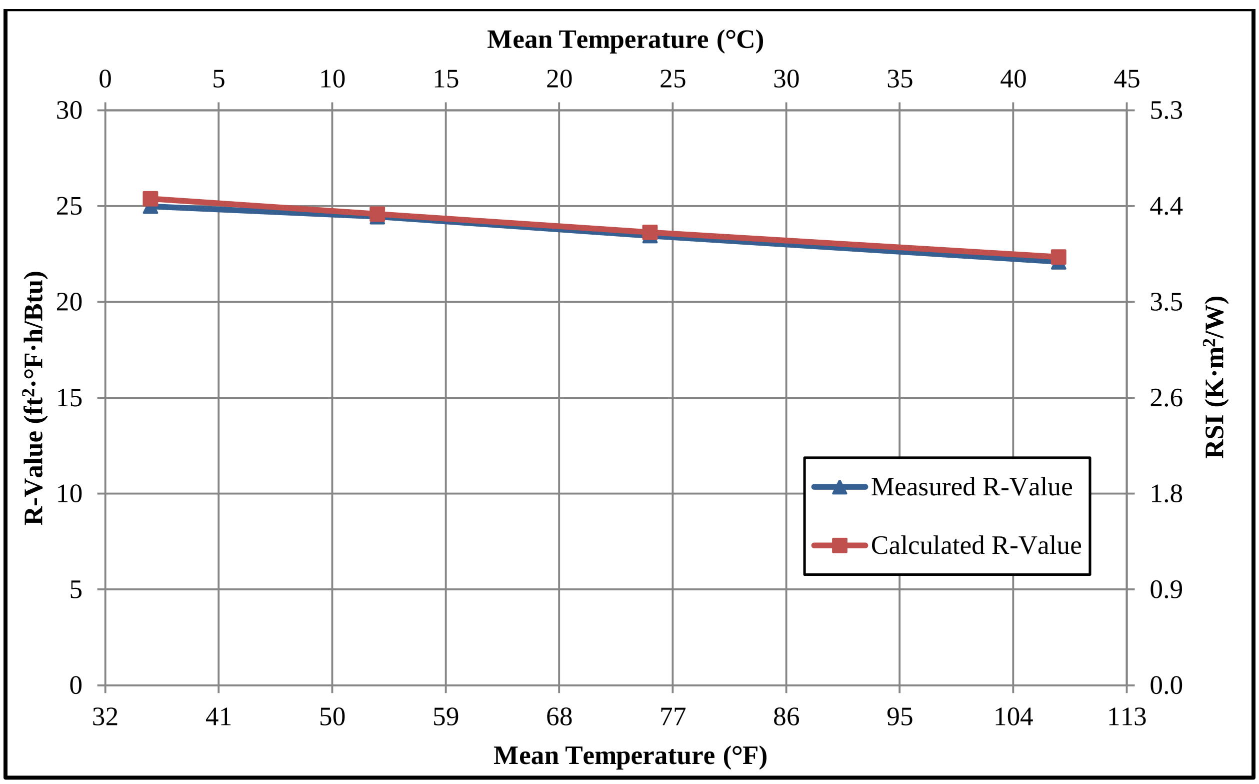

Figure C-4: Measured vs. Calculated Thermal Resistance for Stone Wool R25.21

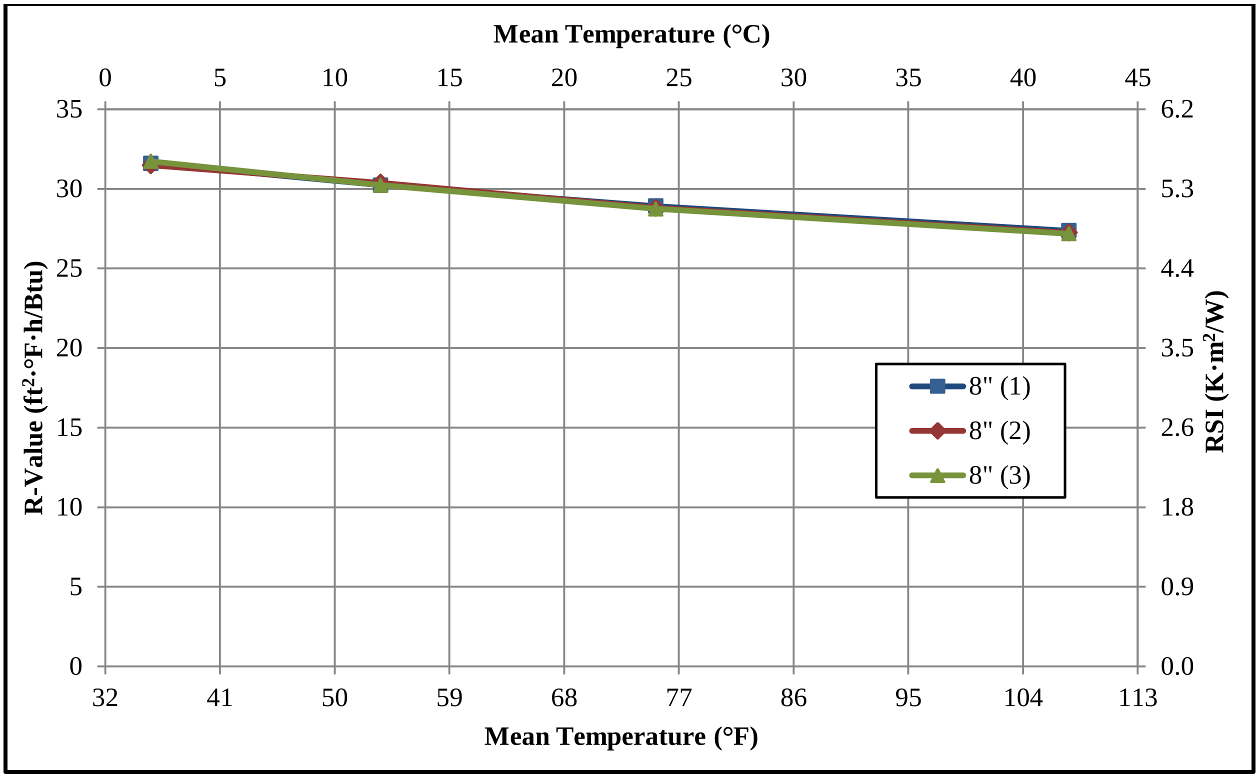

Figure C-5: Stone Wool – R30.21 Two Layer Repeatability

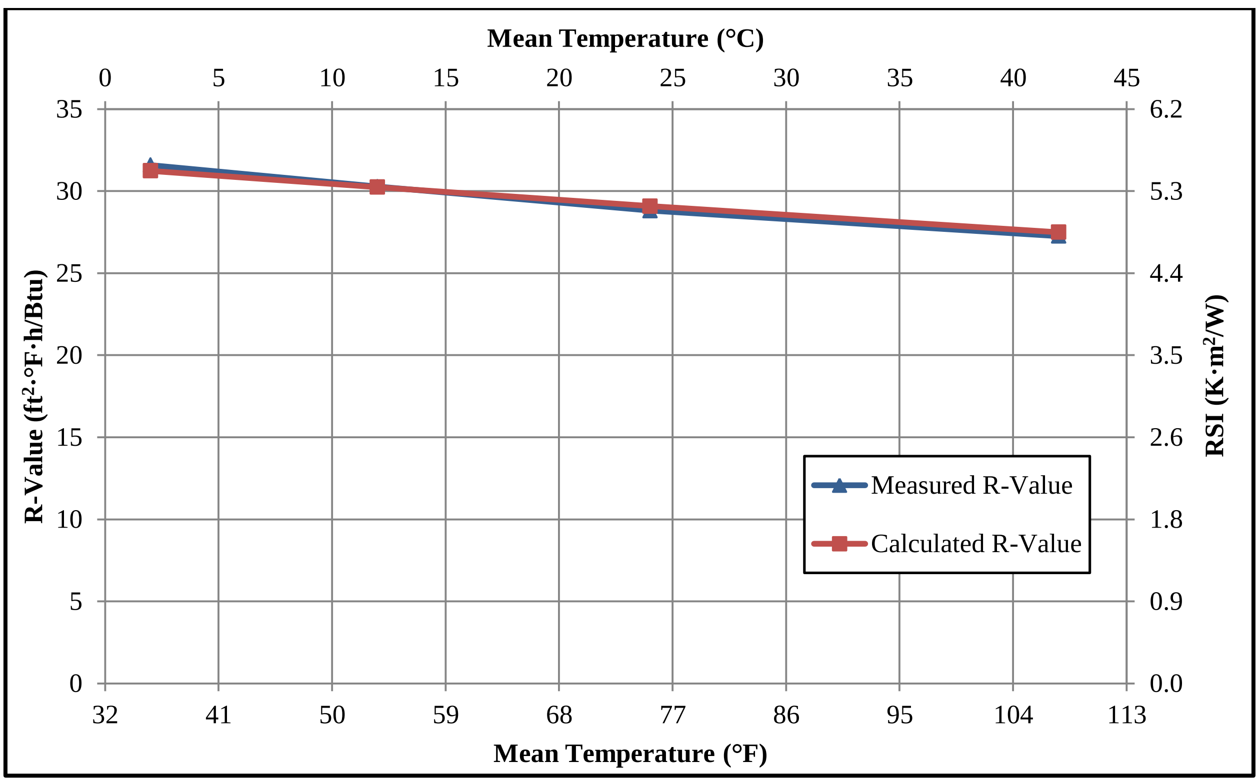

Figure C-6: Measured vs. Calculated Thermal Resistance for Stone Wool R30.21

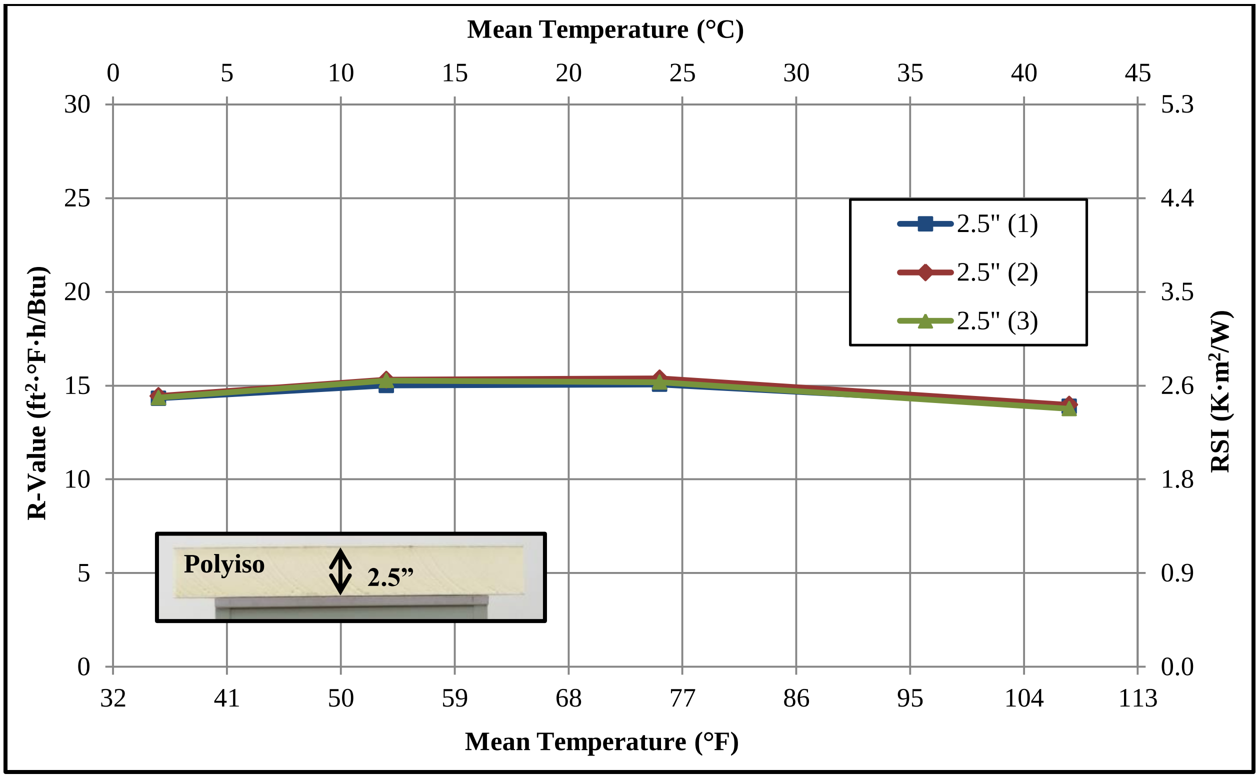

Figure C-7: Polyiso – R25.21 Single Layer Repeatability

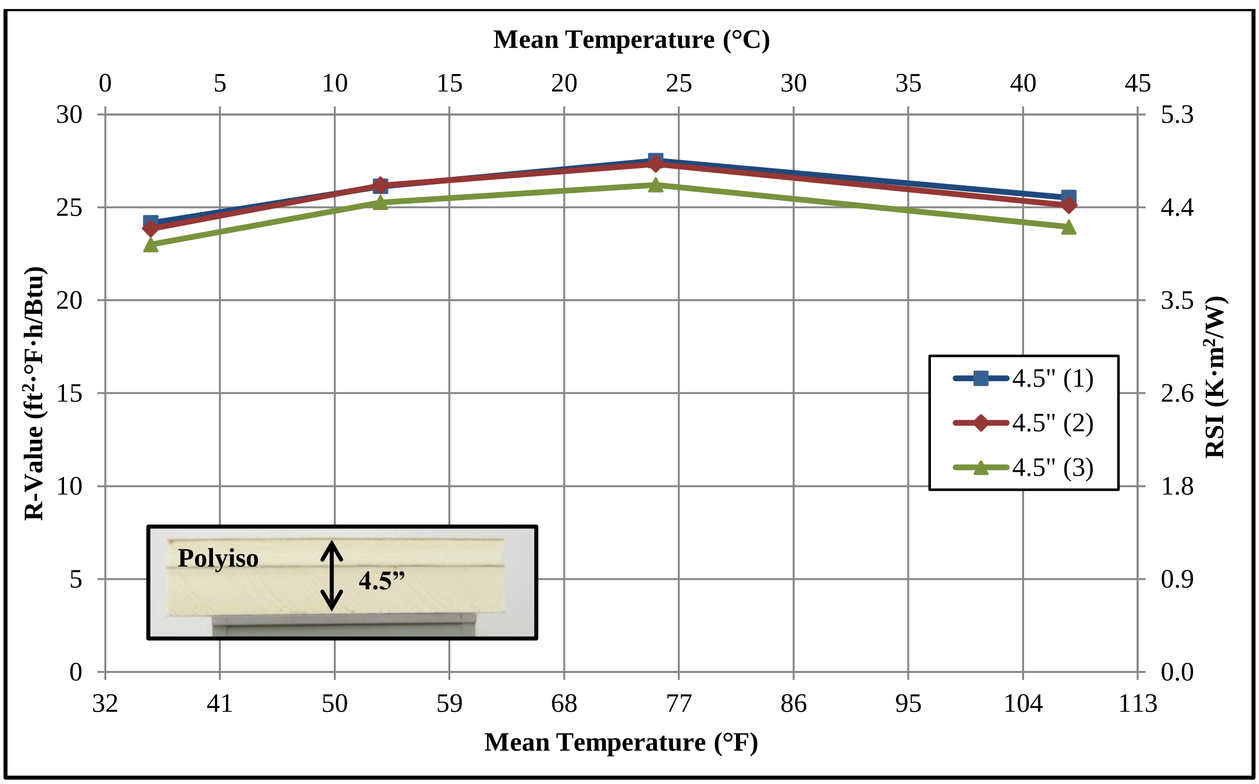

Figure C-8: Polyiso – R25.21 Two Layer Repeatability

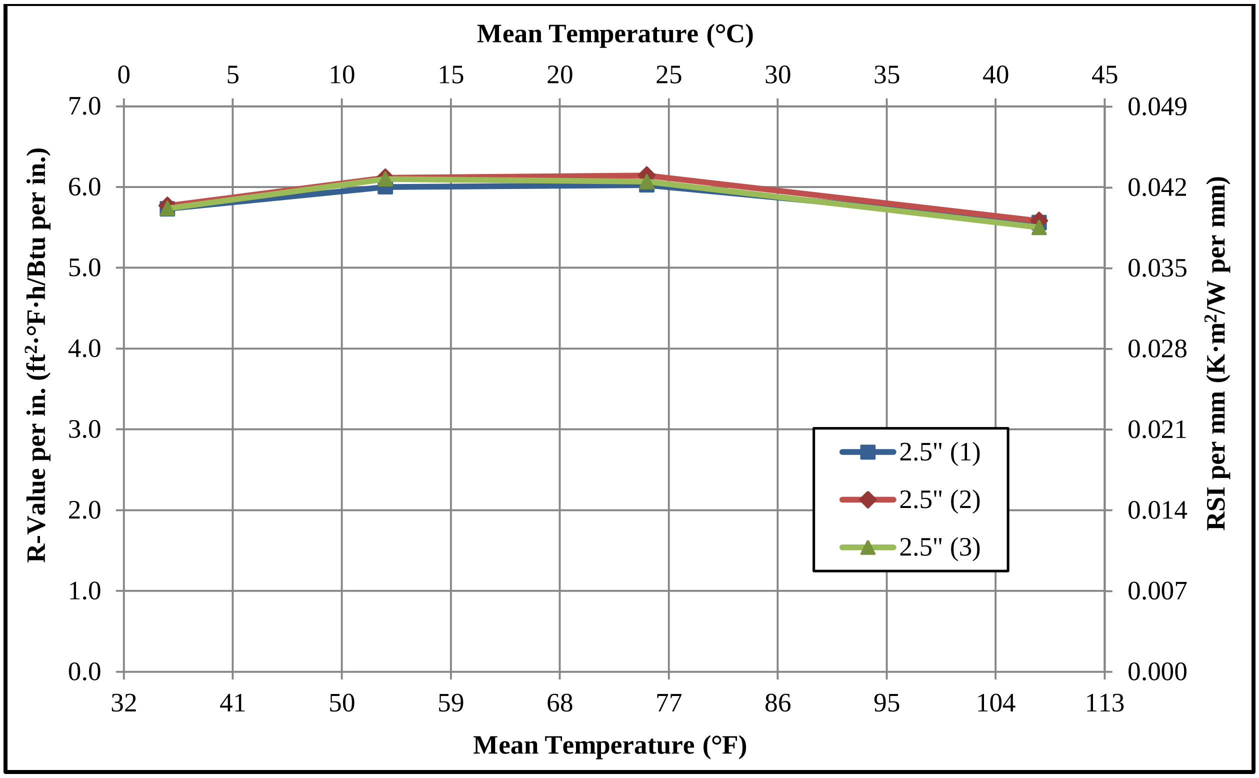

Figure C-9: Polyiso Thermal Resistivity

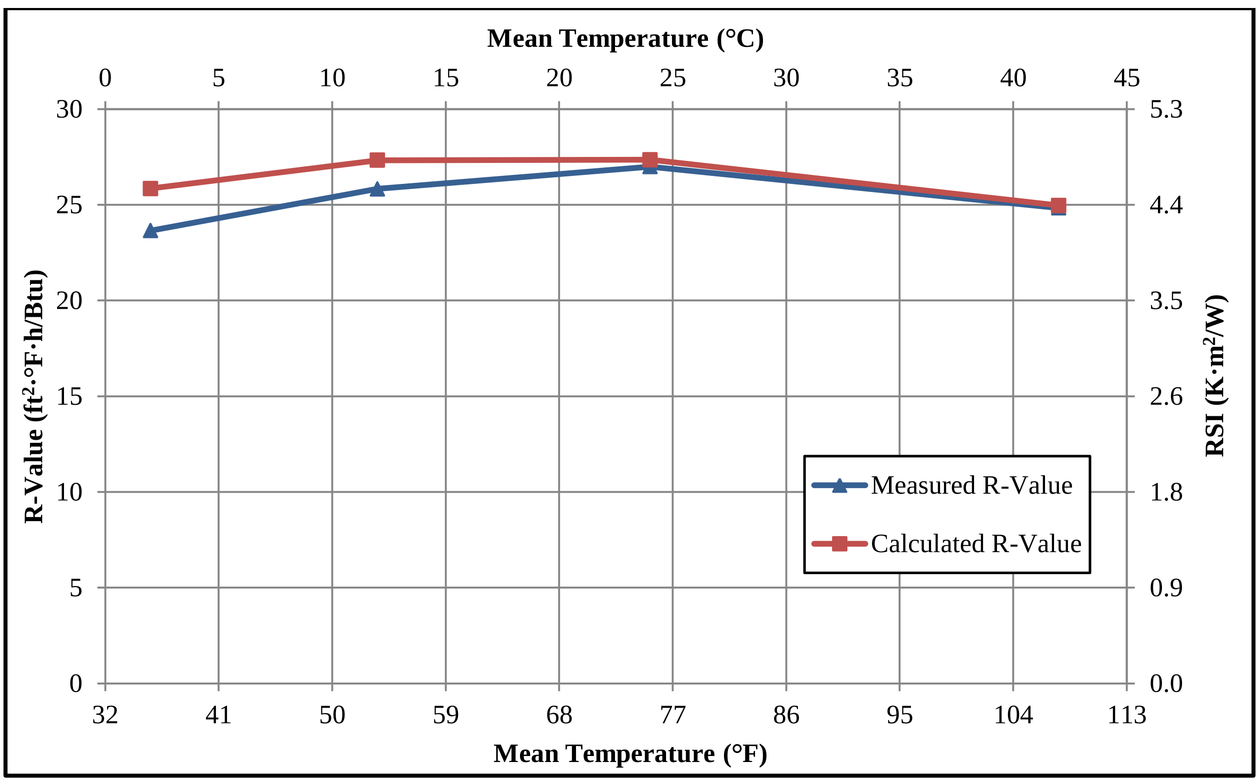

Figure C-8: Measured vs. Calculated Thermal Resistance for Polyiso R25.21

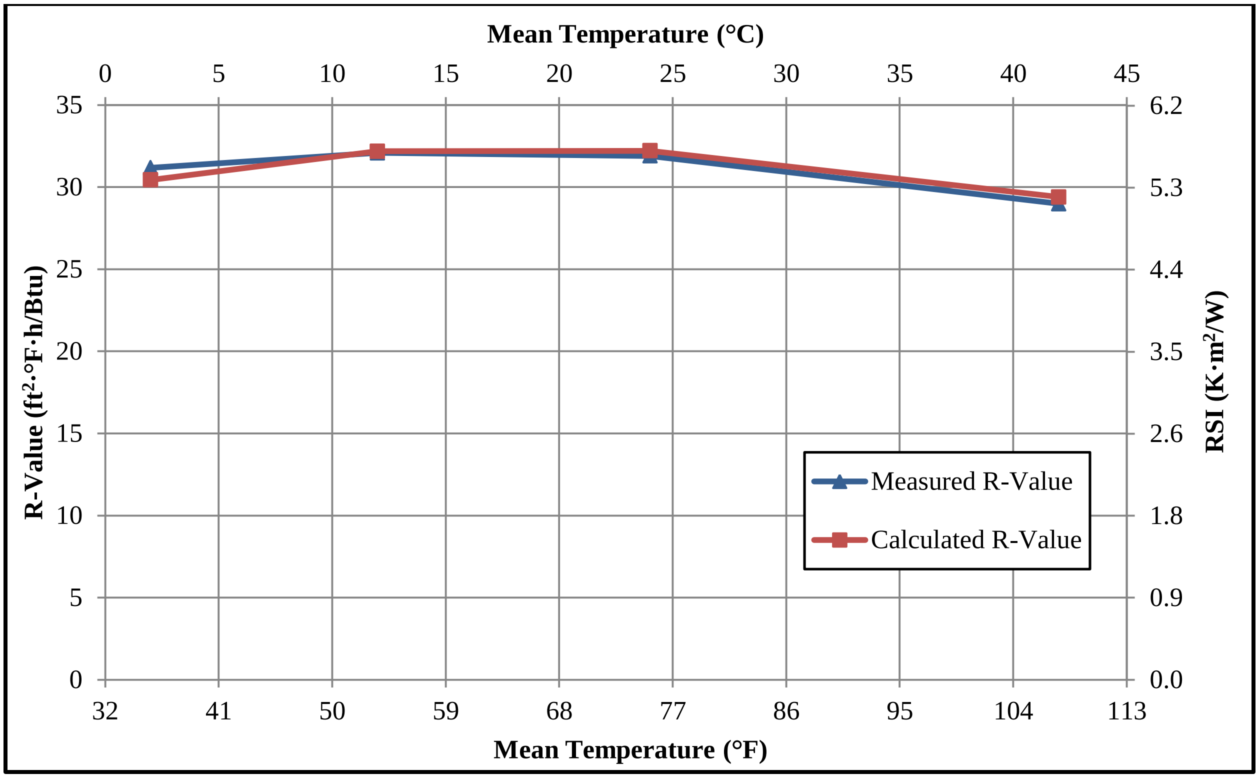

Figure C-9: Measured vs. Calculated Thermal Resistance for Polyiso R30.21

Appendix D: Guarded Hot Box Results

The following are the HFM results used to normalize the measured GHB results.

Table D-11: EPS R26 Temperature Offset Data

HFM - EPS R26					
Measured		Adjusted		Linear Fit HFM	
Tm	R-Value	Tm	R-Value	Slope	-0.10
1.9	26.15	2	26.13	Intercept	26.32
12.0	25.18	12	25.17		
24.4	23.93	24	24.01		
43.2	22.19	42	22.28		

Table D-12: EPS R31 Temperature Offset Data

HFM - EPS R31					
Measured		Adjusted		Linear Fit HFM	
Tm	R-Value	Tm	R-Value	Slope	-0.11
1.7	31.26	2	31.12	Intercept	31.34
11.7	30.02	12	30.04		
24.4	28.56	24	28.74		
42.2	26.85	42	26.78		

Table D-13: Stone Wool R26 Temperature Offset Data

HFM - Stone Wool R26					
Measured		Adjusted		Linear Fit HFM	
Tm	R-Value	Tm	R-Value	Slope	-0.07
1.7	25.00	2	25.07	Intercept	25.21
11.9	24.45	12	24.33		
24.4	23.44	24	23.46		
42.2	22.09	42	22.14		

Table D-14: Stone Wool R31 Temperature Offset Data

HFM - Stone Wool R31					
Measured		Adjusted		Linear Fit HFM	
Tm	R-Value	Tm	R-Value	Slope	-0.11
2.2	31.58	2	31.43	Intercept	31.65
12.1	30.27	12	30.36		
24.4	28.79	24	29.07		
42.6	27.22	42	27.14		

Table D-15: Polyiso R26 Temperature Offset Data

HFM - Polyiso R26							
Measured		Adjusted		Linear Fit HFM			
Tm	R-Value	Tm	R-Value	IF Tm<24C		IF Tm>24C	
2.5	24.10	2	23.65	Slope	0.10	Slope	-0.12
12.3	26.16	12	25.83	Intercept	24.99	Intercept	30.21
24.6	27.33	24	27.00				
42.6	25.23	42	24.84				

Table D-16: Polyiso R31 Temperature Offset Data

HFM - Polyiso R31							
Measured		Adjusted		Linear Fit HFM			
Tm	R-Value	Tm	R-Value	IF Tm<24C		IF Tm>24C	
1.7	31.10	2	31.18	Slope	-0.01	Slope	-0.16
11.8	32.05	12	32.09	Intercept	32.21	Intercept	35.69
23.8	31.89	24	31.89				
42.1	28.97	42	28.98				

Table D-17: GHB – EPS R26 Results – Raw Data

GHB - EPS R26																	
		(1)	(2)	(3)	(4)	(5)	(6)	(7)	(8)	(9)	(10)	(11)	(12)	(13)	(14)	(15)	(16)
System		Guard	Metering	Climatic	ΔT Specimen	Measured Power	Temp. Offset	Watt Offset	Calculated Power	Calculated Heat Flow	RSI	R-Value	Mean Temp	y-int.	Tm	Effective R-Value	% Decrease in R-Value
		°C	°C	°C	°C	W	°C	W	W	W/m²	K m^2/W	ft^2 °F h/Btu	°C		°C	ft^2 °F h/Btu	
Through Fasteners	0	44.13	44.18	4.08	37.00	13.18	0.05	0.085	13.09	8.81	4.20	23.85	24.13	26.17	24	24.65	-
	4	44.31	44.19	4.04	36.80	13.46	-0.12	-0.196	13.66	9.19	4.00	22.74	24.11	25.06	24	23.54	4.51
	6	44.35	44.19	4.07	36.66	13.64	-0.16	-0.268	13.91	9.36	3.92	22.24	24.13	24.56	24	23.04	6.53
	10	44.44	44.22	4.05	36.49	14.06	-0.22	-0.364	14.43	9.71	3.76	21.35	24.13	23.67	24	22.15	10.14
Top Joint		44.12	44.19	4.04	36.66	12.75	0.08	0.126	12.62	8.49	4.32	24.51	24.12	26.83	24	25.31	-
	1/4"	43.91	43.93	4.01	36.24	12.91	0.02	0.037	12.87	8.66	4.18	23.77	23.97	26.07	24	24.55	3.00
	1/2"	44.11	44.20	4.10	36.40	13.28	0.09	0.144	13.14	8.84	4.12	23.38	24.15	25.70	24	24.19	4.46
Bottom Joint		44.16	44.29	4.07	36.50	13.00	0.12	0.206	12.79	8.61	4.24	24.09	24.18	26.41	24	24.89	-
	1/4"	44.26	44.20	4.05	36.48	13.09	-0.05	-0.089	13.18	8.87	4.11	23.36	24.14	25.68	24	24.16	2.93
	1/2"	44.37	44.24	4.08	36.46	13.17	-0.13	-0.223	13.40	9.01	4.04	22.97	24.17	25.30	24	23.78	4.48
Staggered Joints		44.16	44.29	4.07	36.50	13.00	0.12	0.206	12.79	8.61	4.24	24.09	24.18	26.41	24	24.89	-
	1/4"	44.42	44.27	4.07	36.44	13.25	-0.15	-0.244	13.49	9.08	4.01	22.80	24.17	25.12	24	23.60	5.19
	1/2"	44.18	43.87	4.05	35.78	12.95	-0.31	-0.517	13.47	9.06	3.95	22.42	23.96	24.72	24	23.20	6.79

Legend:

- Column 1, 2, 3, 4 and 5 are the measured chamber temperatures and heater power consumption.
- Column 6 is the temperature offset between the metering and guard chambers (column 2- column 1).
- Column 7 is the heat flow offset calculated using column 6 and (Eqn. 4-3).
- Column 8 is the measured heat flow from column 5, normalized for a m^2.
- Column 10 is the calculated thermal resistance (column 4/ column 9); column 11 is the imperial thermal resistance (column 10 × 5.67446).
- Column 12 is the mean temperature of the test (average of column 2 and column 3).
- Column 13 and 14 use the HFM data to normalize the thermal resistance for a mean temperature of 24℃.
- Column 16 is the % decrease in thermal resistance for the test compared to the opaque assembly.

Table D-18: GHB – EPS R31 Results – Raw Data

System		Guard	Metering	Climatic	ΔT Specimen	Measured Power	Temp. Offset	Watt Offset	Calculated Power	Calculated Heat Flow	RSI	R-Value	Mean Temp	y-int.	Tm	Effective R-Value	% Decrease in R-Value
GHB - EPS R31																	
		°C	°C	°C	°C	W	°C	W	W	W/m²	K m^2/W	ft^2 °F h/Btu	°C		°C	ft^2 °F h/Btu	
Through Fasteners	0	44.31	44.23	4.06	37.32	10.55	-0.08	-0.133	10.68	7.19	5.19	29.49	24.14	32.10	24	30.29	-
	4	44.39	44.20	4.08	37.87	11.14	-0.19	-0.313	11.45	7.71	4.91	27.91	24.14	30.53	24	28.72	5.20
	6	44.43	44.21	4.07	37.84	11.37	-0.22	-0.367	11.74	7.90	4.79	27.21	24.14	29.82	24	28.01	7.53
	10	44.55	44.21	4.07	37.89	11.71	-0.34	-0.562	12.27	8.26	4.59	26.06	24.14	28.68	24	26.87	11.31
Top Joint		44.10	44.18	4.08	37.28	10.89	0.08	0.135	10.75	7.24	5.15	29.26	24.13	31.88	24	30.07	-
	1/4"	44.09	44.18	4.03	37.17	11.24	0.09	0.158	11.09	7.46	4.98	28.30	24.11	30.91	24	29.10	3.22
	1/2"	44.11	44.26	4.05	37.05	11.50	0.15	0.245	11.25	7.57	4.89	27.79	24.16	30.41	24	28.60	4.90
Bottom Joint		44.10	44.18	4.08	37.28	10.89	0.08	0.135	10.75	7.24	5.15	29.26	24.13	31.88	24	30.07	-
	1/4"	44.11	44.25	4.05	37.18	11.34	0.14	0.226	11.11	7.48	4.97	28.24	24.15	30.86	24	29.05	3.39
	1/2"	43.95	44.23	4.09	37.28	11.78	0.28	0.461	11.32	7.62	4.89	27.79	24.18	30.41	24	28.60	4.89
Staggered Joints		44.31	44.23	4.06	37.32	10.55	-0.08	-0.133	10.68	7.19	5.19	29.49	24.14	32.10	24	30.29	-
	0"	44.32	44.22	4.06	37.27	10.51	-0.10	-0.172	10.68	7.19	5.19	29.46	24.14	32.08	24	30.27	0.08
	1/4"	44.09	44.21	4.03	37.24	11.52	0.11	0.189	11.33	7.63	4.88	27.73	24.12	30.35	24	28.54	5.79
	1/2"	44.10	44.21	4.07	36.97	11.70	0.11	0.183	11.51	7.75	4.77	27.11	24.14	29.72	24	27.91	7.86
Staggered Joints and Fasteners		44.31	44.23	4.06	37.32	10.55	-0.08	-0.133	10.68	7.19	5.19	29.49	24.14	32.10	24	30.29	-
		43.97	44.19	4.06	35.91	13.20	0.23	0.375	12.82	8.63	4.16	23.64	24.15	26.26	24	24.45	19.29

Table D-19: GHB – Stone Wool R26 – Raw Data

GHB - Stone Wool R26																	
System		Guard	Metering	Climatic	ΔT Specimen	Measured Power	Temp. Offset	Watt Offset	Calculated Power	Calculated Heat Flow	RSI	R-Value	Mean Temp	y-int.	Tm	Effective R-Value	% Decrease in R-Value
		°C	°C	°C	°C	W	°C	W	W	W/m²	K m^2/W	ft^2 °F h/Btu	°C		°C	ft^2 °F h/Btu	
Through Fasteners	0	44.10	44.19	4.07	35.12	13.09	0.09	0.155	12.94	8.70	4.03	22.92	24.13	24.68	24	23.72	-
	4	44.12	44.16	4.06	35.13	13.60	0.04	0.060	13.54	9.11	3.86	21.90	24.11	23.67	24	22.70	4.28
	6	44.13	44.16	4.07	35.13	13.89	0.03	0.051	13.84	9.32	3.77	21.42	24.11	23.18	24	22.22	6.32
	10	44.12	44.13	4.03	34.78	14.39	0.01	0.016	14.37	9.67	3.60	20.43	24.08	22.19	24	21.22	10.52
Top Joint		44.13	44.20	4.06	37.06	12.89	0.07	0.117	12.77	8.60	4.31	24.48	24.13	26.25	24	25.28	-
	1/4"	44.10	44.19	4.02	37.08	13.31	0.09	0.142	13.17	8.86	4.19	23.77	24.10	25.54	24	24.57	2.83
	1/2"	44.11	44.20	4.02	36.96	13.43	0.09	0.155	13.27	8.93	4.14	23.50	24.11	25.27	24	24.30	3.89
Bottom Joint		44.15	44.31	4.05	36.75	13.20	0.16	0.261	12.94	8.71	4.22	23.98	24.16	25.74	24	24.78	-
	1/4"	43.70	44.10	4.03	36.47	14.00	0.39	0.654	13.35	8.98	4.06	23.06	24.11	24.83	24	23.86	3.69
	1/2"	44.14	44.29	4.08	36.40	13.79	0.15	0.250	13.54	9.11	3.99	22.69	24.16	24.46	24	23.49	5.20
Staggered Joints		44.15	44.31	4.05	36.75	13.20	0.16	0.261	12.94	8.71	4.22	23.98	24.16	25.74	24	24.78	-
	1/4"	44.40	44.24	4.02	36.77	13.44	-0.16	-0.261	13.70	9.22	3.99	22.66	24.13	24.43	24	23.46	5.31
	1/2"	44.13	44.15	4.03	36.31	13.82	0.03	0.042	13.78	9.27	3.92	22.25	24.12	24.01	24	23.04	6.99

Table D-20: GHB – Stone Wool R31 – Raw Data

GHB - Stone Wool R31																	
System		Guard	Metering	Climatic	ΔT Specimen	Measured Power	Temp. Offset	Watt Offset	Calculated Power	Calculated Heat Flow	RSI	R-Value	Mean Temp	y-int.	Tm	Effective R-Value	% Decrease in R-Value
		°C	°C	°C	°C	W	°C	W	W	W/m²	K m^2/W	ft^2 °F h/Btu	°C		°C	ft^2 °F h/Btu	
Through Fasteners	0	44.11	44.17	4.07	37.87	11.23	0.06	0.107	11.13	7.49	5.06	28.72	24.12	31.31	24	29.53	-
	4	44.32	44.23	4.07	37.89	11.63	-0.09	-0.152	11.78	7.93	4.78	27.14	24.14	29.73	24	27.95	5.34
	6	44.40	44.21	4.04	37.93	11.79	-0.19	-0.318	12.11	8.15	4.65	26.43	24.14	29.02	24	27.24	7.76
	10	44.39	44.21	4.03	37.85	12.32	-0.18	-0.306	12.63	8.50	4.45	25.30	24.12	27.89	24	26.10	11.58
Top Joint		44.14	44.29	4.03	38.00	11.20	0.15	0.252	10.95	7.37	5.16	29.29	24.16	31.88	24	30.09	-
	1/4"	44.19	44.35	4.05	38.07	11.63	0.16	0.275	11.35	7.64	4.98	28.30	24.20	30.90	24	29.11	3.26
	1/2"	44.14	44.27	4.03	37.92	11.72	0.12	0.203	11.52	7.75	4.89	27.79	24.15	30.38	24	28.59	4.98
Bottom Joint		44.12	44.22	4.04	37.72	11.42	0.11	0.179	11.24	7.56	4.99	28.33	24.13	30.92	24	29.14	-
	1/4"	44.14	44.22	4.04	37.53	11.74	0.08	0.125	11.61	7.82	4.80	27.27	24.13	29.87	24	28.08	3.63
	1/2"	44.39	44.33	4.11	37.26	11.67	-0.06	-0.093	11.76	7.91	4.71	26.75	24.22	29.35	24	27.56	5.41
Staggered Joints		44.12	44.22	4.04	37.72	11.42	0.11	0.179	11.24	7.56	4.99	28.33	24.13	30.92	24	29.14	-
	1/4"	44.47	44.26	4.06	37.68	11.62	-0.21	-0.350	11.97	8.05	4.68	26.57	24.16	29.17	24	27.38	6.03
	1/2"	44.31	44.25	4.07	37.51	12.12	-0.05	-0.091	12.21	8.22	4.57	25.93	24.16	28.52	24	26.74	8.24
Staggered Joints and Fasteners		44.12	44.22	4.04	37.72	11.42	0.11	0.179	11.24	7.56	4.99	28.33	24.13	30.92	24	29.14	-
		44.42	44.21	4.10	37.32	13.39	-0.20	-0.335	13.72	9.23	4.04	22.96	24.18	25.55	24	23.77	18.43

Table D-21: GHB – Polyiso R26 – Raw Data

GHB - Polyiso R26																	
System		**Guard**	**Metering**	**Climatic**	**ΔT Specimen**	**Measured Power**	**Temp. Offset**	**Watt Offset**	**Calculated Power**	**Calculated Heat Flow**	**RSI**	**R-Value**	**Mean Temp**	**y-int.**	**Tm**	**Effective R-Value**	**% Decrease in R-Value**
		°C	**°C**	**°C**	**°C**	**W**	**°C**	**W**	**W**	**W/m²**	**K m^2/W**	**ft^2 °F h/Btu**	**°C**		**°C**	**ft^2 °F h/Btu**	
Through Fasteners	0	44.06	44.24	4.00	38.02	13.29	0.18	0.303	12.99	8.74	4.35	24.70	24.10	27.52	24	25.50	-
	0	44.05	44.23	4.00	37.87	13.43	0.18	0.299	13.13	8.84	4.29	24.34	24.11	27.16	24	25.15	-
	4	44.19	44.22	4.02	37.75	13.78	0.02	0.040	13.74	9.24	4.08	23.20	24.11	26.02	24	24.00	4.56
	6	44.09	44.14	4.01	37.78	14.16	0.05	0.081	14.08	9.47	3.99	22.65	24.08	25.47	24	23.45	6.75
	10	44.05	44.14	4.00	37.66	14.85	0.09	0.150	14.70	9.89	3.81	21.62	24.06	24.43	24	22.42	10.86
Top Joint		44.17	44.30	4.02	36.70	12.63	0.13	0.216	12.41	8.35	4.39	24.96	24.16	27.78	24	25.76	-
	1/4"	44.35	44.30	4.05	36.03	12.46	-0.05	-0.088	12.54	8.44	4.27	24.24	24.13	27.06	24	25.05	2.78
	1/2"	44.08	44.27	4.02	37.74	13.58	0.19	0.322	13.26	8.92	4.23	24.02	24.13	26.84	24	24.82	3.65
Bottom Joint		44.06	44.16	3.98	37.42	13.46	0.10	0.162	13.30	8.95	4.18	23.75	24.07	26.56	24	24.55	-
	1/4"	44.07	44.18	4.00	37.37	13.84	0.12	0.194	13.65	9.19	4.07	23.11	24.09	25.93	24	23.91	2.58
	1/2"	44.12	44.23	4.07	37.36	13.97	0.11	0.176	13.80	9.28	4.02	22.86	24.16	25.68	24	23.67	3.58
Staggered Joints		44.06	44.16	3.98	37.42	13.46	0.10	0.162	13.30	8.95	4.18	23.75	24.07	26.56	24	24.55	-
	1/4"	44.10	44.24	4.04	37.24	13.96	0.14	0.226	13.74	9.25	4.03	22.88	24.14	25.70	24	23.68	3.51
	1/2"	44.13	44.17	4.07	37.17	13.95	0.04	0.067	13.88	9.34	3.98	22.61	24.14	25.43	24	23.41	4.62

Table D-22: GHB – Polyiso R31 – Raw Data

GHB - Polyisol R31																	
System		Guard	Metering	Climatic	ΔT Specimen	Measured Power	Temp. Offset	Watt Offset	Calculated Power	Calculated Heat Flow	RSI	R-Value	Mean Temp	y-int.	Tm	Effective R-Value	% Decrease in R-Value
		°C	°C	°C	°C	W	°C	W	W	W/m²	K m^2/W	ft^2 °F h/Btu	°C		°C	ft^2 °F h/Btu	
Through Fasteners	0	44.16	44.30	4.01	37.18	10.53	0.14	0.229	10.30	6.93	5.36	30.47	24.15	34.32	24	31.28	-
	4	43.92	44.21	4.05	36.85	11.28	0.29	0.478	10.80	7.27	5.07	28.80	24.12	32.65	24	29.61	5.35
	6	44.12	44.37	3.99	36.89	11.51	0.24	0.406	11.11	7.47	4.94	28.04	24.15	31.89	24	28.85	7.77
	10	43.98	44.27	4.03	36.73	12.10	0.29	0.482	11.61	7.82	4.70	26.69	24.15	30.54	24	27.50	12.08
Top Joint		44.11	44.27	4.04	37.11	11.06	0.16	0.265	10.80	7.27	5.11	29.01	24.16	31.83	24	29.82	-
		44.16	44.28	4.01	37.16	10.55	0.12	0.205	10.34	6.96	5.34	30.32	24.15	33.14	24	31.13	-
	1/4"	44.18	44.34	4.03	37.11	10.90	0.17	0.276	10.63	7.15	5.19	29.48	24.19	32.30	24	30.29	2.71
	1/2"	44.16	44.32	4.04	37.10	10.98	0.16	0.267	10.72	7.21	5.15	29.23	24.17	32.05	24	30.04	3.51
Bottom Joint		44.18	44.37	4.04	36.82	10.59	0.19	0.320	10.27	6.91	5.33	30.27	24.20	33.09	24	31.08	-
	1/4"	44.16	44.31	4.06	36.71	10.84	0.15	0.251	10.59	7.13	5.15	29.26	24.19	32.09	24	30.07	3.24
	1/2"	44.15	44.31	4.04	36.77	11.04	0.17	0.277	10.76	7.24	5.08	28.84	24.18	31.66	24	29.65	4.61
Staggered Joints		44.18	44.37	4.04	36.82	10.59	0.19	0.320	10.27	6.91	5.33	30.27	24.20	33.09	24	31.08	-
	1/4"	44.18	44.35	4.06	36.73	11.04	0.17	0.291	10.75	7.23	5.08	28.84	24.21	31.67	24	29.66	4.57
	1/2"	44.16	44.33	4.05	36.70	11.20	0.17	0.288	10.91	7.34	5.00	28.38	24.19	31.21	24	29.19	6.07
Through Joint	3.3" Panel	44.09	44.08	4.02	36.98	16.90	-0.01	-0.013	16.92	11.38	3.25	18.45	24.05	21.26	24	19.25	-
	1/4"	44.12	44.10	4.03	35.60	17.95	-0.01	-0.024	17.98	12.10	2.94	16.72	24.07	19.53	24	17.52	9.01
	1/2"	44.08	44.07	3.99	35.63	18.93	-0.01	-0.015	18.95	12.75	2.79	15.87	24.03	18.68	24	16.66	13.44
Staggered Joints and Fasteners		44.18	44.37	4.04	36.82	10.59	0.19	0.320	10.27	6.91	5.33	30.27	24.20	33.09	24	31.08	-
		44.14	44.27	4.07	36.08	12.61	0.13	0.212	12.40	8.35	4.32	24.55	24.17	27.38	24	25.36	18.40